Department of Applied Chemistry

Stable Hydrogen Isotope Ratios of Individual Hydrocarbons in Sediments and Petroleum

Daniel Dawson

This thesis is presented for the Degree of
Doctor of Philosophy
of
Curtin University of Technology

November 2006

Declaration

To the best of my knowledge and belief this thesis contains no material previously published by any other person except where due acknowledgment has been made.

This thesis contains no material which has been accepted for the award of any other degree or diploma in any university.

Signature:

Date: 13/11/2006

ABSTRACT

Early research into the stable hydrogen isotopic compositions (δD) of petroleum involved bulk deuterium/hydrogen (D/H) measurements which, while providing some useful information, had to contend with the analysis of complex mixtures of hydrocarbons, and alteration resulting from the rapid exchange of nitrogen-, oxygen- and sulphur-bound hydrogen. The use of gas chromatography-isotope ratio mass spectrometry (GC-irMS) overcomes these problems by allowing the analysis of individual compounds containing only the most isotopically conservative aliphatic carbon-bound (C-bound) hydrogen. This project investigates the geochemical utility and reliability of compound-specific δD values, with the aim to better understand and exploit this analytical capability.

To demonstrate the source diagnostic potential of compound-specific δD values, normal and branched alkanes extracted from series of immature bog-head coals (torbanites) were analysed. The torbanites contain immature organic matter predominantly from a single, freshwater algal source, i.e. *Botryococcus braunii* (*B. braunii*). The δD values of *n*-alkanes reflect the climate regime at the time of deposition of the torbanites, and vary mainly in response to the δD values of the source meteoric waters in their depositional environments. *n*-Alkanes from torbanites deposited at high latitude in a glacial climate are depleted in D by up to 70‰ relative to those from a torbanite deposited at low latitude under a tropical climate regime. Torbanites deposited in a mid-latitude region under cool-temperate conditions contain *n*-alkanes with δD values falling in between those of *n*-alkanes from tropical and glacial torbanites. The δD values of the *n*-alkanes also reflect their multiple source inputs. For example, a saw-toothed profile of *n*-alkane δD values in Australian torbanites is attributed to a dual-source system: a predominant *B. braunii* input, with a minor terrestrial plant input to odd-carbon-numbered *n*-alkanes in the range *n*-C_{20} to *n*-C_{29}. The δD values of *n*-alkanes and isoprenoids (pristane and phytane) differ significantly in two Permian torbanites from Australia, thought to be reflective of the offset between the δD values of their precursors in extant organisms. The torbanite data indicate that a biological δD signal has been preserved for at least 260–280 million years, extending the utility of δD values for palaeoclimate studies.

To elucidate the effect of sedimentary processes on the δD values of petroleum hydrocarbons, three sedimentary sequences have been studied. These comprise one from the Perth Basin (Western Australia) and two from the Vulcan Sub-basin (northern Australia) covering a wide range of maturities, i.e. 0.53–1.6% vitrinite reflectance (R_o). The δD values of *n*-alkanes extracted from immature-early mature sediments (marine shales/siltstones and mudstones) are consistent with that expected of marine-derived *n*-alkyl lipids. The hydrocarbons become enriched in D with increasing maturity. The large (ca. 115‰) biologically-derived offset between the δD values of *n*-alkanes and acyclic isoprenoids from immature sediments gradually decreases with increasing maturity, as the isoprenoids become enriched in D more rapidly than the *n*-alkanes. The D-enrichment in isoprenoids correlates strongly with R_o and traditional molecular maturity parameters. This suggests that H/D exchange during maturation occurs *via* a mechanism involving carbocation-like intermediates, which proceeds more rapidly with compounds containing tertiary carbon centres. Significant epimerisation of pristane and phytane coincides with their D-enrichment, suggesting that hydrogen exchange occurs at their tertiary carbons. A mechanism is proposed which can account for both H/D exchange and the epimerisation of pristane and phytane in the sedimentary environment. Pristane and phytane extracted from a post-mature sediment from the Paqualin-1 sequence are significantly enriched in D (ca. 40‰) relative to the *n*-alkanes, indicating that D-enrichment persists at very high maturity, and is more pronounced for the regular isoprenoids than the *n*-alkanes. This supports the notion that H/D exchange causes the observed shift in δD values, rather than free-radical hydrogen transfer. The differences between the δD values of pristane and phytane show opposite trends in the Perth Basin and Vulcan Sub-basin sediments. In the Perth Basin, phytane is enriched in D relative to pristane, likely due to a dominant algal source. In the Vulcan Sub-basin, pristane is enriched in D relative to phytane, and thus is attributed to a lower relative input of algal organic matter. The variance of the δD values of pristane and phytane is generally consistent throughout the maturity range and provides evidence that pristane and phytane exchange hydrogen at similar rates.

δD analysis of crude oils and condensates reservoired in the Perth Basin and Vulcan Sub-basin has been carried out to evaluate potential applications in oil-source correlation. The *n*-alkanes from crude oils and condensates are often more enriched

in D than *n*-alkanes extracted from their supposed source rocks, and the oils also show relatively small differences between the δD values of *n*-alkanes and isoprenoids. These results suggest significant H/D exchange has occurred, implying that the liquids were generated from mature source rocks. A Perth Basin crude oil (Gage Roads-1) thought to be derived from a lacustrine/terrestrial source contains hydrocarbons that are significantly depleted in D relative to Perth Basin oils derived from a marine source, attributed to variability in the isotopic composition of marine and terrestrial source waters. δD values of *n*-alkanes from Vulcan Sub-basin crude oils and condensates are largely consistent with their prior classification into two groups: Group A, having a marine source affinity; and Group B, having a terrigenous source affinity. Some oils and condensates are suggested to be mixtures of Group A and Group B hydrocarbons, or Group A hydrocarbons and other as yet unknown sources. An exception is a former Group A oil (Tenacious-1) containing *n*-alkanes that are enriched in D relative to those from other Group A oils and condensates, attributed to mixing with another source of more mature hydrocarbons. The *n*-alkane δD profile appears to be indicative of source and sedimentary processes. One Perth Basin crude oil (Dongara-14) contains lower-molecular-weight *n*-alkanes that are depleted in D relative to higher-molecular-weight *n*-alkanes, attributed to a mixed marine/terrestrial source. Group A crude oils and condensates from the Vulcan Sub-basin display a 'bowl-shaped' profile of *n*-alkane δD values. An upward inflection in the *n*-alkane δD profile from *n*-C_{11} to *n*-C_{15} is suggested to represent the addition of D-enriched lower-molecular-weight *n*-alkanes from a more mature wet gas/condensate to an initial charge of lower maturity oil.

Ultimately, this project has demonstrated that the δD values of individual petroleum hydrocarbons can be used to elucidate the nature of source organic matter and depositional environments. The preservation potential of lipid δD values is greater than previously thought, although it is clear that H/D exchange accompanying maturation can have a significant effect on the δD values of certain hydrocarbons. Thus, great care must be taken when interpreting δD values of individual hydrocarbons, particularly those derived from sediments of high thermal maturity.

ACKNOWLEDGEMENTS

First and foremost, I would like to give a special thank you to my principal supervisor Associate Professor Kliti Grice. Her tireless effort, guidance and encouragement over the past 3–4 years have been invaluable. Thanks to Kliti I have had the 'whole' PhD experience, including opportunities to publish journal articles, and travel the world attending and presenting this research at national and international conferences, as well as achieving my academic goals. One could only hope that other PhD students have the experiences that I've been fortunate enough to have during my postgraduate tenure. I would also like to thank my associate supervisor Emeritus Professor Robert Alexander, who on many occasions has given me valuable second opinions and useful feedback on scientific results, draft publications and thesis chapters. A big thank you to Dr Paul Greenwood for proof-reading this thesis.

I would like to thank Mr Geoff Chidlow and Mrs Sue Wang for technical assistance with gas chromatography-mass spectrometry and gas chromatography-isotope ratio mass spectrometry, respectively. Their extensive knowledge, experience, and patience have been invaluable to me over the past 3–4 years.

Geological samples for a project of this nature are precious, and not always easy to obtain. Thus, I would like pass on my utmost gratitude to the following companies (and specific staff) for openly providing samples and other valuable scientific information: Origin Energy (Dr Rob Willink and Mr Bruce Thomas); and Geoscience Australia (Drs Dianne Edwards and Chris Boreham).

A big thank you goes to staff and students (past and present) of the Department of Applied Chemistry, and particularly those of the Centre for Applied Organic Geochemistry, for creating an enjoyable and stimulating environment in which to conduct research.

I would like to thank the Department of Education, Science and Training for awarding me a stipend in the form of an Australian Postgraduate Award research scholarship.

Last but certainly not least, I would like to thank my family for their love, encouragement and financial support over the past 3–4 years, and for playing the most important role in making me the person I am today.

PREFACE

The purpose of this preface is to provide an overview of the layout of this thesis. The introduction chapter (Chapter 1) is a brief description of the basic principles of petroleum and stable isotope geochemistry. Chapter 1 also describes the scope and significance of this project. More detailed introductory and background information is included in the individual introduction sections of Chapters 4, 5 and 6, which also discuss the results obtained from each part of this study. The summary and conclusions sections of Chapters 4, 5 and 6 are presented in point-form detailing the specific findings, while Chapter 7 summarises the overall conclusions of these individual chapters and the project. Chapters 2 and 3 describe experimental and analytical techniques, as well as the geological samples used for this study.

Chapter 4 of this thesis includes details that were originally published as Dawson *et al.* (2004). Chapter 5 comprises the results published as Dawson *et al.* (2005a; 2005b) and, in part, as Dawson *et al.* (2006). Selected information in Chapter 6 has been accepted for publication, in part, as Dawson *et al.* (2006). For full publication details, see the following page.

PUBLICATIONS ARISING FROM THIS STUDY

Dawson, D., Grice, K., Wang, S.X., Alexander, R., Radke, J., 2004. Stable hydrogen isotopic composition of hydrocarbons in torbanites (Late Carboniferous to Late Permian) deposited under various climatic conditions. Organic Geochemistry 35, 189-197.

Dawson, D., Grice, K., Alexander, R., 2005a. Effect of maturation on the indigenous δD signatures of individual hydrocarbons in sediments and crude oils from the Perth Basin (Western Australia). Organic Geochemistry 36, 95-104.

Dawson, D., Grice, K., Alexander, R., 2005b. Stable hydrogen isotope ratios of sedimentary hydrocarbons: A Potential method for assessing thermal maturity? Australian Petroleum Production and Exploration Association Journal 45, 253-260.

Dawson, D., Grice, K., Alexander, R., Edwards, D.S., 2006. The effect of source and maturity on the stable isotopic compositions of individual hydrocarbons in sediments and crude oils from the Vulcan Sub-basin, Timor Sea, northern Australia. Organic Geochemistry (in press).

TABLE OF CONTENTS

LIST OF FIGURES

LIST OF TABLES

CHAPTER 1

1 INTRODUCTION

1.1 PETROLEUM GEOCHEMISTRY

Petroleum geochemistry is concerned with the processes involving sedimentary organic matter that lead to the formation and accumulation of crude oil and natural gas. These processes include the production, accumulation and preservation of organic matter in depositional environments, its senescence and burial in the sediment (Sec. 1.1.1), and finally its alteration under thermal stress (maturation) in the subsurface which can lead to the formation of liquid and gaseous hydrocarbons (petroleum, Sec. 1.1.2). Certain hydrocarbons can be related to natural products of living organisms which are the precursors of sedimentary organic matter, and thus can provide information about the depositional palaeoenvironment in which the precursor organism lived. Relating sedimentary hydrocarbons to their biological precursors is often done *via* structural correlation and/or *via* the use of stable isotopes (Sec. 1.2). The following sections describe the basic principles of petroleum geochemistry.

1.1.1 Sediments

Sediment is defined as unconsolidated grains of minerals, organic matter or pre-existing rocks that can be transported by water, ice or wind, and deposited in various environments (e.g. Figure 1.1). The organic matter in sediments derives from the remains of extant organisms including algae, bacteria and higher plants. Sedimentary rocks result from the accumulation and lithification of sediment in the subsurface. Fine-grained sedimentary rocks (sediments) containing ≥1% organic matter and ≥0.5 wt.% total organic carbon (TOC) are potential petroleum source rocks. If buried and heated (matured) sufficiently, source rocks can generate petroleum (Sec. 1.1.2) which may (or may not) be trapped in a reservoir.

Maturation is the chemical change in sedimentary organic matter, induced by burial and the action of temperature and pressure. Thermally-driven chemical reactions may convert the organic matter into petroleum. The extent of maturation

can be determined using a combination of non-biomarker (e.g. vitrinite reflectance, Rock Eval pyrolysis; Appendix 1) and biomarker/molecular parameters, most of which are described in detail by Peters and Moldowan (1993) and Peters *et al.* (2005).

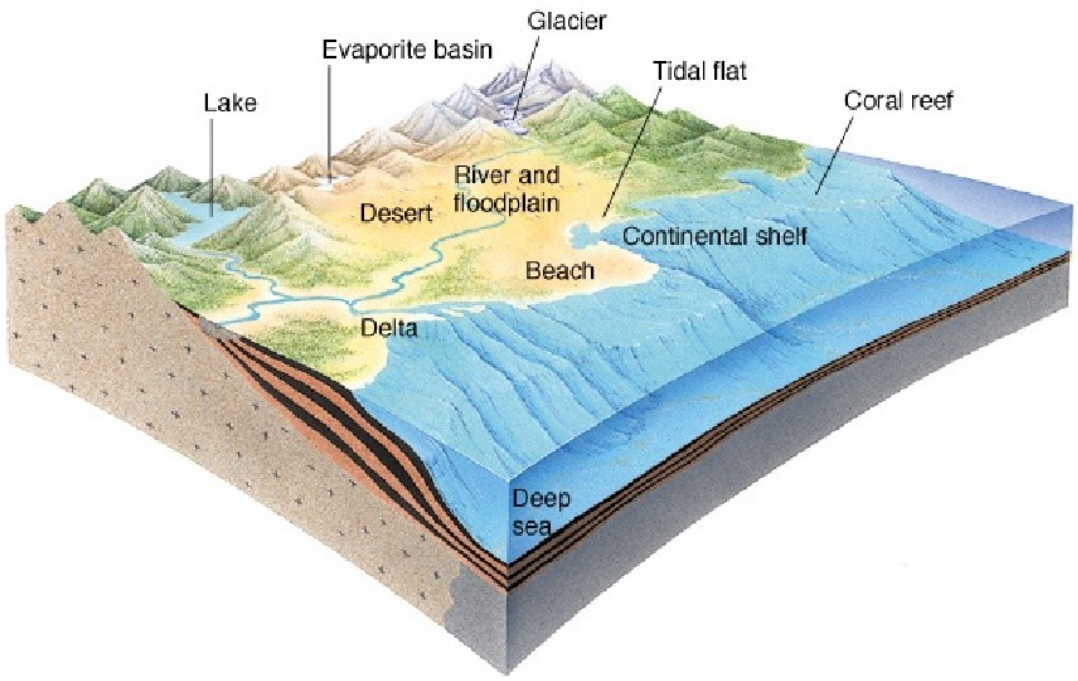

Figure 1.1 Depositional environments

Sedimentary organic matter comprises two general fractions: (i) bitumen (Sec. 1.1.2), a low-molecular-weight component which can be extracted from a source rock using common organic solvents; and (ii) kerogen, a high-molecular-weight component which is insoluble in these solvents. The degradation and alteration (biological, physical and chemical) of the organic material during transport, burial and early maturation can lead to stable, complex macromolecules (kerogen) which can be preserved in sedimentary horizons. This process is known as diagenesis, and occurs up to an equivalent vitrinite reflectance of 0.6% (Peters and Moldowan, 1993). Kerogens can be classified into three main types: I, II (II-S) and III. Type I kerogen is typically formed from algal organic matter deposited in a lake (lacustrine setting), and is highly oil-prone. Type II kerogen is usually derived from a mixture of terrestrial and marine organic matter deposited in a marine environment, and is oil-prone. Type II-S is similar to type II except it has high sulfur content. Type III

kerogen is formed mainly from terrestrial/woody matter typically deposited in a deltaic/paralic marine setting, and is gas-prone.

Deep in the subsurface and with increasing temperatures, a process known as catagenesis thermally decomposes part of the macromolecular structure of kerogen to form petroleum (Sec. 1.1.2). Catagenesis occurs at a maturity level equivalent to the vitrinite reflectance range of 0.6–2.0%, which includes the oil-generative window (Peters and Moldowan, 1993). A schematic diagram showing the relationship of diagenesis, catagenesis and metagenesis (gas production at high thermal stress) is shown in Figure 1.2.

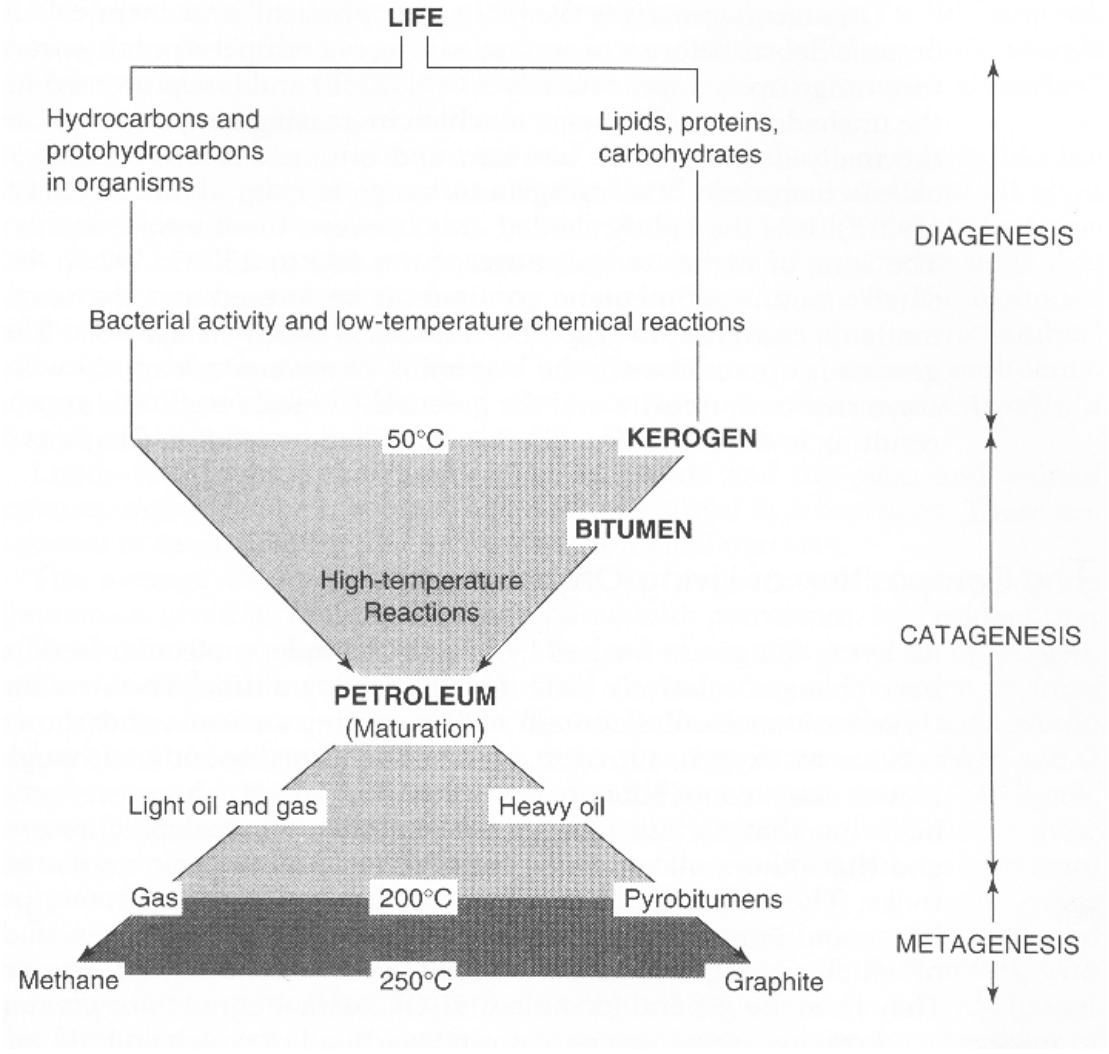

Figure 1.2 The origin and maturation of petroleum (Hunt, 1996)

1.1.2 Petroleum

Petroleum is a complex mixture of hydrocarbons found in the Earth. It includes hydrocarbon gases, bitumen, migrated crude oil and pyrobitumen, but not kerogen. Bitumen is free organic matter within a source rock which is compositionally similar to crude oil. However, unlike crude oil which has migrated out of the source rock, bitumen is indigenous to the rock in which it is found.

The hydrocarbons in petroleum can be divided into a number of polarity-based fractions. These include saturated hydrocarbons (aliphatic and cycloaliphatic); aromatic hydrocarbons; more polar compounds containing nitrogen, sulfur and oxygen (NSO); and (in some cases) metal porphyrin complexes containing vanadium, nickel and occasionally iron (Hunt, 1996). The aliphatic hydrocarbon fraction consists primarily of normal and branched alkanes, which are mainly derived from biological precursors. Cycloaliphatic hydrocarbons comprising monocyclic (e.g. alkylcyclopentanes, alkylcyclohexanes) and multi-ring compounds (e.g. hopanes, steranes) also occur in this fraction. The aromatic hydrocarbons range from benzene to polycyclic aromatic hydrocarbons (e.g. phenanthrenes). Examples of NSO compounds are aliphatic and aromatic carboxylic acids, carbazoles, phenols, and complex structures derived from sterols. Within the myriad of compound structures, hydrogen can be bound a number of different ways, i.e. either to primary, secondary or tertiary carbon atoms in alkyl moieties (aliphatic C-bound hydrogen); to carbon atoms in aromatic rings (aromatic C-bound hydrogen); and to nitrogen, oxygen or sulfur atoms in polar compounds (N, O, S-bound hydrogen). The way hydrogen is bound has implications in terms of its reactivity, e.g. towards hydrogen exchange as is discussed in more detail in Chapter 5 of this thesis.

The majority of compounds in petroleum are formed synthetically in the subsurface. Commonly referred to as geosynthetic products, these include many aromatic hydrocarbons and several saturated hydrocarbons (e.g. monomethylalkanes) and NSO compounds (e.g. carbazoles). The geosynthetic formation process results in a host of alkylated, dealkylated and isomerised aromatic components (e.g. Radke *et al.*, 1982; van Aarssen *et al.*, 1999; Bastow *et al.*, 2000) with non-isoprenoidal carbon skeletons, and hence cannot be directly related to natural product precursors of algae, bacteria and higher plants. Geosynthetic compounds generally have no structural similarities to any biological precursors, however their distributions can

give insights into the types of chemical processes that occur in the subsurface during petroleum generation (e.g. Radke *et al.*, 1982; Bastow *et al.*, 2000).

Some petroleum hydrocarbons formed *via* degradation of the macromolecular structure of kerogen, with minimal alteration of their carbon skeletons, can be directly related to their biological precursors. These compounds are commonly referred to as 'biomarkers', and have useful applications in petroleum geochemistry. The carbon skeleton of a biomarker is often a diagenetically altered (e.g. dehydrated or aromatised) analogue of the precursor. Likewise its isotopic composition may be diagnostic of a supposed precursor or sedimentary process. The diagenetic processes which convert biochemicals to biomarkers do not fractionate the stable isotopes of carbon to any significant extent (Freeman *et al.*, 1990). Biomarkers can be source-specific or non-specific. For example isorenieratane (Appendix 2, **I**) and some related aromatic compounds are biomarkers derived from isorenieratene (**II**), found in Chlorobiaceae (green sulfur bacteria). Thus isorenieratane is a specific biomarker for green sulfur bacteria, and therefore photic zone euxinic (presence of hydrogen sulfide, anoxic) depositional conditions for geological samples (e.g. Grice *et al.*, 2005a). Other biomarkers can have multiple origins in which case they are of more limited diagnostic value, for example the C_{20} isoprenoid phytane (**III**), which can derive from the lipids of archaea, bacteria and chlorophyll *a* (**IV**) in algae and/or higher plants, and from bacteriochlorophylls (**V**) *a* and *b* of purple sulfur bacteria. Biomarkers are present in both sediments/source rocks and crude oils, and are quite often used in petroleum geochemistry for oil-oil and oil-source correlations (e.g. see Chapter 6). They are used to provide an indication of alteration events such as maturation (e.g. see Chapter 5) and biodegradation, as well as to provide information about depositional environments. A range of parameters are typically used, based on the distributions of both saturated and aromatic compounds. The stable isotopic compositions of biomarkers and other compounds are also useful for geochemical applications (Sec. 1.2). A comprehensive review of biomarker science and its applications in petroleum geochemistry is presented in Peters and Moldowan (1993) and Peters *et al.* (2005).

.

1.2 STABLE ISOTOPE GEOCHEMISTRY

Stable isotope geochemistry is based upon the relative and absolute concentrations of the elements and their stable isotopes in the Earth. There are a number of stable isotopes of interest to organic geochemists (e.g. Table 1.1). The stable isotopes of carbon and hydrogen are the most useful natural tracers in sedimentary organic matter because they are usually the most abundant elements. Thus the stable isotopes of carbon and hydrogen will be discussed exclusively in this thesis.

Table 1.1 Natural abundances (atom %) of stable isotopes

Carbon	Hydrogen	Oxygen	Sulfur	Nitrogen
^{12}C (98.899)	^{1}H (99.985)	^{16}O (99.759)	^{32}S (95.018)	^{14}N (99.9634)
^{13}C (1.111)	^{2}D (0.0105)	^{17}O (0.0374)	^{34}S (4.215)	^{15}N (0.3663)
		^{18}O (0.2039)		

1.2.1 Stable isotopes

Stable isotopes as opposed to radiogenic (unstable) isotopes do not decay, thus their natural abundances (e.g. see Table 1.1) remain relatively constant, even over geological timescales. However, variations in stable isotopic composition, or 'isotopic fractionations', occur in nature as a result of chemical and physical processes, due to different isotopes of an element having subtly different chemical and physical properties. Equilibrium processes (Sec. 1.2.2) and kinetic processes (Sec. 1.2.3) can lead to stable isotopic fractionation.

1.2.2 Equilibrium isotope effects

Equilibrium isotope effects occur as a result of temperature-dependent equilibrium isotope-exchange reactions. These reactions result in a change of the isotope distribution between different chemical substances, between different phases, or between individual molecules (Hoefs, 1987). For example, the equilibrium reaction:

$$A_1 + B_2 \rightleftharpoons A_2 + B_1$$

where subscripts indicate that species A and B contain either the light (1) or heavy (2) isotope.

In these cases, there is no net change in the chemical system, i.e. the products are chemically identical to the reactants, with the exception being that the stable isotopes are distributed differently between them. A real example is the evaporation/condensation cycle of water, where:

$$H_2O_{vapour} + D_2O_{liquid} \rightleftharpoons HDO_{vapour} + HDO_{liquid} \rightleftharpoons D_2O_{vapour} + H_2O_{liquid}$$

This physical process results in a change in the distribution of hydrogen (and oxygen) isotopes between the liquid and vapour phases (see Chapter 4). Kinetic fractionation occurs when the water vapour is removed before condensation can occur (see Sec. 1.2.3).

1.2.3 Kinetic isotope effects

Kinetic isotope effects occur when an irreversible chemical reaction takes place resulting in a change in the chemical system. As a simple example, a unidirectional chemical reaction always shows a depletion of the heavy isotope in the reaction products relative to the reactants. This occurs due to the slower reaction rate of the heavier isotopic species. For example, in a reaction of reactant A to product B, there may be two (or more) competing unidirectional isotopic reactions:

$$A_1 \xrightarrow{k_1} B \qquad\qquad A_2 \xrightarrow{k_2} B$$

where k is the rate constant.

In this theoretical example, say the rate determining step involves the breakage of a bond. It is generally easier to break the bonds of molecules that contain the lighter

isotopes, because the vibrational frequency of such bonds tends to be higher. Thus, in this case, $k_1 > k_2$, and therefore more of the lighter isotope will be incorporated into the product. A real example is when water evaporates and the water vapour is removed immediately, e.g. three competing unidirectional isotopic reactions:

$$H_2O_{liquid} \xrightarrow{k_1} H_2O_{vapour}$$

$$HDO_{liquid} \xrightarrow{k_2} HDO_{vapour}$$

$$D_2O_{liquid} \xrightarrow{k_3} D_2O_{vapour}$$

where in this case $k_1 > k_2 > k_3$ because the lighter isotopic species of water evaporate preferentially (see Chapter 4). Thus the net process results in water vapour that is enriched in protium (^1H).

1.2.4 Standards and notation

Stable carbon and hydrogen isotopic compositions are determined not as absolute isotopic abundances, but as ratios of a heavy isotope to a light isotope relative to a standard. For example, stable carbon isotopic compositions are determined as a ratio of carbon-13 (^{13}C) to carbon-12 (^{12}C) relative to the international standard Pee Dee Belemnite (PDB), a marine limestone from the Pee Dee formation in South Carolina (USA). For stable hydrogen isotopic composition, the ratio is deuterium (^2H or D) to protium relative to Standard Mean Ocean Water (SMOW). Stable isotopic compositions are expressed as a delta (δ) value (e.g. $\delta^{13}C$ for carbon, δD for hydrogen) in units of per mil (‰) or parts per thousand, as calculated using equation 1.

$$\delta_{sample} = \frac{R_{sample} - R_{standard}}{R_{standard}} \text{ x } 1000\ ‰ \qquad \text{(Equation 1)}$$

where R is the ratio of heavy to light isotope.

The PDB and SMOW international standards are assigned an arbitrary δ value of 0‰. It should be noted that PDB was exhausted several years ago, and has been replaced by calibrating another carbonate (NBS-19) relative to PDB (Urey *et al.*, 1951; Craig, 1957). The new calibration scale is termed 'VPDB' (Vienna PDB). SMOW was believed to represent (isotopically) an average isotopic composition of the world's oceans (being the largest reservoir of hydrogen and oxygen) based on data accumulated over time (Werner and Brand, 2001). However the standard was not available as a reference material, and therefore was defined relative to another water standard (NBS-1, also now exhausted) which deviated by 47.6‰ from the current δD scale (Werner and Brand, 2001). Thus a new reference material was developed with an isotopic composition equivalent to that of SMOW, which led to the current 'VSMOW' (Vienna SMOW) scale. Another primary international standard for δD determinations is Standard Light Antarctic Precipitation (SLAP), which is strongly depleted in D (δD = -428‰).

Throughout the text and figures in this thesis, stable isotopic compositions will be referred to as δ values, or as an expression of heavy/light isotope (e.g. D/H or $^{13}C/^{12}C$), with the suffix of compositions or signatures. When making comparisons between the isotopic compositions of two materials, or describing changes in isotopic composition, the following terms are used: (i) higher and lower δ values (e.g. higher indicating more of the heavy isotope); (ii) isotopically heavier and lighter (e.g. heavier meaning more of the heavy isotope); (iii) more/less positive (e.g. more positive meaning more of the heavy isotope) and more/less negative δ values; and (iv) enriched and depleted in a particular isotope (e.g. for hydrogen, enriched or depleted in D).

1.2.5 Stable isotope analysis

Stable isotopic compositions are most effectively determined using mass spectrometric methods (Hoefs, 1987). The two general methods of analysis are bulk isotope analysis, and compound-specific isotope analysis.

Bulk isotope analysis

Bulk isotope analysis involves measurement of the stable isotopic composition of the total carbon, hydrogen, oxygen, nitrogen or sulfur within a sample, thus it represents the average of all compounds in complex mixtures. The entire sample, for example a whole crude oil, undergoes quantitative combustion, oxidation, reduction and/or pyrolysis to convert the element of interest into a gaseous analyte (e.g. see Chapter 3) which is amenable to high-precision isotopic analysis by an isotope ratio mass spectrometer (irMS). The process also converts by-products into a form that will not interfere isobarically with the analyte of interest (e.g. see Chapter 3).

Compound-specific isotope analysis

Compound-specific isotope analysis (CSIA) involves measurement of the stable isotopic composition of individual compounds in a complex mixture. The original method for determining the discrete isotopic value of an individual compound required lengthy offline laboratory procedures to isolate components of interest for analysis *via* the bulk method, taking great care to avoid isotopic fractionation. Furthermore, complete offline separation is often not possible for such complex mixtures such as petroleum. However, the development of gas chromatography-isotope ratio mass spectrometry (GC-irMS) has allowed online GC separation of components of a complex mixture prior to combustion/pyrolysis (see above) and analysis by the irMS (Matthews and Hayes, 1978). GC-irMS instruments have been developed with the capability of measuring $^{13}C/^{12}C$ (Matthews and Hayes, 1978), $^{18}O/^{16}O$ and $^{15}N/^{14}N$ (Brand *et al.*, 1994), and recently D/H (Burgoyne and Hayes, 1998).

CSIA offers numerous advantages over the bulk isotope analysis method. The $\delta^{13}C$ analysis of individual sedimentary hydrocarbons can provide evidence for their diverse origins (e.g. Freeman *et al.*, 1990; Hayes *et al.*, 1990; Rieley *et al.*, 1991). This level of detail can not be obtained *via* bulk analysis, which provides the average value of all of the constituents present in the material analysed. Secondary processes (e.g. migration contamination, biodegradation; see Sec. 1.2.6 and 1.2.7) may alter the isotopic compositions of certain compound classes. Some processes will affect this to a greater extent than others, thus the bulk isotopic composition of the sample

averages both source and altered signatures. For example, bulk isotope analysis of hydrogen in petroleum samples has to contend with the rapid exchange of aromatic, O-, N- and S-bound hydrogen. The analysis of individual petroleum hydrocarbons such as *n*-alkanes by CSIA allows the measurement of the most isotopically conservative aliphatic C-bound hydrogen. This often allows source isotopic signatures to be identified, as well as recognition of secondary alteration effects by comparing the isotopic signatures of compounds with low and high resistance to secondary alteration.

1.2.6 Stable carbon isotopes in organic matter

Carbon is the fundamental element of organic compounds. It is an essential element for plants and animals, ultimately derived from atmospheric carbon dioxide assimilated by plants during photosynthesis. Carbon has two stable isotopes, ^{12}C and ^{13}C. Photosynthetic carbon fixation favours the lighter ^{12}C isotope, therefore biosynthesised organic compounds are depleted in ^{13}C relative to their carbon source. The present day environmental distributions of stable carbon isotopes are controlled by several factors, including (see Hayes, 1993): (i) $\delta^{13}C$ of the carbon source, and its availability; (ii) the photosynthetic pathway (and the associated complex fractionations) involved in the uptake of carbon dioxide; (iii) isotopic fractionations associated with biosynthesis (e.g. lipids versus protein and sugar biosynthesis); and (iv) other physiological factors including cell size and geometry (Goericke *et al.*, 1994; Popp *et al.*, 1998), growth rates of phytoplankton (Laws *et al.*, 1995), and the plant-water use efficiency of terrestrial plants (i.e. C3, C4 and CAM) (Ehleringer *et al.*, 1993). The measurement of $\delta^{13}C$ values is useful in petroleum geochemistry because it can enable the reconstruction of ancient biogeochemical processes relating to the carbon cycle in ancient depositional environments (Freeman *et al.*, 1990), which would have played a major role in the production of the source organic matter for present-day reservoired crude oils.

The $\delta^{13}C$ values of petroleum components, including whole crude oils or bitumens, their fractions, and individual compounds, have been used to determine the geological age of source rocks, as well as the nature of their depositional environment and source organic matter (e.g. Gilmour *et al.*, 1984; Sofer, 1984; Bjorøy *et al.*, 1991; Chung *et al.*, 1992; Murray *et al.*, 1994; Andrusevich *et al.*,

1998; Santos Neto and Hayes, 1999). A summary of previous work is described in the introduction of Chapter 6. In the subsurface, maturation has been reported to affect the stable carbon isotopic composition of petroleum (Clayton, 1991; Clayton and Bjorøy, 1994). $\delta^{13}C$ values of kerogen, source rock extracts and crude oils and their associated fractions, and individual compounds (e.g. *n*-alkanes) have been found to generally increase with thermal maturity (e.g. see Chapter 5). The enrichment of ^{13}C in kerogen is thought to be a result of the thermal release of isotopically light products (Clayton, 1991). For crude oils, the ^{13}C enrichment is probably due to mixing of isotopically light bitumen with isotopically heavier generated products (Clayton, 1991). Other secondary processes such as biodegradation have been reported to alter $\delta^{13}C$ values. It is widely accepted that the $\delta^{13}C$ values of natural gas components (C_1–C_5) are significantly altered by biodegradation (e.g. Pallasser, 2000). Slight to moderate biodegradation has been shown to affect the $\delta^{13}C$ values of light hydrocarbons (C_5–C_9) (George *et al.*, 2002). There is no evidence of any significant fractionation of carbon isotopes in higher molecular weight *n*-alkanes (C_{14}–C_{29}) with biodegradation (Sun *et al.*, 2005). In the majority of cases, biodegradation leads to an enrichment of ^{13}C in residual compounds, with the level of enrichment gradually decreasing with increasing molecular weight (e.g. George *et al.*, 2002; Sun *et al.*, 2005). This is thought to be a result of kinetic isotope fractionation (Sec. 1.2.3), where molecules containing more of the lighter isotope are preferentially degraded. A sequential loss of *n*-alkanes with ongoing biodegradation leads to a depletion of ^{13}C in residual saturated fractions, while residual aromatic and NSO hydrocarbon fractions become relatively enriched in ^{13}C (Sun *et al.*, 2005).

1.2.7 Stable hydrogen isotopes in organic matter

Hydrogen is the lightest chemical element and the most abundant in the universe, and is present in water and all organic compounds. Hydrogen consists of two naturally-occurring stable isotopes, ^{1}H and D. The water in the world's oceans constitutes the largest natural reservoir of hydrogen, and is fundamental in the global hydrological cycle. In marine and terrestrial environments, ocean water, and/or meteoric water produced *via* operation of the hydrological cycle, is used by inhabiting organisms. Thus, the distribution of stable hydrogen isotopes in present

day environments is predominantly controlled by a variety of naturally occurring processes in the global hydrological cycle (see Chapter 4), and the hydrogen bound in the biosynthetic products of photoautotrophs will (isotopically) reflect the source water (see Chapter 4). Hydrogen has the largest mass difference (2:1) between its two stable isotopes and thus, the largest natural variation in stable isotope ratios. This makes the measurement of δD values an attractively sensitive technique for geochemical applications.

To date there has been relatively limited research into the D/H composition of petroleum, particularly using a compound-specific approach. The reports that exist have investigated the relationships between δD values of whole crude oils and bitumens, and their source (including organic matter type and depositional conditions), thermal maturity, as well as the effects of secondary processes such as biodegradation, mixing and migration (e.g. Hoering, 1977; Rigby *et al.*, 1981; Yeh and Epstein, 1981; Smith *et al.*, 1982; Santos Neto and Hayes, 1999; Li *et al.*, 2001; Schimmelmann *et al.*, 2004; Radke *et al.*, 2005; Sun *et al.*, 2005; Xiong *et al.*, 2005; Pedentchouk *et al.*, 2006). For a more comprehensive review of this work, see Chapters 5 and 6.

Depending on the extent of the chemical reactions during petroleum formation, the distribution of stable hydrogen isotopes in petroleum hydrocarbons may be representative of the source waters present in their precursors' depositional environment (e.g. see Chapter 4). Indeed, maturation has been reported to affect the distribution of stable hydrogen isotopes in organic matter, with a gradual D-enrichment with ongoing maturation based on bulk δD measurements (e.g. Rigby *et al.*, 1981; for a review see Chapter 5). Published research on the effects of other secondary processes on the distribution of stable hydrogen isotopes in petroleum samples appears to be limited to one report on the in vitro biodegradation of a North Sea crude oil (Pond *et al.*, 2002), and another on a selection of Liaohe Basin (NE China) crude oils representing a natural sequence of increasing degree of in-reservoir biodegradation (Sun *et al.*, 2005). Pond *et al.* (2002) studied the effect of slight-moderate aerobic biodegradation on the δD values of individual *n*-alkanes in a crude oil, and found that shorter chain *n*-alkanes (*n*-C_{15} to *n*-C_{18}) degrade fastest, and show the largest D-enrichment (~12–25‰). The δD values of longer chain *n*-alkanes (*n*-C_{19} to *n*-C_{27}) only showed a 5‰ D-enrichment with ongoing biodegradation. Sun *et*

al. (2005) found that stable hydrogen isotopes in *n*-alkanes are significantly fractionated with moderate-heavy biodegradation, resulting in enrichment in D of up to 35‰. The D-enrichment was evident throughout the range *n*-C_{16} to *n*-C_{27}, indicating that in-reservoir biodegradation fractionates hydrogen isotopes in longer chain *n*-alkanes to a larger extent than in-vitro (laboratory) biodegradation (e.g. Pond *et al.*, 2002).

1.3 SCOPE AND SIGNIFICANCE OF THIS STUDY

The scope of the present study is to determine the source and palaeoenvironmental (i.e. depositional environment) information that can be obtained from the distributions of stable hydrogen isotopes in individual hydrocarbons of sedimentary organic matter. Limited work in this area in the past has been based on bulk D/H compositions which, while providing some useful information, has to contend with the analysis of complex mixtures and the rapid exchange of N, O and S-bound hydrogen (see Chapter 5). δD CSIA of isotopically conservative aliphatic C-bound hydrogen avoids these problems. This allows for generation of a whole host of new results, hence the requirement of extensive knowledge about the various processes that determine the D/H composition of individual hydrocarbons in petroleum.

In order to demonstrate the information attainable from the distribution of C-bound stable hydrogen isotopes, the δD values of normal and branched alkanes extracted from a series of immature bog-head coals (torbanites) were measured. The well-preserved organic matter in these samples has a predominant algal source (*Botryococcus braunii*). This and their thermal immaturity make these samples ideal for δD analysis and interpretation. The δD values of hydrocarbons in the coals were interpreted in terms of their palaeolatitude (palaeoclimate) of deposition, which varied from equatorial (tropical) to mid-latitude (cool-temperate) to high-latitude (glacial). This research is detailed in Chapter 4 of this thesis.

Implicit in the interpretation of δD values of sedimentary organic matter is an understanding of the effect of sedimentary processes, such as maturation, on the δD

values of individual petroleum hydrocarbons. To this end, three sedimentary sequences from Australia covering a wide range of maturity have been studied as described in Chapter 5. The effect of maturation, *via* hydrogen exchange reactions, on the δD values of individual compounds containing only aliphatic C-bound hydrogen (i.e. normal and branched alkanes) was assessed. Hydrogen can be bound to either primary, secondary or tertiary carbon in alkyl moieties, and the relative exchange rates of these different types of bound hydrogen with ongoing maturation (geological timescales) was studied in terms of the rate of change of δD values of normal versus branched hydrocarbons. Aromatic C-bound hydrogen and N, O and S-bound hydrogen were not studied considering the relatively rapid rate of exchange of this hydrogen, even on laboratory timescales. Potential mechanisms of hydrogen exchange have been discussed based on previously published work. In addition, an analysis of the diastereomers (stereoisomers of a compound with more than one chiral centre where only one of the chiral centres has a different configuration) of two regular isoprenoids, pristane and phytane, was undertaken in order to elucidate the usefulness of stereochemical changes as a proxy for hydrogen exchange, and to provide insight into potential mechanisms. A new mechanism of hydrogen exchange has been proposed, extending on previous work. The thermally-induced changes in the novel parameters determined in this study were compared to traditional maturity parameters.

Finally, in Chapter 6 a series of crude oils and condensates generated from the sequences mentioned above were analysed for oil-source correlation purposes. The results are compared with previously published work based on comprehensive molecular and stable carbon isotope analysis. Compound-specific δD results were validated using the more traditional bulk δD analysis. The δD values of *n*-alkanes and regular isoprenoids from the crude oils and condensates were compared to that obtained from their supposed source rocks, and interpreted in terms of source and maturity.

The ability to understand and track the origin, generation and maturity of petroleum is critical to the exploration and production of oil and gas reserves. Hydrogen processes are fundamental to the understanding of petroleum formation and generation. The capability of measuring the δD values of individual compounds in petroleum provides a new method of monitoring hydrogen processes in the

subsurface, and allows insights into the potential chemical mechanisms that form this complex mixture of hydrocarbons. This project aims to better understand and exploit this analytical capability.

CHAPTER 2

2 GEOLOGICAL SAMPLES

2.1 TORBANITES

Torbanites are organic-matter-rich sediments containing high amounts of organic matter, with high petroleum potential. Their total organic carbon (TOC) contents range from 30 to 70 wt.% (Boreham, 1994). The organic matter in torbanites is largely derived from the Chlorophyceae *Botryococcus braunii* (*B. braunii*) (Hutton *et al.*, 1980; Largeau *et al.*, 1984; Derenne *et al.*, 1988; Gatellier *et al.*, 1993; Boreham, 1994; Audino *et al.*, 2001a; Grice *et al.*, 2001), with some torbanites being composed of up to 90% of *B. braunii* remains (Derenne *et al.*, 1988). *B. braunii* is a colonial unicellular organism that can flourish in most climates, including temperate, tropical and arctic zones, and has been reported to occur exclusively in fresh and brackish waters (Tyson, 1995). There is, however, one report of *B. Braunii* occurring in a sulfide-rich hypersaline deposit (Grice *et al.*, 1998b), attributed to periodic freshwater incursions (containing *B. braunii*) into a marine, sulfide-rich environment, leading to the preservation of its lipids *via* early diagenetic sulfurisation.

Five torbanites from Australia and Scotland covering the Late Carboniferous to the Late Permian were analysed (Table 2.1). The torbanites were deposited in inland lakes, each under a different climate regime including glacial, cool-temperate and tropical. The torbanite from Torbane Hill, Scotland (Figure 2.1d) was deposited during the Late Carboniferous when Laurasia (the ancient super-continent in the northern hemisphere) was located in low latitudes (Figure 2.1a). Climate conditions in Scotland at this time were tropical with extensive plant growth. Two torbanites from the southern hemisphere (Temi, Eastern Australia; Figure 2.1e) were deposited during the Early Permian under glacial conditions. Gondwana (the ancient super-continent in the southern hemisphere) was located in high latitudes (Figure 2.1b) as a result of a southward migration that began during the Early Carboniferous (White, 1993). At the Carboniferous–Permian boundary it is believed that a vast sheet of ice covered almost half of the Australian continent (Frakes, 1979; White, 1993). The Gondwana ice sheet receded towards the Middle Permian as the climate became

warmer, and there was a rapid rise in sea level during the Late Permian as the ice sheet melted (White, 1993). During the Late Permian Gondwana was located in lower latitudes (Figure 2.1c) and experienced a cool-temperate climate, when two other torbanites from the southern hemisphere (Newnes, Eastern Australia; Figure 2.1e) were deposited.

The torbanite from Scotland is from the Carboniferous Lower Coal Measures found at Boghead on the Torbane Hill estate, close to Bathgate (Figure 2.1d) (Beveridge *et al.*, 1991). The torbanites from Temi came from what is commonly called the Murrurundi deposit which is located due north of Murrurundi in the Liverpool Ranges on the northern margin of the Sydney Basin (Figure 2.1e). The deposit occurs in the Temi Formation which, in the Temi area, is approximately 30 m thick and comprises mostly sandstone, shale, conglomerate, carbonaceous shale and coal. The Newnes torbanites come from the contiguous Newnes-Glen Davis deposit that is located on the western margin of the Sydney Basin, 40 km north of Lithgow (Figure 2.1e). The torbanite occurs in a seam, associated with bituminous coal and shale, approximately 60 m below the top of the Illawarra Coal Measures.

Table 2.1 Torbanites used in this study

Sample #	Location	Age	Climate
3733	Newnes, Australia	Late Permian	Cool-Temperate
3736	Newnes, Australia	Late Permian	Cool-Temperate
3740	Temi, Australia	Early Permian	Glacial
3742	Temi, Australia	Early Permian	Glacial
3755	Torbane Hill, Scotland	Late Carboniferous	Tropical

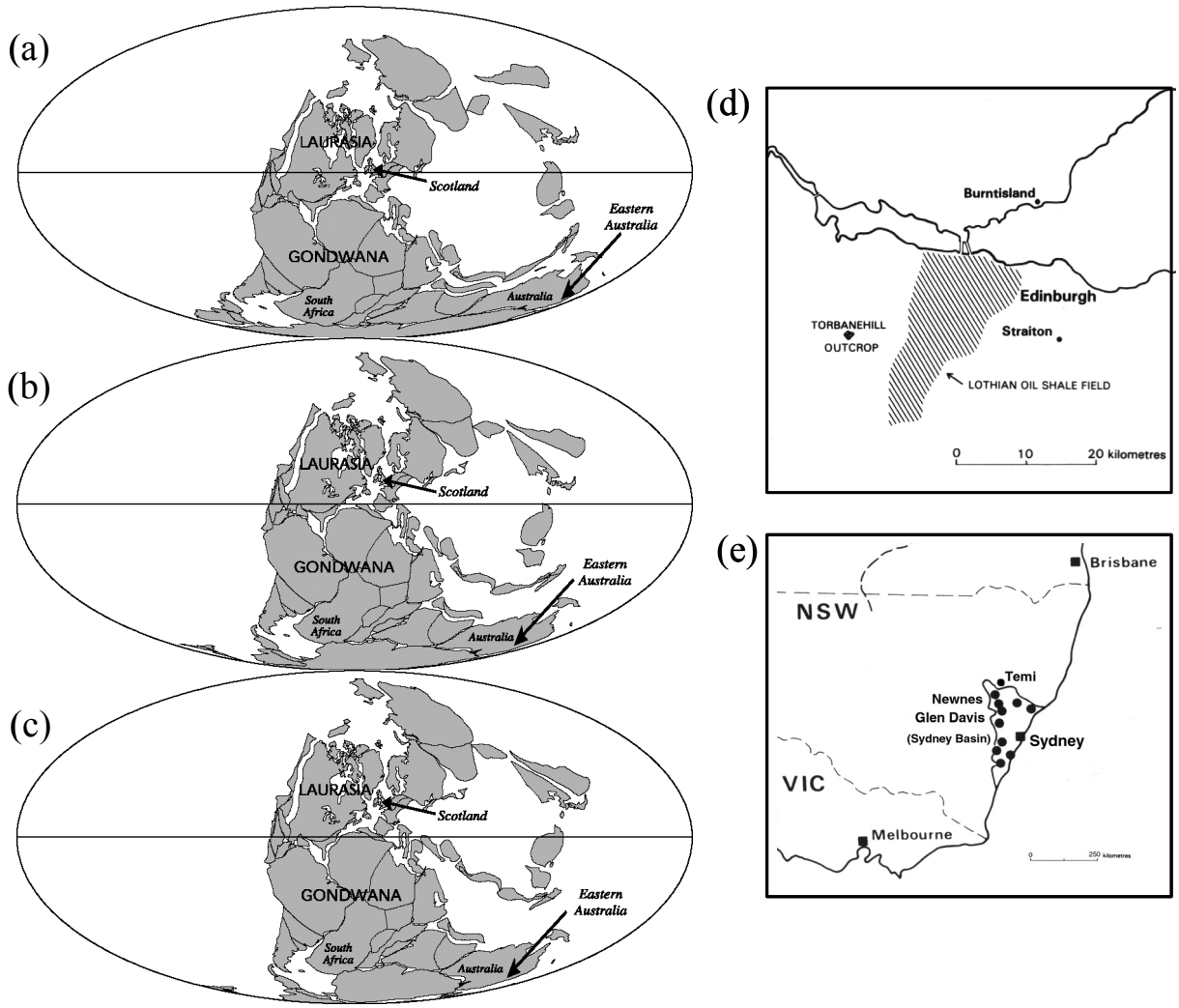

Figure 2.1 Palaeogeographic world maps (Scotese, 1997), (a) Late Carboniferous, 310 Ma.; (b) Early Permian, 280 Ma.; and (c) Late Permian, 260 Ma; and present day maps showing the location of torbanite deposits in (d) Scotland (Beveridge *et al.*, 1991), and (e) Eastern Australia (Hutton *et al.*, 1980)

2.2 PERTH BASIN SEDIMENTS AND CRUDE OILS

The Perth Basin is located in southwest Western Australia (WA). It is a deep and linear north-south trending trough extending over 1,000 km from Geraldton in the north to the south coast of WA (Figure 2.2). The basin covers an area of approximately 45,000 km^2 onshore, and 98,000 km^2 offshore.

Perth Basin sediments comprise rocks of Permian to Early Cretaceous age. The main depocentre is the Dandaragan Trough, where up to 15 km of Permian and Mesozoic sediments were deposited. The Dandaragan Trough is bound by the Beagle Ridge to the north and west, and by the Harvey Ridge to the south. Offshore and west of the city of Perth is the Vlaming Sub-basin which contains about 10 km of Cretaceous and Tertiary sediments. The regional stratigraphy of the study area is summarised in Figure 2.2.

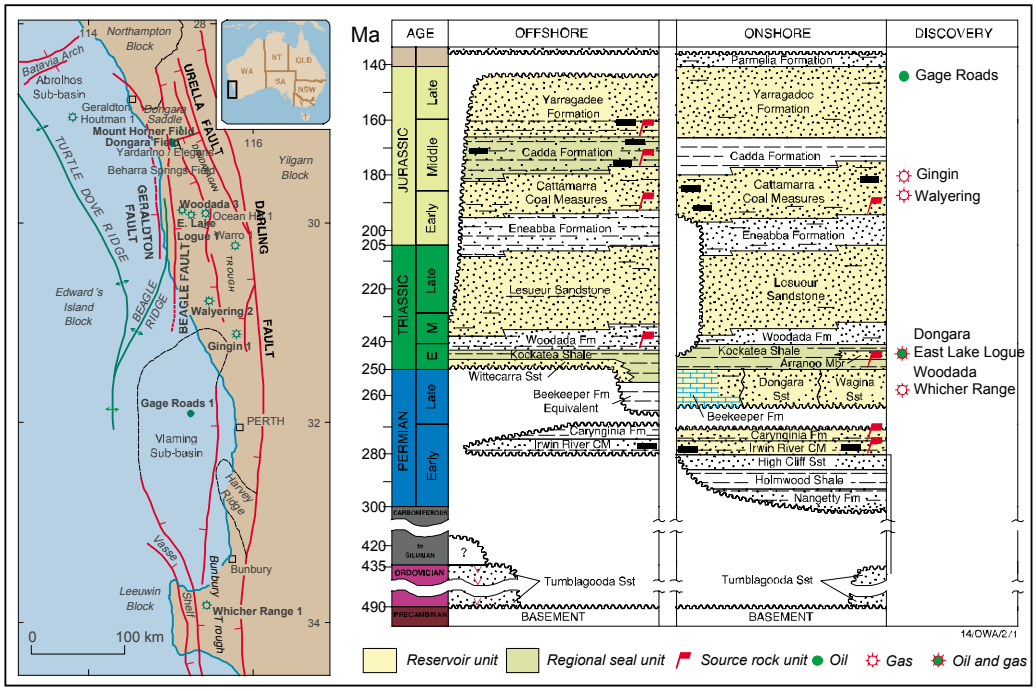

Figure 2.2 A map and stratigraphic column of the Perth Basin (Boreham *et al.*, 2001). The hydrocarbon discoveries, and wells in bold on the map, are the samples used in Chapter 6.

The Perth Basin sediments used in this study (Table 2.2) are all from the Lower Triassic Hovea Member (Sapropelic Interval) of the Kockatea Shale (Thomas and Barber, 2004; Thomas *et al.*, 2004). The Kockatea Shale is a marine sequence of

shale and siltstone, with a low amount of coaly material making the determination of maturity by vitrinite reflectance difficult (Kantsler and Cook, 1979). The Sapropelic Interval of the Hovea Member is believed to be a source from which much of the oil and gas in the northern Perth Basin originates (Thomas and Barber, 2004), and has recently been suggested to have been deposited under photic zone euxinic conditions (Grice *et al.*, 2005a; 2005b). Photic zone euxinia may occur in anaerobic zones of stratified water columns (in lake or marine environments) with restricted water circulation. Here, conditions are favourable for the growth of sulphate-reducing bacteria, and considerable sulphide accumulation may occur. At a depth where there is enough light for photosynthesis to take place, and where the upper sulphide limit coincides with a lower oxygen limit (the chemocline), anoxygenic green sulfur bacteria can thrive. The depositional conditions are therefore anoxic and restricted, and free H_2S is prevalent in the water column.

The Perth Basin crude oils used in this study (Table 2.3) are reservoired in various geological units, ranging from Late Permian to Late Jurassic in age. There is geochemical evidence (see Chapter 6) indicating that the East Lake Logue-1 condensate, and the Dongara-14 and Woodada-3 crude oils are sourced primarily from the Early Triassic Hovea Member (Sapropelic Interval) of the Kockatea Shale, a source from which much of the oil and gas in the northern Perth Basin is thought to originate (Thomas and Barber, 2004). Another potentially significant source is the Early Permian Irwin River Coal Measures (Summons *et al.*, 1995; Volk *et al.*, 2004).

Table 2.2 Perth Basin sediment samples used in this study

Well	Depth/m (ft)	Maturity
BMR-10	973-976 (3193-3203)	Immature
BMR-10	989-991 (3245-3250)	Immature
Dongara-4	1674 (5491)	Early mature
Dongara-4	1675 (5495.5)	Early mature
Dongara-4	1678 (5505)	Early mature
Yardarino-2	2289 (7509)	Mature
Yardarino-2	2290 (7512.5)	Mature
Arrowsmith-1	2494 (8181)	Late mature
Arrowsmith-1	2678 (8187)	Late mature

Table 2.3 Perth Basin crude oil and condensate samples used in this study

Well	Sample Type	Reservoir Unit	Reservoir Age
Whicher Range-1	Yellow-brown condensate	Sue Coal Measures[b]	Late Permian
Woodada-3	Crude oil	Beekeeper Fm[a]	Late Permian
East Lake Logue-1	Yellow condensate	Beekeeper Fm[a]	Late Permian
Dongara-14	Brown, heavy oil	Dongara Sst[a]	Late Permian
Gingin-1	Yellow condensate	Cattamarra Coal Measures[b,c,d]	Early Jurassic
Walyering-2	Yellow-brown condensate	Cattamarra Coal Measures[b,c,d]	Early Jurassic
Gage Roads-1*	Brown, heavy oil	Yarragade Fm[b,c]	Late Jurassic

[a]Thomas and Barber (2004); [b]Summons *et al.* (1995); [c]Kantsler and Cook (1979); [d]Thomas and Brown (1983); *Vlaming Sub-basin, southern offshore Perth Basin; Fm, Formation; Sst, Sandstone

2.3 VULCAN SUB-BASIN SEDIMENTS AND CRUDE OILS

The Vulcan Sub-basin is a northeast-southwest-trending Mesozoic extensional depocentre in the western Bonaparte Basin (Figure 2.3) and comprises a complex series of horsts, grabens and terraces. The major grabens are the Swan and Paqualin, which contain up to 3 km of Late Jurassic marine mudstones (Vulcan Formation) some of which are the most organic matter-rich sediments in the sub-basin. Widespread fluvial-deltaic sedimentation occurred in the Early and Middle Jurassic (Plover Formation), including organic matter-rich marine mudstones and coaly coastal plain facies. The regional stratigraphy of the study area is summarised in Figure 2.4. The Vulcan Sub-basin sediment samples used in this study (Table 2.4) consisted of eight sediments each from the Paqualin-1 well (Paqualin Graben, Figure 2.3) and the Vulcan-1B well (Swan Graben, Figure 2.3), all from the lower Vulcan Formation (Figure 2.4). Eleven crude oils and condensates reservoired in various geological units in the Vulcan Sub-basin (Table 2.5), ranging from Middle Jurassic to Late Cretaceous in age, were used in this study.

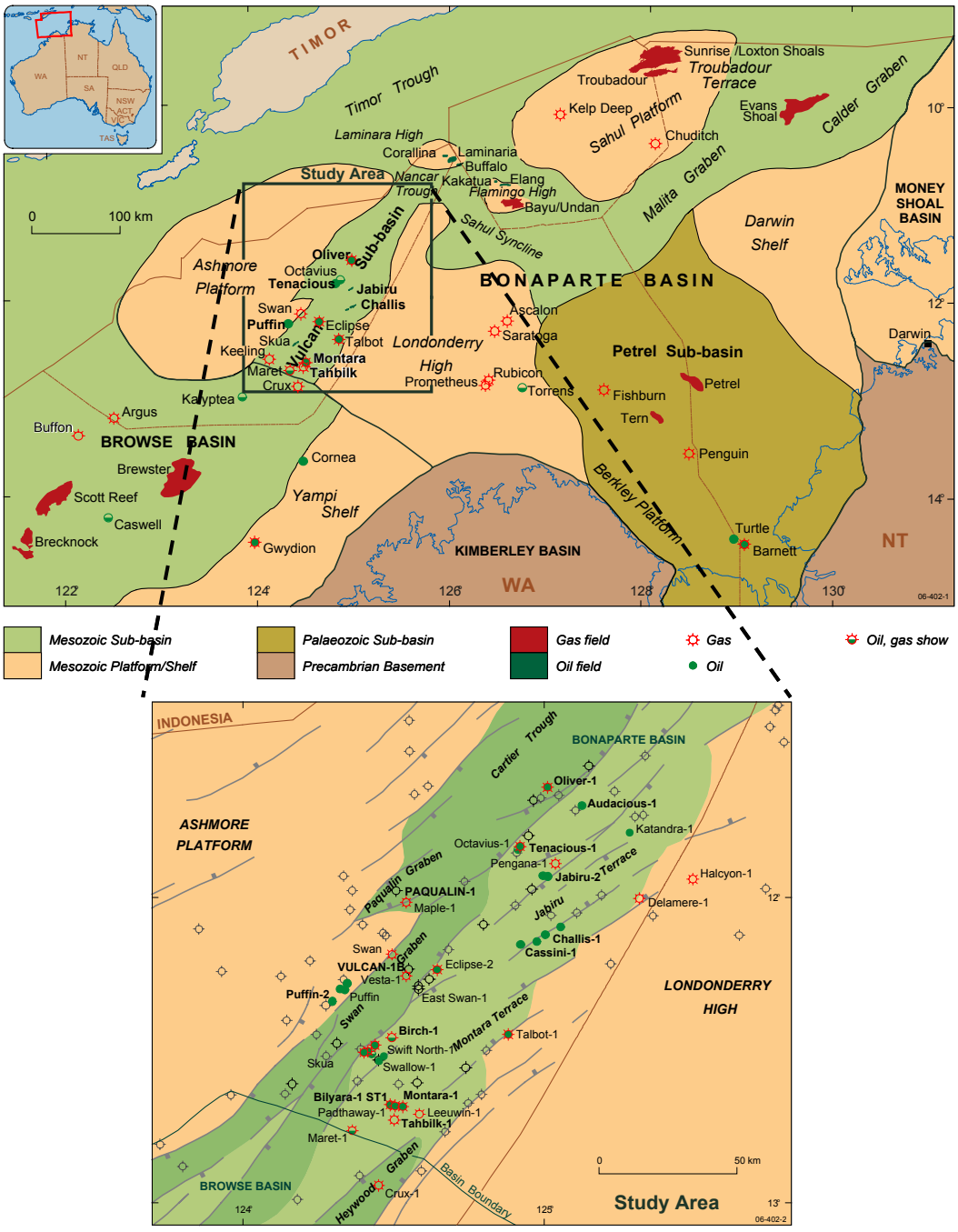

Figure 2.3 A map of the Vulcan Sub-basin (Edwards *et al.*, 2004) showing the location of Paqualin-1 and Vulcan-1B wells, and other petroleum exploration wells. The wells shown in bold are the samples used in Chapter 6.

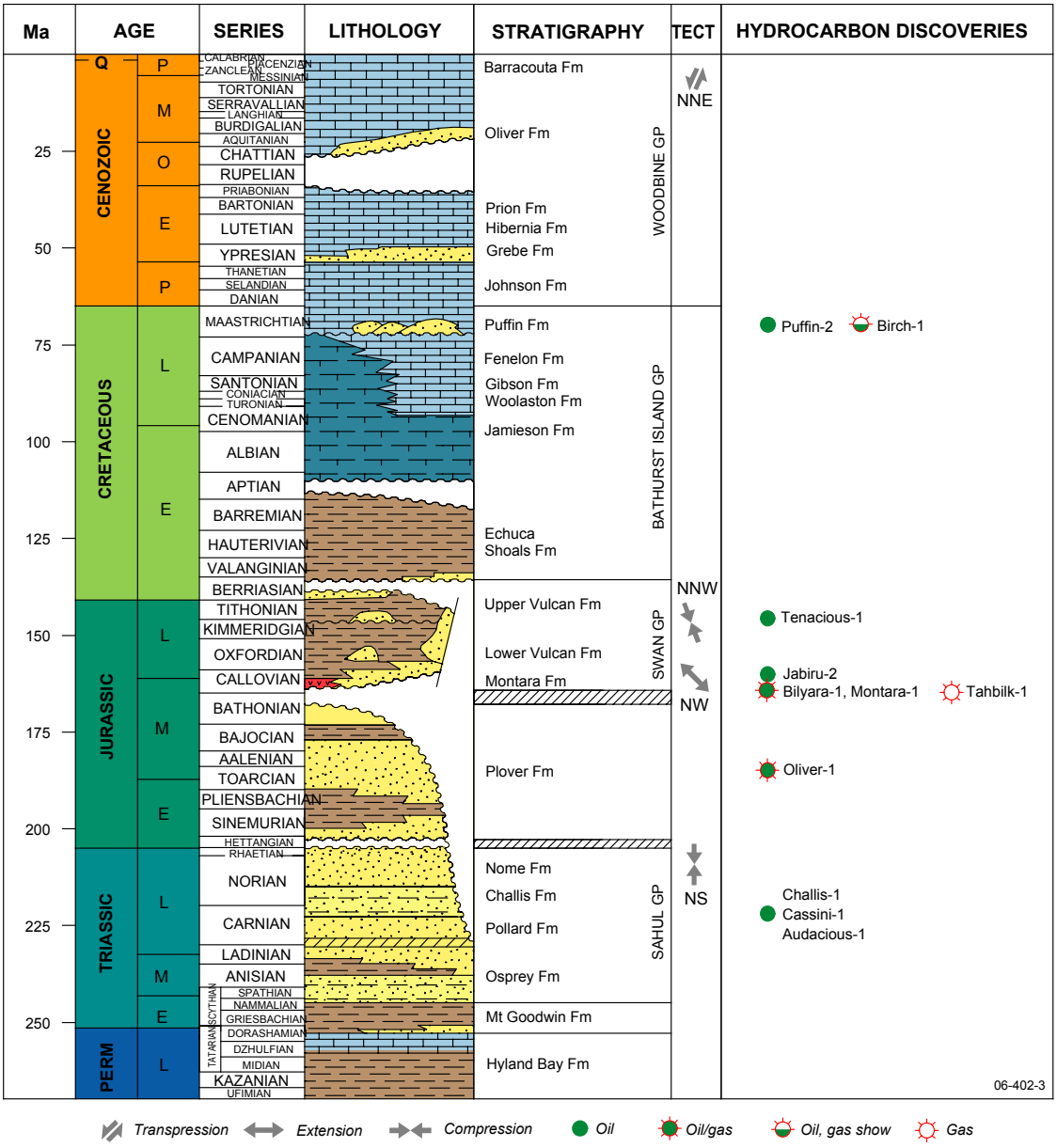

Figure 2.4 A stratigraphic column for the Vulcan Sub-basin (Edwards *et al.*, 2004). The hydrocarbon discoveries are the samples used in Chapter 6.

Table 2.4 Vulcan Sub-basin sediment samples

Well, Depth (m)	Maturity*
Paqualin-1	
3159	Early mature
3354	Mature
3402	Mature
3444	Mature
3504	Mature
3594	Late mature
3654	Late mature
3864	Post mature
Vulcan-1B	
3014	Early mature
3155	Mature
3240	Mature
3292	Mature
3380	Mature
3444	Late mature
3624	Late mature
3679	Post mature

*See Chapter 5

Table 2.5 Vulcan Sub-basin crude oils and condensates

Well name	Sample Type	Reservoir Unit[a]	Reservoir Age
Birch-1	Brown, light oil	Puffin Fm	Late Cretaceous
Cassini-1	Brown, light oil	Challis Fm	Late Triassic
Jabiru-2	Brown, light oil	Montara Fm	Middle Jurassic
Tenacious-1	Brown, light oil	Lower Vulcan Fm	Late Jurassic
Challis-1	Brown, light oil	Challis Fm	Late Triassic
Oliver-1	Yellow-brown, medium-light oil	Plover Fm	Middle Jurassic
Montara-1	Yellow-brown, medium-light oil	Montara Fm	Late Jurassic
Bilyara-1	Yellow-brown, medium-light oil	Montara Fm	Late Jurassic
Tahbilk-1	Yellow-brown condensate	Montara Fm	Late Jurassic
Puffin-2	Brown, light oil	Puffin Fm	Late Cretaceous
Audacious-1	Yellow, light oil	Plover Fm	Middle Jurassic

[a] Edwards *et al.* (2004); Fm, Formation

CHAPTER 3

3 EXPERIMENTAL

3.1 MATERIALS AND REAGENTS

Solvents

n-Pentane (AR grade, APS chemicals) and dichloromethane (AR grade, Chemsupply) were purified *via* distillation using a fractionating column. *n*-Hexane, methanol (ChromAR grade, Mallinckrodt Chemicals) and cyclohexane (Nanograde, Mallinckrodt Chemicals) were used without further purification.

Drying and neutralising agents

Anhydrous magnesium sulphate (AR grade, Unilab) was pre-rinsed with solvent before use as a drying agent. For use as a neutralising agent, sodium bicarbonate (AR grade, Chemsupply) was dissolved in milli-Q water until saturated.

Silica gel

Silica gel 60 (0.063–0.200 mm, MERCK) for column chromatography was activated at 120ºC for 8 hours, and pre-rinsed with solvent prior to use.

Molecular sieves

Type 5A (MERCK) and ZSM-5 (PQ Zeolites) molecular sieves were activated at 250ºC for 8 hours prior to use.

Copper (precipitated)

Precipitated copper powder (BDH chemicals) was activated by rinsing with 3M hydrochloric acid (2 mL), and then sequentially rinsing with milli-Q water (2 mL), methanol (2 mL) and dichloromethane (2 mL) before use.

Hydrofluoric acid

For digestion of molecular sieves, hydrofluoric acid (50% w/v, MERCK) was used without further purification.

Compressed gases

High purity nitrogen (BOC Gases Australia Ltd.) was used for solvent removal, without further purification.

3.2 GEOCHEMICAL TECHNIQUES

3.2.1 Sample preparation

Sediments and crude oils

The sediment samples were surface-extracted with a solution of dichloromethane and methanol (9:1 v/v, respectively) covering the sample (2 x 30 minutes), and dried prior to grinding. The sediment samples were ground to a particle size of 150 μm or less using a ring-mill (Rocklabs). Bulk crude oil samples were sub-sampled appropriately to ensure homogeneity.

3.2.2 Extraction of soluble organic matter from sediments

Soxhlet extraction

In a typical extraction, the ground sediment was accurately weighed into a pre-extracted (9:1 v/v dichloromethane/methanol) cellulose thimble. The top of the thimble was plugged with pre-extracted glass wool. The extraction was performed using a Soxhlet apparatus, with a mixture of dichloromethane and methanol (9:1 v/v, respectively). Fresh solvent was introduced as required, and the extraction was allowed to proceed for at least 72 hours or until the solvent became colourless.

Accelerated solvent extraction

Accelerated solvent extractions (ASE) were performed at Geoscience Australia (Canberra, ACT, Australia) using a method optimised by Calvo *et al.* (2003). In a typical extraction, the ground sediment was accurately weighed into a pre-extracted stainless steel extraction cell containing a glass-fiber filter paper. The cell was loaded into the turret of a Dionex ASE 200 (Dionex, Sunnyvale, CA, USA). Extraction was carried out as follows: (1) the cell was preheated at 100ºC for 2 min; (2) a mixture of dichloromethane and methanol (9:1 v/v, respectively) was pumped into the cell up to a pressure of 6895 kPa (1000 p.s.i.) with 5 min thermal equilibration; (3) 6895 kPa was maintained for 2 min (static time) after which the solvent residue was purged with high-purity (HP) compressed nitrogen (BOC Gases Australia Ltd.), flushing the solvent-extract from the cell into a 60 mL collection vial; and (4) the solvent residue was purged with HP compressed nitrogen. Step 3 was repeated 5 times for each cell with the introduction of fresh solvent after each static phase. A final volume of approximately 30 mL of solvent-extract was obtained in the collection vial. The majority of solvent was removed using a ThermoSavant SC210A SpeedVac Plus concentrator with a ThermoSavant RVT400 Refrigerated Vapour Trap (Thermo Electron, Waltham, MA, USA), and a Büchi 168 Vacuum/Distillation Controller (Büchi, Flawil, Switzerland) with a diaphragm vacuum pump. Remaining solvent was removed carefully under HP nitrogen.

3.2.3 Fractionation of crude oils and sediment extracts using column chromatography and molecular sieves

Small-scale column chromatography

In a typical small-scale fractionation (Bastow *et al.*, 2006), the sample (up to 20 mg) was applied to the top of a small column (5.5 x 0.5 cm i.d.) of activated silica gel (pre-rinsed with *n*-pentane). The aliphatic hydrocarbon (saturated) fraction was eluted with pentane (2 mL); the aromatic fraction with a solution of dichloromethane and pentane (2 mL, 3:7, respectively); and the NSO fraction with a solution of equal parts of dichloromethane and methanol (2 mL).

Large-scale column chromatography

In a typical large-scale fractionation, the sample (up to 100 mg) was applied to the top of a large column (20 x 0.9 cm i.d.) of activated silica gel which was packed as a slurry in *n*-pentane. The aliphatic hydrocarbon (saturate) fraction was eluted with pentane (35 mL); the aromatic fraction with a solution of dichloromethane and pentane (40 mL, 3:7, respectively); and the polar fraction with a solution of equal parts of dichloromethane and methanol (40 mL).

Type 5A molecular sieving

In a typical separation, a saturated fraction was obtained using the small-scale silica-gel chromatographic method (see above) using cyclohexane in place of pentane. Alternatively, for an existing saturate fraction in pentane, the solvent was removed carefully using a heated sand bath (60ºC), and the resulting dry fraction made up in cyclohexane (2 mL). A portion of the resulting saturate fraction in cyclohexane (~ 1750 μL) was added to a 2 mL autosampler vial half-filled with activated 5A molecular sieves. The autosampler vial was capped and placed into a pre-heated aluminium block (85ºC) for at least 8 hours. The resulting cool solution was then filtered through a small column of silica (0.5 x 0.5 cm i.d., pre-rinsed with cyclohexane), and the sieves rinsed thoroughly with cyclohexane (approx. 3 x 1 mL), yielding the branched/cyclic fraction (5A excluded). Excess cyclohexane was removed under a slow stream of nitrogen.

ZSM-5 molecular sieving

In a typical separation, the branched/cyclic (5A excluded) hydrocarbon fraction was transferred (in a minimum amount of pentane) onto a small column (7–8 cm x 0.5 cm i.d.) of activated ZSM-5 molecular sieves (pre-rinsed with pentane), and allowed to stand (1–5 minutes). The sieves were rinsed with pentane (approx. 2 mL) yielding the branched/cyclic fraction (ZSM-5 excluded).

Recovery of included hydrocarbons from molecular sieves

The dry sieves were transferred to a 15 mL Teflon test-tube. Hydrofluoric acid (HF, 20–30 drops) was added along with pentane (2–3 mL) to cover the mixture. The solution was stirred magnetically in an ice bath until the sieves had dissolved (45–60 minutes), and the HF was neutralised with a saturated sodium bicarbonate solution. The remaining pentane was filtered through a small column of anhydrous magnesium sulfate. The aqueous solution was further extracted with pentane (approx. 5 x 1 mL). Excess pentane was removed carefully using a heated sand bath (60ºC).

3.3 ANALYTICAL METHODS AND INSTRUMENTATION

3.3.1 Gas chromatography-mass spectrometry

Acquire (full-scan) mode for compound identification

Gas chromatography-mass spectrometry (GC-MS) was performed using a HP 5973 mass-selective detector (MSD) interfaced to HP 6890 gas chromatograph (GC) fitted with a 60 m x 0.25 mm i.d. fused silica open tubular capillary column coated with a 0.25 μm (5%-phenyl)-methylpolysiloxane stationary phase (HP-5MS, Agilent J&W). For routine analysis the GC oven was programmed from 40 to 310ºC at 3ºC/minute with initial and final hold times of 1 and 30 minutes, respectively. Samples (dissolved in *n*-pentane or *n*-hexane) were injected (split/splitless injector) by a HP 6890 series auto-sampler using pulsed-splitless mode. Ultra-high purity (UHP) helium (further purified using an in-line OMI^{TM} Indicating Purifier, Supelco, Bellefonte, PA) was used as the carrier gas at a flow rate of 1.1 mL/min with the injector operating at constant flow. In full-scan mode, the MS was typically operating at an ionisation energy of 70 eV, a source temperature of 180ºC, an electron multiplier voltage of 1800 V and a mass range of 50 to 550 AMU.

Selected-ion monitoring mode for the analysis of the diastereomers of pristane and phytane

GC-MS analysis for the determination of pristane and phytane diastereomer ratios was carried out under two sets of conditions: (i) an initial set of conditions developed by Hansen *et al.* (2003), and (ii) an improved set of conditions (G. Chidlow, pers. comm.) developed during this study. The chromatographic separation characteristics of each set of conditions are presented in Chapter 5. Both sets of conditions use the same MSD and GC equipment described above.

(i) Under the initial conditions (Hansen *et al.*, 2003), the GC was fitted with a 50 m x 0.15 mm i.d. fused-silica open tubular narrow-bore column coated with a 0.25 μm 5% phenyl/95% dimethylpolysiloxane stationary phase (BP-5, SGE). The GC oven was programmed from 50 to 145ºC at 1ºC/minute, held isothermally for 60 minutes and then programmed from 145 to 290ºC at 5ºC/minute, with initial and final hold times of 1 and 15 minutes, respectively. Samples (dissolved in *n*-hexane) were injected (split/splitless injector) by a HP 6890 series auto-sampler using splitless mode. The same carrier gas described above was used at an initial flow rate of 1 mL/min with the injector operating at constant pressure of 414 kPa (60 psi). The MS conditions were identical to those described above (full-scan mode), with the exception that the MSD was operated in selected ion monitoring (SIM) mode (monitoring *m/z* 169, 183 and 197).

(ii) Under the improved conditions (G. Chidlow, pers. comm.), the GC was fitted with a 60 m x 0.25 mm i.d. WCOT fused silica capillary column coated with a 0.25 μm phenyl arylene polymer stationary phase (DB-5MS, Agilent J&W). The GC oven was programmed from 50 to 145ºC at 1ºC/minute, held isothermally for 60 minutes and then programmed from 145 to 300ºC at 5ºC/minute, with initial and final hold times of 1 and 40 minutes, respectively. The injection conditions, carrier gas type and flow rate were identical to that described in (i) above, with the injector operating at a constant pressure of 117 kPa (16.9 psi). The MS conditions were identical to those described in (i) above.

3.3.2 Gas chromatography-isotope ratio mass spectrometry

Gas chromatography-isotope ratio mass spectrometry (GC-irMS) was performed on a Micromass IsoPrime mass spectrometer interfaced to a HP 6890 GC for determination of compound-specific stable carbon isotopic compositions ($\delta^{13}C$), or an Agilent Technologies 6890N GC for stable hydrogen isotopic compositions (δD). In both cases, the GC was fitted with the same column used for GC-MS analysis (acquire mode). During the analysis of samples, the GC oven, carrier gas and injection conditions were identical to those described above for GC-MS analysis (acquire mode). During the analysis of a mixture of organic reference compounds (decane, undecane, dodecane and methyldecanoate), the GC oven was programmed from 50 to 310ºC at 10ºC/min with initial and final hold times of 1 and 10 minutes, respectively.

$\delta^{13}C$ values were calculated by integration of the *m/z* 44, 45 and 46 ion currents of the CO_2 peaks produced by combustion of the chromatographically separated compounds using copper oxide pellets (4 mm x 0.5 mm, isotope grade, Elemental Microanalysis Ltd.) at 850ºC. The compositions are reported relative to CO_2 reference gas pulses (Coleman Instrument grade, BOC Gases Australia Ltd.) of known $^{13}C/^{12}C$ content into the mass spectrometer. The $^{13}C/^{12}C$ content of the CO_2 reference gas was monitored daily *via* analysis of the mixture of reference compounds (see above). Average values of at least three analyses and standard deviations are reported. Isotopic compositions are given in the delta notation relative to Vienna Peedee belemnite (VPDB).

δD values were calculated by integration of the *m/z* 2 and 3 ion currents of the H_2 peaks produced by pyrolysis of the chromatographically separated compounds using chromium powder (350–400 μm, IsoScience Australia Pty. Ltd.) at 1050ºC. An interfering species, H_3^+ is formed in the ion source of the mass spectrometer as a result of H_2^+ ion and H_2 molecule collisions (Coplen, 1988). The amount of H_3^+ formed depends on the partial pressure of hydrogen, and the species interferes isobarically at *m/z* 3. Thus, contributions from H_3^+ produced in the ion source are corrected by performing *m/z* 3 measurements at two different pressures of the H_2 reference gas to determine the H_3^+ factor. An electrostatic sector is used to separate HD^+ from the leading edge of the large signal produced at *m/z* 4 by the constant flow of helium (carrier gas) into the mass spectrometer. δD values are reported relative to

that of H_2 reference gas pulses produced by allowing hydrogen (UHP, BOC Gases Australia Ltd.) of a known D/H content into the mass spectrometer. The D/H content of the H_2 reference gas was monitored daily *via* analysis of the mixture of reference compounds (see above). Average values of at least four analyses and standard deviations are reported. An internal standard (squalane) with a predetermined δD value of -167‰ was added to samples to monitor accuracy and precision of δD measurements. Isotopic compositions are given in the delta notation relative to Vienna Standard Mean Ocean Water (VSMOW).

3.3.3 Elemental analysis-isotope ratio mass spectrometry

Bulk isotope analyses were performed on a Micromass IsoPrime isotope ratio mass spectrometer interfaced to a EuroVector EuroEA3000 elemental analyser. For bulk $\delta^{13}C$ analysis, the sample was accurately weighed into a small tin capsule which was then folded and compressed thoroughly to remove atmospheric gases. The capsule is dropped by an autosampler into a combustion reactor at 1025ºC. The sample and capsule melt in an atmosphere temporarily enriched with oxygen, where the tin promotes flash combustion. The combustion products, entrained in a constant flow of helium, pass through an oxidation catalyst (chromium oxide). The oxidation products then pass through a reduction reactor at 650ºC containing copper granules, where any oxides of nitrogen (NO, N_2O and N_2O_2) are reduced to N_2 and excess oxygen is removed. The resulting gas species then pass through a magnesium perchlorate filter to remove water. The remaining CO_2, along with N_2 and SO_2 (if present) are separated on a 3 m chromatographic column (PoropakQ) at ambient temperature, before passing through a thermal conductivity detector (TCD), then into the irMS. The isotopic compositions are calculated and reported as above for GC-irMS analysis.

For bulk δD analysis, the sample is accurately weighed into a small silver capsule which is then folded and dropped into a pyrolysis reactor containing glassy carbon chips held at 1260ºC. The sample is pyrolysed to form H_2 and CO, along with N_2 if applicable. The pyrolysis products are separated on a 1 m 5A molecular sieve packed chromatographic column held in an oven at 80ºC (isothermal), before passing through a TCD, then into the irMS. δD values are calculated and reported as above for GC-irMS analysis.

CHAPTER 4

4 STABLE HYDROGEN ISOTOPIC COMPOSITION OF HYDROCARBONS IN TORBANITES DEPOSITED UNDER DIFFERENT CLIMATIC CONDITIONS

4.1 INTRODUCTION

Stable hydrogen isotopic compositions (δD) of organic compounds preserved in sediments are of interest to organic geochemists and palaeoclimatologists because they can reflect the isotopic composition of water that existed in the depositional environment. The transport of water and the energy exchanged as it is converted from one physical state to another are important drivers in weather and climate, thus hydrogen isotopic fractionations are thought to be related to a wide variety of naturally occurring processes associated with the hydrological cycle (e.g. Craig, 1961; Craig *et al.*, 1963; Dansgaard, 1964; Craig and Gordon, 1965) (Sec. 4.1.1). Most photoautotrophs utilize water as a hydrogen source, and the D concentration in the source water is reflected in the D/H composition of the photoautotrophic organism (e.g. Sessions *et al.*, 1999). The magnitude of the isotopic fractionation between water and lipids biosynthesised by the organisms can vary significantly, depending on environmental conditions (physical processes), and biosynthetic pathways (chemical processes). The remains of previously-living organisms ultimately become incorporated in sediments and constitute a source of organic matter for petroleum (see Chapter 1).

Compound-specific D/H analysis has been used only recently in the reconstruction of palaeoenvironments. δD values of lipid biomarkers from peat deposits (Xie *et al.*, 2000) and sediments (Sauer *et al.*, 2001) have been used as a proxy for palaeoenvironmental and palaeoclimatic conditions. Andersen *et al.* (2001) reported δD values of individual *n*-alkanes and isoprenoids as evidence of large and rapid climate variability during the Messinian salinity crisis. Li *et al.* (2001) analysed crude oils from the Western Canada sedimentary basin to assess the usefulness of the technique for petroleum correlation and palaeoenvironmental reconstruction.

The study of palaeoenvironments is important in the understanding of present day changing climates and environments. Understanding past events (e.g. mass extinctions) can give insights into the potential effects of significant climate change on life as it exists today. In terms of petroleum geochemistry, an understanding of the palaeoenvironment where a petroleum source rock was deposited can contribute to the current understanding of petroleum formation and generation, and assist in future petroleum exploration strategies. This chapter comprises the results of a study involving the D/H analysis of individual hydrocarbons from a selection of well-characterised torbanites (commonly referred to as bog-head coals; see Chapter 2) with similar biological inputs and of similar thermal maturity, but from various palaeogeographical locations and deposited under different climatic conditions. The present study was carried out in order to elucidate the potential of compound-specific D/H analysis for palaeoenvironment reconstruction, and to further investigate the preservation potential of indigenous δD signatures in ancient sedimentary organic matter.

4.1.1 Hydrogen isotopic fractionations in the hydrological cycle

Water is ubiquitous on the Earth's surface, and is the main source of hydrogen in the natural environment. In the hydrological cycle, water undergoes numerous physical processes, mainly relating to phase transitions, and the isotopes of hydrogen undergo considerable fractionations during these processes. Isotopic fractionations occur as a result of changes in isotope distribution between the different phases. For example, evaporation-condensation processes involve the changing of the physical state of water between the liquid and gaseous (vapour) phases, and fractionations occur due to differences in the vapour pressures of the different isotopic species of water (Hoefs, 1987). Evaporation is a process whereby water changes from liquid to vapour. It has been shown that water vapour formed due to evaporation is depleted in the heavy isotopes D and ^{18}O (Craig and Gordon, 1965; Hoefs, 1987), and therefore the remaining liquid is enriched in these species. This occurs due to the vapour pressure of the heavier isotopic species of water, e.g. $HD^{18}O$ and $H_2{}^{18}O$, being slightly lower than that of the light isotopic species, e.g. $H_2{}^{16}O$. Condensation is a process whereby water vapour changes to the liquid phase. The heavier isotopic species of water condense preferentially because their saturation vapour pressures are

lower than that of the lighter isotopic species; therefore the heavier isotopes D and ^{18}O concentrate in the liquid phase (Craig and Gordon, 1965 and references therein). A simple model that can be used to describe isotopic behaviour in the hydrological cycle is the Rayleigh distillation process (Sec. 4.1.1.1). All water in the hydrological cycle originates from ocean water which, as a result of the operation of the hydrological cycle, leads to meteoric waters initially in the form of atmospheric precipitation (e.g. rain, snow).

4.1.1.1 Ocean water

The oceans constitute 97.25% of the hydrosphere, covering 70% of the Earth's surface with a total volume of 1.37 x 10^9 km^3 of water (Criss, 1999). Ocean water generally has a uniform isotopic composition of 0±5‰ relative to VSMOW (Craig and Gordon, 1965), with values outside this range being confined to surface waters which have been affected by evaporation, formation of sea ice, or addition of meteoric waters (Criss, 1999). The evaporation of ocean water resulting in the formation of water vapour (in the form of clouds) is the first stage of the hydrological cycle. The Rayleigh process assumes that the majority of ocean water evaporates in tropical regions. The vapour formed as a result of evaporation is isotopically lighter than the ocean water. Subsequently, the water vapour is transported to higher latitudes, and due to the prevailing low temperatures, condensation takes place resulting in precipitation. During rain out there is further isotopic fractionation, which in turn affects the isotopic composition of the resulting meteoric waters (Sec. 4.1.1.2).

4.1.1.2 Meteoric waters

Meteoric waters are waters that are produced through operation of the hydrological cycle. Meteoric waters include rain and snow, and its derivative forms of streamflow, lake water, soil water, glacier ice, and shallow groundwater (Criss, 1999). The δD values of meteoric waters are almost always more negative than ocean water. The isotopic values of meteoric waters vary principally with temperature, but also with other factors including altitude, latitude and proximity to the ocean (Craig, 1961; Dansgaard, 1964; Kehew, 2001). When evaporated water

condenses in a cloud and produces raindrops, isotopic depletion of the cloud takes place through concentration of the heavy stable isotopes in the liquid phase (see above). Studies of the isotopic effects associated with precipitation have been undertaken previously by Craig (1961) and Dansgaard (1964).

In terms of the global hydrological cycle, as clouds move to higher latitudes (i.e. from the equator towards the poles), the rain out of heavy isotopes causes the cloud to become isotopically lighter. Consequently, precipitation in regions of high latitude (e.g. polar, glacial regions) is depleted in the heavy stable isotopes relative to precipitation in areas of low latitude (equatorial, tropical regions). The isotopic values of meteoric waters around the world vary in a highly characteristic manner, and conform closely to an empirical relationship known as the "meteoric water line", or MWL (Figure 3.1; Criss, 1999).

In terms of terrestrial (localised) hydrological cycles (e.g. Figure 4.2), the D/H composition of precipitated water can also vary with elevation (altitude), and distance from the ocean (continentality). With increasing altitude, meteoric precipitation becomes progressively depleted in heavy isotopes (Craig, 1961; Dansgaard, 1964; Kehew, 2001), although the reason for this behaviour is not well understood. With increasing distance from the ocean, meteoric precipitation also becomes progressively depleted in heavy isotopes as a result of raining out (see above and Figure 4.2), although this effect is highly variable (Criss, 1999 and references therein). In localised areas, these effects lead to a large variation in δD values of meteoric waters produced from the terrestrial hydrological cycle.

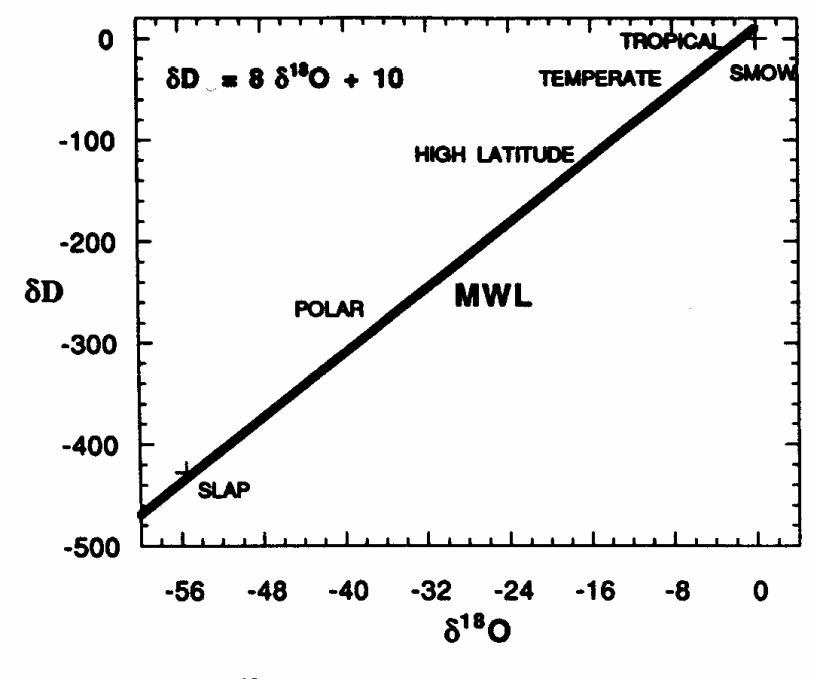

Figure 4.1 Meteoric water line indicating the change in δD and $\delta^{18}O$ during the progression from the tropics to temperate zones to high-latitude regions, and the positions of the SMOW (Standard Mean Ocean Water) and SLAP (Standard Light Antarctic Precipitation) isotopic standards (Criss, 1999)

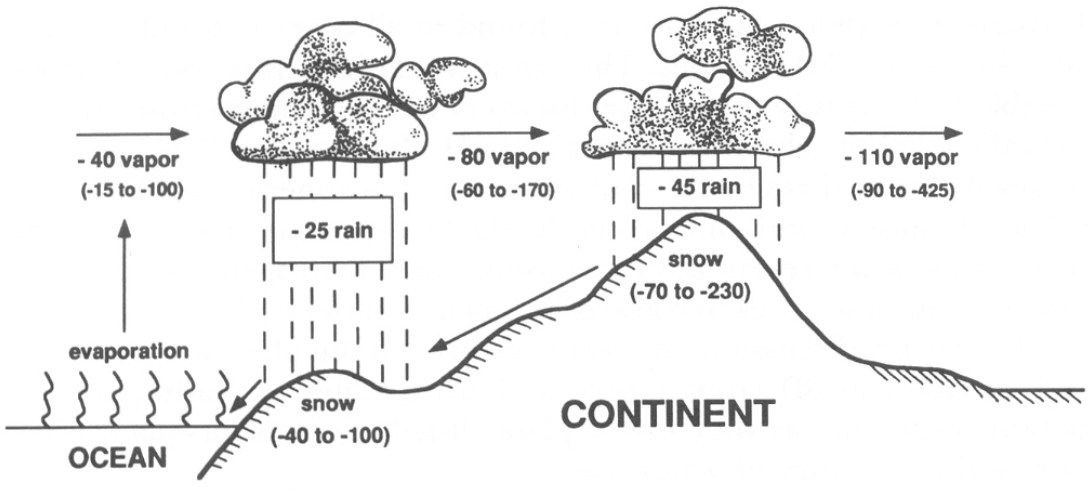

Figure 4.2 Variation of the stable hydrogen isotopic composition of water in the terrestrial hydrological cycle. The quoted values are what can be expected at mid-latitudes; values in parentheses are ranges reported in the literature and depend upon latitude and time of year (Dawson, 1993 and references therein)

4.1.2 Biological fractionation of hydrogen isotopes

Hydrogen isotopic studies of present-day organisms have shown that biosynthetically produced lipids are depleted in D relative to the total biomass (e.g. Estep and Hoering, 1981). Furthermore, different classes of biologically produced lipids within organisms vary significantly in δD (e.g. Sessions, 2001). For example, polyisoprenoid lipids are generally found to be depleted in D relative to acetogenic (*n*-alkyl) lipids (Estep and Hoering, 1980; Sessions *et al.*, 1999). The magnitude of the D/H fractionation between growth water and *n*-alkyl lipids is ca. -150‰, while the fractionation between water and isoprenoid lipids is ca. -235‰ (e.g. Smith and Epstein, 1970; e.g. Estep and Hoering, 1980; Sessions *et al.*, 1999). The reason for this difference is not well understood, although it is probably a result of isotope effects during biosynthesis of the different lipid classes. Assuming that biosynthetic processes have always produced lipids that are depleted in D relative to biomass, and *n*-alkyl and isoprenoid lipids with different δD values, this so-called 'biological signature' may be reflected in their diagenetic products in the sedimentary environment.

As well as variations in lipid δD values within organisms, there are also variations between different organisms, for example between algae (aquatic plants) and terrestrial plants. Algae have lipid δD values which are directly related to the δD of their growth water (Sternberg, 1988; Sessions *et al.*, 1999; Andersen *et al.*, 2001). Terrestrial plants are more exposed to the external environment, and use water produced by the complex terrestrial hydrological cycle (Sec. 4.1.1.2). An additional source of isotopic fractionation associated with terrestrial plants is evapotranspiration, which is the evaporative loss of the light isotopic species of water on leaf surfaces, resulting in an enrichment of D (see Sec. 4.1.1) in the remaining water (Dongmann *et al.*, 1974). Of course, freshwater algae are also associated with a terrestrial environment, and their lipid δD values can therefore be influenced by processes such as surface evaporation of lake water.

4.1.3 Preservation of biological hydrogen isotopic signatures in the sedimentary environment

Biological D/H signatures have been shown to be preserved in ancient, immature sediments. Hoering (1977), Rigby *et al.* (1981) and Smith *et al.* (1982) measured the δD values of bulk organic matter, and individual fractions from a series of crude oils, and coal and shale extracts ranging in geological age from Late Tertiary to Precambrian. Extracts of geologically young (Late Tertiary), immature samples had a wide variation in δD between fractions, with the saturated hydrocarbon fraction (i.e. lipid fraction) being significantly depleted in D relative to the bulk organic matter.

Andersen *et al.* (2001) reported δD values of individual *n*-alkanes and isoprenoids as evidence of large and rapid climate variability during the Messinian salinity crisis. They found that the isotopic data tracked climatically driven hydrologic changes in response to extreme evaporation. The isotopic signatures reported by Anderson *et al.* (2001) were most likely primary signatures (i.e. not diagenetically altered), as the depletion of D in the isoprenoid 5α-cholestane relative to the C_{22} *n*-alkane was consistent with that found in modern biological samples (Estep and Hoering, 1980; Sessions *et al.*, 1999). In this case, it was shown that primary δD signatures were preserved for approximately 6 million years (Ma). More recently, Yang and Huang (2003) demonstrated the preservation potential of lipid δD values in Miocene lacustrine sediments and plant fossils at Clarkia, northern Idaho, USA. They reported the δD values of individual lipids isolated from plant fossils and water-lain sediments. At that time, the Clarkia sediments they studied comprised the oldest reported samples (15–20 Ma) where original compound-specific δD values appear to have been preserved.

4.1.4 Aims of this study

The specific aims of the present study include:

(i) The evaluation of established fractionation procedures (silica gel chromatography combined with molecular sieving) for GC-MS characterisation, to determine their suitability for preparation of samples for CSIA of C-bound hydrogen. A particular focus is the evaluation of a molecular

sieving method using a series of model compounds to ensure there was no isotopic fractionation.

(ii) Applying fractionation procedures to extractable organic matter from a suite of torbanites, with the aim of obtaining baseline resolution of *n*-alkanes and selected branched alkanes.

(iii) Measurement of δD values of *n*-alkanes, pristane and phytane (containing only C-bound hydrogen), with use of both external and internal standards to monitor accuracy and precision of measurements.

(iv) Interpretation of results based on previous work relating to the depositional characteristics (primarily palaeoclimate of deposition) of the torbanites, and their specific source organic matter inputs. Establishing the extent of preservation of lipid δD values.

4.2 RESULTS AND DISCUSSION

4.2.1 Geochemistry

Comprehensive organic geochemical analyses of the torbanites used in this study, including thorough biomarker studies, have been done previously by Boreham *et al.* (1994), Audino *et al.* (2001a; 2001b; 2002) and Grice *et al.* (2001). In summary, the saturated hydrocarbons present in these samples comprise the common regular isoprenoids, pristane (**VI**) and phytane (**III**), *n*-alkanes ranging from *n*-C_{14} to around *n*-C_{30}, a high relative abundance of hopanes maximising at the C_{30} $\alpha\beta$-hopane (**VII**), and other less ubiquitous hydrocarbons (e.g. drimanes). The torbanites lack the traditional *B. braunii* biomarkers, e.g. botryococcane (**VIII**), lycopane (**IX**) and cyclobotryococcanes (e.g. C_{34}: **X**), derived from the recognised lipids of two distinct races, B and L, although it has been suggested the algal biomass may have been subjected to reworking by heterotrophic bacteria (Derenne *et al.*, 1988; Audino *et al.*, 2001a). A feature common to all torbanites is the presence of *n*-alkanes mainly

attributed to the highly aliphatic, non-hydrolysable and insoluble biomacromolecule (algaenan) found in their outer cell walls (Berkaloff *et al.*, 1983; Largeau *et al.*, 1984; Kadouri *et al.*, 1988; Derenne *et al.*, 1989; 1992; Gelin *et al.*, 1994; Berthéas *et al.*, 1997). Furthermore, the A race of *B. braunii* produce long chain *n*-alkadienes and *n*-alkatrienes (Metzger *et al.*, 1986) which may contribute to the long chain *n*-alkanes in torbanites. In addition a new class of biomarkers, the macrocyclic alkanes (e.g. **XI**), have been reported in all torbanites examined from various geographical locations, ranging in age from the Late Carboniferous to the Late Permian (Audino *et al.*, 2001b; Grice *et al.*, 2001). The macrocyclic alkanes are thought to be formed from the algaenan of *B. braunii via* an olefin metathesis reaction (Audino *et al.*, 2002).

The torbanites used in this study have TOC contents of 52 to 59 wt.% (Table 4.1). The sediments do not differ significantly in maturity, and are relatively immature (i.e. before the onset of oil generation) with C_{31}-homohopane 22*S*/(22*S* + 22*R*) ratios (Ensminger *et al.*, 1977, see Appendix 1) ranging between 0.37 and 0.55 (Table 4.1), and T_{max} values from Rock-Eval pyrolysis (Appendix 1) between 446 to 460ºC (Table 4.1). The torbanites contain type I organic-matter based on hydrogen and oxygen indices (HI, OI; Table 4.1; Appendix 1) from Rock-Eval pyrolysis.

Table 4.1 Geochemical parameters of the torbanites

Sample #	TOC (wt.%)[a]	T_{max} (ºC)[a]	HI (mg HC/g TOC)[a]	OI (mg CO_2/g TOC)[a]	$C_{31}\alpha\beta22S$/ ($C_{31}\alpha\beta22S$+$C_{31}\alpha\beta22R$)
3733	59	460	974	51	0.39
3736	59	460	997	10	0.39
3740	52	446	1150	8	0.39[b]
3742	56	446	1145	6	0.37[b]
3755	52	455	1174	4	0.55[b]

[a]Determined by Boreham *et al.* (1994); [b]Determined by Audino *et al.* (2001a); TOC, total organic carbon; HI, hydrogen index; OI, oxygen index

4.2.2 Stable carbon isotopic analysis

Previous studies of organic-matter with large contributions from *B. braunii* have shown the organic carbon to be significantly enriched in ^{13}C relative to that derived

from other aquatic plants (Boreham, 1994; Grice *et al.*, 2001). Measurement of the $\delta^{13}C$ of individual *n*-alkanes (predominantly from *B. Braunii,* see Sec. 2.1) in some Australian torbanites revealed a 'saw-toothed' $\delta^{13}C$ profile in the higher-molecular-weight range (*n*-C_{20} to *n*-C_{30}) (Grice *et al.*, 2001). The odd-carbon-numbered *n*-alkanes from *n*-C_{21} to *n*-C_{29} are depleted in ^{13}C relative to even-carbon-numbered *n*-alkanes from *n*-C_{20} to *n*-C_{30}. This is consistent with a predominant source from the algenan of *B. braunii* (see Sec. 2.1), while the ^{13}C-depletion in odd *n*-alkanes >*n*-C_{21} is attributed to a contribution from terrestrial plant waxes (Boreham, 1994; Grice *et al.*, 2001). The $\delta^{13}C$ values of *n*-alkanes in these samples showed no apparent relationship with palaeolatitude/palaeotemperature.

4.2.3 Stable hydrogen isotopic analysis

The δD values of individual *n*-alkanes from the five torbanites were measured. The δD values of pristane and phytane were measured in two Australian (Temi) torbanites. *n*-Alkanes were separated from the branched and cyclic compounds by treating the saturated hydrocarbon fractions with 5A molecular sieves (see Chapter 3 and Sec. 4.2.3.1). Standard deviations for at least three replicate analyses are mostly within 5‰. In a minimal number of cases, for peaks of relatively low intensity or where minor co-elution was evident, standard deviations are as high as 15‰.

4.2.3.1 Evidence against isotopic fractionation during separation procedures

A brief experiment was performed to ensure that isotopic fractionation did not occur during separations on silica gel or during 5A molecular sieving. A mixture of six individual *n*-alkanes (undecane, *n*-C_{11}; tridecane, *n*-C_{13}; tetradecane, *n*-C_{14}; heptadecane, *n*-C_{17}; nonadecane, *n*-C_{19}; and pentacosane, *n*-C_{25}) was analysed by gas chromatography-isotope ratio mass spectrometry (GC-irMS; Figure 4.3). The mixture was then subjected to the separation procedures, which included silica gel chromatography, adduction into 5A molecular sieves, recovery from 5A molecular sieves *via* digestion with hydrofluoric acid, and finally careful evaporative-removal of solvent (concentration) using a heated sand bath (Chapter 3). The recovered *n*-alkanes were then re-analysed by GC-irMS. Table 4.2 summarises the results of these analyses, and Figure 4.4 is a plot of δD values versus carbon number for each

of the *n*-alkanes. The precision of GC-irMS analysis is 5‰ or better (e.g. Table 4.2) for peaks of suitable intensity, and in the case of GC-irMS, for peaks that are resolved to the baseline. The δD values obtained from each analyses are precise with standard deviations being less than 4‰. The δD values from the two analyses are in relatively good agreement with the spread of data ranging from 4–13‰ (Figure 4.4). Therefore, it was concluded that there is no evidence for significant fractionation of hydrogen isotopes during the separation procedures.

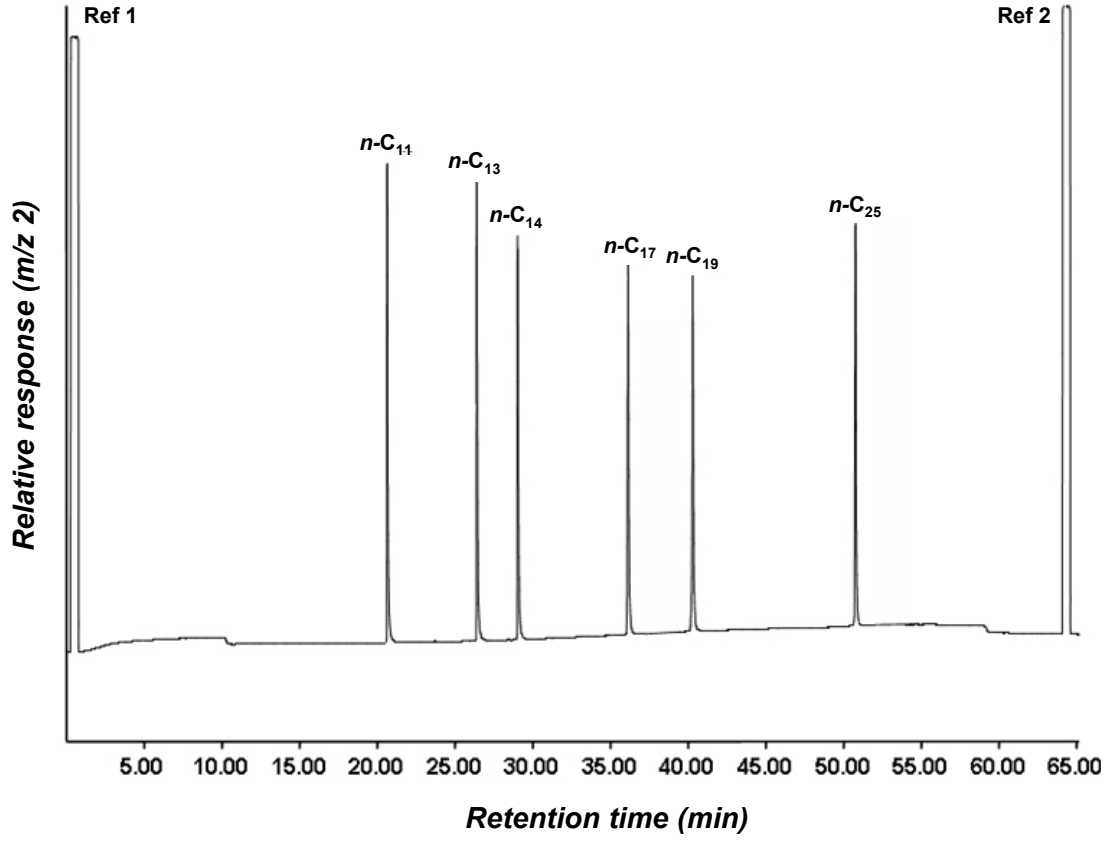

Figure 4.3 GC-irMS chromatogram (*m/z* 2) of a mixture of *n*-alkanes, including undecane (*n*-C_{11}), tridecane (*n*-C_{13}), tetradecane (*n*-C_{14}), heptadecane (*n*-C_{17}), nonadecane (*n*-C_{19}) and pentacosane (*n*-C_{25}). Ref is the hydrogen reference gas peak. Concentration is approx. 200–250 ng μL^{-1} per component (1 μL injection, pulsed-splitless).

Table 4.2 δD values of six *n*-alkanes obtained from compound-specific isotope analysis (CSIA δD) before and after treatment of the mixture with 5A molecular sieves*

Compound	CSIA δD (‰)	CSIA δD after molecular sieving (‰)	ΔδD (‰)
Undecane	-214 (2)[5]	-205 (3)[3]	7
Tridecane	-48 (2)[5]	-54 (1)[3]	-6
Tetradecane	-120 (1)[5]	-124 (0)[3]	-4
Heptadecane	-229 (1)[5]	-222 (1)[3]	7
Nonadecane	-258 (1)[5]	-245 (2)[3]	13
Pentacosane	-121 (1)[5]	-113 (4)[3]	8

*Numbers in parentheses are standard deviations, superscript numbers are number of replicate analyses; ΔδD, difference between the δD value after molecular sieving and the δD value before molecular sieving (relative to VSMOW)

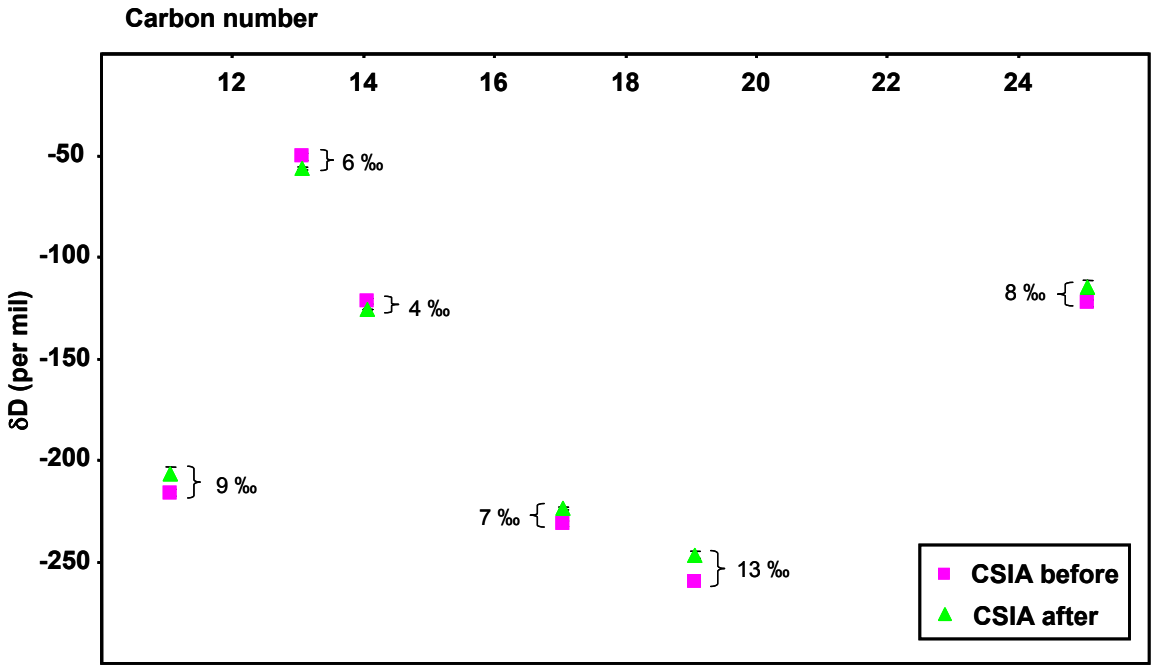

Figure 4.4 Plot of δD values versus carbon number for six *n*-alkanes, comparing δD values measured by compound-specific isotope analysis (CSIA) before and after treatment with 5A molecular sieves. The spread of data is indicated by curly brackets and labels. Error bars indicate the standard deviation of at least 3 replicate analyses. Where error bars are not visible, the error is smaller than the size of the symbol.

4.2.3.2 *n*-Alkanes

δD values of individual *n*-alkanes from the torbanites are plotted in Figure 4.5. The error bars indicate the standard deviation for at least three replicate measurements. Where error bars are not visible, the error is smaller than the size of the symbol. The *n*-alkanes from the Scottish torbanite (Torbane Hill, #3755) have δD values between -140 and -160‰. The *n*-alkanes from two Eastern Australian torbanites (Newnes, #3733 and #3736) have δD values between -150 and -200‰. The *n*-alkanes from two other Eastern Australian torbanites (Temi, #3740 and #3742) have δD values between -180 and -230‰. Hydrogen isotopic measurements of *n*-alkanes from the two Newnes torbanites were limited to between three and five compounds due to their low relative abundance in these samples (e.g. Figure 4.6a).

The δD values of *n*-alkanes in the various torbanites appear to correlate with the palaeolatitude/palaeoclimate at the time the samples were deposited. The *n*-alkanes in the two torbanites deposited under glacial conditions (#3740 and #3742) are significantly depleted in D (ca. 40 to 70‰) relative to the *n*-alkanes in a torbanite deposited under tropical conditions (#3755). The *n*-alkanes in torbanites deposited under cool to temperate conditions (#3733 and #3736) have δD values that generally fall in between those of the *n*-alkanes from tropical and glacial samples. The difference in δD values of the *n*-alkanes from samples deposited under different climate regimes is consistent with the variation in the δD of precipitation with latitude, which contributes to meteoric waters that are used by photosynthetic organisms. The isotopic effects associated with precipitation have previously been studied by Craig (1961) and Dansgaard (1964) (see Sec. 4.1.1.2). Areas of the plot shown in Figure 4.5 have been assigned a depositional climate based on the δD composition of the *n*-alkanes in the various sediments.

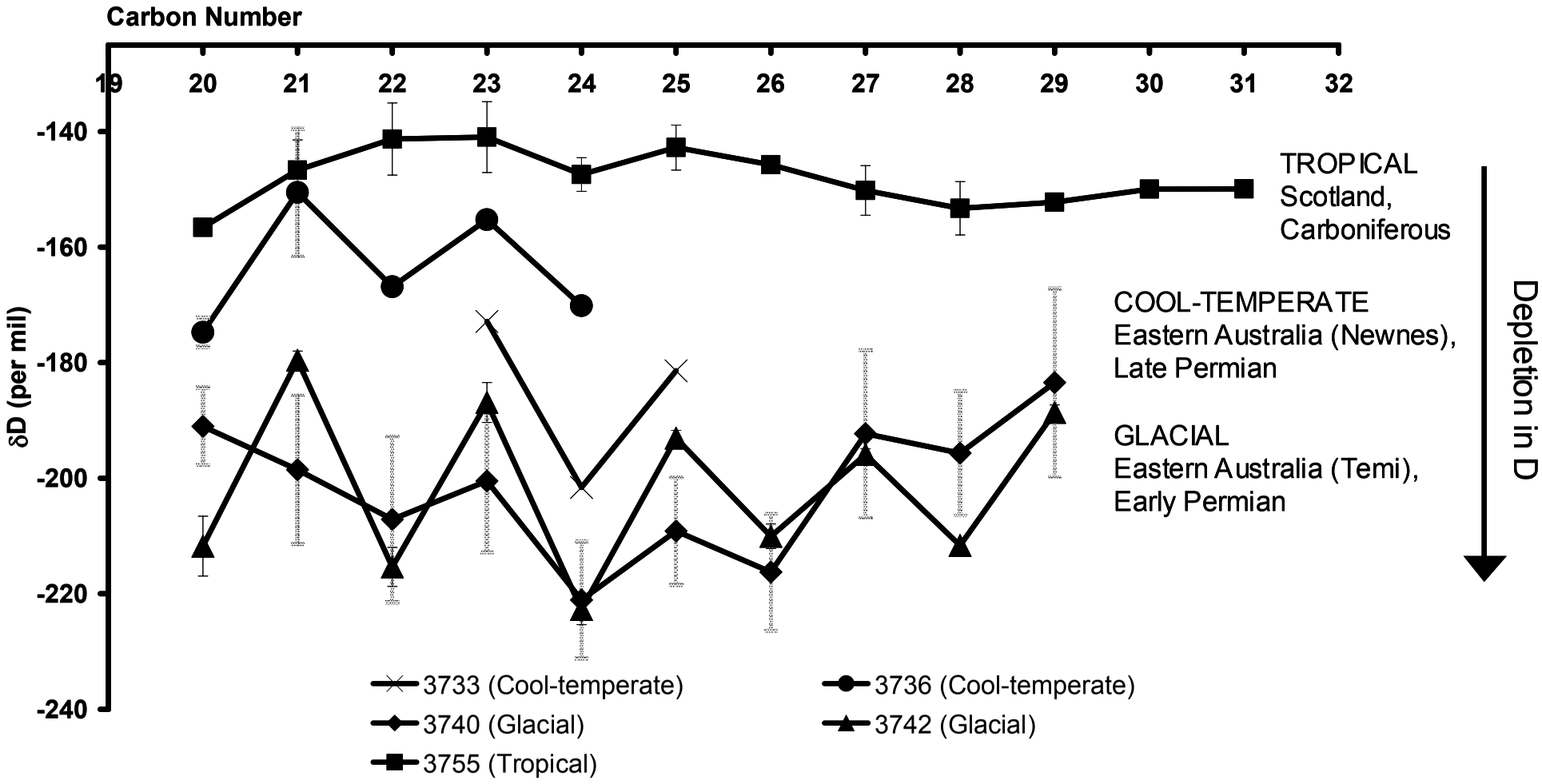

Figure 4.5 Stable hydrogen isotopic compositions of individual *n*-alkanes in five torbanites (Late Carboniferous-Late Permian) from various palaeogeographical locations deposited under various climatic conditions

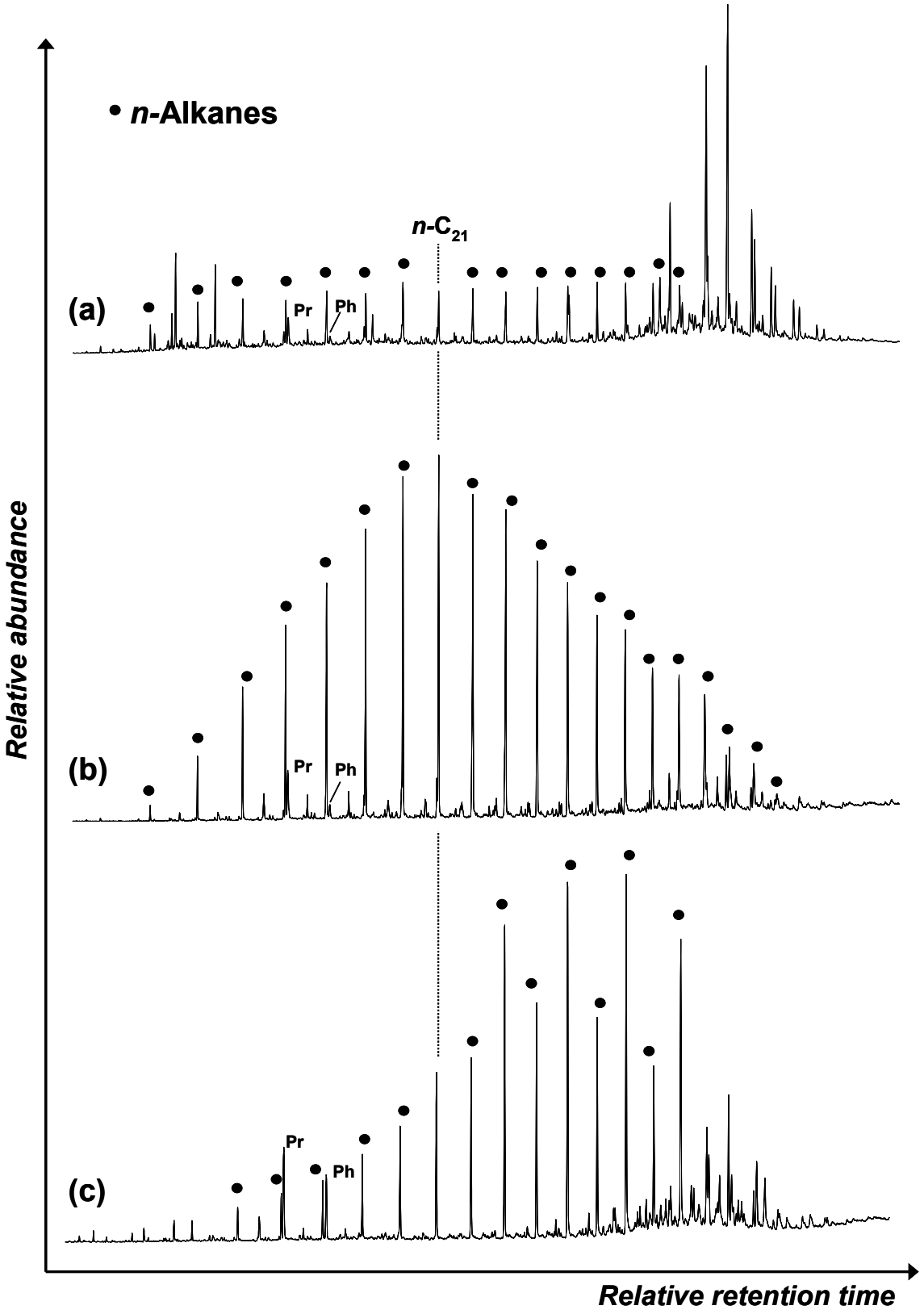

Figure 4.6 GC-MS total-ion chromatograms of the saturate fractions of torbanites (a) #3733, (b) #3755 and (c) #3740

Since the torbanites were deposited in freshwater, inland lakes, it is important to also consider the effect of surface evaporation of the lake-water when interpreting the differences seen in the δD values of the *n*-alkanes in torbanites deposited at different palaeolatitudes. The δD values of lake-waters predictably indicate their meteoric parentage (Criss, 1999), however surface evaporation is an important process which affects all surface waters, especially shallow lakes. Of course, such effects are most pronounced in windy, hot, or arid areas (Criss, 1999). Surface waters become enriched in heavy isotopes as a result of evaporation (see Sec. 4.1.1 and 4.1.2). Although the δD composition of the water in the lake will be affected by evaporation to some extent, meteoric precipitation is most likely the dominant process in determining the isotopic composition of the lake-water in this case, considering the significant difference in the depositional latitude of each torbanite. However, the fact that the δD values of *n*-alkanes from the two torbanites deposited under cool-temperate conditions are spread over a wider range than the δD values of *n*-alkanes from the two torbanites deposited under glacial conditions, is possibly a result of an evaporation effect, where the δD values of *n*-alkanes from torbanite #3736 (-150 to -175‰) are indicative of a more evaporative environment in comparison to the δD values of *n*-alkanes from torbanite #3733 (-170 to -200‰).

It cannot be completely excluded that δD composition of the organic matter has been altered to some extent by diagenetic transformations in the subsurface, even considering that these sediments are relatively immature (pre-oil generation based on homohopane distributions, Sec. 2.1). It has been shown that exchange between C-bound hydrogen and water-derived hydrogen occurs during artificial maturation of organic matter (see Chapter 5), and consequently, the δD values of *n*-alkanes in the samples investigated might have been affected by hydrogen exchange reactions between organic-matter and formation waters during natural maturation. However, there is evidence that hydrogen exchange processes have not altered the indigenous isotopic signatures to a large extent (see below).

A feature of the results obtained from this study is a saw-toothed profile of δD values for the *n*-alkanes (C_{20}–C_{29}) in the Australian torbanites (#3733, #3736, #3740 and #3742, Figure 4.5). This type of profile has previously been identified with the $\delta^{13}C$ values of C_{20} to C_{30} *n*-alkanes in these samples (Sec. 4.2.2), with approximately a 3–5‰ shift in $\delta^{13}C$ between odd and even *n*-alkanes. However, the odd-even trend

in $\delta^{13}C$ values is opposite to that seen here with the δD values, where the odd-carbon-numbered *n*-alkanes are enriched in D relative to the even-carbon-numbered *n*-alkanes. The saw-toothed profile of $\delta^{13}C$ values was explained by a dual-source system with contributions from both *B. braunii* and terrestrial plants (Boreham, 1994; Grice *et al.*, 2001). The same explanation can be applied to the profile of δD values, where the even-carbon-numbered *n*-alkanes are ascribed a predominant *B. braunii* source (i.e. algaenan), while the D-enriched odd-carbon-numbered *n*-alkanes are probably related to a dominant terrestrial plant source of these compounds. The terrestrial plant contribution causes a relative enrichment in D due to isotopic effects during evaporation of water from leaf surfaces and by transpiration in the plants (Dongmann *et al.*, 1974; Estep and Hoering, 1980 and references therein; Farquhar and Gan, 2003; Gan *et al.*, 2003). Further evidence of a terrestrial plant contribution to higher-molecular-weight odd-carbon-numbered *n*-alkanes is seen in the GC-MS total-ion-chromatograms for the saturate fractions of the Australian sediment extracts. There is an odd-over-even preference for *n*-alkanes in the higher-molecular-weight region (e.g. *n*-C_{22} to *n*-C_{29}, Figure 4.6c). It is likely that hydrogen exchange processes brought about by maturation have had only a minor effect (if any) on the δD values of odd *n*-alkanes in the Australian torbanites, since predominant odd *n*-alkanes >*n*-C_{21} can be considered as preserved genuine biological lipids. Hydrogen exchange reactions between organic-matter and formation waters might essentially affect hydrocarbons generated during maturation, and would probably result in a more homogeneous profile of δD values.

4.2.3.3 Acyclic isoprenoids

δD values of the acyclic isoprenoids pristane and phytane from the branched and cyclic fractions of two Australian torbanites (Temi, Early Permian) were measured. Pristane and phytane from torbanite #3740 have δD values of -283±2‰ and -259±2‰ respectively (Figure 4.7). Pristane and phytane from torbanite #3742 have δD values of -277±2‰ and -268±3‰, respectively (Figure 4.7). Pristane and phytane in the Temi torbanites (#3740 and #3742) are strongly depleted in D (ca. 60 to 80‰) compared to the *n*-alkanes in the same sample (Figure 4.7). The offset between the δD values of isoprenoids and *n*-alkanes is similar to the offset seen in

modern biological samples (e.g. Estep and Hoering, 1980; Sessions *et al.*, 1999), indicating that an apparent biological signal has been preserved for at least 260–280 million years. Significant diagenetic effects would more likely result in a more homogeneous distribution of δD values (see Chapter 5). Unfortunately the δD values of pristane and phytane in the other torbanites could not be measured due to the low relative abundance of these compounds (e.g. Figure 4.6a, b). However, because the torbanites appear to have had a similar thermal history (based on various maturity parameters, Sec. 2.1), and similar source inputs (Berkaloff *et al.*, 1983; Largeau *et al.*, 1984; Kadouri *et al.*, 1988; Derenne *et al.*, 1989; Derenne *et al.*, 1992; Gelin *et al.*, 1994; Berthéas *et al.*, 1997), it is assumed that indigenous signals are also preserved in these samples. This lends credence to the interpretation given for the observed differences between δD values of *n*-alkanes present in the torbanites (Sec. 4.2.3.2).

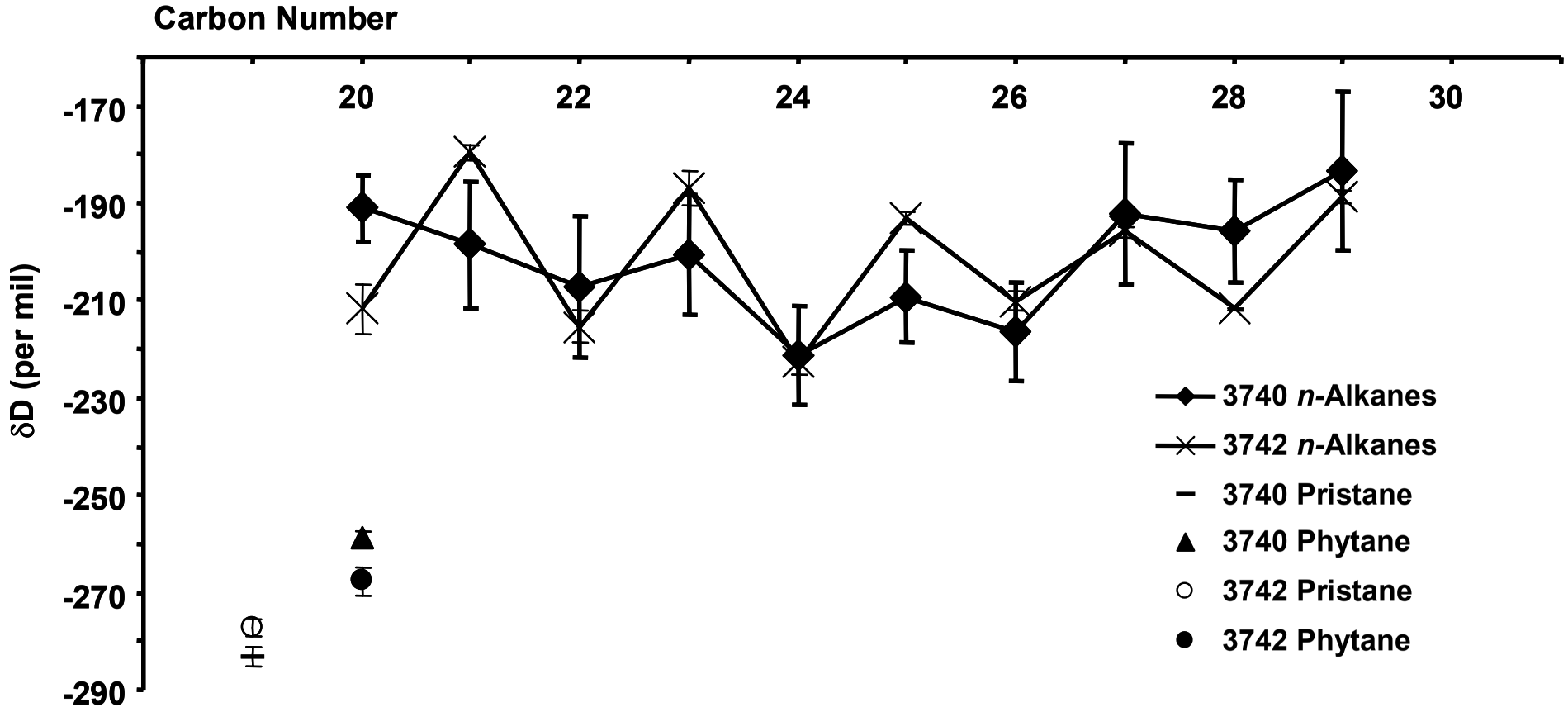

Figure 4.7 Stable hydrogen isotopic composition of individual *n*-alkanes, pristane and phytane in two Australian torbanites (Temi, Early Permian).

There is a significant difference between the δD values of pristane and phytane of the Temi torbanites, phytane being enriched in D ca. 24‰ relative to pristane. Li *et al.* (2001) reported that phytane is mostly enriched in D relative to pristane, and suggested this to be consistent with different origins of pristane and phytane or different isotope effects for their derivation from a common precursor (e.g. phytol, **XII**). Further evidence for different origins of pristane and phytane in the Temi torbanites is apparent from their $\delta^{13}C$ values, where phytane is ca. 2–3‰ depleted in ^{13}C relative to pristane (Grice *et al.*, 2001). While pristane was speculated to be attributed mainly to the phytyl side chain of chlorophyll *a* of cyanobacteria, the ^{13}C-depleted phytane was attributed to a contribution from a ^{13}C-depleted source such as glyceroldiether lipids (e.g. **XIII**) of methylotrophic bacteria (Grice *et al.*, 2001).

4.3 SIGNIFICANCE

The *n*-alkanes from the low-maturity torbanites appear to preserve δD values that correlate with the palaeolatitude at the time of deposition. This, along with the observed offset between the δD values of isoprenoids and *n*-alkanes in the torbanites (similar to that observed in modern biological samples) is significant. The fact that primary hydrogen isotopic signatures appear to have been preserved for at least 260–280 million years indicates that the preservation potential of lipid δD values is much greater than previously thought. This clearly demonstrates how the measurement of δD values of individual compounds in sedimentary organic matter can be very useful for palaeoenvironmental reconstructions, providing diagenetic and catagenetic processes (e.g. maturation, see Chapter 5) have not played a significant role.

4.4 SUMMARY AND CONCLUSIONS

1. The separation procedures performed on the torbanite solvent extracts, including silica gel chromatography and 5A molecular sieving, do not fractionate hydrogen isotopes to any significant extent.

2. δD values of *n*-alkanes in the torbanites analysed in this study appear to reflect the depositional palaeolatitude/palaeoclimate of the sediments, attributed to the δD composition of meteoric waters in the environment where the sediments were deposited.

3. A saw-toothed profile of δD values identified for the *n*-alkanes in the Australian torbanites is attributed to a dual-source system with predominant *B. braunii* input, and terrestrial plant input to the odd-carbon-numbered *n*-alkanes.

4. The significant depletion of deuterium in two acyclic isoprenoids (pristane and phytane) relative to the *n*-alkanes in two Australian torbanites is similar to the offset seen in modern biological samples, indicating that an apparent biological signal has been preserved for at least 260–280 million years. There is no evidence that diagenetic and catagenetic have affected the δD values of the compounds analysed.

5. A smaller but distinct difference observed between the δD values of pristane and phytane of the Temi torbanites is suggested to be caused by either different sources for the two isoprenoids, or isotope effects associated with their derivation from a common precursor (e.g. phytol). There is additional evidence for different origins of pristane and phytane from the $\delta^{13}C$ values of these compounds.

CHAPTER 5

5 EFFECT OF MATURATION ON THE INDIGENOUS δD SIGNATURES OF INDIVIDUAL HYDROCARBONS

5.1 INTRODUCTION

For the δD values of sedimentary hydrocarbons to reflect that of their biosynthetic precursors (e.g. see Chapter 3), the δD signature of the precursor must be preserved throughout sedimentation, burial and the diagenetic and catagenetic processes that can lead to the formation of petroleum. It is believed that diagenetic and catagenetic effects over extended periods of geological time (millions of years) promote significant hydrogen exchange (Sec. 5.1.1) between organic hydrogen and hydrogen species in the surrounding environment (Rigby *et al.*, 1981; Alexander *et al.*, 1984; Schimmelmann *et al.*, 1999; Leif and Simoneit, 2000; Schimmelmann *et al.*, 2001; Sessions *et al.*, 2004). Thermal maturation in particular has been found to play a significant role in the alteration of indigenous δD signatures (Rigby *et al.*, 1981).

Until recently, the ability to study the distribution of stable hydrogen isotopes in sedimentary organic matter has been limited to δD measurements of bulk organic matter or whole fractions from crude oils or sediment extracts. Aside from the fact that bulk isotopic measurements of sedimentary organic matter do not reflect the diverse origins of individual compounds, another major disadvantage in terms of bulk D/H analysis of complex mixtures of hydrocarbons in petroleum is the variation in reactivity of different organic compounds towards hydrogen exchange. For example, N, O, S-bound hydrogen will exchange relatively quickly (see Sec. 5.1.1), and the presence of these moieties in complex mixtures can result in rapid alteration of any indigenous D/H signature. On the other hand, aliphatic C-bound hydrogen is less prone to exchange (see Sec. 5.1.1). The isotopic analysis of individual aliphatic compounds containing only C-bound hydrogen (e.g. *n*-alkanes) is attractive, because aliphatic C-bound hydrogen is probably the most isotopically conservative (Sessions *et al.*, 2004). The recent advent of compound specific hydrogen isotope analysis has

allowed the measurement of the D/H composition of individual compounds in complex mixtures (Burgoyne and Hayes, 1998; Hilkert *et al.*, 1999).

An understanding of the effect of diagenetic and catagenetic processes (e.g. maturation) on indigenous hydrogen isotopic compositions is important in the interpretation of δD values of sedimentary hydrocarbons. Previous work based on bulk D/H analysis provides evidence of homogenistation and gradual D-enrichment of sedimentary organic matter with increasing thermal maturity (Hoering, 1977; Rigby *et al.*, 1981; Smith *et al.*, 1982), resulting in a progressive loss of the indigenous (source) D/H signature. The ability to gauge the extent of secondary alteration is therefore essential before source interpretation of δD values is carried out. The work presented here extends the previous work based on bulk measurements, *via* the analysis of individual hydrocarbons in petroleum, to assess the effect of subsurface processes on the δD values of compounds with different reactivity's towards hydrogen exchange (Sec. 5.1.1). In addition, the ability to use δD values of individual hydrocarbons to determine the level of maturity of sedimentary organic matter is assessed. To achieve this, the δD values of *n*-alkanes, pristane and phytane from sedimentary sequences covering a range of maturity (%R_o 0.53–1.6) from the northern Perth Basin (on-shore, Western Australia), and Paqualin-1 and Vulcan-1B from the Vulcan Sub-basin (offshore, northern Australia) were investigated.

5.1.1 Hydrogen exchange in organic compounds

Hydrocarbons contain hydrogen atoms which occupy a range of molecular positions. For example, hydrogen can be bound either to primary, secondary or tertiary carbon atoms in alkyl moieties (aliphatic C-bound hydrogen); to carbon atoms in aromatic rings (aromatic C-bound hydrogen); and to nitrogen, oxygen or sulfur atoms in polar compounds (N, O, S-bound hydrogen). The hydrogen bond strength varies significantly for different types of bonds, which is an important factor in determining exchangeability and therefore the rate of hydrogen exchange at various positions in organic molecules. For example, aliphatic C-bound hydrogen is linked *via* a strong covalent bond, and is often referred to as 'non-exchangeable hydrogen' (e.g. Epstein *et al.*, 1976; Schimmelmann, 1991). In contrast, aromatic C-bound hydrogen is more prone to exchange due to the enhanced stability of aromatic

systems and their ability to stabilize charged transition states; while N, O, S-bound hydrogen is linked *via* weaker hydrogen bonds making exchange even more favourable.

The rate of exchange of bound hydrogen in alkyl moieties is dependent on the extent of substitution of carbon atoms within the alkyl chain. For example, molecules containing tertiary (3º) carbon atoms, i.e. those substituted with three other carbon atoms or alkyl groups (tri-substituted), will exchange their hydrogen more easily and more rapidly compared to molecules containing only secondary (2º, di-substituted) or primary (1º, mono-substituted) carbon atoms. This is chemically explicit in terms of heterolytic and homolytic cleavage processes, and occurs due to the ability of additional alkyl groups to stabilize charged transition states (e.g. carbocations or radicals) *via* inductive and resonance effects.

Although aliphatic C-bound hydrogen is often considered as non-exchangeable hydrogen, it may well be exchangeable under certain physical and chemical conditions during petroleum generation in the subsurface over geological time. These conditions have been reproduced in the laboratory in order to simulate sedimentary processes. The following sections comprise a review of previous studies on the exchange of C-bound hydrogen in model compounds (Sec. 5.1.1.1), and in sedimentary organic matter during artificial (Sec. 5.1.1.2) and natural (Sec. 5.1.1.3) maturation.

5.1.1.1 Exchange of carbon-bound hydrogen in model compounds

There have been few publications relating to alkyl hydrogen exchange of model aliphatic compounds under laboratory conditions. Those that exist generally investigate the exchange of C-bound hydrogen in the presence and absence of catalysts (e.g. clay), and discuss exchange rates, and potential mechanisms of hydrogen exchange.

Alexander *et al.* (1984) heated *meso*-pristane (**VI**) with a deuterated clay (montmorillonite) at 160ºC for 670 h, and found that 63% of the total pristane (based on GC-MS analysis) was deuterated. They also found that 40% of methyl hydrogen, and 40% of methylene (2º carbon) and methine (3º carbon) hydrogen were replaced by deuterium based on ^{1}H NMR spectroscopic analysis. Estimated exchange half-

times were 2.1 and 1.5 years for primary and secondary hydrogen respectively, which are much slower than those determined for naphthalene (**XIV**) under similar conditions (Alexander *et al.*, 1982; Alexander *et al.*, 1983; Sessions *et al.*, 2004). Sessions *et al.* (2004) used compound-specific isotope-ratio mass spectrometry to analyse *n*-icosane (*n*-C_{20}) which was incubated with heavy water (D_2O) on montmorillonite or silica at various temperatures. They reported exchange half-times ranging from ~10,000 years at 60ºC to ~100,000 years at 7ºC. These exchange half-times were faster than that reported for *n*-hexane (*n*-C_6) without a catalyst by Koepp (1978). The higher exchange rate was attributed to the presence of a mineral catalyst. Larcher *et al.* (1986) studied alkyl hydrogen exchange in a series of acyclic isoprenoid acids when heated at 160ºC in the presence of deuterated montmorillonite. Analysis of the methyl ester derivatives by GC-MS indicated that all of the isoprenoid acids had undergone hydrogen exchange with water adsorbed on the clay surface, and exchange was most rapid at the carbon adjacent to the carboxyl group (Larcher *et al.*, 1986).

The laboratory conditions under which alkyl hydrogen exchange has been observed in model compounds suggests that similar processes could occur in sedimentary organic matter and during petroleum generation.

5.1.1.2 Exchange of carbon-bound hydrogen during artificial maturation of sedimentary organic matter

A number of techniques have been used to artificially mature sedimentary organic matter. The techniques involve heating a sample in either an open or closed system. Open systems allow the generated reaction products to continuously exit the system, while closed systems trap evolved products meaning they continue to be exposed to, and involved in, the maturation process. Artificial maturation experiments can also be performed under anhydrous or hydrous conditions. Hydrous experiments appear to more accurately reproduce the natural maturation process, and thus have been used more widely. The following examples from the literature use the closed-system hydrous pyrolysis technique. As for the model compound research described above, these reports discuss the exchange of C-bound hydrogen in the

presence and absence of catalysts, and discuss exchange rates, and potential mechanisms of hydrogen exchange (Sec. 5.2.5).

Koepp (1978) used isotope-ratio mass spectrometry to measure the bulk D/H composition of petroleum fractions and individual model compounds incubated with D_2O without a catalyst. They reported exchange half-times for saturated and aromatic fractions which were 3 to 4 orders of magnitude faster than model saturated and aromatic compounds (Koepp, 1978; Sessions *et al.*, 2004), which was most likely due to the presence of more reactive compounds in the complex fractions (Sessions *et al.*, 2004). Hoering (1984) subjected pre-extracted Messel Shale to pyrolysis at 330ºC for 3 days in the presence of excess water (H_2O and D_2O). When the reaction was performed in heavy water, extensive deuteration of a variety of hydrocarbon types (including *n*-alkanes) was evident. More recently, Leif and Simoneit (2000) conducted an additional series of pyrolysis experiments on Messel Shale using model aliphatic compounds (*n*-alkanes and *n*-alkenes) as 'probe' molecules. They pyrolysed the compounds in both D_2O and shale/D_2O (and shale/H_2O), and found that in the absence of shale only the *n*-alkenes incorporated deuterium from D_2O. The presence of shale resulted in more deuterium incorporation into the *n*-alkenes, a minor amount of deuterium incorporation into *n*-alkanes, and hydrogenation of *n*-alkenes to *n*-alkanes. Schimmelmann *et al.* (1999) artificially matured immature source rock chips in isotopically distinct waters using hydrous pyrolysis, and found that at temperatures ≥300ºC significant hydrogen exchange occurred between the water and the organic hydrogen. Furthermore, depending on temperature, time and kerogen type, it was shown that 45–79% of C-bound hydrogen in matured kerogen was derived from water, while bitumen and expelled oil had a slightly lower percentage (36–78%) of water-derived hydrogen (Schimmelmann *et al.*, 1999).

From the work described above, it is clear that water-derived hydrogen can exchange with aliphatic C-bound hydrogen during artificial maturation of sedimentary organic matter.

5.1.1.3 Exchange of carbon-bound hydrogen during natural maturation of sedimentary organic matter

Hydrogen exchange processes occurring during diagenesis and maturation will result in D/H changes of the organic matter as a result of isotope exchange with H and D in the surrounding environment. Published work on maturation in natural systems provides evidence of gradual D-enrichment of organic matter with increasing thermal maturity (Hoering, 1977; Rigby *et al.*, 1981; Smith *et al.*, 1982; Li *et al.*, 2001).

In the past, bulk hydrogen isotopic analysis has been used to study the effect of maturation on the D/H composition of sedimentary organic matter. Hoering (1977) measured the bulk δD values of three fractions (saturated, aromatic and NSO) from a suite of crude oils and sediment extracts from various locations in the United States, Iran, Finland and Australia. The samples ranged in geological age from Pilocene to Precambrian. He reported that older samples, having experienced a longer and higher thermal history, contained organic matter with a relatively homogeneous and D-enriched D/H composition. The extract of an immature shale had a wider variation in the δD values of its individual fractions, with the saturated hydrocarbon fraction being depleted in D relative to the aromatic and NSO fractions. Furthermore, the NSO fraction was significantly enriched in D relative to the aromatic fraction (Hoering, 1977), reflecting the presence of hydrogen which is more reactive towards hydrogen exchange. Rigby *et al.* (1981) reported bulk δD values of crude oils and coals (and their saturated fractions) from the Gippsland and Bass Basins of Australia. Vitrinite reflectance measurements of the coals ranged from 0.45 to 1.04% with increasing depth. In all cases, the saturated fractions were depleted in deuterium relative to their parent coals, with the magnitude of depletion being larger in less mature samples. The deuterium content of the saturated fractions was shown to increase with increasing maturity. Further work on Australian coals was carried out by Smith *et al.* (1982), who also found that original hydrogen isotopic differences between the parent coals and their fractions were progressively lost with increasing maturity. More recently, Lis *et al.* (2005) investigated the D/H composition of type-II kerogens from the New Albany Shale (Illinois Basin, USA) and the Exshaw Formation (Alberta Basin, Canada). In both suites, the δD values of non-

exchangeable (i.e. aliphatic) hydrogen increase with maturation from immature through to post mature.

A significant finding of the pioneering work in the 1970's and 1980's (summarised above) was the apparent preservation of biosynthetic D/H signatures in aliphatic fractions of immature sedimentary organic matter, evidenced by the relative depletion of deuterium in these fractions, relative to the aromatic and NSO fractions which would have exchanged hydrogen to a large extent. Indeed, aliphatic C-bound hydrogen is the most isotopically conservative hydrogen moiety (Sessions *et al.*, 2004; see Sec. 5.1.1).

The recent advent of compound specific hydrogen isotope analysis (see Chapter 1) has allowed investigations of the effect of maturation on the D/H composition of individual compounds. Li *et al.* (2001) measured the isotopic composition of carbon-bound hydrogen in individual *n*-alkanes and acylic isoprenoids from a series of crude oils from the Western Canada Sedimentary Basin. They observed a significant enrichment in deuterium in *n*-alkanes (ca. 40‰) from highly mature crude oils relative to those from marginally mature crude oils.

5.1.1.4 Summary

The laboratory conditions under which alkyl hydrogen exchange has been observed in model compounds suggests that these processes could occur in the sedimentary environment at subsurface temperatures and in the presence of mineral catalysts (i.e. in the source rock matrix). In addition, it is clear that water-derived hydrogen can exchange with aliphatic C-bound hydrogen during artificial maturation of sedimentary organic matter. There is a gradual D-enrichment of sedimentary organic matter in geological samples with increasing thermal maturity, a trend evident in various geological locations worldwide (Hoering, 1977; Rigby *et al.*, 1981; Smith *et al.*, 1982; Li *et al.*, 2001). The D-enrichment is likely to be due to hydrogen exchange between the organic matter and D-rich formation waters in the subsurface. Figure 5.1 shows the range of chemical moieties of a hypothetical kerogen structure, highlighting the different types of bound hydrogen discussed above.

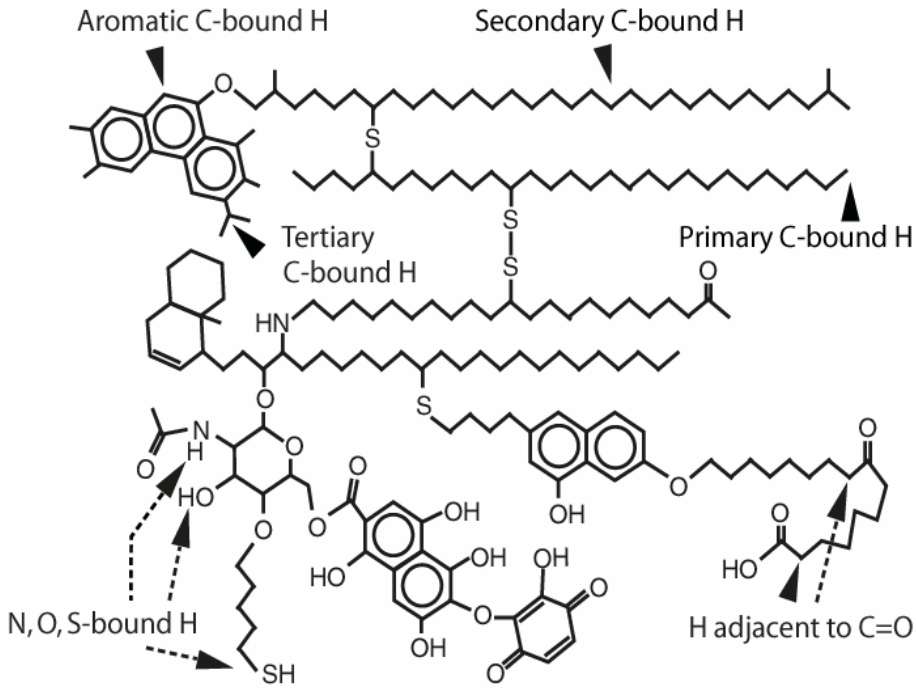

Figure 5.1 Hypothetical kerogen structure containing various types of organic moieties and bound hydrogen including primary, secondary or tertiary aliphatic C-bound hydrogen; aromatic C-bound hydrogen; and N, O, S-bound hydrogen (after Schimmelmann *et al.*, 2006)

5.1.2 Aims of this study

The specific aims of the present study include:

(i) Fractionation of the extractable organic matter from immature to post mature Perth Basin (WA) and Vulcan Sub-basin (Timor Sea) sediments to obtain baseline resolution of *n*-alkanes, pristane and phytane, followed by measurement of their δD values.

(ii) Interpretation of the results based on the source, and thermal maturity of the hydrocarbons, with comparison to molecular and stable carbon isotopic results.

(iii) Investigating whether a mechanism of hydrogen exchange can be proposed, extending previous studies, and based on the analysis in this study of stereochemical conversions of the diastereomers of pristane (**VI**) and phytane (**III**).

5.2 RESULTS AND DISCUSSION

5.2.1 Geochemistry

5.2.1.1 Perth Basin sediments

Detailed organic geochemical analyses of sediments from the Kockatea shale have been carried out previously by Thomas and Barber (2004), including Rock-Eval pyrolysis, thermal maturity estimates and biomarker distributions. The Hovea member of the Kockatea shale is characterised by fossiliferous, Type II organic-matter-rich shales (typically 1–5 wt.% TOC) (Thomas and Barber, 2004). Due to the difficulties associated with the direct measurement of vitrinite reflectance of sediments from the Kockatea Shale (Kantsler and Cook, 1979), Thomas and Barber (2004) used basin-wide burial history modelling to calculate equivalent vitrinite reflectance values (R_e) for the samples. The Perth Basin sediments range in maturity from immature through to late mature (%R_e = 0.53 to 1.13, Table 5.1). The saturated hydrocarbons comprise *n*-alkanes ranging from *n*-C_8 to around *n*-C_{35}, the common regular isoprenoids pristane and phytane, and a high relative abundance of hopanes and steranes in the samples of lower relative maturity.

Table 5.1 Geochemical parameters of the Perth Basin sediment extracts.

Well, Depth m (ft)	R_e (%)[a]	*Ts*/(*Ts*+*Tm*)
BMR 10 973–976 (3193–3203)	0.53	0.30
BMR 10 989–991 (3245–3250)	0.53	0.25
Dongara 4 1674 (5491)	0.60	0.32
Dongara 4 1675 (5495.5)	0.60	0.34
Dongara 4 1678 (5505)	0.60	0.38
Yardarino 2 2289 (7509)	0.78	0.76
Yardarino 2 2290 (7512.5)	0.78	0.79
Arrowsmith 1 2494 (8781)	1.13	0.89
Arrowsmith 1 2678 (8787)	1.13	0.80

R_e, equivalent vitrinite reflectance
Ts/(*Ts*+*Tm*), maturity parameter based on the 18α(H)- and 17α(H)-trisnorhopanes (Appendix 1)
[a] Determined by Thomas and Barber (2004)

5.2.1.2 Vulcan Sub-basin sediments

Previous organic geochemical studies on Paqualin-1 sediments include work carried out by Smith and Sutherland (1991), van Aarssen *et al.* (1998a; 1998b) and Edwards *et al.* (2004). Smith and Sutherland (1991) published Rock-Eval and vitrinite reflectance data, and performed pyrolysis gas chromatography on samples from the sequence for organic matter characterisation. van Aarssen *et al.* (1998a; 1998b) analysed aromatic biomarkers from thirteen sediment extracts from Paqualin-1 for stratigraphic correlation and palaeoclimate reconstruction purposes. Edwards *et al.* (2004) also published Rock-Eval and vitrinite reflectance data, and calculated some biomarker parameters for oil-source correlations (see Chapter 6). All of the data in the above studies indicate that the Paqualin-1 sequence contains Type II/III kerogen. Source rocks within the Paqualin-1 well in the Paqualin Graben (Figure 2.3) have been identified within the lower Vuclan Formation (Caroll and

Syme, 1994; Edwards *et al.*, 2004). In that part of the sequence, TOC averages around 2 wt.% and hydrogen indices range from 40 to 300 mg HC/g TOC (e.g. Table 5.2). The Paqualin-1 sediments used in this study range in maturity from early mature through to post mature based on vitrinite reflectance measurements (%R_o = 0.62 to 1.6), while T_{max} ranges from 441 to 455ºC (Table 5.2). The saturated hydrocarbons in Paqualin-1 comprise *n*-alkanes ranging from *n*-C_{11} to around *n*-C_{34} and the common, regular isoprenoids pristane and phytane. Hopanes and steranes are present in relatively high abundance in the immature samples, and in lower abundance in the more mature samples.

Geochemical analyses of Vulcan-1B sediments in the Vulcan-1B well, located in the Swan Graben (Chapter 2), have been carried out previously by Edwards *et al.* (2004), and included Rock-Eval pyrolysis and molecular characterisation. The lower Vulcan Formation in the Swan Graben comprises organic matter-rich mudstones (average TOC = 2 wt.%) that, like Paqualin-1, contain predominately type II/III kerogen. Hydrogen indices range from 150 to 400 mg HC/g TOC (Edwards *et al.*, 2004; e.g. Table 5.3). The Vulcan-1B sediments used in this study range in maturity from early mature to post mature (%R_o = 0.69 to 1.3; Table 5.3). The R_o data available throughout the Vulcan-1B well have been measured by three separate laboratories, and there are large discrepancies in the measurements. This is possibly due to (Kennard *et al.*, 1999; D. Edwards, pers. comm.): (i) the occurrence of perhydrous vitrinite which suppresses R_o, a likely explanation because it is well documented in the North West Shelf using the fluorescence alteration of multiple macerals (FAMM) technique (e.g. Wilkins *et al.*, 1992); (ii) overheating of the samples during collection and drying of drill chips on the drilling rig resulting in overestimated R_o, which is unlikely because there is no evidence of unusually high maturities from the geochemical analysis; and/or (iii) operator biases. The saturated hydrocarbons in Vulcan-1B comprise *n*-alkanes ranging from C_{11} to C_{33} and the regular isoprenoids pristane and phytane. Hopanes and steranes are present in high relative abundance in the less mature samples, and in low relative abundance in more mature samples. Source-specific saturated biomarker ratios (e.g. $C_{29}/(C_{29}+C_{27})$ steranes, $C_{19}/(C_{19}+C_{23})$ tricyclic terpanes; Appendix 1) indicate that the Vulcan-1B sediments contain a mixture of marine-algal organic matter and varying amounts of terrestrial plant debris which has been reworked by bacteria (Edwards *et al.*, 2004).

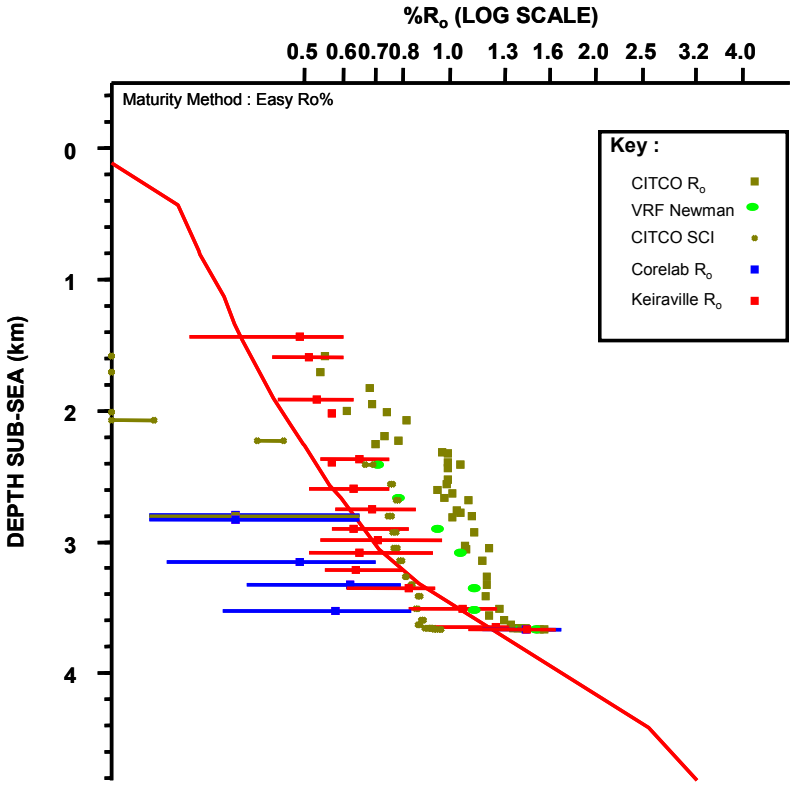

Figure 5.2 Observed vs. computed maturity plot (geohistory model) for Vulcan-1B (Kennard *et al.*, 1999).

Table 5.2 Geochemical parameters of the Paqualin-1 sediment extracts used in this study.

Well, Depth (m)	R_o (%)[a]	TOC (wt.%)[a]	T_{max} (°C)[a]	HI (mg HC/g TOC)[a]	OI (mg CO_2/g TOC)[a]
Paqualin-1					
3159	0.62	1.91	441	286	109
3354	0.80	1.69	441	167	n/a
3402	0.82	n.d.	n.d.	n.d.	n.d.
3444	0.82	1.91	445	150	170
3504	0.83	1.97	441	122	93
3594	1.0	2.43	450	101	43
3654	1.2	1.85	448	98	90
3864	1.6	1.78	455	75	125

R_o, vitrinite reflectance; TOC, total organic carbon; HI, hydrogen index; OI, oxygen index; n.d., not determined; [a] Geoscience Australia Petroleum Wells Database, http://dbforms.ga.gov.au/www/npm.well.search

Table 5.3 Geochemical parameters of the Vulcan-1B sediment extracts used in this study.

Well, Depth (m)	R_o (%)[a]	TOC (wt.%)	T_{max} (°C)	HI (mg HC/g TOC)	OI (mg CO_2/g TOC)
3014	0.69	1.39	439	243	133
3155	0.77	1.54	439	197	122
3240	0.83	1.74	439	183	82
3292	0.86	1.59	440	156	102
3380	0.93	1.80	441	122	151
3444	1.0	1.92	431	215	170
3624	1.17	2.40	430	174	172
3679	1.3	n.d	n.d.	n.d.	n.d.

R_o, vitrinite reflectance; TOC, total organic carbon; HI, hydrogen index; OI, oxygen index; n.d., not determined; [a] Data extrapolated from a thermal geohistory model (Kennard *et al.*, 1999)

5.2.2 Stable carbon isotopic analysis

The stable carbon isotopic compositions ($\delta^{13}C$) of individual *n*-alkanes (ca. *n*-C_{12} to *n*-C_{33}), pristane and phytane were measured in extracts of the Perth Basin and Vulcan Sub-basin sediments. Standard deviations for at least three replicate analyses were ≤0.4‰.

5.2.2.1 Perth Basin sediments

The $\delta^{13}C$ values of *n*-alkanes, pristane and phytane from the nine sediments range from -30 to -35‰ (isotopically depleted in ^{13}C), characteristic of Early Triassic sedimentary organic matter (Morante *et al.*, 1994; Summons *et al.*, 1995). Isotopically light organic carbon during the Permian/Triassic geological period has been reported previously in sedimentary organic matter from the Bonaparte, Bowen, Canning, Canarvon and Perth Basins of Australia (Summons *et al.*, 1995; Foster *et al.*, 1997), and globally in marine limestones and terrestrial organic carbon (Morante *et al.*, 1994; Wignall and Twitchett, 1996; Krull *et al.*, 2000). This worldwide

negative $\delta^{13}C$ excursion is believed to be related to a global event at the Permian/Triassic boundary which caused the most severe mass-extinction of the past 500 million years (Erwin, 1994; Benton, 2003).

Pristane and phytane derive from the phytyl side-chain of chlorophyll *a* and/or *b* (**XV**) of algae and cyanobacteria, therefore the $\delta^{13}C$ values of these isoprenoids are robust indicators of the isotopic composition of photosynthetic organisms (Schouten *et al.*, 1998). Conversely, *n*-C_{14} to *n*-C_{18} alkyl carbon chains can be derived from both autotrophic and heterotrophic organisms, and therefore the $\delta^{13}C$ values of these straight-chain compounds may represent the average isotopic composition of multiple sources. If derived from primary producers *via* the classical mevalonate pathway, pristane and phytane should be enriched in ^{13}C relative to *n*-C_{14} to *n*-C_{18} by ca. 1.5‰ (Hayes, 1993). The difference ($\Delta\delta^{13}C$) between the average $\delta^{13}C$ value of *n*-C_{17} and *n*-C_{18} alkanes and the average $\delta^{13}C$ value of pristane and phytane calculated for the Perth Basin samples used in this study falls between 0 and -3.3‰, i.e. pristane and phytane are generally enriched in ^{13}C relative to *n*-C_{17} and *n*-C_{18} alkanes which is consistent with a relatively high input from primary producers (algae) to the organic matter. Grice *et al.* (2005a) compared the $\delta^{13}C$ values of pristane and phytane to those of the *n*-C_{17} and *n*-C_{18} alkanes extracted from a drill core (Hovea-3) covering the Permian-Triassic boundary from the onshore Perth Basin. A plot of the $\Delta\delta^{13}C$ values versus depth (Figure 5.3) showed that the *n*-C_{17} and *n*-C_{18} were depleted in ^{13}C relative to pristane and phytane by up to 1.6‰ (on average) in the Triassic, providing evidence of high primary productivity (Grice *et al.*, 2005a). This was supported by other independent evidence such as an abundance of metalloporphyrins from chlorophylls and bacteriochlorophylls (Grice *et al.*, 2005a). The fact that pristane and phytane in the Perth Basin samples used for this study are in some cases markedly more enriched in ^{13}C than *n*-C_{17} and *n*-C_{18} (by up to 3.3‰) may be attributed to their derivation *via* the pyruvate/glyceraldehyde-3-phosphate biosynthetic pathway. When derived *via* this pathway, pristane and phytane have been found to be enriched in ^{13}C by 2–5‰ relative to *n*-C_{17} and *n*-C_{18} (Schouten *et al.*, 1998).

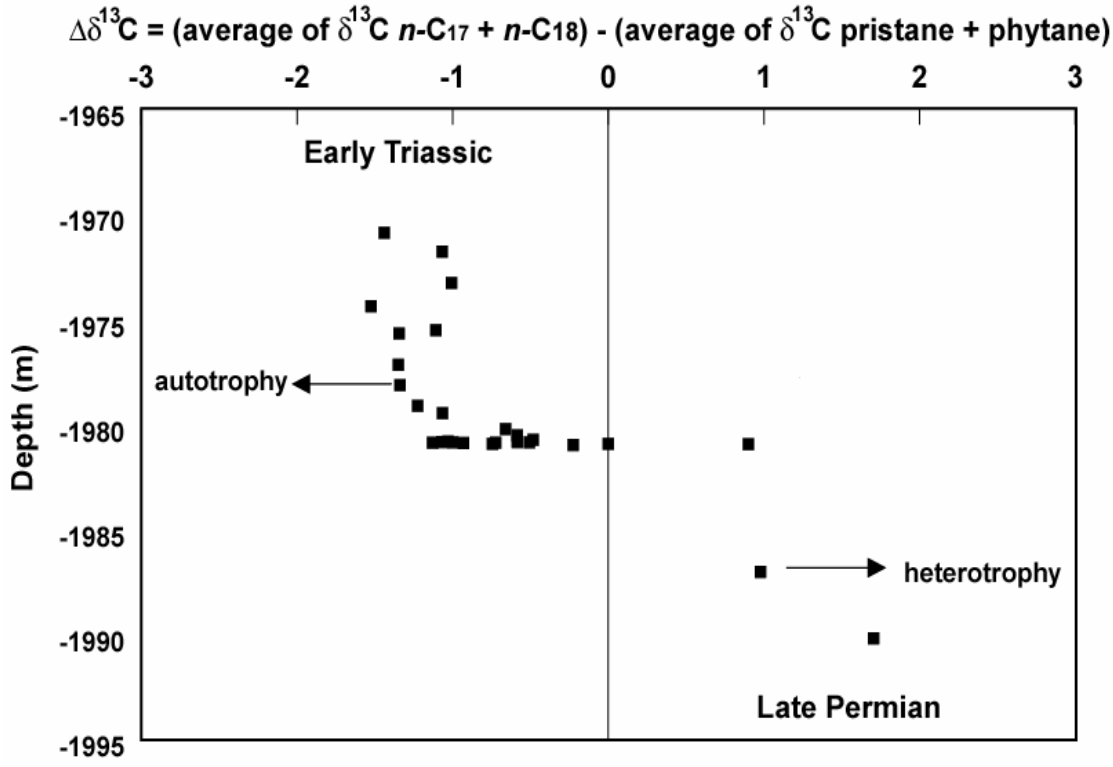

Figure 5.3 Plot of $\Delta\delta^{13}C$ (see above for definition) versus depth for a series of Late Permian-Early Triassic Perth Basin sediment extracts (Hovea-3) (Grice *et al.*, 2005a).

Although the Perth Basin sample set used in this study represents a substantial maturity range of $\%R_e$ 0.53 to 1.13, there is no indication that increasing thermal maturity has significantly affected the $\delta^{13}C$ values of *n*-alkanes, pristane or phytane. Note that other studies have shown that thermal maturation can significantly affect the $^{13}C/^{12}C$ composition of petroleum hydrocarbons (Clayton, 1991; Clayton and Bjorøy, 1994).

5.2.2.2 Vulcan Sub-basin sediments

The $\delta^{13}C$ values of *n*-alkanes (Figure 5.4a), pristane and phytane from the eight Paqualin-1 sediments (obtained from K. Grice) generally fall within a narrow range, from -26 to -31‰, while the $\delta^{13}C$ values of the same compounds from the eight Vulcan-1B sediments (*n*-alkanes: Figure 5.4b) range from -26 to -30‰. Two Paqualin-1 samples however, from depths 3444 m and 3864 m, have $\delta^{13}C$ values of normal and branched alkanes that are significantly heavier, ranging from -24 to -26‰ (average -24.9‰) and -23 to -25‰ (average -24.2‰), respectively. Paqualin-1

3864m is significantly more thermally mature (post-mature, $\%R_o$ = 1.6), and this may have affected the $\delta^{13}C$ values. The effect of maturity leads to an enrichment in ^{13}C, thought to be a result of the release of ^{13}C-depleted components (Clayton, 1991). In the case of Paqualin-1 (3444 and 3864 m), the significant differences in $\delta^{13}C$ values cannot be explained by maturity differences alone. In addition, Paqualin-1 3444 m is mature ($\%R_o$ = 0.82), but contains normal and branched alkanes that are more enriched in ^{13}C than those from two late mature samples (3594 and 3654 m, $\%R_o$ = 1.0 and 1.2, respectively). At present it is unclear why this is the case, although this is one of a number of inconsistencies that occur in this part of the Paqualin-1 sequence, including a reversal of molecular maturity parameters (van Aarssen *et al.*, 2004). The $\delta^{13}C$ values of *n*-alkanes extracted from sediments from the Vulcan-1B well also appear to have been affected by maturation. Notably, the deepest sample analysed (3624 m) has *n*-alkanes which are significantly enriched in ^{13}C (by ca. 1.2–1.6‰) relative to those from the other samples. The data also have interesting implications in terms of the $\delta^{13}C$ compositions of Vulcan Sub-basin crude oil and condensate components (see Chapter 6).

The $\Delta\delta^{13}C$ values (see Sec. 5.2.2.1) calculated for the Paqualin-1 samples used in this study fall between 0.2 and 2.6‰, and for the Vulcan-1B samples (where $\delta^{13}C$ measurements were made) between 1.5 and 2.7‰, i.e. *n*-C_{17} and *n*-C_{18} alkanes are generally enriched in ^{13}C relative to pristane and phytane. These results are in contrast to those reported by Grice *et al.* (2005a) for the Triassic samples from the Perth Basin (Sec. 5.2.2.1), and thus are probably attributed to a lower relative algal input to the organic matter in the Vulcan Sub-basin samples. Indeed, the Permian core samples analysed by Grice *et al.* (2005a) (see Sec. 5.2.2.1 and Figure 5.3) also showed an enrichment of ^{13}C in *n*-C_{17} and *n*-C_{18} hydrocarbons relative to pristane and phytane, attributed to heterotrophic processing of primary photosynthate or a high input of ^{13}C-enriched bacterial biomass (Summons *et al.*, 1994; Grice *et al.*, 2005a).

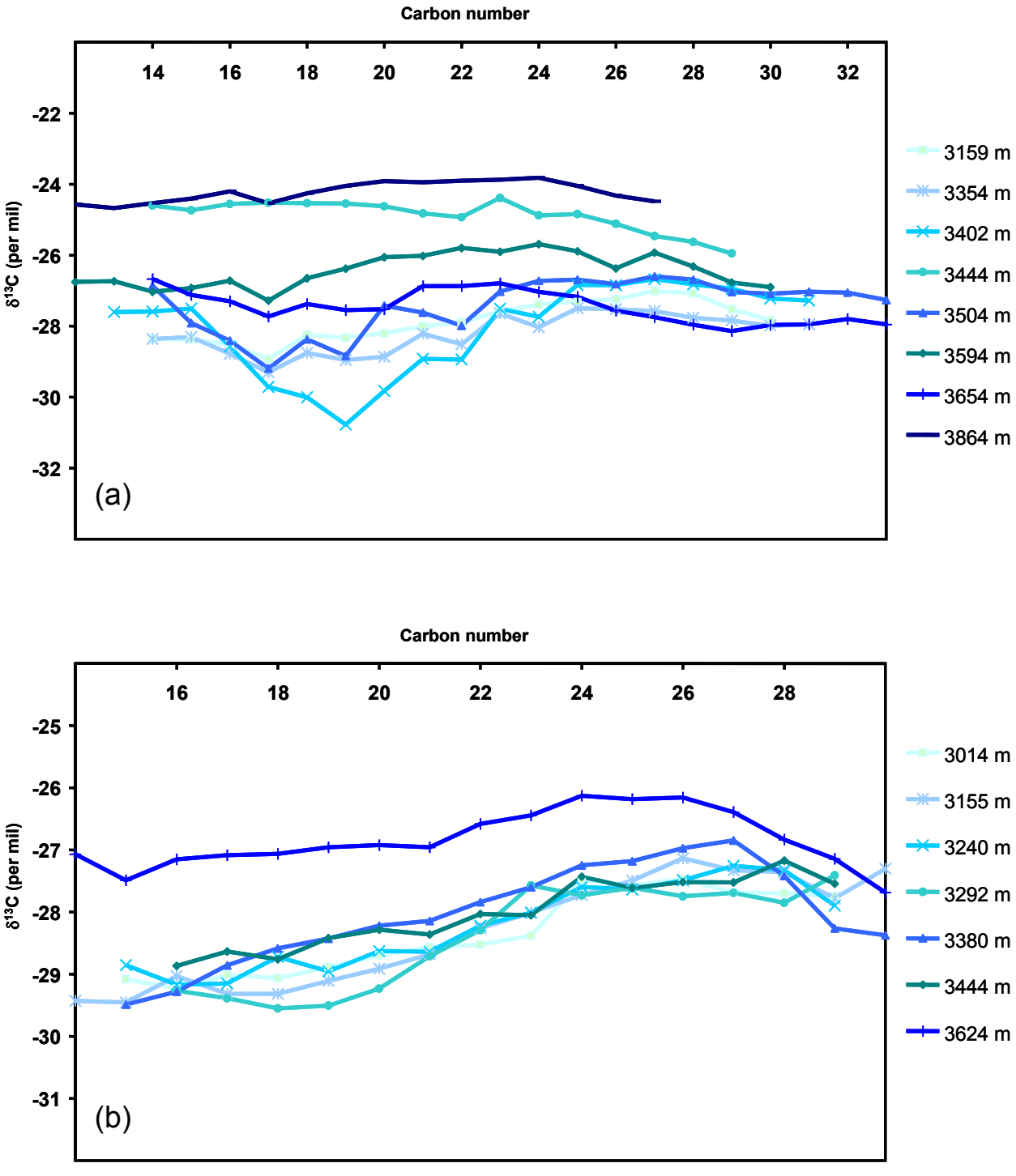

Figure 5.4 Plots of carbon number versus $\delta^{13}C$ value for *n*-alkanes extracted from Vulcan Sub-basin sediments from the (a) Paqualin-1 well (obtained from K. Grice); and (b) Vulcan-1B well.

5.2.3 Stable hydrogen isotopic analysis

The δD values of the *n*-alkanes (ca. *n*-C_{12} to *n*-C_{32}), pristane and phytane were measured in extracts of nine sediments from four wells in the Perth Basin, and sixteen from two wells in the Vulcan Sub-basin. Standard deviations for at least three replicate analyses were mostly within 5‰, but for peaks of relatively low intensity or where minor co-elution was evident, standard deviations were as high as 16‰ (e.g. Table 5.4).

5.2.3.1 Perth Basin sediments

The range of δD values of *n*-alkanes (ca. C_{12} to C_{32}), and the δD values of pristane and phytane from extracts of the Perth Basin sediments are summarized in Table 5.4. The ΔδD values, determined by subtracting the average δD value of the *n*-alkanes from the average δD value of pristane and phytane, are also shown in Table 5.4. The δD values of the *n*-alkanes, pristane and phytane from four extracts, each representing a particular level of maturity (immature, early mature, mature and late mature) are plotted in Figure 5.5 (NB. the plots for the samples of corresponding maturities are virtually identical).

Table 5.4 δD values of *n*-alkanes, pristane (Pr) and phytane (Ph), and corresponding ΔδD values (see below for definition) for the Perth Basin sediment extracts

Well, Depth m (ft)	*n*-Alkanes δD Range (‰)*	δD Pr (‰)*	δD Ph (‰)*	ΔδD (‰)
BMR 10 973–976 (3193–3203)	-183 to -128 (13)[4]	-267 (7)[5]	-249 (4)[5]	-115
BMR 10 989–991 (3245–3250)	-188 to -130 (8)[5]	-278 (3)[3]	-266 (1)[3]	-116
Dongara 4 1674 (5491)	-175 to -140 (8)[5]	-217 (3)[5]	-185 (0)[3]	-43
Dongara 4 1675 (5495.5)	-157 to -112 (6)[5]	-208 (6)[5]	-166 (7)[5]	-55
Dongara 4 1678 (5505)	-165 to -116 (5)[4]	-175 (6)[5]	-168 (2)[3]	-29
Yardarino 2 2289 (7509)	-146 to -109 (8)[3]	-153 (3)[3]	-144 (1)[3]	-23
Yardarino 2 2290 (7512.5)	-166 to -123 (7)[3]	-159 (7)[3]	-141 (3)[3]	-6
Arrowsmith 1 2494 (8781)	-145 to -80 (4)[3]	-102 (16)[3]	-97 (16)[3]	3 (0)
Arrowsmith 2678 (8787)	-123 to -73 (3)[3]	-121 (4)[3]	-108 (4)[3]	-19

ΔδD, difference between the average δD value of Pr and Ph and the average δD value of the *n*-alkanes (relative to VSMOW); * Numbers in parenthesis are standard deviations (average is shown for *n*-alkanes), superscript numbers are number of replicate analyses.

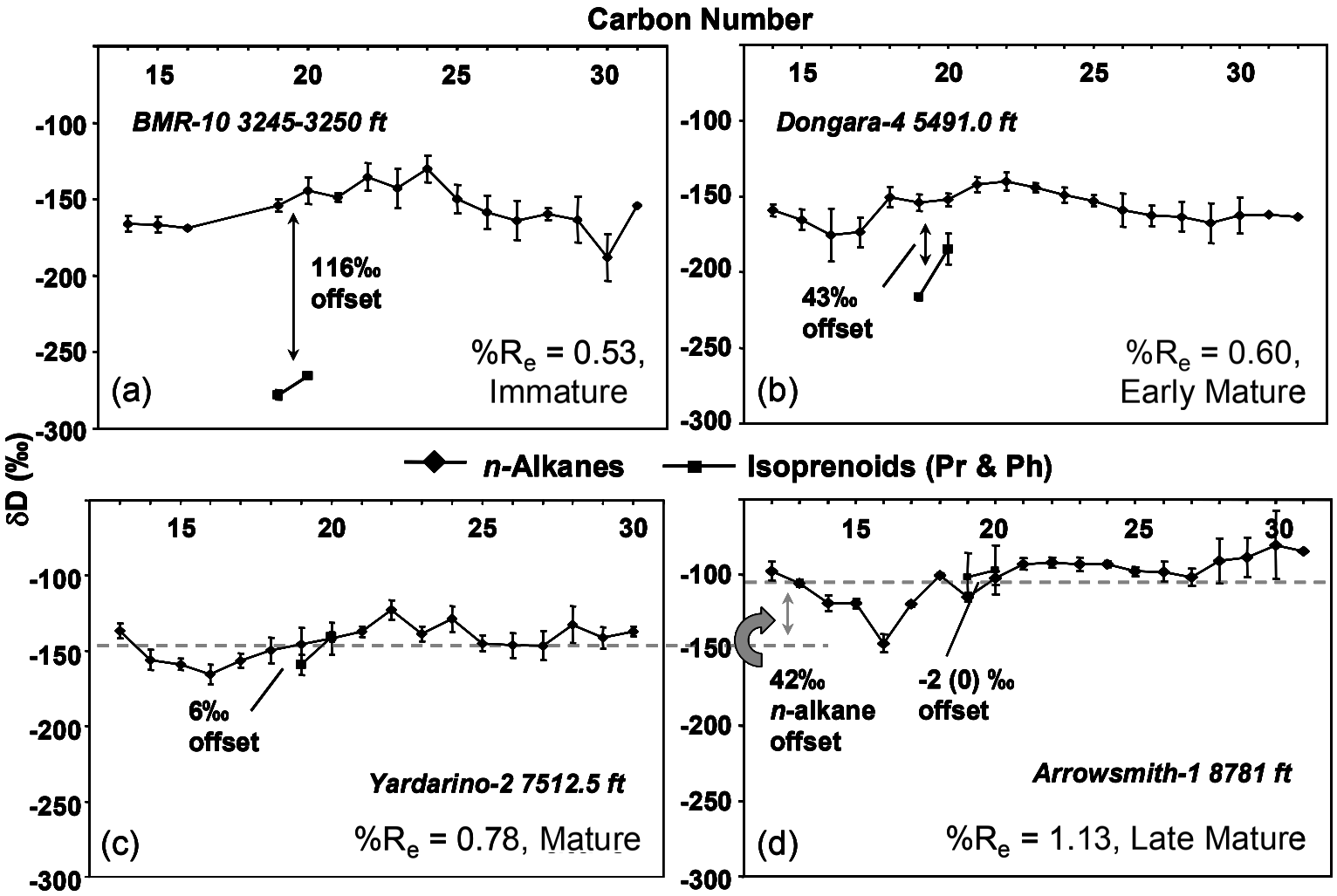

Figure 5.5 δD values of *n*-alkanes (ca. C_{12} to C_{32}), pristane and phytane from four Perth Basin sediments: (a) BMR 10 989–991 m (3245–3250 ft), immature; (b) Dongara 4 1674 m (5491 ft), early mature; (c) Yardarino 2 2290 m (7512.5 ft), mature; and (d) Arrowsmith 1 2494 m (8781 ft), late mature.

The δD values of pristane and phytane in the Perth Basin samples average between -272 and -99‰, with the isoprenoids in the more mature samples being more enriched in D. Phytane in the immature sediments is enriched in D by ca. 12 to 18‰ relative to pristane (Table 5.4). This is consistent with previous research by Li *et al.* (2001), who attribute the difference between the δD values of pristane and phytane to either different origins of these isoprenoids or different isotopic effects during their derivation from a common precursor, e.g. phytol. Interestingly, a similar difference between the δD values of pristane and phytane is retained with increasing maturity, although the magnitude of the difference varies between 5 and 42‰ (see Table 5.4). This indicates that both pristane and phytane exchange hydrogen at similar rates, thus retaining the difference between their δD values, even though source signatures are progressively lost with ongoing isotope exchange.

Extracts from the two immature sediments from the BMR 10 well contain pristane and phytane that are significantly depleted in D by ca. 114 to 116‰ (Table 5.4) relative to the *n*-alkanes in the same sample (e.g. Figure 5.5). Extracts from three early mature sediments from the Dongara 4 well contain pristane and phytane that are ca. 30 to 55‰ depleted in D (Table 5.4) relative to the *n*-alkanes (e.g. Figure 5.5). Extracts from two mature sediments from the Yardarino 2 well contain pristane and phytane that are depleted in D by ca. 6 to 23‰ (Table 5.4) relative to *n*-alkanes of this sample (e.g. Figure 5.5). Extracts from two late mature sediments from the Arrowsmith 1 well contain pristane and phytane that are ca. 0 to 19‰ depleted in D (Table 5.4) relative to the *n*-alkanes (e.g. Figure 5.5).

The large offset between the δD values of pristane and phytane relative to those of the *n*-alkanes (ca. -114 to -116‰) from the immature sediments appears to reflect the isotopic compositions of their precursors (i.e. biosynthesized *n*-alkyl and isoprenoid lipids), where the isoprenoid components are depleted in deuterium relative to the *n*-alkyl components (see Chapter 4). In fact, the average δD value of the *n*-alkanes (-143 and -156‰), and the average δD value of pristane and phytane (-258 and -272‰) in the two immature sediments are in good agreement with the range of reported δD values of precursor *n*-alkyl lipids (-250 to -150‰) and phytol (-357 to -278‰), respectively (e.g. Estep and Hoering, 1980; Sessions *et al.*, 1999). With increasing maturity, the difference between the δD values of *n*-alkanes and

isoprenoids gradually decreases (Figure 5.5). Pristane and phytane become more enriched in D with increasing maturity, while the *n*-alkanes generally remain at a constant composition, until late maturity (%R_o = 1.13) where there is a significant enrichment of D (ca. 42‰) in *n*-alkanes. This indicates that primary *n*-alkane D/H signatures are probably best preserved in immature sediments, with enrichment in D occurring at higher maturities attributed to isotopic exchange associated with maturation reactions (Sec. 5.1.1.3). Thus the biological δD signature is lost at high maturity levels. It is evident that the isoprenoids become enriched in D more rapidly than the *n*-alkanes, suggesting that isotopic enrichment (hydrogen isotopic exchange) occurs *via* a mechanism that proceeds faster with compounds containing tertiary carbon centres. One could envisage a mechanism involving carbocation-like intermediates, since carbocation formation is more favourable with molecules containing tertiary carbon centres compared to straight-chain molecules with only primary and secondary carbons. Further discussion of potential mechanisms is provided in Section 5.2.5.

The δD values of *n*-alkanes from the nine extracts average between -158 and -96‰ (range of δD values of *n*-alkanes for each sample is shown in Table 5.4). Based on bulk isotopic measurements of crude oils generated from marine source rocks, Santos Neto and Hayes (1999) suggested that marine-derived *n*-alkanes are likely to have δD values near -150‰ if no significant isotopic exchange has occurred as a result of secondary reactions. Indeed, the natural hydrogen isotopic fractionation between environmental water and *n*-alkyl lipids biosynthesized by autotrophs is approximately -147±5‰ (Smith and Epstein, 1970), and the isotopic composition of ocean water is near 0‰ (see Chapter 4). The δD values measured for *n*-alkanes from the immature-early mature sediments analysed in this study average -158 to -132‰, respectively, consistent with that expected for marine-derived organic matter. The samples of higher maturity, however, contain *n*-alkanes that are somewhat more enriched in D (mature-late mature, averaging -126 to -96‰, respectively), with the exception of Yardarino 2 7512.5 ft (averaging -144‰).

There is compelling evidence that hydrogen exchange significantly alters the D/H composition of sedimentary organic matter during thermal maturation (e.g. Hoering, 1977; Rigby *et al.*, 1981; Smith *et al.*, 1982; Li *et al.*, 2001; this study). However, kinetic isotope effects associated with thermal cracking of hydrocarbons might also

play a role. Tang *et al.* (2005) proposed a quantitative kinetic model to simulate the large D (and ^{13}C) enrichments observed in *n*-alkanes during artificial thermal maturation of a North Sea crude oil under anhydrous, closed-system conditions. Under the conditions used, the average *n*-alkane δD values increased by ~50‰ at an R_e of 1.5%. In addition, the amount of D-enrichment increased with increasing *n*-alkane carbon number, thought to be a combined result of greater thermal cracking of longer-chain *n*-alkanes, and the generation of isotopically lighter, shorter-chain compounds (Tang *et al.*, 2005). While the data reported by Tang *et al.* (2005) are consistent with changes in D/H compositions observed during the natural maturation of sedimentary organic matter, it is difficult to envisage how a process such as thermal cracking could produce consistent δD values in *n*-alkanes and isoprenoids in samples (regardless of age and maturity) from various geological locations worldwide (e.g. see above). Therefore, it is suggested that hydrogen exchange, and the associated equilibrium isotope effects, is the primary process in determining the D/H composition of mature sedimentary organic matter.

Figure 5.6 is a depth profile of the average δD value of the *n*-alkanes, and the δD values of pristane and phytane from the Perth Basin sediments. The general trend of D-enrichment with depth/maturity is clearly evident in both compound classes, with the rate of enrichment being more rapid in isoprenoids relative to *n*-alkanes. The figure also clearly shows that the δD values of pristane and phytane change in a similar fashion with maturation, suggesting they exchange hydrogen at similar rates.

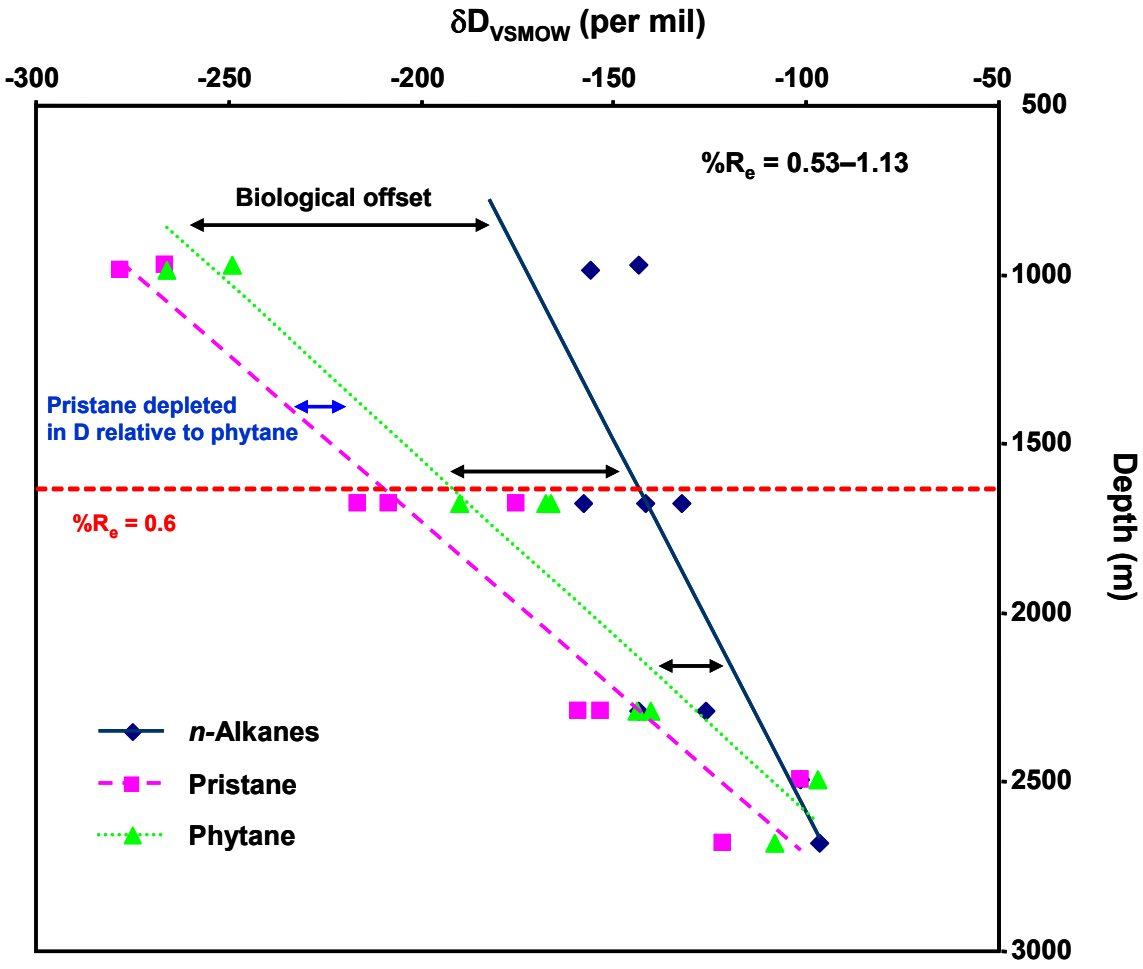

Figure 5.6 A depth profile of the average δD value of *n*-alkanes, and the δD value of pristane and phytane from the Perth Basin sediments (Table 5.4).

Of course, it is possible (although unlikely) that the *n*-alkanes and isoprenoids exchange hydrogen at the same rate. In such a case, the observed change in the δD values of the *n*-alkanes and the isoprenoids would be consistent with the extent to which the compounds are out of isotopic equilibrium (A.L. Sessions, personal communication). For example, if the equilibrium fractionation between pristane/phytane and the matrix of exchangeable hydrogen was, say -110‰, then we might expect the δD values of pristane and phytane to change markedly from the initial δD value of around -250‰ with ongoing exchange. However, the δD values of the *n*-alkanes would probably change only by a small amount (relative to the change in δD values of pristane and phytane) with ongoing exchange, considering that the

average initial δD value of the *n*-alkanes is around -150‰. In other words, for a given increment in hydrogen exchange, there is a larger change in the δD value of the isoprenoids compared to that of the *n*-alkanes, even though the two compound classes hypothetically exchange hydrogen at the same rate. This notion is depicted in Figure 5.7.

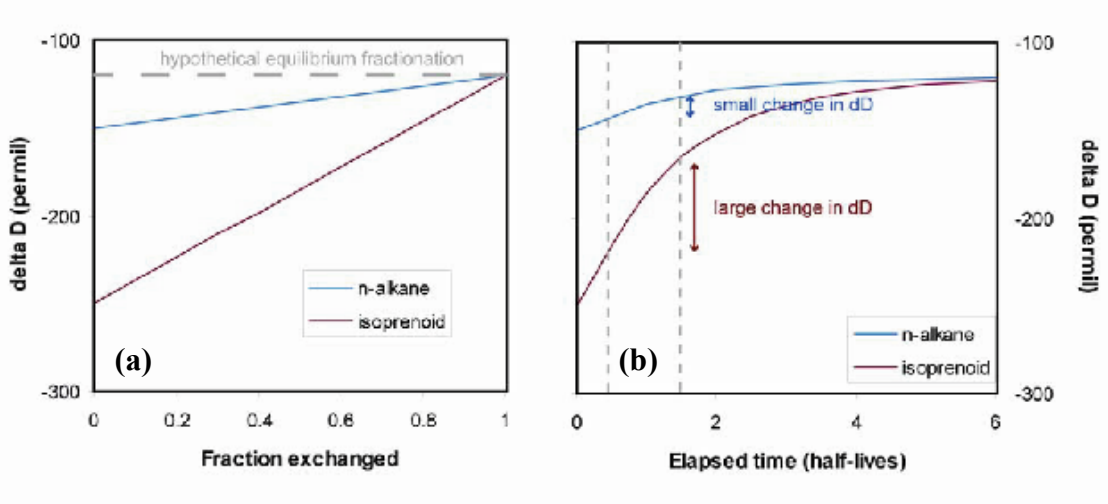

Figure 5.7 Plot of hypothetical data for (a) δD value versus fraction of total hydrogen exchanged, and (b) δD value versus elapsed time (half-lives) for an *n*-alkane and an isoprenoid (A.L. Sessions, pers. comm.).

5.2.3.2 Vulcan Sub-basin sediments

The range of δD values of *n*-alkanes (ca. C_{13} to C_{31}), and the δD values of pristane and phytane from extracts of the Vulcan Sub-basin sediments are summarized in Table 5.5. The δD values of *n*-alkanes from the eight Paqualin-1 extracts average between -136 and -108‰, and the *n*-alkanes from the eight Vulcan-1B extracts average between -146 and -110‰ (Figure 5.8). The δD values of *n*-alkanes extracted from the sediments of lowest maturity are consistent with a marine source, i.e. marine mudstones of the lower Vulcan Formation, while the samples of higher maturity contain *n*-alkanes that are somewhat more enriched in D. The δD values of pristane and phytane in the Paqualin-1 samples average between -165 and -68‰, and in Vulcan-1B between -166 and -105‰ (Table 5.5). The

difference between the δD values of the *n*-alkanes and regular isoprenoids decreases with increasing maturity. Pristane and phytane are more rapidly enriched in D with ongoing maturation, similar to that observed in the Perth Basin. The enrichment of D in hydrocarbons from Paqualin-1 appears to occur at lower maturity (based on R_o) compared to Vulcan-1B and Perth Basin sediments. In particular, from the shallowest Paqualin-1 sample (3159m, $\%R_o = 0.62$) to the sample immediately below (3354m, $\%R_o = 0.8$), there is a significant enrichment of D in pristane and phytane (ca. 60‰), resulting in a change in ΔδD value from -29 to +21‰. This is not consistent with samples of corresponding maturity (i.e. similar R_o) from Vulcan-1B and the Perth Basin. The significantly positive ΔδD values are maintained in the deeper, more mature Paqualin-1 samples. It appears that the Paqualin-1 sediments below ~3159 m are more mature than indicated by R_o values, suggesting that the available R_o data do not accurately reflect maturity in this case. Although maturity is the most likely explanation for the observed differences between the δD values of isoprenoids and *n*-alkanes from Paqualin-1, alternatively the isoprenoids from the least mature Paqualin-1 sample may be derived from a different or additional relatively D-depleted source. Pristane and phytane extracted from a post-mature Paqualin-1 sediment ($\%R_o = 1.6$) are significantly enriched in D (ca. 40‰) relative to the *n*-alkanes. This indicates that D-enrichment persists at very high maturity, and continues to be more rapid for regular isoprenoids than *n*-alkanes. Published equilibrium fractionation factors between C-bound hydrogen and water for primary, secondary and tertiary C-H (Sessions *et al.*, 2004 and references therein) do not allow for more positive δD values for isoprenoids relative to *n*-alkanes. However uncertainties in these data are very large, and the approach used to calculate the factors did not take into account the isotope effects associated with solubility and adsorption processes, which could be important factors to consider in sedimentary organic matter (Sessions *et al.*, 2004). Furthermore, the experiments performed to measure equilibrium fractionations were exchange reactions catalysed by enzymes at 35ºC, with no data available to extrapolate the results to other temperatures (Sessions *et al.*, 2004). The field data presented herein indicate that the δD values of isoprenoids can be more positive than *n*-alkanes, however there is a need for further experimental and more comprehensive field data to support this finding. The data presented herein also provide further evidence that free-radical hydrogen transfer is

unlikely to have caused the observed shift in δD values of isoprenoids and *n*-alkanes. The current understanding of free-radical hydrogen transfer suggests that *n*-alkanes could be affected to a larger extent than regular isoprenoids by such a process (Pedentchouk *et al.*, 2006). Thus, significant D-enrichment in regular isoprenoids is more likely to be a result of H/D exchange reactions which favour the primary and secondary carbons adjacent to tertiary carbon centres (see also Sec. 5.2.5 and 5.2.6).

Pristane is enriched in D relative to phytane by up to 22‰ throughout the Paqualin-1 sequence, while a similar trend is evident in Vulcan-1B where pristane is enriched by up to 26‰ relative to phytane (Table 5.5). This is opposite to the trend observed for the Perth Basin samples, where pristane is consistently depleted in D relative to phytane, but again indicates that pristane and phytane exchange hydrogen at similar rates during maturation. The enrichment of D in pristane relative to phytane in the Vulcan Sub-basin sediments could be attributed to a lower relative algal input to the isoprenoids in these samples. This is opposite to that observed in the Perth Basin samples (see Sec. 5.2.2.1 and 5.2.2.2), where they are considered to be from a dominant algal source. Indeed, a significant terrestrial (higher plant) source may have contributed to the pristane of Paqualin-1, considering that tocopherol (**XVI**) of higher plants is another natural product precursor of pristane (Goosens *et al.*, 1984). This higher plant source of pristane could be relatively enriched in D as a result of the evapotranspiration isotope effects that occur in plants (see Chapter 4).

Figure 5.8 shows two depth profiles of the δD values of the *n*-alkanes (average), pristane and phytane from the Paqualin-1 (a), and Vulcan-1B (b) sediment extracts. Again, the general trend of D-enrichment with depth/maturity is clearly evident, with the enrichment being more marked in isoprenoids relative to *n*-alkanes. The figure also shows that the δD values of pristane and phytane change in a similar fashion with maturation, suggesting they exchange hydrogen at similar rates.

Table 5.5 δD values of *n*-alkanes (range), pristane (Pr) and phytane (Ph), and ΔδD values (see below for definition).

Well, Depth (m)	*n*-Alkanes δD Range (‰)*	δD Pr (‰)*	δD Ph (‰)*	ΔδD (‰)
Paqualin-1				
3159	-145 to -129 (6)[3]	-158 (5)[4]	-172 (4)[4]	-29
3354	-143 to -92 (6)[3]	-105 (6)[5]	-109 (4)[5]	21
3402	-129 to -112 (5)[3]	-110 (3)[5]	-112 (5)[5]	11
3444	-138 to -109 (8)[5]	-112 (5)[3]	-114 (3)[3]	13
3504	-129 to -106 (9)[4]	-89 (5)[3]	-97 (5)[3]	27
3594	-125 to -106 (3)[4]	-88 (3)[3]	-94 (5)[3]	27
3654	-115 to -96 (5)[3]	-87 (2)[3]	-99 (1)[3]	13
3864	-117 to -92 (8)[3]	-57 (4)[5]	-79 (5)[5]	40
Vulcan-1B				
3014	-154 to -125 (5)[3]	-168 (9)[3]	-165 (7)[3]	-21
3155	-150 to -123 (6)[3]	-169 (9)[3]	-178 (11)[3]	-34
3240	-142 to -119 (5)[3]	-125 (5)[3]	-129 (3)[3]	8
3292	-141 to -124 (3)[3]	-136 (8)[3]	-148 (8)[3]	-9
3380	-130 to -105 (3)[3]	-119 (8)[3]	-126 (3)[3]	-1 (0)
3444	-123 to -104 (3)[3]	-100 (3)[4]	-126 (8)[3]	3 (0)
3624	-117 to -101 (8)[3]	-110 (15)[4]	-116 (3)[4]	-3 (0)
3679	-120 to -107 (6)[3]	-102 (4)[3]	-108 (7)[3]	9

ΔδD, difference between the average δD value of Pr and Ph and the average δD value of the *n*-alkanes (relative to VSMOW); * Numbers in parentheses are standard deviations (average is shown for *n*-alkanes), superscript numbers are number of replicate analyses.

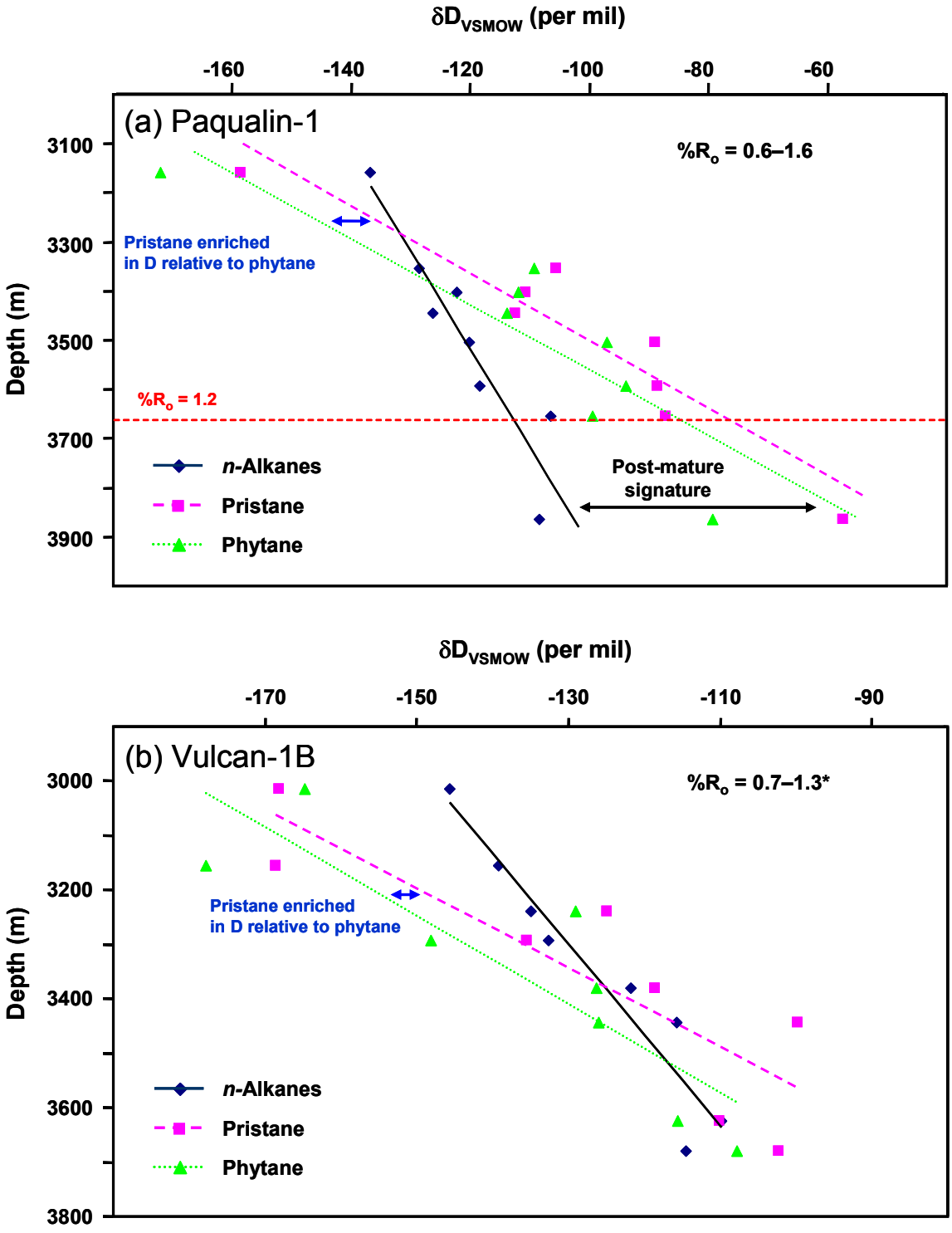

Figure 5.8 Depth profiles of the δD values of *n*-alkanes (average), pristane and phytane from (a) Paqualin-1 and (b) Vulcan-1B sediment extracts. * R_o data extrapolated from a thermal geohistory model (Kennard *et al.*, 1999).

5.2.3.3 Other sedimentary sequences

Since publication of the δD analysis of samples from the Perth Basin described above (Dawson *et al.*, 2005a, 2005b), similar research outcomes have been reported and published on other samples from various locations worldwide (Radke *et al.*, 2005; Pedentchouk *et al.*, 2006).

Radke *et al.* (2005) investigated the influence of thermal maturity on the δD values of saturated hydrocarbons (*n*-alkanes and isoprenoids) from two sediment sections from Poland (Kupferschiefer) and Germany (Posidonia Shale). The Early Permian Kupferschiefer (KS) samples covered a maturity range from early mature to late mature ($\%R_o$ = 0.65 – 1.3), and the Jurassic Posidonia Shale (PS) samples from immature to late mature ($\%R_o$ = 0.48 – 1.06). The δD values of *n*-alkanes from the KS samples average between -136 and -72‰, while the *n*-alkanes from the PS samples average between -167 and -100‰. The *n*-alkanes in the most mature KS sample were enriched in D by 37‰ relative to an early mature sample, while the *n*-alkanes in the most mature PS sample were enriched in D by ca. 67‰ relative to those from the immature sample. The δD values of pristane and phytane in the KS samples average between -275 and -81‰, and in PS samples between -317 and -123‰, the isoprenoids in the more mature samples being enriched in D. The *n*-alkanes and isoprenoids all become enriched in D with increasing maturity, with D-enrichment being more rapid for the isoprenoids compared to the *n*-alkanes.

A similar trend of enrichment of deuterium in *n*-alkanes and isoprenoids was seen by Pedentchouk *et al.* (2006), who studied a continuous 450 m core of Early Cretaceous, lacustrine sediments from West Africa. The sediments covered a maturity range from immature to early mature ($\%R_o \sim 0.55 – 0.7$). The δD value of the C_{17} *n*-alkane ranges between -135 and -90‰, and is most enriched in D in the samples of highest maturity. The δD values of pristane and phytane fall between -230 and -110‰ over the maturity range.

5.2.4 Comparison of δD values to traditional molecular maturity parameters

A comparison of δD values of individual compounds to traditional maturity parameters, such as R_o and various molecular parameters was undertaken in order to further assess whether changes in D/H composition are related to maturation. The

parameters were calculated using the areas under relevant peaks in a GC-MS total-ion chromatogram (or extracted ion chromatograms where applicable).

5.2.4.1 Perth Basin

For reasons unknown, the majority of commonly used molecular maturity parameters calculated for the Perth Basin sediments were anomalous, evident from their lack of correlation with equivalent vitrinite reflectance (R_e). The anomalous parameters included the saturated molecular parameters based on the C_{31}–C_{35} 17α-hopanes [22*S*/(22*S*+22*R*)], and C_{29} 5α,14α,17α(H)-steranes [20*S*/(20*S*+20*R*)]; and the aromatic molecular parameters such as those based on the distribution of phenanthrene and the methylphenanthrene isomers (e.g. MPI-1; Appendix 1), and the distributions of dimethylnaphthalenes (e.g. DNR-1; Appendix 1) and trimethylnaphthalenes (e.g. TNR-1; Appendix 1). However, the maturity parameter based on the 18α(H)- and 17α(H)-trisnorhopanes (*Ts*/(*Ts*+*Tm*); Appendix 1) (Seifert and Moldowan, 1978) was calculated and appeared to reflect the relative maturities of the samples (Table 5.1). This traditional biomarker maturity parameter has been plotted against the R_e values in Figure 5.9a, for each of the Perth Basin sediments. *Ts*/(*Ts*+*Tm*) correlates well with the R_e values (R^2 = 0.8). Figure 5.9b displays a plot of the average δD value of pristane and phytane versus the R_e values for each of the nine sediments. The average δD values of pristane and phytane also correlate well with the R_e values (R^2 = 0.76; Fig. Figure 5.9b), clearly showing that the isotopic enrichment in the isoprenoids is proportional to maturation.

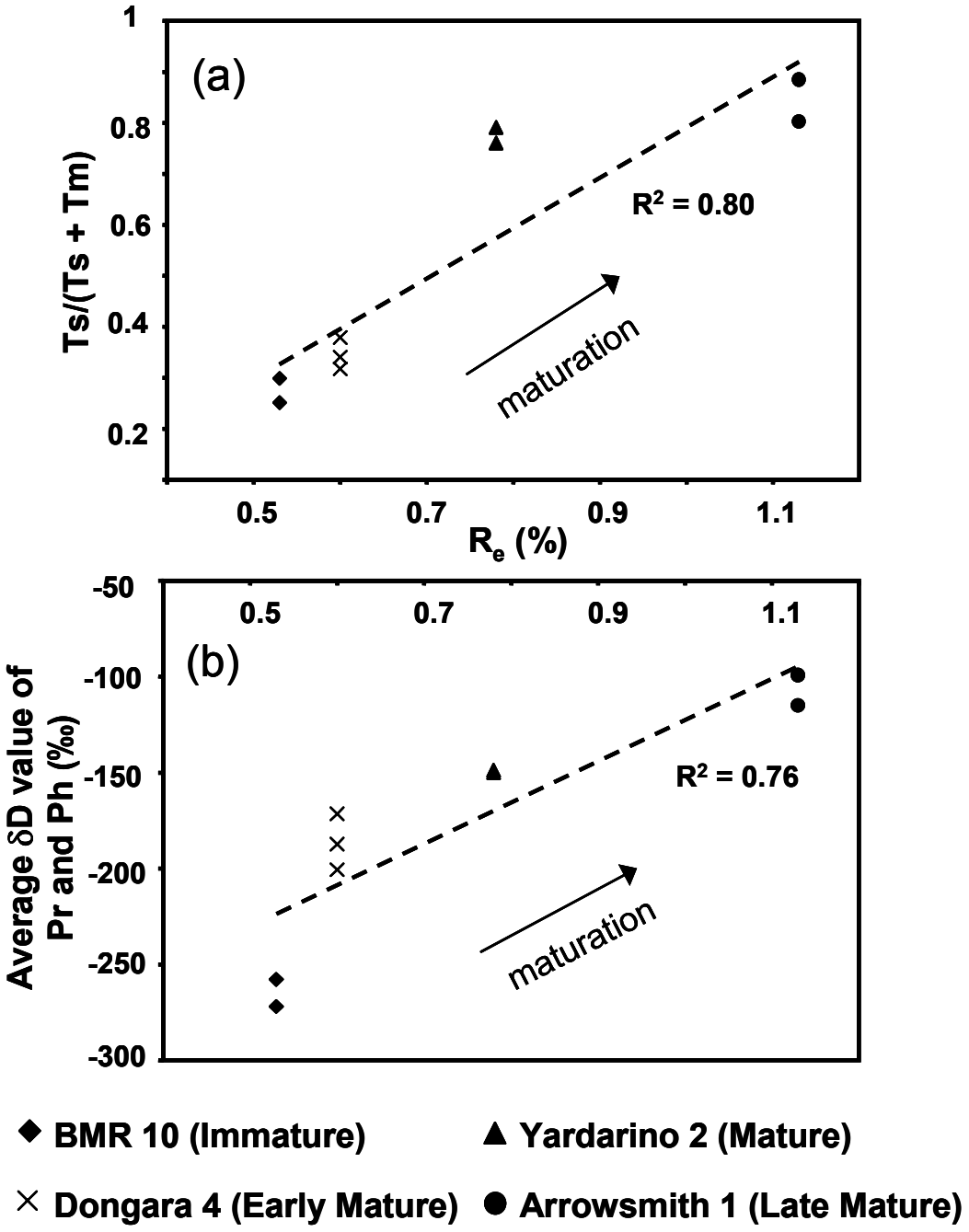

Figure 5.9 Plot of (a) *Ts*/(*Ts*+*Tm*), and (b) average δD value of pristane (Pr) and phytane (Ph), versus the equivalent vitrinite reflectance (R_e) values for the Perth Basin sediments.

5.2.4.2 Vulcan Sub-basin

Various molecular maturity parameters were calculated for the Paqualin-1 and Vulcan-1B sediment extracts. The saturated hydrocarbon parameters were not useful in this case because many of the required components (e.g. hopanes and steranes) were not detected in the more mature samples. However, the aromatic molecular parameters MPI-1 (Radke and Welte, 1983) and TNR-1 (Alexander *et al.*, 1985) appear to reflect the relative maturities of the Paqualin-1 sediments, and correlate strongly with R_o (R^2 = 0.81 and 0.87, respectively; see Figure 5.10).

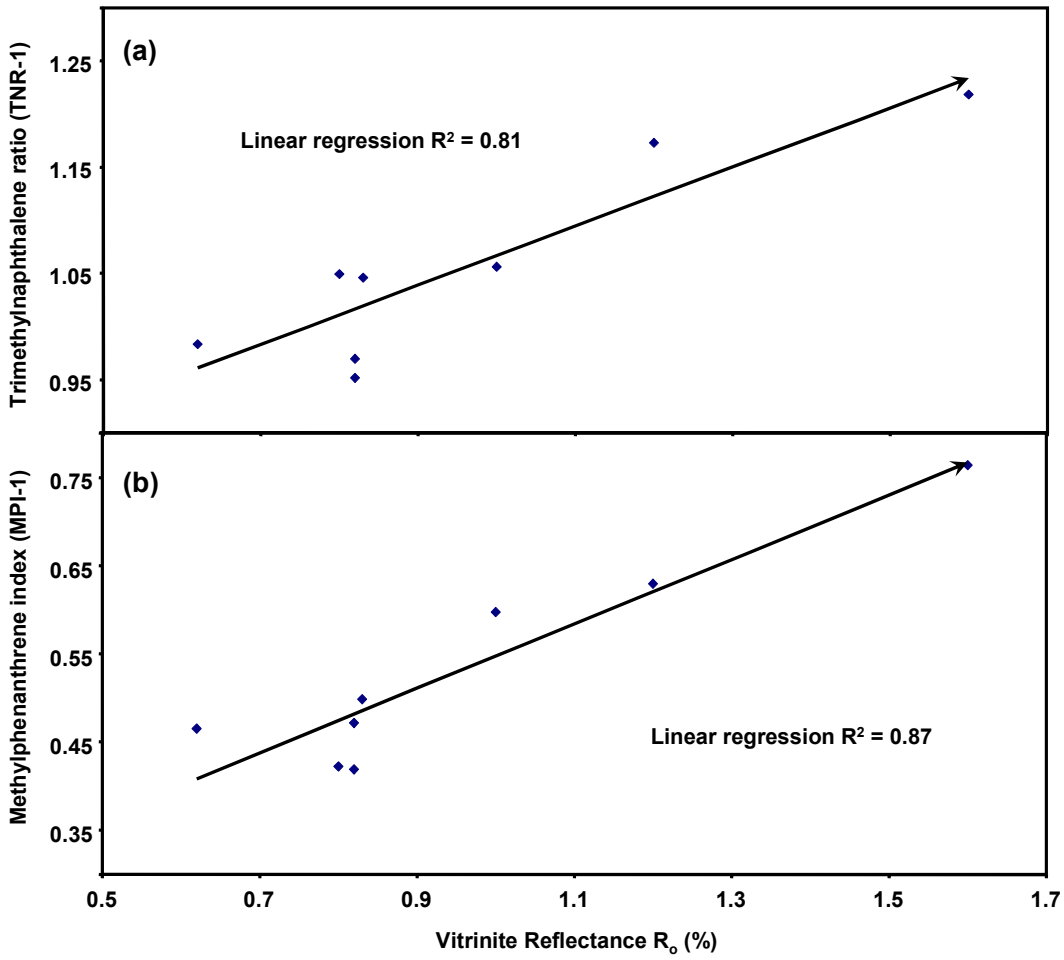

Figure 5.10 Plot of (a) trimethylnaphthalene ratio (TNR-1), and (b) methylphenanthrene index (MPI-1), versus vitrinite reflectance (R_o) values for the Paqualin-1 sediment extracts. The direction of the arrow indicates increasing maturity.

Figure 5.11 displays plots of R_o (a), TNR-1 (b) and MPI-1 (c), versus the average δD value of pristane and phytane for the Paqualin-1 sediment extracts. The least mature Paqualin-1 sample (3159m, R_o = 0.62) plots as an outlier on all three due to a marked depletion of D in pristane and phytane, which could be attributed to an additional or different input to the isoprenoids in this sample. Excluding this outlier, the average δD values of pristane and phytane correlate strongly with R_o, TNR-1 and MPI-1 (R^2 = 0.79, 0.75 and 0.86, respectively).

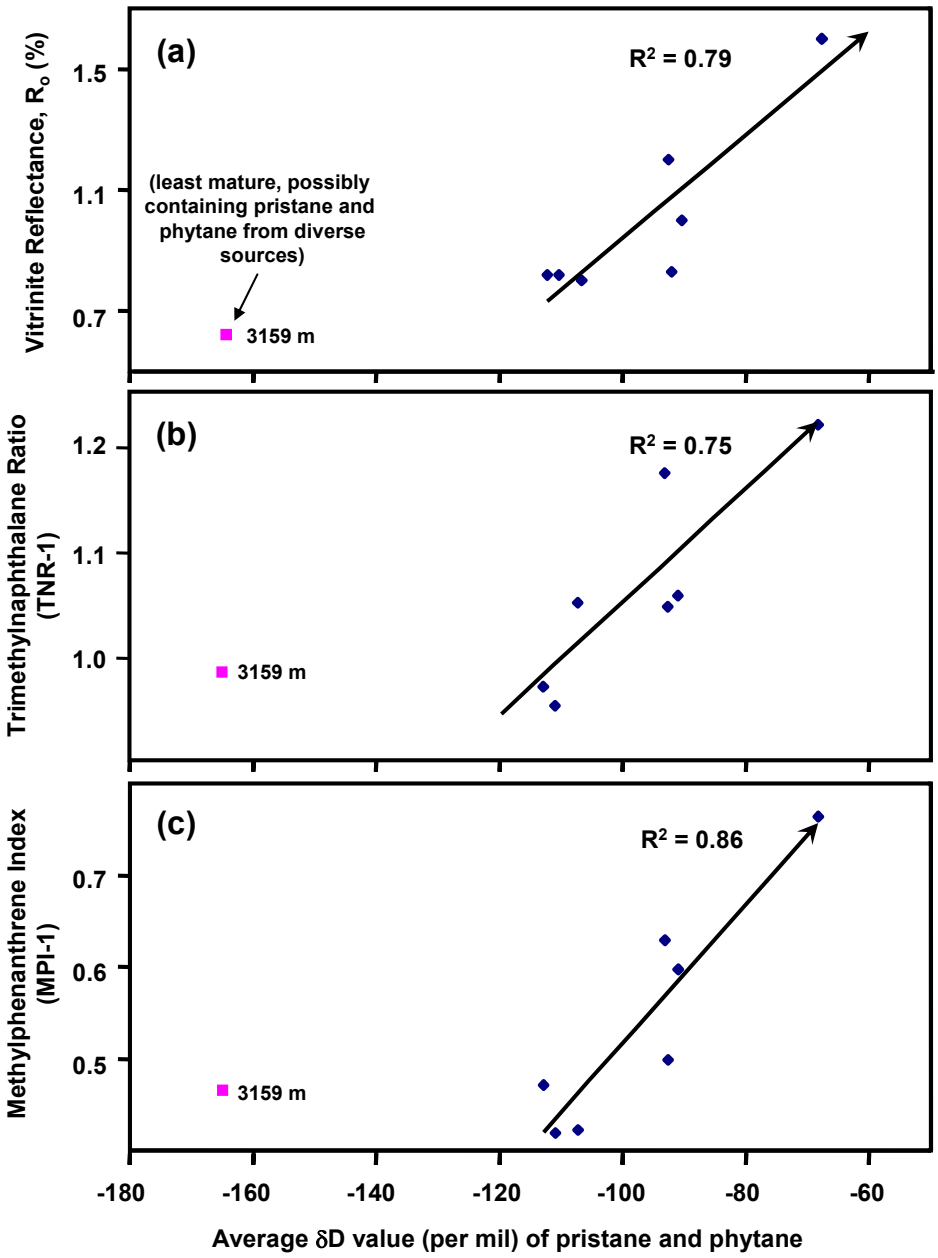

Figure 5.11 Plot of (a) vitrinite reflectance (R_o), (b) trimethylnaphthalene ratio (TNR-1), and (c) methylphenanthrene index (MPI-1), versus the average δD value of pristane and phytane for the Paqualin-1 sediment extracts. The direction of the arrow indicates increasing maturity.

The aromatic molecular parameter MPI-1 appears to reflect the relative maturities of the Vulcan-1B sediments. Figure 5.12 displays plots of R_o and MPI-1 versus the average δD value of pristane and phytane for the Vulcan-1B sediment extracts. The two least mature Vulcan-1B samples (3014 m and 3155m, R_o = 0.69 and 0.77, respectively) plot as outliers due to a marked depletion of D in pristane and phytane. This is similar to the least mature sample in the Paqualin-1 well (see above), and could also be attributed to an additional or different input to the isoprenoids. The average δD values of pristane and phytane correlate strongly with R_o and MPI-1 (R^2 = 0.70 and 0.76, respectively). These data provide further evidence that the isotopic enrichment in isoprenoids is proportional to maturation within the investigated range of maturity.

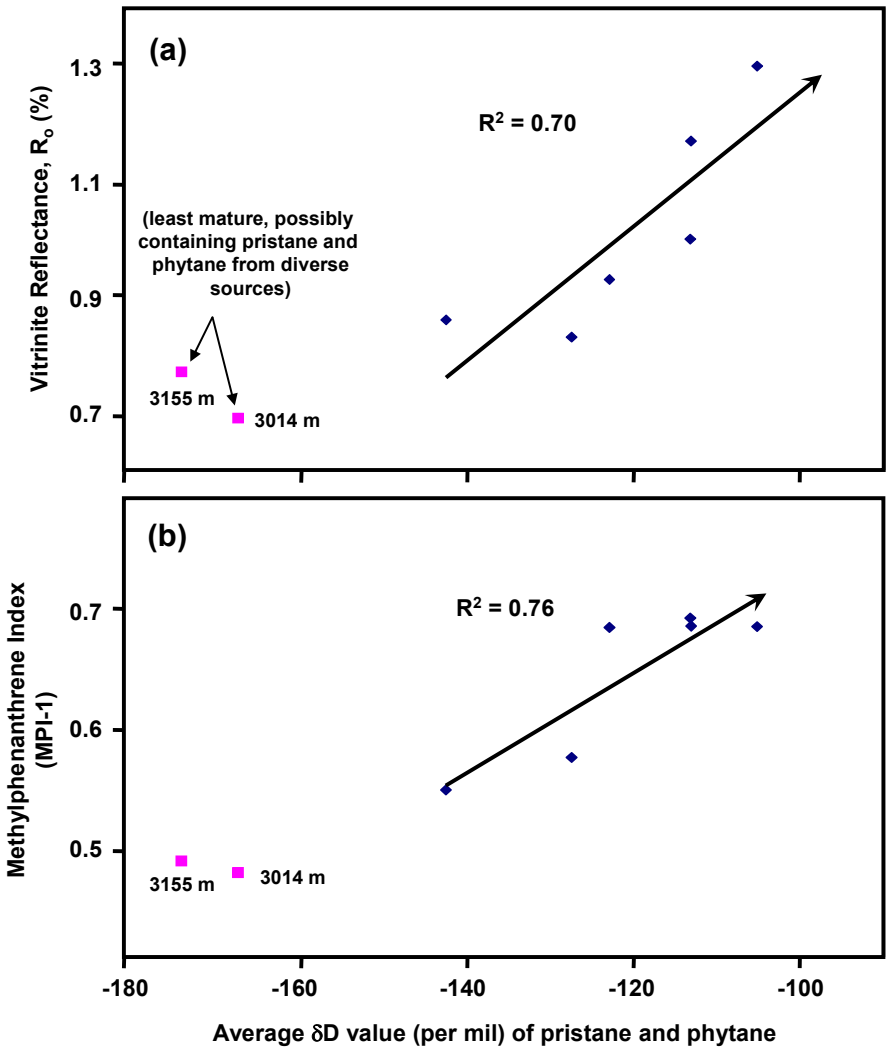

Figure 5.12 Plot of (a) vitrinite reflectance (R_o), and (b) methylphenanthrene index (MPI-1), versus the average δD value of pristane and phytane for the Vulcan-1B sediment extracts. The direction of the arrow indicates increasing maturity.

5.2.5 Possible mechanisms of hydrogen exchange during maturation

A number of simple mechanisms of hydrogen exchange (and associated D-enrichment) have been put forward based on artificial maturation experiments. Hoering (1984) suggested thermal generation of organic free radicals from the kerogen (e.g. see (2) below), followed by successive, multiple exchange with D_2O. In summary, organic (alkyl) free radicals and hydrogen atoms can be formed *via* thermal cleavage of bonds in the kerogen. Free radical reactions can then propagate to yield hydrocarbons with multiple deuterated sites. The suggested source of deuterium for organic deuteration is heavy water (HDO, D_2O), which could exchange with a hydrogen radical (1). Propagation steps could involve the generation of an alkene and a hydrogen atom from an alkyl free radical (2), with the alkene then being susceptible to attack by a deuterium atom (3). This would result in migration of the radical site to form a secondary free radical, which could in turn form an isomerised alkene (4) for further deuteration. Alkene isomerisation and free radical site migration could continue (5) until termination of the free radical reaction *via* e.g. radical recombination. The net process is summarised in (6).

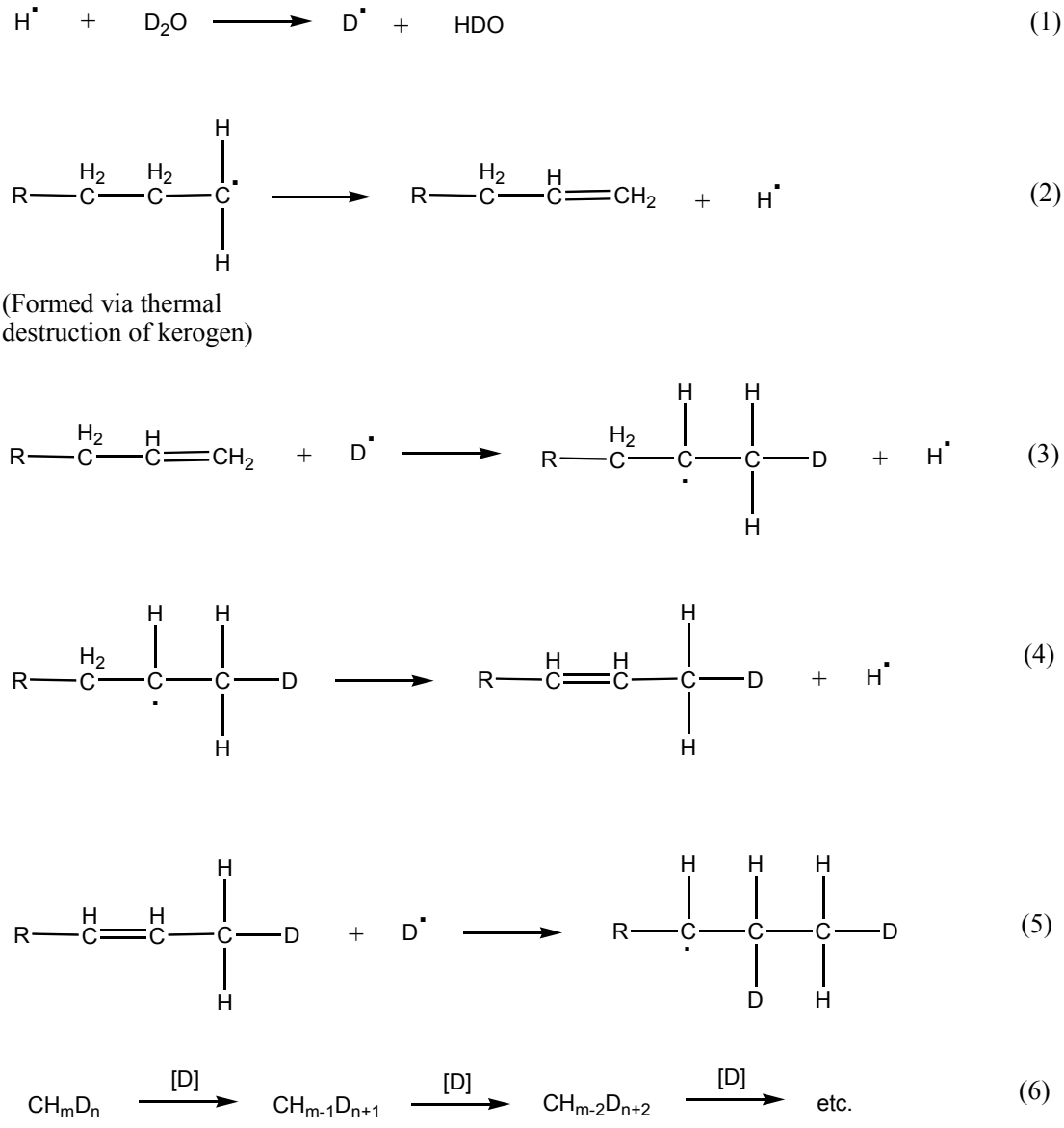

(Hoering, 1984)

Ross (1992) re-evaluated the mechanism proposed by Hoering (1984). Firstly, he suggested that the initial propagation step where radical displacement of D• by H• in D_2O occurs (1) is an unlikely process. Instead, Ross (1992) suggests that substances such as phenols, carboxylic acids or H_2S can exchange ionically with D_2O, and the resulting deuterated species can take part in free radical H/D exchange with alkyl radicals formed from the thermal destruction of kerogen. A numerical simulation of the mechanism put forward by Hoering (1984) produced a series of profiles showing the position and relative amount of deuterium substitution in *n*-alkanes. It was shown

that there were marked differences between the natural and simulated profiles, the statistically derived distributions being much narrower than the natural distributions. This provided statistical evidence against homogeneous, single-site, sequential H/D exchange. Instead, Ross (1992) suggested that the deuterated *n*-alkanes are generated by a series of multiple exchanges taking place simultaneously at various sites along the carbon chain, possibly occurring at the organic-mineral interface. The mechanistic details are not discussed, however hydrogen exchange at clay mineral surfaces has been studied previously by Alexander *et al.* (1984). The mechanism they propose for a branched alkyl moiety (Figure 5.13) is firstly, interaction of the moiety with a Lewis acid site on the clay surface which polarises a carbon-hydrogen bond, generating a carbocation-like species. Hydrogen attached to a tertiary carbon will interact preferentially with the clay to form a carbocation-like species of higher stability than one formed at a secondary or primary carbon. This interaction results in enhanced acidity of the hydrogen attached to carbons that are adjacent to tertiary carbon centres, making them susceptible to exchange with other hydrogen present in the system. Exchange is thought to occur *via* an adsorbed alkene-like intermediate (e.g. Figure 5.13), which is stabilised by conjugated substituents (Morrison and Boyd, 1992). Pristane contains four tertiary carbon atoms, each with hydrogen that could preferentially interact with Lewis acid sites on clay surfaces, and therefore promote hydrogen exchange at various positions in the pristane molecule (e.g. Figure 5.14).

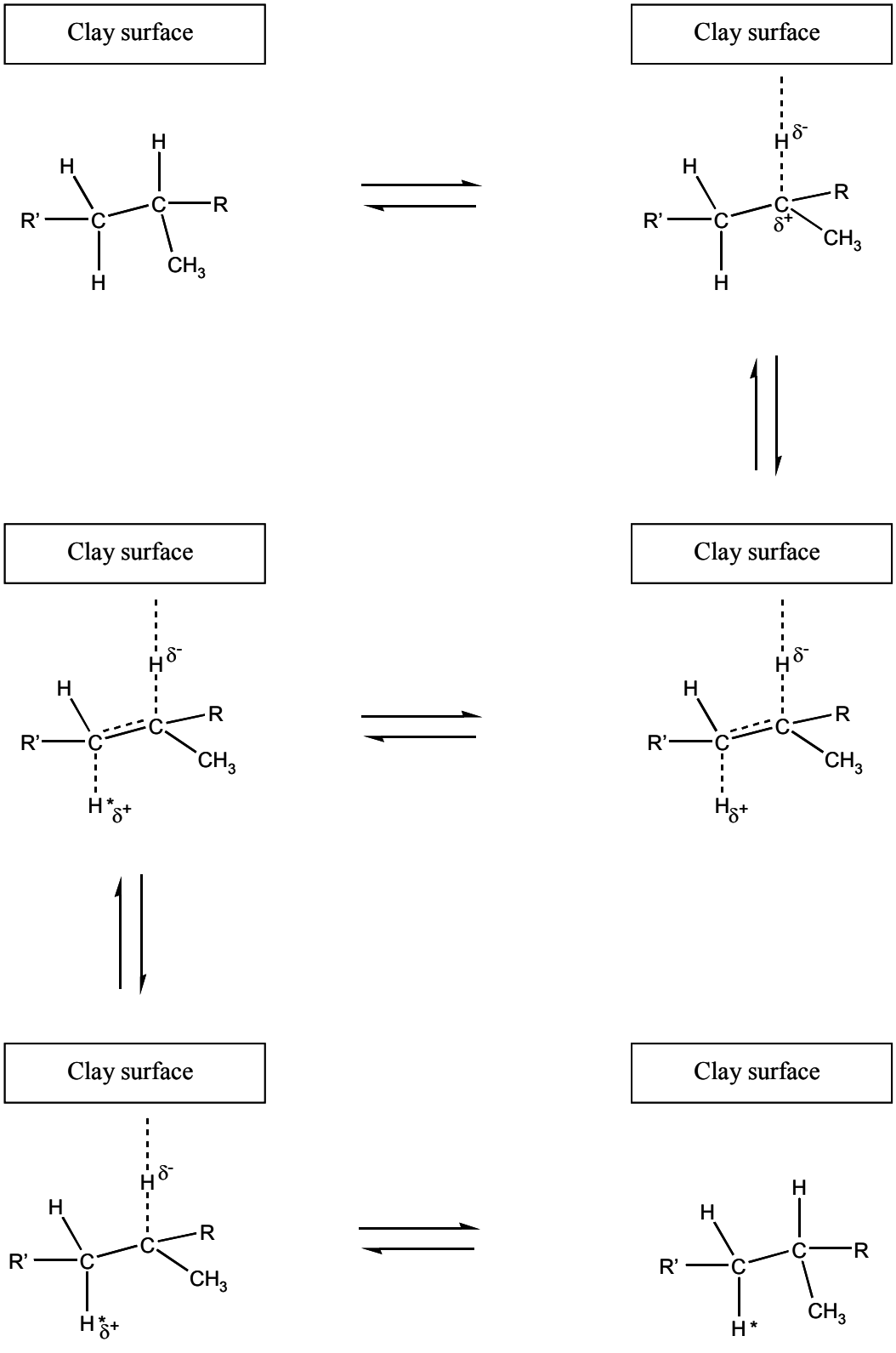

Figure 5.13 Reaction mechanism for clay-catalysed hydrogen exchange in a branched alkyl moiety (Alexander *et al.*, 1984).

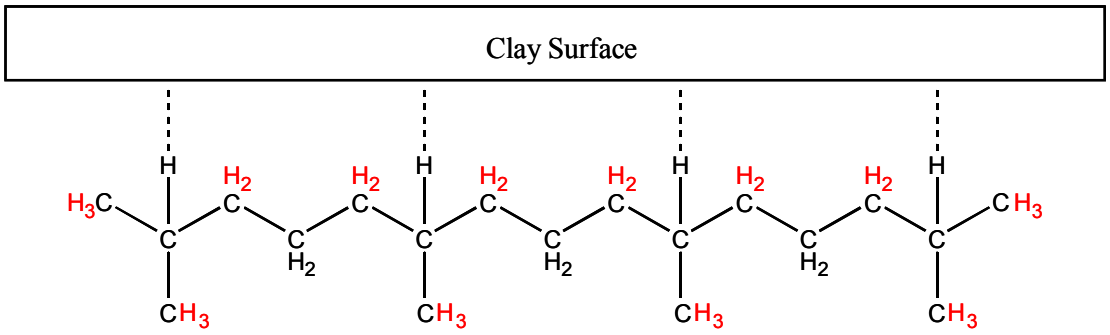

Figure 5.14 Adsorption of the tertiary C-bound hydrogen atoms in pristane onto a clay surface. The hydrogen in red is susceptible to exchange *via* the mechanism shown in Figure 5.13.

The possibility of hydrogen exchange occurring at various positions in the pristane molecule is supported by Hoering (1984), who reported a bimodal D-substitution profile with maxima at D_0 (no deuterium substitution) and D_7 (7 atoms of deuterium substituting for hydrogen), indicating there is different rates of exchange at two different sites in the molecule.

An overall hydrogen exchange mechanism suggested by Leif and Simoneit (2000) involved breakdown of kerogen *via* free radical hydrocarbon cracking to form *n*-alkanes and terminal *n*-alkenes, followed by rapid isomerisation of the terminal *n*-alkenes to internal *n*-alkenes *via* ionic acid-catalyzed isomerisation. The latter provides a mechanism for exchange taking place simultaneously at various sites along a carbon chain as suggested by Ross (1992) (see above). Upon saturation of the internal *n*-alkenes, *n*-alkanes with water-derived deuterium would be formed, preventing further exchange *via* isomerisation. A range of potential mechanisms of hydrogen exchange in moieties derived from a hypothetical kerogen molecule is displayed in Figure 5.15.

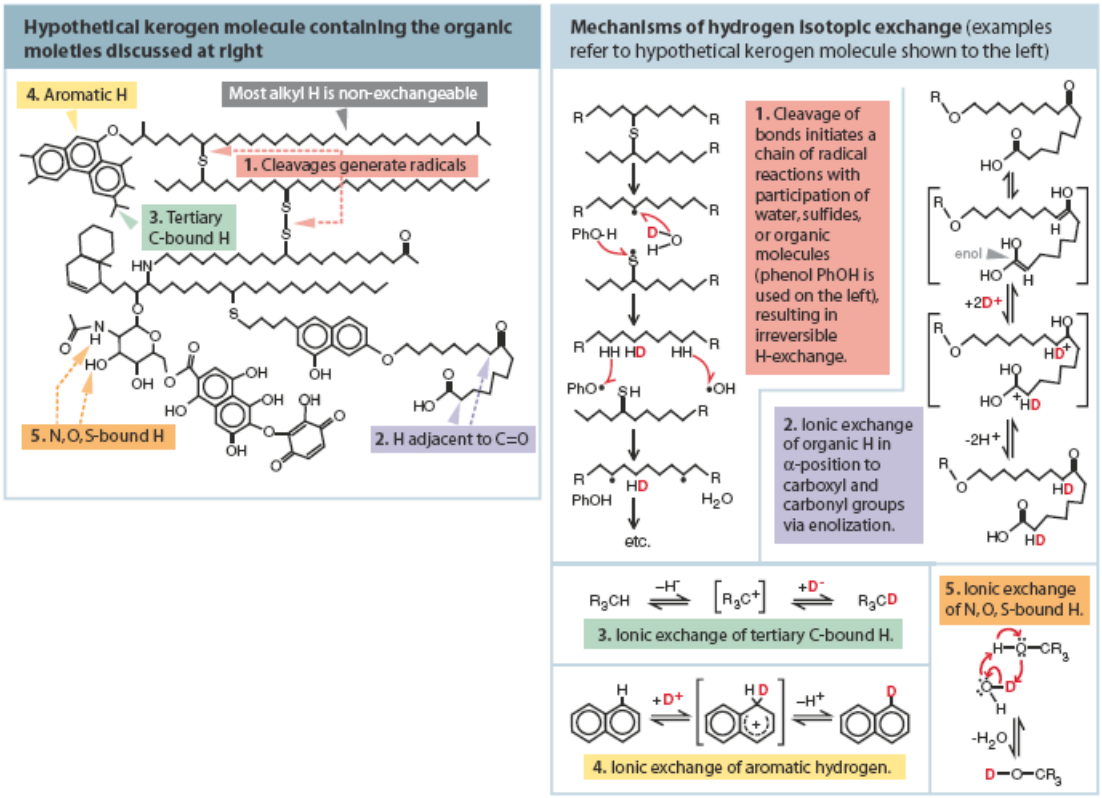

Figure 5.15 Potential mechanisms of hydrogen exchange in chemical moieties derived from kerogen including primary, secondary or tertiary aliphatic C-bound hydrogen; aromatic C-bound hydrogen; and N, O, S-bound hydrogen (Schimmelmann *et al.*, 2006).

5.2.6 Stereochemistry as a proxy for hydrogen exchange

Structural changes of molecules, such as stereochemical inversion or rearrangement of chiral compounds, could provide insight into the mechanism of hydrogen exchange in natural samples. The work by Alexander *et al.* (1984) proposes a mechanism for clay-catalysed alkyl hydrogen exchange (summarised above, Figure 5.13) where it is implicit that the clay-adsorbed intermediate is alkene-like and planar, but not free of the surface. This implies that, if the adsorbed hydrogen was attached to an asymmetric carbon, isomerisation of this chiral centre would not be possible. Indeed, Alexander *et al.* (1984) have shown that hydrogen exchange in pristane is most rapid at positions adjacent to tertiary carbon centres, indicating that the carbocation-like intermediate forms preferentially at the tertiary carbon and exchange is facilitated at the primary and secondary carbon atoms. No detectable exchange was observed at the tertiary carbons in pristane under the conditions used (see Sec. 5.1.1.1). To support the lack of exchange at tertiary carbons, Alexander *et al.* (1984) analysed the diastereomers of pristane using high-

resolution GC and found that there was no change in their relative abundance, indicating that no significant isomerisation had occurred at the two chiral carbons. However, pristane and phytane epimerisation appears to occur in sediments at a relatively fast rate (Patience *et al.*, 1978; Hansen *et al.*, 2003; this study). In order to study this further in natural systems, measurement of the ratios of the diastereomers of pristane and phytane in the Perth Basin and Vulcan Sub-basin sediment extracts was undertaken.

The pristane molecule is symmetrical, with two chiral centres at C-6 and C-10 giving rise to three diastereomers (**VI**), 6(*R*),10(*R*)-pristane (*RR*); 6(*S*),10(*S*)-pristane (*SS*) and 6(*R*),10(*S*)-pristane (*RS*, *meso*). All three can be found in sedimentary organic matter, but only *meso*-pristane retains the configuration of the precursor and the *RR* and *SS* enantiomers are suggested to form from the isomerisation of the *meso* compound during maturation (Patience *et al.*, 1978). For example, the immature Messel shale (Eocene, Germany) contains only *meso*-pristane, while the thermally mature Irati shale (Permian, Brazil) contains a 1:1 mixture of the *meso* and *RR*/*SS* isomers respectively (Patience *et al.*, 1978). Isomerisation of the chiral centres of pristane would inherently involve a hydrogen exchange process, and possible mechanisms are discussed in other sections (Sec. 5.2.5 and 5.2.6.3). Phytane has three chiral centres at C-6, C-10 and C-14, giving rise to eight diastereomers (**III**), with the eight possible configurations at the chiral centres being *RRR*, *SSS*, *RRS*, *SSR*, *RSR*, *SRS*, *SRR* and *RSS,* respectively. All eight have been reported to occur in sedimentary organic matter (Patience *et al.*, 1980). The diastereomers of pristane and phytane co-elute on GC columns using conventional techniques. The GC method used in this study (see Chapter 3) allowed partial separation of the diastereomers (Hansen *et al.*, 2003). This method was developed from the work of Cox *et al.* (1974), who similarly achieved partial peak separation of the diastereomers of pristane, and found that the two enantiomers *RR* and *SS* co-elute as the first peak and the *RS* isomer (*meso* compound) as the second (e.g. Figure 5.16a). Under the GC conditions used for this study, all eight diastereomers of phytane elute as two partially resolved peaks (e.g. Figure 5.16a), each presumably containing four diastereomers.

Hansen *et al.* (2003) studied the effects of maturation and biodegradation on the diastereomers of pristane and phytane. They introduced the parameters PrDR

(pristane diastereomer ratio) and PhDR (phytane diastereomer ratio). The former is calculated by dividing the area under the *meso*-pristane peak of the doublet by the area under the peak representing the *RR* and *SS* enantiomers formula (i.e. *RS*/(*RR*+*SS*). However, for the purpose of this study and for easier comparison to PhDR, we will represent PrDR as the area under the peak representing the *RR* and *SS* enantiomers divided by the area under the *meso*-pristane peak, i.e. (*RR*+*SS*)/*RS* (denoted as PrDR'). PhDR is calculated by dividing the area under the left peak by the area under the right peak of the phytane doublet (Hansen *et al.*, 2003).

It would be most suitable to use pristane rather than phytane for the purpose of monitoring relative abundances of diastereomers, since pristane has a lower number of isomers and their elution characteristics have been established. The diastereomer analysis of Perth Basin samples presented in Dawson *et al.* (2005a) denoted that the calculated PrDRs were anomalous, attributed partially to the lower chromatographic resolution of the pristane diastereomers relative to those of phytane (e.g. Figure 5.16a). The method of analysis has since been refined (see Chapter 3) resulting in an improvement of separation of the pristane (and phytane) diastereomers (compare Figure 5.16a and Figure 5.16b), therefore the samples have been re-analysed and the new data are presented herein.

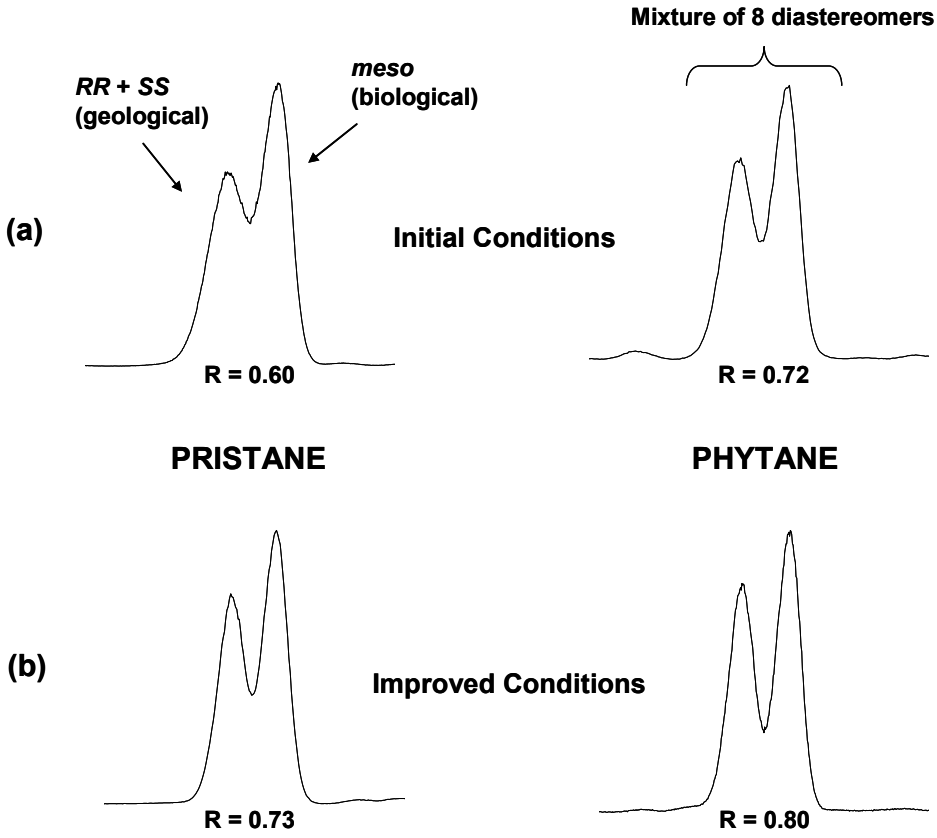

Figure 5.16 Separation of the diastereomers of pristane and phytane using gas chromatography. The conditions (also see Chapter 3) were (a) Column: SGE BP-5, 50 m x 0.15 mm i.d., 0.25 μm film thickness (f.t.); Temperature program: 50 to 145ºC at 1ºC min^{-1}, isothermal (60 min), then 145 to 290ºC at 5ºC min^{-1}, isothermal (15 min) (initial conditions); and (b) Column: J&W Scientific DB-5MS, 60 m x 0.25 mm i.d., 0.25 μm f.t.; Temperature program: 50 to 145ºC at 1ºC min^{-1}, isothermal (60 min), then 145 to 300ºC at 5ºC min^{-1}, isothermal (40 min) (improved conditions). Conventional chromatographic resolution (R) is calculated using the equation $R = [2(t_{R,X} - t_{R,Y})]/(W_{b,X} + W_{b,Y})$, where t_R is the retention time, and W_b is the peak width at baseline, of components X and Y.

Crocetane (**XVII**) is present in some sediment extracts and crude oils and has been shown to coelute with phytane (Barber *et al.*, 2001), and can therefore interfere with the calculation of PhDR. The Perth Basin sediments used for this study are known not to contain crocetane (K. Grice, pers. comm.), despite its previous identification in shallower (681.2–681.5m and 856.7–856.8m) BMR-10 (Perth Basin) bitumen (Greenwood and Summons, 2003), and several Perth Basin crude oils (Barber *et al.*, 2001; Greenwood and Summons, 2003). The Vulcan Sub-basin sediments are also known not to contain crocetane (K. Grice, pers. comm.).

5.2.6.1 Perth Basin sediments

The plots in Figure 5.17 show (a) PrDR' versus the δD value of pristane, and (b) PhDR versus the δD value of phytane, for each of the Perth Basin samples. With a progressive enrichment of D in pristane and phytane, PrDR' and PhDR increase and approach value of 1 from initial values of 0.71 and 0.77 respectively. The values increase in a linear fashion with a moderate-strong relationship (R^2 = 0.74 and 0.95 for PrDR' and PhDR respectively) up to PrDR' and PhDR values of 0.93 and 0.95, respectively for two late-mature samples. Patience *et al.* (1978) suggested that an equilibrium mixture of approximately 1:1 of the *RS* and *RR/SS* diastereomers of pristane would be reached as a result of conversion due to maturation. They suggested this loss of stereospecificity with increasing maturity to be analogous to that observed with hopanes. Using pristane as a model, an equilibrium mixture of the diastereomers of phytane can be expected in crude oils and mature sediments. In fact, Patience *et al.* (1980) separated the diastereomers of phytane in a crude oil into two partially resolved peaks with a 1:1 ratio, and Mackenzie *et al.* (1980) found that the extent of isomerisation of phytane with maturation appeared to be virtually identical to that of pristane.

The values of PrDR' and PhDR obtained from the immature Perth Basin sediments (0.71 and 0.77 respectively) suggest that significant epimerisation has already occurred. For example, a PrDR' of 0.71 indicates that the diastereomer mixture consists of approximately 40% of the *RR and SS* isomers and 60% of the *meso* isomer. Hence, there has been approximately 70% conversion of *meso*-pristane to *RR*- and *SS*-pristane in these immature samples, even though pristane appears to have largely retained the isotopic composition of its precursor (see Sec. 5.2.3.1). The degree of conversion approaches 85–90% at an early mature level. Indeed, the extent of isomerisation would suggest significant hydrogen exchange has occurred and thus significant scrambling of indigenous δD signatures would be expected. This is not the case with immature and early mature Perth Basin samples (Sec. 5.2.3.1).

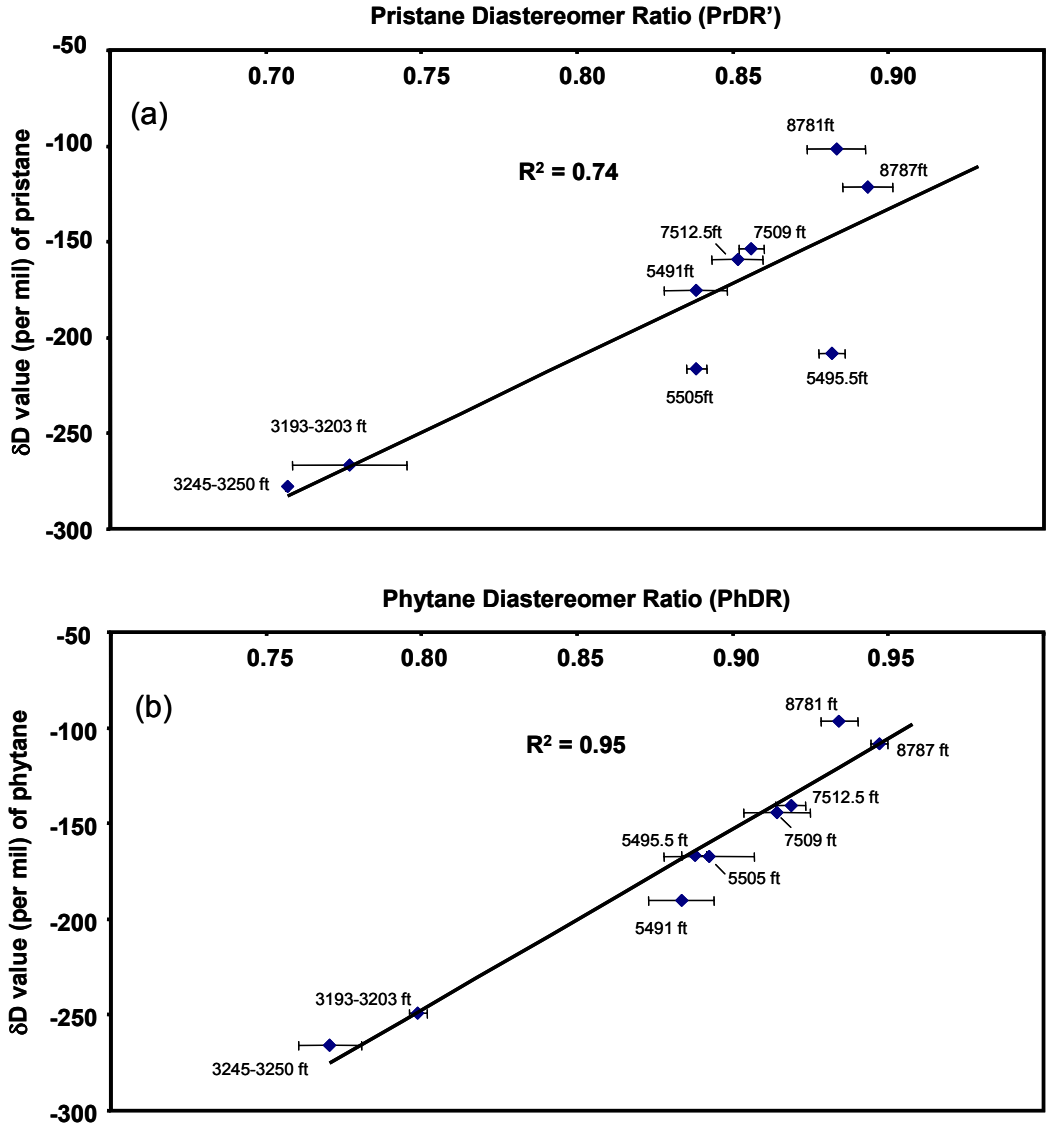

Figure 5.17 Plot of (a) the δD value of pristane versus the pristane diastereomer ratio (PrDR') and (b) the δD value of phytane versus the phytane diastereomer ratio (PhDR) for the Perth Basin samples.

5.2.6.2 Vulcan Sub-basin sediments

The plots in Figure 5.18 show (a) PrDR' versus the δD value of pristane, and (b) PhDR versus the δD value of phytane, for the Paqualin-1 and Vulcan-1B sediment extracts, superimposed on the data obtained from the Perth Basin sediment extracts. It is evident that both PrDR' and PhDR for the Vulcan Sub-basin sediments plot in the top right-hand area of the chart, indicating significant epimerisation of pristane and phytane in these samples. Indeed, 85–90% epimerisation of pristane and phytane is evident in the least mature sample in the Vulcan Sub-basin set (early mature, $\%R_o$

= 0.62). This is consistent with results obtained from the Perth Basin samples (Sec. 5.2.6.1), where 85–90% epimerisation had also occurred in early mature samples.

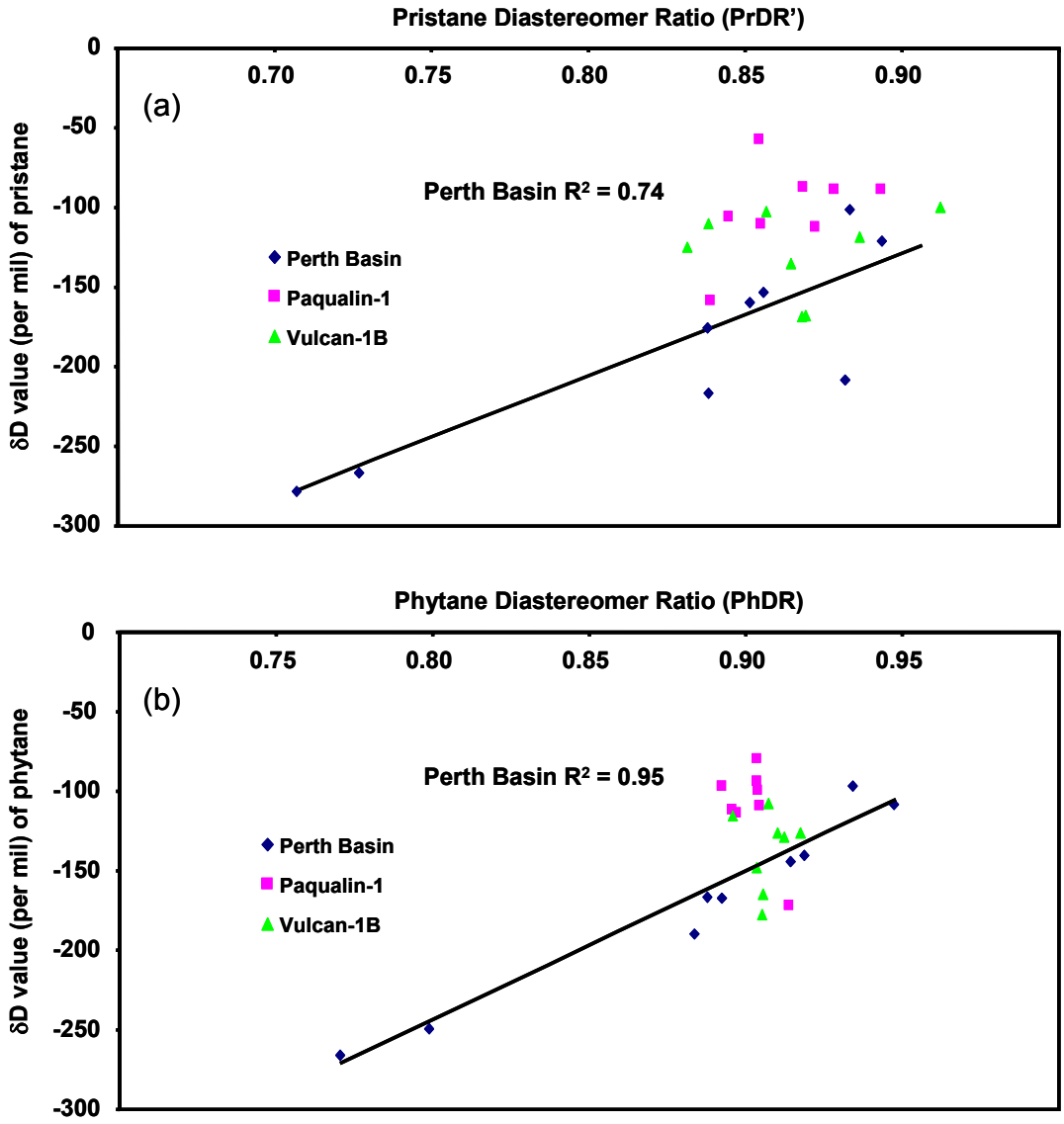

Figure 5.18 Plot of (a) the δD value of pristane versus the pristane diastereomer ratio (PrDR') and (b) the δD value of phytane versus the phytane diastereomer ratio (PhDR) for the Vulcan Sub-basin sediment extracts, superimposed on the data obtained from the Perth Basin sediment extracts.

5.2.6.3 Mechanism

The analysis of the diastereomers of pristane and phytane described above confirms that significant epimerisation of the natural pristane and phytane diastereomers occurs relatively early in the maturation process. However, the δD

values of pristane and phytane in immature samples suggest that they retain the isotopic composition of their precursors (Sec. 5.2.3).

Isomerisation of the chiral centres of optically active compounds inherently involves a hydrogen exchange process. A mechanism proposed by Patience *et al.* (1978) for the isomerisation of pristane, similar to that suggested by Ensminger (1977) for the loss of stereospecificity of hopanes, involves abstraction by a carbocation of a hydride ion at the chiral carbon, with the carbocation being formed in the presence of a Lewis acid catalyst (e.g. clay mineral) and a proton donor. The resulting tertiary carbocation could then isomerise and abstract a hydride ion from a donor molecule to form a different diastereomer. Alternatively, the isomerised carbocation could lose H^+ to form an alkene, and then reduction at the appropriate position would give the same net result (Patience *et al.*, 1978). Presumably, the same mechanism would be applicable to the isomerisation of phytane. The experiments performed by Alexander *et al.* (1984) indicated that a free carbocation was not formed and there was no increase in the abundance of the *RR* or *SS* diastereomers relative to the *meso* isomer. This clearly showed that under the conditions where appreciable exchange was shown to occur at both primary and secondary carbons, no significant isomerisation had occurred at the two chiral centres. The absence of epimerisation, and therefore (presumably) hydrogen exchange at the tertiary carbons in pristane, is not consistent with observations from the natural geochemical maturation of sedimentary organic matter (Patience *et al.*, 1978; Hansen *et al.*, 2003; this study). Thus, a mechanism is proposed which can account for both hydrogen exchange and epimerisation in the sedimentary environment (Figure 5.19), extending on the work by Alexander *et al.* (1984).

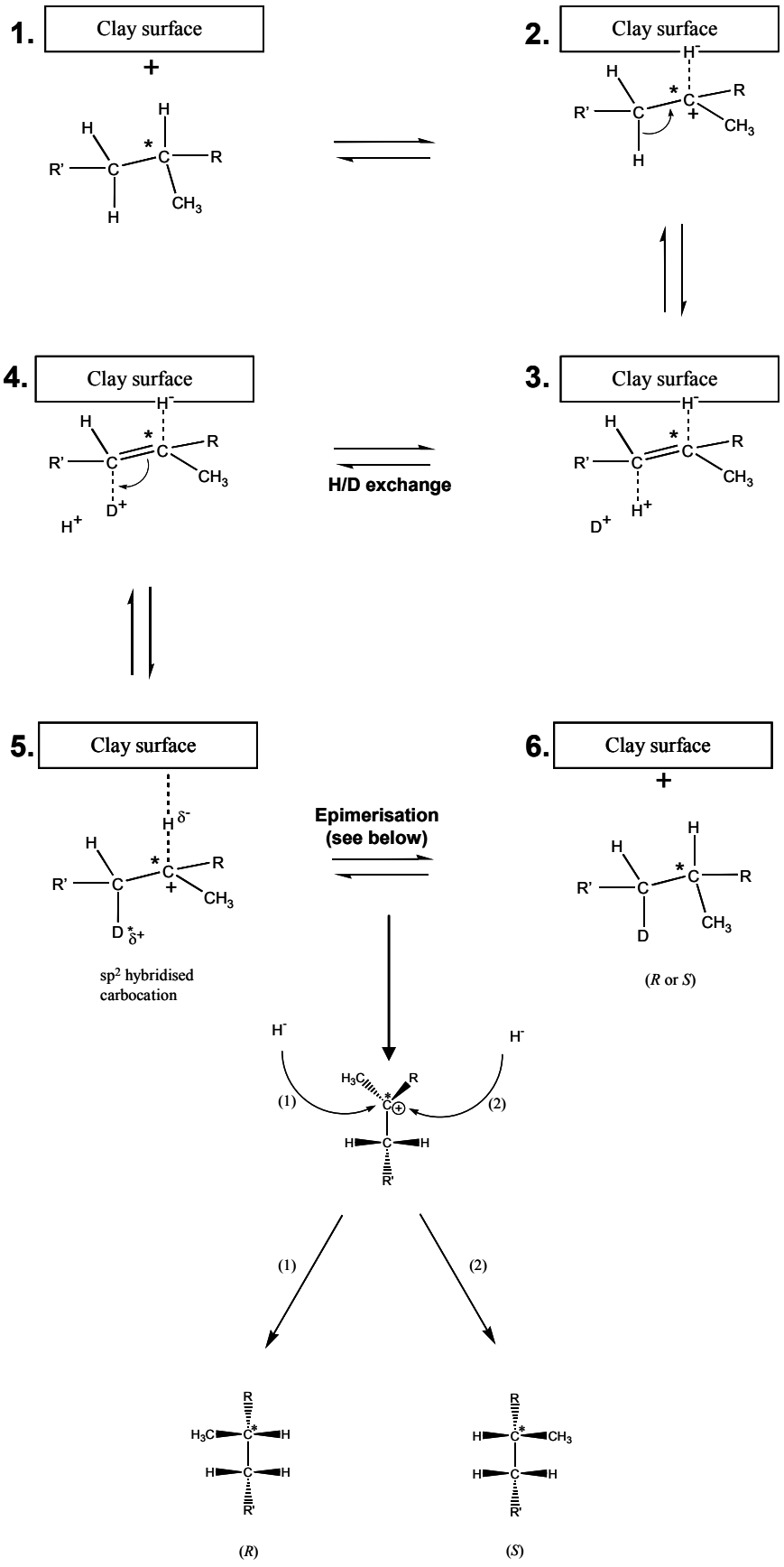

Figure 5.19 Mechanism of hydrogen exchange (after Alexander *et al.*, 1984), and epimerisation of a chiral centre, where R' ≥ R in terms of substituent priority, and R ≠ CH_3. * denotes a chiral centre.

In the proposed mechanism (refer to Figure 5.19), a chiral compound approaches the clay surface (1) and one of the hydrogen atoms bound to the tertiary (chiral) carbon adsorbs to the positively-charged clay surface (2). This permits a positive charge to develop at the tertiary carbon, facilitating the formation of an intermittent alkene structure (3). The hydrogen attached to the carbon adjacent to the tertiary carbon may then detach, and exchange with other ^{1}H or D atoms in the system (4). The resulting sp^2 hybridised tertiary carbocation (5) may then undergo ^{1}H (or D) reattachment resulting in additional hydrogen exchange along with epimerisation of the chiral centre (6).

In summary, while significant epimerisation of pristane (e.g. 70–75% conversion of *meso*-pristane to *RR/SS*-pristane) and phytane appears to occur early in maturation, continuing epimerisation (from 80–95% conversion) has been shown to be directly related to a progressive enrichment of D in pristane and phytane with increasing maturity (from immature to late mature). However, the epimerisation mechanism appears not to be a significant process in altering the δD values of pristane and phytane during early maturation. Two immature Perth Basin samples ($\%R_o$ = 0.53), after 70–75% epimerisation, contain pristane with a δD value indicative of the precursor. Perhaps H/D exchange and epimerisation proceed *via* different mechanisms during the early stages of maturation.

5.3 SIGNIFICANCE

The δD values of the *n*-alkanes, pristane and phytane (and presumably other hydrocarbons) are affected by thermal maturation. The hydrocarbons become enriched in D (*via* hydrogen exchange) with increasing maturity, with the isoprenoids becoming enriched more rapidly than the *n*-alkanes. The results provide an insight into chemical processes which may occur in the subsurface during petroleum formation and generation. In addition, the results suggest that δD values of individual hydrocarbons may be used to assess the thermal maturity of sedimentary organic matter. Finally, the results further emphasize the care needed when interpreting δD values of hydrocarbons in sediments of high thermal maturity, particularly those hydrocarbons with a high reactivity towards H-exchange. It is

suggested that samples retaining an offset between the δD values of *n*-alkanes and isoprenoids will have relatively well preserved D/H compositions.

5.4 SUMMARY AND CONCLUSIONS

1. The δD values of *n*-alkanes from low maturity sediments (immature-early mature) are consistent with that expected for predominantly marine-derived organic matter, i.e. the Kockatea Shale, a marine sequence of shale and siltstone of the Perth Basin, and marine mudstones of the lower Vulcan Formation in the Vulcan Sub-basin.

2. The *n*-alkanes, pristane and phytane of immature sediments have δD values that represent the expected isotopic composition of their precursors, i.e. biosynthesised *n*-alkyl and isoprenoid lipids. With increasing maturity, pristane and phytane become rapidly enriched in D while the *n*-alkanes generally remain at a constant isotopic composition, until a mature-late mature level is reached where there is a significant enrichment of D in *n*-alkanes. The enrichment of D in hydrocarbons from Paqualin-1 appears to occur at lower maturity (based on R_o) compared to Vulcan-1B and Perth Basin sediments. In particular, the shallowest to the next Paqualin-1 sample shows a significant enrichment of D in isoprenoids. This is not consistent with the results obtained for samples of corresponding maturity from Vulcan-1B and the Perth Basin, thus it appears that the deeper Paqualin-1 sediments are more mature than suggested by R_o values. Alternatively, the isoprenoids from the least mature Paqualin-1 sample may derive from an additional, relatively D-depleted source. Pristane and phytane extracted from a post-mature Paqualin-1 sediment are significantly enriched in D relative to the *n*-alkanes, indicating that rapid D-enrichment in regular isoprenoids continues at very high maturity. This is not consistent with published equilibrium fractionation factors between C-bound hydrogen and water for primary, secondary and tertiary C-H. It also suggests that free-radical hydrogen transfer is unlikely to have caused the observed shift in δD values of isoprenoids

and *n*-alkanes, and instead supports a hydrogen exchange process which occurs preferentially at primary and secondary carbons in isoprenoids.

3. Phytane is enriched relative to pristane in extracts of immature Perth Basin sediments, and this signature is retained with ongoing maturation, indicating the two isoprenoids exchange hydrogen at similar rates. In the Vulcan Sub-basin, pristane is enriched in D relative to phytane throughout the maturity range, opposite to that observed in the Perth Basin. The differences in δD values of pristane and phytane are suggested to be due to different isotopic effects during their derivation from a common precursor, or different sources for the isoprenoids. The differences observed between the basins may be attributed to a dominant algal source for organic matter in the Perth Basin, with the Vulcan Sub-basin having a lower relative algal input.

4. The enrichment of D in pristane and phytane with increasing maturity correlates strongly with changes in traditional maturity parameters, providing further evidence that D-enrichment is associated with thermal maturation.

5. Significant epimerisation of pristane and phytane during early maturation suggests that hydrogen exchange occurs at the tertiary carbons of these hydrocarbons, and that a free carbocation is formed in the process. However, the epimerisation mechanism does not appear to be a significant process in altering the δD values of pristane and phytane during early maturation, since immature samples contain pristane and phytane with δD values which are thought to represent isotopic composition of their precursor(s). In the studied range of maturity in the Perth Basin, the pristane and phytane diastereomer ratios (PrDR' and PhDR, respectively) correlate linearly with the progressive enrichment of D in pristane and phytane. The evidently more mature Vulcan Sub-basin sediments have PrDRs and PhDRs which were all close to equilibrium values.

6. A mechanism has been proposed which can account for both H/D exchange, and epimerisation of pristane and phytane in the sedimentary environment. Upon interaction with a clay surface, a chiral compound forms an intermittent alkene structure *via* a tertiary carbocation-like species. The hydrogen attached to the carbon adjacent to the tertiary carbon may then detach, and exchange with other

^{1}H or D atoms. Then the resulting sp^2 hybridised tertiary carbocation undergoes ^{1}H (or D) reattachment resulting in additional hydrogen exchange along with epimerisation of the chiral centre.

CHAPTER 6

6 STABLE HYDROGEN ISOTOPIC COMPOSITIONS OF HYDROCARBONS FOR OIL-SOURCE CORRELATION IN AUSTRALIAN PETROLEUM SYSTEMS

6.1 INTRODUCTION

Oil-source rock correlations are based on the principle that certain compositional parameters of migrated crude oils are comparable to those of the bitumen remaining in their source rocks (Peters and Moldowan, 1993). To achieve a robust correlation, a combination of geochemical parameters are commonly used (e.g. Sec. 6.1.1 and 6.1.2). Typically, molecular distributions, and/or stable carbon isotopic compositions ($\delta^{13}C$) of *n*-alkanes, have been used to determine whether a genetic relationship exists between crude oils and potential source rocks (e.g. Seifert and Moldowan, 1978; Seifert and Moldowan, 1981; Mackenzie *et al.*, 1982; Summons *et al.*, 1995; Boreham *et al.*, 2001; Edwards *et al.*, 2004; Thomas and Barber, 2004).

The ability to accurately correlate a crude oil to its source rock is important in petroleum exploration and production. Oil-source correlations can be used to establish and constrain petroleum systems, and in turn improve exploration success. There have been only a few reported cases where hydrogen isotopic compositions of individual compounds have been used for oil-source correlation purposes, thus the robustness of the technique has not been rigorously tested. The present study aims to further investigate the potential of δD values of individual compounds in crude oils and source rock extracts as an oil-source correlation tool. In this chapter, the application of δD values of individual petroleum hydrocarbons for oil-source correlation purposes is presented. Crude oils from the Perth Basin (Western Australia) and the Vulcan Sub-basin (offshore, Northern Australia) were analysed to evaluate their source and thermal maturity and complement previous reported work based on molecular distributions and stable carbon isotopic analysis (Summons *et al.*, 1995; Boreham *et al.*, 2000; Boreham *et al.*, 2001; Edwards *et al.*, 2004).

6.1.1 Correlation based on molecular distributions

Oil-source correlation based on molecular distributions is commonly achieved using gas chromatography-mass spectrometry to analyse hydrocarbon fractions from crude oils and source rock extracts (e.g. Seifert and Moldowan, 1978; Seifert and Moldowan, 1981; Mackenzie *et al.*, 1982; Peters and Moldowan, 1993; Peters *et al.*, 2005). The distributions of compound classes such as *n*-alkanes, hopanes, steranes and alkylaromatics (e.g. naphthalenes and phenanthrenes), and specific biomarker compounds (e.g. isorenieratane; see Chapter 1) can be used for correlation purposes. Molecular parameters are routinely used for oil-oil and oil-source correlations, but also as indicators for maturation, biodegradation and depositional environments.

Oil-prone, lacustrine and marine source rocks (Type I and II, respectively) generate crude oils containing an abundance of biomarkers useful for oil-source correlation. However gas-prone, coaly source rocks (Type III) generate gases and/or condensates consisting of mainly gasoline-rage hydrocarbons. Biomarkers and other high-molecular-weight components are commonly present in low quantities or absent in condensates, making oil-source correlation using molecular parameters difficult or impossible. In these cases the $\delta^{13}C$ values of *n*-alkanes are often useful for oil-source correlation (Sec. 6.1.2).

6.1.2 Correlation based on stable carbon isotopic composition

The $\delta^{13}C$ of sedimentary organic matter has been used to study secular change in the global carbon cycle (e.g. Chung *et al.*, 1992; Summons *et al.*, 1995; Andrusevich *et al.*, 1998). These secular changes in the geological past have resulted in changes in the $\delta^{13}C$ of inorganic carbon sources (e.g. CO_2) available for photosynthesis. Indeed, the $\delta^{13}C$ of sedimentary organic matter is dependent on the $\delta^{13}C$ of atmospheric CO_2 (Hayes, 1993) and other factors (see Chapter 1). Therefore, $\delta^{13}C$ values of petroleum hydrocarbons often relate to the age (time of deposition) of their source rock (e.g. Chung *et al.*, 1992; Summons *et al.*, 1995; Andrusevich *et al.*, 1998).

Isotopic compositions can be determined using either bulk isotope analysis or compound-specific isotope analysis (see Chapter 1). Bulk isotopic analysis of organic carbon has been used to classify marine and non-marine (terrestrial) crude oils by plotting the bulk $\delta^{13}C$ values of the C_{15+} saturate fractions versus those of

their aromatic fractions (e.g. Figure 6.1; AGSO and GEOMARK Research Inc., 2001), and to infer genetic relationships between lipids in living organisms and their diagenetic products (Sofer, 1984). Chung *et al.* (1992) classified 621 post-Ordovician marine crude oils into four groups, in terms of their depositional environment and the geological age of their source, on the basis of $\delta^{13}C$ values (in conjunction with pristane/phytane ratios and sulfur contents). More recently, Andrusevich *et al.* (1998) reported bulk $\delta^{13}C$ values of the C_{15+} saturate and aromatic hydrocarbon fractions of 514 crude oils, and found that both fractions become enriched in ^{13}C with decreasing geological age including three major shifts at the Cambrian/Ordovician, Triassic/Jurassic and Paleogene/Neogene boundaries.

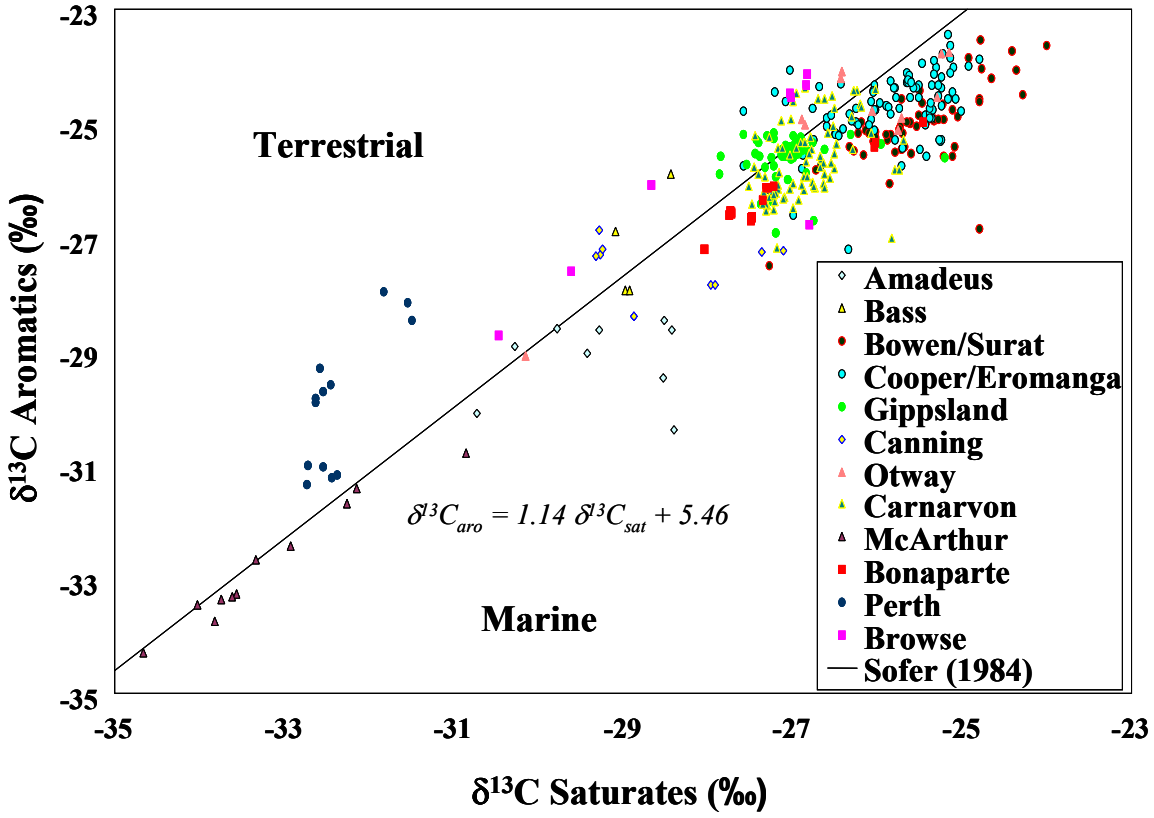

Figure 6.1 Plot of the $\delta^{13}C$ value of C_{15}+ aromatic fractions versus the $\delta^{13}C$ value of C_{15}+ saturated fractions (Sofer plot) for several hundred crude oils from various Australian sedimentary basins (AGSO and GEOMARK Research Inc., 2001)

Although bulk $\delta^{13}C$ analysis can be useful in oil-source correlations, it does not allow the isotope signature of specific source components to be identified. Isotopic analysis of organic carbon in individual compounds (CSIA, see Chapter 1) is a more powerful tool in the analysis of petroleum, because the $\delta^{13}C$ values of individual

sedimentary hydrocarbons provide evidence for their diverse origins (e.g. Freeman *et al.*, 1990; Hayes *et al.*, 1990; Grice *et al.*, 1996; Schouten *et al.*, 1998). The $\delta^{13}C$ values of *n*-alkanes (together with biomarker distributions) have been used on numerous occasions for oil-source correlations. For example, a suite of crude oils from the Perth Basin (Western Australia) have been classified based on the age of their source (see Sec. 6.2.2.1), with the majority of oils from the northern on-shore part of the basin having been attributed to an Early Triassic source rock (Summons *et al.*, 1995; Thomas and Barber, 2004). Edwards *et al.* (2004) categorised a series of Vulcan Sub-basin crude oils and condensates into two end-member groups, based on different relative inputs of marine and terrestrial organic matter to the oils (see Sec. 6.2.2.2).

The average $\delta^{13}C$ value of the *n*-alkanes in some cases may be indicative of the $\delta^{13}C$ value of the bulk crude oil, considering they are (generally) a quantitatively important component of oils. In these cases, compound-specific *n*-alkane data may not provide any additional information than bulk isotopic analysis. However in many cases, certain *n*-alkanes in crude oils vary significantly in $\delta^{13}C$ as a result of their derivation from a diverse range of isotopically-distinct precursors. Thus, the profile of $\delta^{13}C$ values of *n*-alkanes within oils can vary in response to variations in source inputs, which can be very useful in oil-source correlations. $\delta^{13}C$ analysis has been used effectively in the past to study the origin of *n*-alkanes in source rocks and crude oils. Murray *et al.* (1994) stated that the shape of *n*-alkane $\delta^{13}C$ profiles in crude oils is primarily determined by their source rock's depositional setting. For example, negatively-sloping *n*-alkane $\delta^{13}C$ profiles are characteristic of crude oils derived from fluvio-deltaic and freshwater transitional depositional environments, attributed to an abundance of terrestrial plant matter in the source (Murray *et al.*, 1994). Relatively flat or positively-sloping profiles are typical of marine and lacustrine-sourced crude oils (Murray *et al.*, 1994; Summons *et al.*, 1995; Xiong *et al.*, 2005). Variations in the *n*-alkane $\delta^{13}C$ profiles of oils can indicate contributions from multiple source-types. The profile of *n*-alkane $\delta^{13}C$ values can also be affected by secondary processes such as thermally-induced hydrocarbon cracking (e.g. Tang *et al.*, 2005), in-reservoir mixing of different oils (e.g. Rooney *et al.*, 1998) and migration contamination, and these factors must be taken into account when interpreting *n*-alkane $\delta^{13}C$ profiles in crude oils.

6.1.3 Aims of this study

The specific aims of the present study include:

(i) Fractionation of the Perth Basin and Vulcan Sub-basin crude oils and condensates, including isolation of *n*-alkanes from branched and cyclic compounds. Measurement of the δD values of *n*-alkanes, pristane and phytane.

(ii) Measurement of the bulk δD values of the whole crude oils and condensates, for comparison to the compound-specific isotopic results.

(iii) Interpretation of results based on the source (e.g. depositional environment, facies), maturity, and the effect of other secondary processes (e.g. in-reservoir mixing) on the Perth Basin and Vulcan Sub-basin crude oils and condensates.

(iv) Comparison of results obtained from the crude oils to those obtained from their supposed source rocks.

6.2 RESULTS AND DISCUSSION

6.2.1 Geochemistry

6.2.1.1 Perth Basin crude oils

The Perth Basin crude oils and condensates used in this study have been analysed previously by Summons *et al.* (1995), Boreham *et al.* (2000), Thomas and Barber (2004) and Grice *et al.* (2005b). Summons *et al.* (1995) used the $\delta^{13}C$ values of *n*-alkanes in combination with the distributions of diagnostic biomarkers in a suite of Perth Basin crude oils for oil-source correlation in the northern on-shore Perth Basin. These parameters allowed classification of the Perth Basin oils according to the geological age of their source. The marine-derived Dongara-14 crude oil and East Lake Logue-1 condensate from the Early Triassic Kockatea Shale have relatively low Pr/Ph ratios (Table 6.1; Appendix 1) consistent with deposition of their source rock in an anoxic setting. The Perth Basin crude oils have varying quantities of rearranged

steranes (diasteranes) and rearranged hopanes (diahopanes), attributed to local lithological and maturity differences (Summons *et al.*, 1995).

A C_{33} *n*-alkylcyclohexane (C_{33}ACH) is present in the Woodada-3 and Dongara-14 crude oils. This compound was formally identified by McIldowie and Alexander (2005) as *n*-heptacosylcyclohexane (**XVIII**). This biomarker has been found in high relative abundance in a lower Triassic source rock (Hovea Member, Kockatea Shale) and associated crude oils from the northern onshore Perth Basin (Jefferies, 1984; Summons *et al.*, 1995; Thomas and Barber, 2004), and in a Permian-Triassic marine section from Eastern Greenland (Grice *et al.*, 2005c). A specific source of the C_{33}ACH has not been identified, although it has been suggested to be a biomarker for the Permian-Triassic mass extinction, possibly derived from a phytoplankton source that first bloomed during the extinction interval, and thrived in the aftermath (Grice *et al.*, 2005c). In the Perth Basin, the C_{33}ACH is thought to be characteristic of organic matter derived from the Kockatea Shale, although its absence is equivocal (Boreham *et al.*, 2000). The biomarker was not found in any significant amounts in the East Lake Logue-1 condensate, also thought to be derived from organic matter in the Kockatea Shale.

Boreham *et al.* (2000) plotted three aromatic maturity ratios for the Perth Basin crude oils: TMNr (trimethylnaphthalene ratio), TeMNr (tetramethylnaphthalene ratio) and PMNr (pentamethylnaphthalene ratio) in a ternary diagram (van Aarssen *et al.*, 1999) (Figure 6.2; Appendix 1) All crude oils plot near the centre of the diagram, within the so-called 'maturity centre' (van Aarssen *et al.*, 1999). The maturity centre is defined as the area within a 10% margin around a single point on the diagram representing a case where TMNr, TeMNr and PMNr are determined only by thermal stress. Samples that deviate from the maturity centre are affected by additional secondary processes (see Appendix 1). Based on the ternary plot of the naphthalene parameters (Figure 6.2), it was determined that the Perth Basin crude oils had not been affected to any large extent by in-reservoir mixing of oils of different maturities, by biodegradation, or by migration contamination (Boreham *et al.*, 2000).

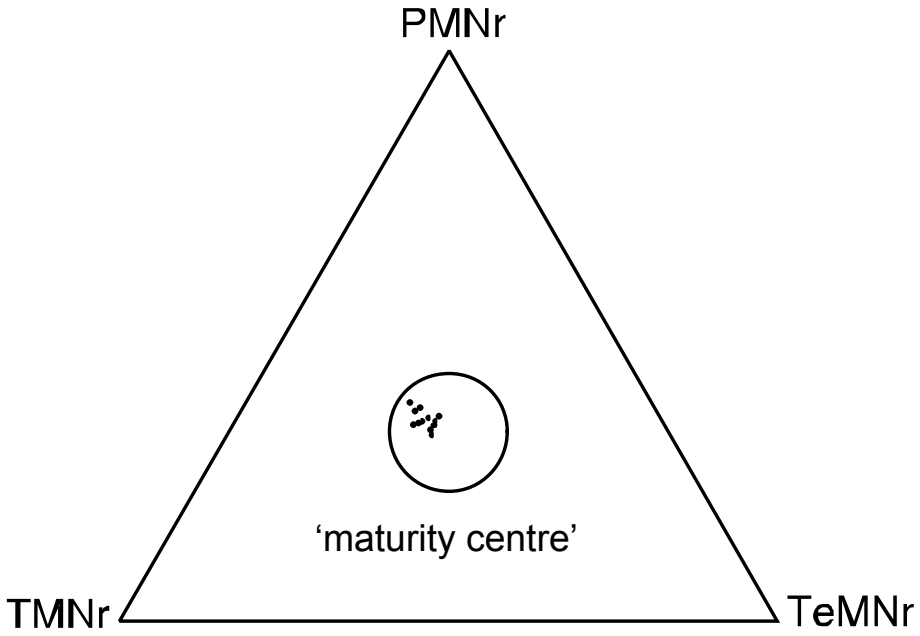

Figure 6.2 Ternary plot of the trimethylnaphthalene ratio (TMNr), tetramethylnaphthalene ratio (TeMNr), and pentamethylnaphthalene ratio (PMNr) for a suite of Perth Basin crude oils including those used for this study (Boreham *et al.*, 2000). All oils are inside the 'maturity centre'

Thomas and Barber (2004) performed a comprehensive oil-source correlation in the northern Perth Basin, based on biomarker distributions, and stable carbon isotopic analyses. A series of discriminating features included *n*-alkane profiles (Appendix 1), Pr/Ph ratios, sterane distributions, tricyclic and tetracyclic terpane distributions, *n*-alkane $\delta^{13}C$ profiles, the presence of C_{33}ACH, and the occurrence of a series of rare aromatic biomarkers including phytanyltoluene and long-chain alkylnaphthalenes (Thomas and Barber, 2004). It was concluded that the majority of crude oils and condensates from the northern Perth Basin were sourced from the Hovea Member (Sapropelic Interval) of the Kockatea Shale, with an exception being the Woodada-3 crude oil which was believed to be derived from a mixture of Triassic and Permian sources. The presence of the C_{33}ACH, together with a distinct sterane distribution and waxy *n*-alkane distribution (Summons *et al.*, 1995) for Woodada-3 indicate a contribution from the Early Triassic Hovea Member (Thomas and Barber, 2004). However the *n*-alkane $\delta^{13}C$ profile (Sec. 6.2.2.1) and relatively high Pr/Ph ratio (2.5) suggest a contribution from a Permian source.

Grice *et al.* (2005b) established an oil-source correlation for the northern onshore Perth Basin based on unusual aromatic and polar biomarkers, which were attributed ultimately to a green sulfur bacterial (GSB) source. The GSB biomarkers were

identified in Early Triassic sediments from a drill core (Hovea-3) in this part of the basin (Grice *et al.*, 2005a). Crude oils (e.g. Dongara) and condensates previously associated with the Early Triassic source rock in the northern onshore Perth Basin (Summons *et al.*, 1995; Boreham *et al.*, 2000; Thomas and Barber, 2004) were also found to contain GSB biomarkers (Grice *et al.*, 2005a; 2005b). This provided additional evidence for photic zone euxinic depositional conditions for the Early Triassic source rock. Other crude oils and condensates, including Gage Roads-1 (crude oil), contained no trace of GSB biomarkers (Grice *et al.*, 2005a; 2005b). Indeed, Gage Roads-1 is reservoired in a different geological province (Vlaming Sub-basin, southern offshore Perth Basin), and is thought to be derived from sources in the Jurassic Yarragadee Formation and Cattamarra Coal Measures (Summons *et al.*, 1995).

Table 6.1 Various geochemical parameters for the Perth Basin crude oils and condensates used in this study

Well	HPI	Pr/Ph	C_{33}ACH
Whicher Range-1	0.13	3.3	absent
Woodada-3	0.72	2.5	present
East Lake Logue-1	0.12	1.7	absent
Dongara-14	n.d.	1.3	present
Gingin-1	0.18	2.6	absent
Walyering-2	0.13	2.9	absent
Gage Roads-1	0.67	2.9	absent

HPI, Higher plant index (Appendix 1); Pr/Ph, pristane to phytane ratio; C_{33}ACH, C_{33} *n*-alkylcyclohexane; n.d., not determined

6.2.1.2 Vulcan Sub-basin crude oils

Organic geochemical analysis of the Vulcan Sub-basin crude oils has been carried out previously by Edwards *et al.* (2004) and Liu *et al.* (2005). Based on molecular analysis (Edwards *et al.*, 2004), and total scanning fluorescence spectral signatures (Liu *et al.*, 2005), the Vulcan Sub-basin crude oils and condensates were separated into two end member groups (A and B). Group A oils are characterised by a high proportion of lower-molecular-weight compounds where the *n*-C_{7+} alkanes

maximise at around *n*-C_{10} (e.g. Challis, Jabiru, Tenacious). Group B oils have a high proportion of waxy (>C_{22}) *n*-alkanes maximising at *n*-C_{17} or higher (e.g. Montara, Bilyara; Edwards *et al.*, 2004). Oils possibly derived from multiple sources were thought to be those at Audacious, Oliver, Puffin and Tahbilk (Edwards *et al.*, 2004). Group A oils were correlated with Late Jurassic marine mudstones of the Lower Vulcan formation, while Group B oils were suggested to be sourced from the Middle Jurassic fluvio-deltaic mudstones of the Plover Formation, and have a significant component of terrestrially-derived organic matter.

Group A and B oils have also been discriminated using some source-specific terpane and sterane biomarker parameters (Edwards *et al.*, 2004). For example, the Group A oils have lower C_{19}/C_{23} tricyclic terpane ratios relative to Group B oils, indicative of a stronger marine influence. In addition, there is a greater abundance of the algal-derived C_{27} sterane within the Group A oils compared to the Group B oils. The Group A and B oils and condensates are all characterised by dominant C_{30} hopanes, and minor differences in the C_{27}–C_{35} hopane series are evident between Groups A and B. The classification of Group A and B oils is largely supported by Total Scanning Fluorescence spectral signatures (Liu *et al.*, 2005).

The ratios of C_{27} diasterane/C_{27} sterane versus C_{30} diahopane/C_{30} hopane for the Vulcan Sub-basin oils and condensates used in this study (or samples from representative wells) are listed in Table 6.2 and plotted in Figure 6.3. Diasterane/sterane and diahopane/hopane ratios (Appendix 1) generally increase with increasing maturity. The Group A oils show a trend of increasing maturity in the order of Birch, Challis, Cassini, Tenacious and Jabiru (Figure 6.3). There is also a trend of increasing maturity in Group B oils from Montara to Bilyara. Audacious-1 (mixed oil) appears to be the most mature, while Tahbilk-1 (mixed oil) appears to be the least mature. The relatively high abundance of rearranged steranes and rearranged hopanes in general in the Vulcan Sub-basin oils and condensates (Edwards *et al.*, 2004) is indicative of their derivation from a clay-rich source rock (Peters and Moldowan, 1993).

The naphthalene parameters TMNr, TeMNr and PMNr (van Aarssen *et al.*, 1999) for selected Vulcan Sub-basin crude oils and condensates (or samples from representative wells) are listed in Table 6.2, and a ternary plot of the parameters is shown in Figure 6.4. The majority of the Vulcan Sub-basin oils plot within the maturity centre (Edwards *et al.*, 2004). However, Tenacious-1 plots slightly away

from the centre towards the TMNr corner, indicating mixing with more mature hydrocarbons (Edwards *et al.*, 2004). In a 1:1 mixture of a high maturity and low maturity oil, the distribution of TMNs will largely reflect the larger relative contribution of TMNs from the high maturity oil to the mixture (van Aarssen *et al.*, 1999). The TMNr, TeMNr and PMNr values generally indicate medium to high levels of maturity.

Table 6.2 Various geochemical parameters for the Vulcan Sub-basin crude oils and condensates used in this study (Edwards *et al.*, 2004).

Well name (classification*)	19T/23T	27diaS/27S	30diaH/30H	TMNr	TeMNr	PMNr
Birch-1 (A)	0.83	1.89	0.17	n/a	n/a	n/a
Cassini-1 (A)	0.96	1.97	0.21	n/a	n/a	n/a
Jabiru-2/1A# (A)	0.98	4.11	0.41	0.77	0.70	0.47
Tenacious-1 (A)	0.66	3.50	0.33	0.70	0.60	0.39
Challis-1/2A# (A)	1.04	2.14	0.20	0.73	0.62	0.43
Oliver-1 (A+B)	1.08	5.38	0.39	n/a	n/a	n/a
Montara-1/2# (B)	2.14	2.91	0.21	0.82	0.78	0.55
Bilyara-1 (B)	1.79	5.30	0.38	0.82	0.78	0.55
Tahbilk-1 (A+?)	0.66	1.27	0.06	0.79	0.74	0.59
Puffin-2 (A+?)	0.69	2.16	0.26	0.71	0.62	0.43
Audacious-1 (A+?)	1.29	6.93	0.49	n/a	n/a	n/a

* Classification based on work by Edwards *et al.* (2004) where A = high marine influence, B = high terrestrial-plant influence, and ? = an unknown source; # Data from a different but representative well; 19T/23T, ratio of C_{19} to C_{23} tricyclic terpanes; 27diaS/27S, ratio of $C_{27}\beta\alpha$-diasterane (*20S*) to $C_{27}\alpha\alpha\alpha$-sterane (*20R*); 30diaH/30H, ratio of C_{30} diahopane to $C_{30}\alpha\beta$-hopane; TMNr, trimethylnaphthalene ratio; TeMNr, tetramethylnaphthalene ratio; PMNr, pentamethylnaphthalene ratio (see Appendix 1).

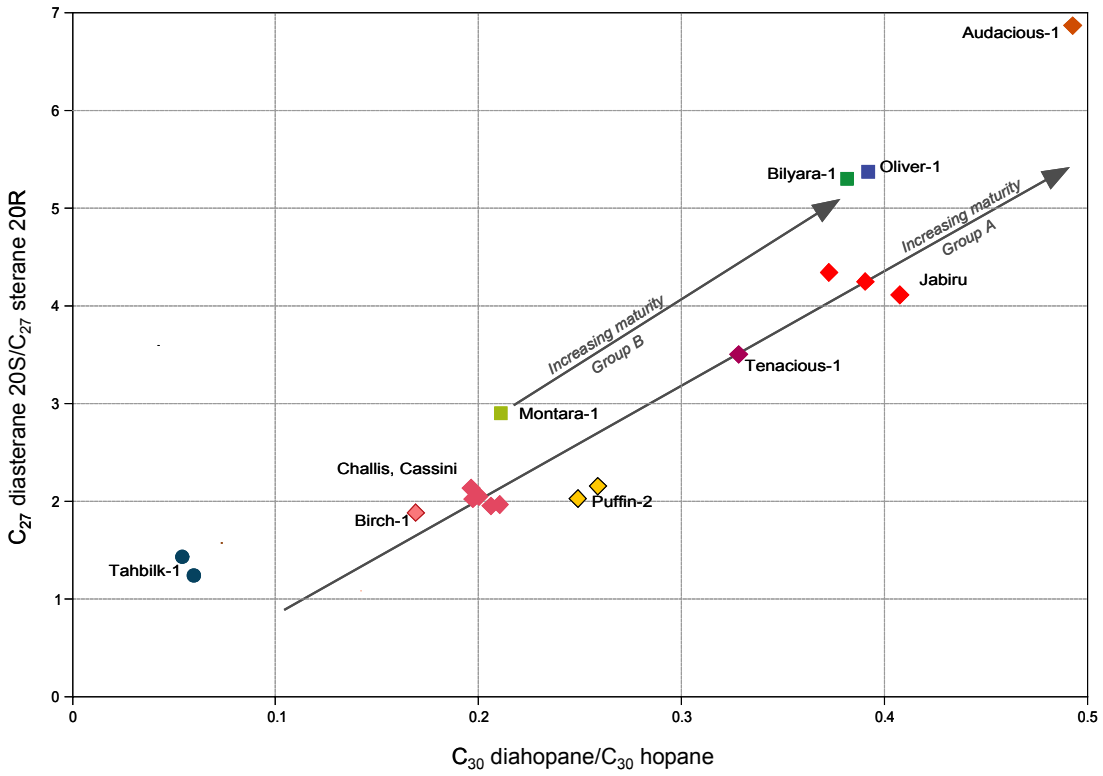

Figure 6.3 Plot of C_{27} diasterane 20*S*/C_{27} sterane 20*R* versus C_{30} diahopane/C_{30} hopane for most of the Vulcan Sub-basin crude oils and condensates (or representative samples) analysed in this study (Edwards *et al.*, 2004), demonstrating their relative maturities. Data for multiple wells are displayed for several samples.

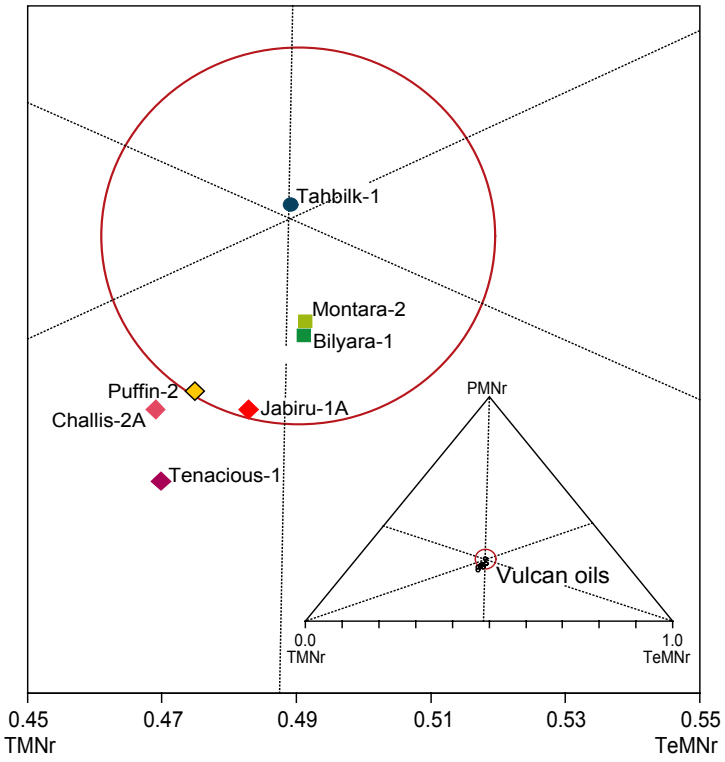

Figure 6.4 Ternary plot of the trimethylnaphthalene ratio (TMNr), tetramethylnaphthalene ratio (TeMNr), and pentamethylnaphthalene ratio (PMNr) for selected Vulcan Sub-basin crude oils and condensates (or representative samples) used for this study (Edwards *et al.*, 2004)

6.2.2 Stable carbon isotopic analysis

The stable carbon isotopic compositions ($\delta^{13}C$) of individual *n*-alkanes were measured in the Perth Basin and Vulcan Sub-basin crude oils and condensates. The $\delta^{13}C$ values of the two regular isoprenoids pristane and phytane were measured in the Perth Basin crude oils and condensates only. Standard deviations for at least three replicate analyses are within 0.4‰.

6.2.2.1 Perth Basin crude oils

The results of $\delta^{13}C$ analysis of the Perth Basin crude oils used in this study have been published previously by Summons *et al.* (1995) and Boreham *et al.* (2000) and Boreham *et al.* (2001). $\delta^{13}C$ analysis was also carried out as part of this study, the results of which have been published previously by Thomas and Barber (2004). The pertinent results are discussed below.

Summons *et al.* (1995) used the $\delta^{13}C$ values of *n*-alkanes (together with biomarker distributions, see Sec. 6.2.1.1) to classify a suite of Perth Basin crude oils based on the age of their source (Permian, Early Triassic and Jurassic). The $\delta^{13}C$ data obtained in the present study were consistent with that obtained by Summons *et al.* (1995). The $\delta^{13}C$ values of *n*-alkanes for the Perth Basin oils and condensates analysed in this study are shown in Figure 6.5. The oil and condensate from an Early Triassic source (Dongara-14, East Lake Logue-1) have *n*-alkanes which are isotopically very light (ca. -34‰) in comparison to those from Jurassic-sourced oils and condensates (Gage Roads-1, Gingin-1; ca. -24‰), and a Permian-sourced condensate (Whicher Range-1; ca. -25‰). Isotopically light organic (and inorganic) carbon is a global feature of the Early Triassic (see Chapter 5), and the $\delta^{13}C$ values of hydrocarbons from the Early Triassic-sourced oils and condensates are consistent with those from Early Triassic Perth Basin sediments (Hovea Member, Kockatea Shale) reported in Chapter 5. Another Early Triassic-sourced oil (Woodada-3), and a Jurassic-sourced condensate (Walyering-2) have *n*-alkanes with intermediate $\delta^{13}C$ values (ca. -30‰).

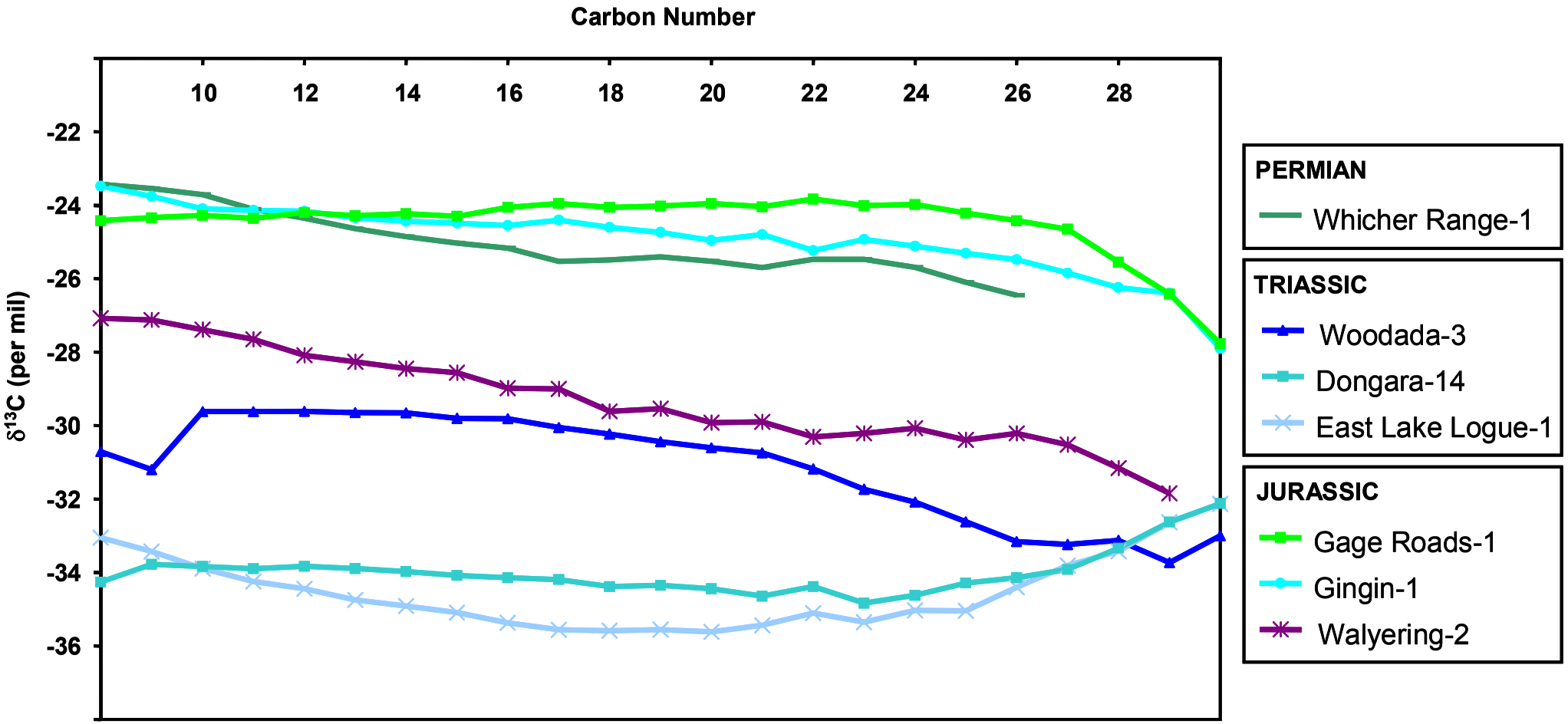

Figure 6.5 Plot of carbon number versus $\delta^{13}C$ value for *n*-alkanes in Perth Basin crude oils and condensates

It is unusual that the *n*-alkanes from Woodada-3 (Early Triassic) are enriched in ^{13}C (by ca. 4‰) relative to the other Early Triassic-sourced oil and condensate analysed in this study (Figure 6.5). This phenomenon was also identified in several bitumens and kerogen from the Woodada-2 section (Summons *et al.*, 1995), and has been attributed to the possible incorporation of reworked, ^{13}C-enriched organic matter of Permian age (Jefferies, 1984; Thomas and Barber, 2004), or can also be attributed to a change in the organofacies type, i.e. from wood-charcoal-dominated to algal-dominated (Summons *et al.*, 1995; Foster *et al.*, 1997). In addition, a trend towards heavier $\delta^{13}C$ values for shorter-chain *n*-alkanes in Woodada-3 has been attributed to a contribution from an isotopically heavier Permian condensate (Summons *et al.*, 1995; Thomas and Barber, 2004). Work by Boreham *et al.* (2000) suggested that Woodada-3 was indeed a 'vagrant' oil. Using statistical principle-component cluster analysis of molecular parameters and bulk carbon isotopes, the oil was quite different to other northern onshore Perth Basin oils (Boreham *et al.*, 2000). Furthermore, Thomas and Barber (2004) identified a series of features which correlate Perth Basin crude oils to a particular source, and these features in Woodada-3 were consistent with a mixture of Permian and Triassic sources (see Sec. 6.2.1.1). Another possibility is that the Woodada-3 oil has been affected by higher thermal maturity in the Woodada area (Thomas and Barber, 2004). Higher thermal maturity can result in an enrichment of ^{13}C in *n*-alkanes (Clayton, 1991; Clayton and Bjorøy, 1994; see Chapter 5). However condensate recovered from the nearby East Lake Logue-1 well has a typical Early Triassic isotopic signature of approximately -35‰, which is clearly not affected by maturity to any significant extent (Thomas and Barber, 2004).

The profile of $\delta^{13}C$ values of *n*-C_8 to *n*-C_{27} from Gage Roads-1 oil is relatively flat, indicative of a lacustrine source, but can also be a characteristic of marine-derived crude oils (Murray *et al.*, 1994; Summons *et al.*, 1995) (see Sec. 6.1.2). However, a higher plant index (HPI, Appendix 1) of 0.67, and a high relative abundance of *n*-C_{23} to *n*-C_{29} indicates a significant terrestrial input. Furthermore, Volk *et al.* (2004) reported a strong terrestrial signature for a Gage Roads-2 fluid inclusion (FI) oil, based on an odd-over-even preference of *n*-alkanes in the *n*-C_{25} to *n*-C_{31} range, high C_{29} sterane content, high HPI and other evidence based on source-specific aromatic hydrocarbons.

The profile of $\delta^{13}C$ values of *n*-alkanes from Dongara-14 displays an interesting trend. The lower molecular weight *n*-alkanes (*n*-C_8 to *n*-C_{26}) are depleted in ^{13}C relative to the higher molecular weight *n*-alkanes (*n*-C_{27} to *n*-C_{33}) by about 2‰. Potential reasons for this trend include possible in-reservoir mixing of different oils, migration contamination, or a single mixed marine/terrestrial source rock for this oil. The molecular analysis (Sec. 6.2.1.1) showed no evidence of significant in-reservoir mixing of oils of different maturities or migration contamination. In addition, a high relative abundance of both lower and higher molecular weight *n*-alkanes in the Dongara-14 crude oil suggests both series are indigenous to the oil. Therefore, a single mixed marine/terrestrial source rock is suggested to have caused the observed profile of $\delta^{13}C$ values of *n*-alkanes in Dongara-14.

The $\delta^{13}C$ values of pristane and phytane in the Perth Basin crude oils were also measured as part of this study, and range between -32.3 and -25.1‰. The $\delta^{13}C$ values of pristane and phytane, like the $\delta^{13}C$ values of the *n*-alkanes, reflect the age of the source rock. For example, pristane and phytane from Early Triassic-sourced oils and condensates are depleted in ^{13}C ($\delta^{13}C$ ca. -32‰) relative to that from Jurassic-sourced oils and condensates ($\delta^{13}C$ ca. -26‰). The difference between the average $\delta^{13}C$ value of *n*-C_{17} and *n*-C_{18} alkanes and the average $\delta^{13}C$ value of pristane and phytane, respectively ($\Delta\delta^{13}C$ values) for the Early Triassic-sourced oils and condensates range between -0.7 and -3.5‰. Thus pristane and phytane are enriched in ^{13}C relative to *n*-C_{17} and *n*-C_{18} alkanes indicating a relatively high algal input, consistent with that observed for the Early Triassic source rock in the northern Perth Basin (see Chapter 5). The $\Delta\delta^{13}C$ value for Woodada-3 (-0.7‰) is more positive than those for other Early Triassic-sourced oils and condensates (Dongara-14, -2.2‰; East Lake Logue-1, -3.5‰), further evidence for a contribution from a Permian source (see above). The Permian-sourced Whicher Range-1 condensate has a $\Delta\delta^{13}C$ value of 2.2‰, i.e. *n*-C_{17} and *n*-C_{18} alkanes are enriched in ^{13}C relative to pristane and phytane, indicating a relatively lower algal input to this condensate. These results are consistent with that observed in some Permian sediments from the Perth Basin (Grice *et al.*, 2005a; see Chapter 5).

6.2.2.2 Vulcan Sub-basin crude oils

$\delta^{13}C$ analysis of the Vulcan Sub-basin crude oils used in this study has been carried out previously by Edwards *et al.* (2004), and the $\delta^{13}C$ values of the *n*-alkanes again classified the Vulcan Sub-basin crude oils and condensates into two groups (see also Sec. 6.2.1.2). The $\delta^{13}C$ values of the *n*-alkanes in the Vulcan Sub-basin oils (Edwards *et al.*, 2004) are plotted in Figure 6.6. The $\delta^{13}C$ values of *n*-alkanes from Group B oils (Montara-1, Bilyara-1) range between -25 and -27‰ (average -26.1‰), in the Group A oils (Jabiru, Birch, Challis, Puffin, Tenacious) between -25 and -31‰ (average -27.9‰), and the mixed oils (Oliver, Audacious) between -25 and -28‰ (average -26.9‰). The *n*-alkanes in the Group B oils are significantly more enriched in ^{13}C (by ca. 1.8‰). The relatively less mature Vulcan Sub-basin sediments (Chapter 5) have *n*-alkane $\delta^{13}C$ values which are similar to those of the Group A oils, i.e. a marine signature. In contrast, the more mature sediments contain *n*-alkanes which are more enriched in ^{13}C (see Chapter 5), having similar $\delta^{13}C$ values to *n*-alkanes from Group B oils. However, based on maturity-dependent hopane (e.g. *Ts/Ts+Tm*, 22*S*/22*S*+22*R*) and sterane (e.g. $C_{29}\alpha\alpha\alpha$ 20*S*/$C_{29}\alpha\alpha\alpha$ 20*S*+20*R*, $C_{29}\alpha\beta\beta$ 20*S*+20*R*/$C_{29}\alpha\alpha\alpha+\alpha\beta\beta$ 20*S*+20*R*) parameters (Edwards *et al.*, 2004), the Group B oils were not generated at higher thermal maturities than the Group A oils (see also Figure 6.3). Consequently, the enrichment of ^{13}C in *n*-alkanes in Group B oils was attributed to an increased input of terrestrial-plant organic matter to the source rock (Edwards *et al.*, 2004). The compound-specific data were supported by bulk $\delta^{13}C$ analysis of the saturated hydrocarbon fractions of the crude oils and condensates (Edwards *et al.*, 2004).

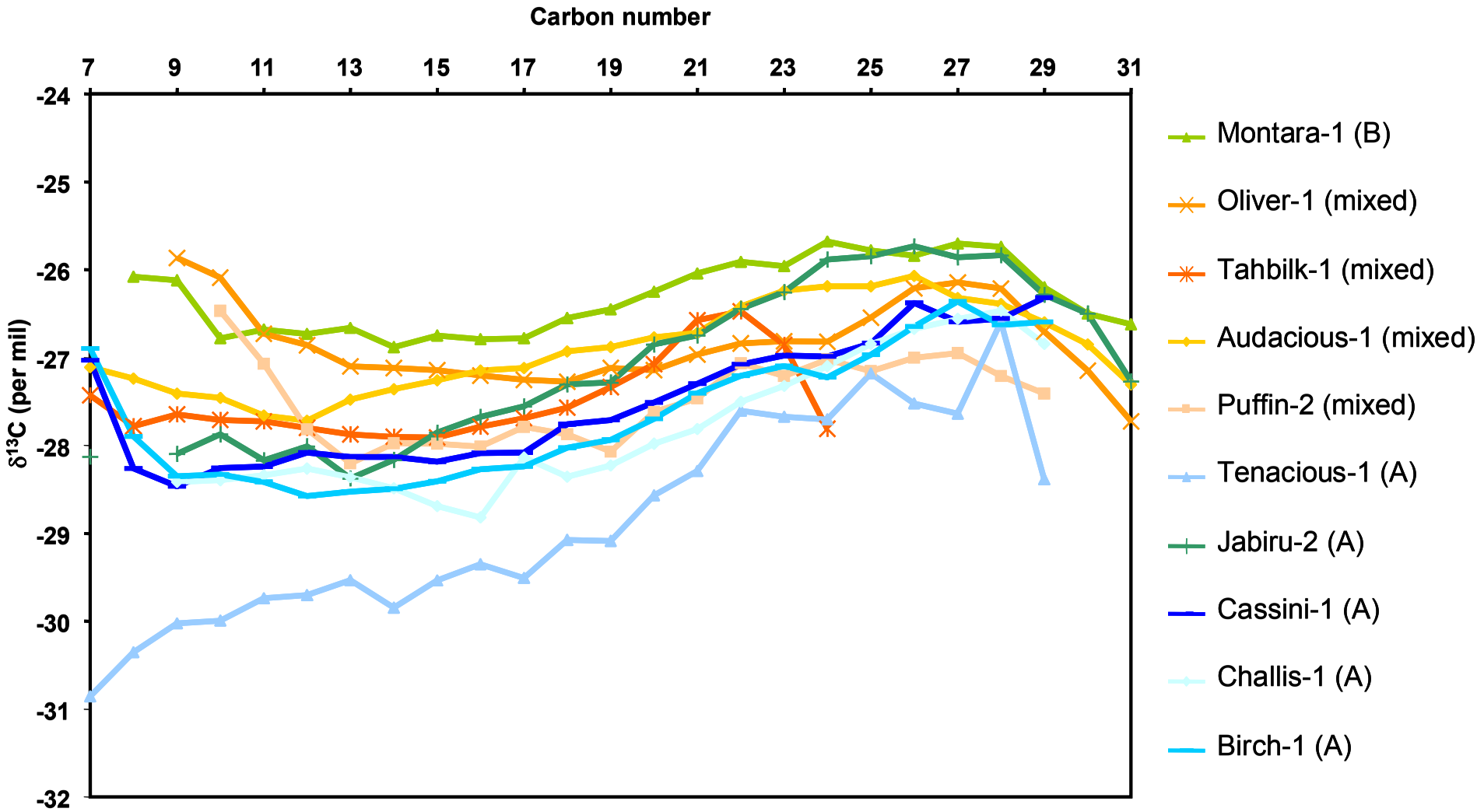

Figure 6.6 Plot of carbon number versus $\delta^{13}C$ value for *n*-alkanes in Vulcan Sub-basin crude oils and condensates (Edwards *et al.*, 2004)

6.2.3 Bulk stable hydrogen isotopic analysis of Perth Basin and Vulcan Sub-basin crude oils and condensates

Bulk δD values of the Perth Basin and Vulcan Sub-basin crude oils and condensates were determined using elemental analysis-isotope ratio mass spectrometry (Chapter 2). The results are summarised in Table 6.3 and Table 6.4. Standard deviations for at least two replicate analyses are within 4‰. The bulk δD values of the Perth Basin crude oils and condensates range from -179 to -121‰, and in most cases vary quite significantly (up to 32‰) from the average δD values of the *n*-alkanes (Table 6.3) obtained from CSIA (Sec. 6.2.4). The bulk δD values of the Vulcan Sub-basin crude oils and condensates range from -127 to -103‰, and are consistent with average δD values of the *n*-alkanes, which range from -133 to -102‰ (Table 6.4). Indeed, *n*-alkanes are a quantitatively important component of crude oils that have not been affected by secondary processes (e.g. biodegradation) to any significant extent.

Small differences in δD between whole oils and individual fractions have been observed in previously reported data sets. Rigby *et al.* (1981) analysed twelve crude oils from the Gippsland Basin, south-eastern Australia. The δD values of the saturated fractions differed from the bulk oil by less than 5‰ on average, and in a small number of cases up to 10 to 14‰. Yeh and Epstein (1981) published δD values of whole oils and individual fractions, for two crude oils from Saskatchewan (Canada) and Utah (USA). The difference in δD values between the whole oils and their fractions was less than 2‰. Santos Neto and Hayes (1999) reported bulk δD values of whole oils, and their saturated fractions, from twenty-one marine-evaporitic, lacustrine and mixed oils from the onshore Potiguar Basin, northeastern Brazil. The differences between the δD values of the bulk oil and saturated fractions were mostly less than 5‰, and in two or three samples up to 8 to 10‰. Schimmelmann *et al.* (2004) reported δD values of seventy-five Australian terrestrially-sourced oils and their fractions, and individual compounds in twenty eight of them. They found that in most cases, sub-fractions had similar δD values to their parent whole oils. δD values of saturated and *n*-alkane fractions were generally within 5‰ of the whole oil δD values. Crude oils from the Otway Basin (south-eastern Australia) were an exception, with saturated fractions being depleted in D by

22‰ or more relative to the whole oil and other fractions (Schimmelmann *et al.*, 2004). These data reported in the literature are consistent with the data obtained for the Perth Basin crude oils and condensates analysed in this study, where the *n*-alkanes are depleted in D relative to the bulk oil by up to 32‰ (on average), with an exception being Gage Roads-1 where the *n*-alkanes are enriched in D by 19‰ (on average) relative to the bulk oil (Table 6.3).

Table 6.3 Bulk δD values and average *n*-alkane δD values of Perth Basin crude oils and condensates determined by elemental analysis-isotope ratio mass spectrometry

Well name	Bulk δD_{oil} (‰)*	Average $\delta D_{n\text{-alkanes}}$ (‰)*	ΔδD (‰)
Whicher Range-1	-141 (1)[2]	-116 (3)[4]	-25
Woodada-3	-121 (1)[3]	-89 (3)[5]	-32
East Lake Logue-1	-129 (1)[3]	-117 (4)[4]	-12
Dongara-14	-130 (4)[2]	-125 (2)[3]	-5
Gingin-1	-143 (3)[2]	-125 (3)[4]	-18
Walyering-2	-131 (2)[2]	-104 (3)[5]	-27
Gage Roads-1	-179 (1)[2]	-198 (2)[4]	19

* Numbers in parentheses are standard deviations (average is shown for *n*-alkanes), superscript number are number of replicate analyses; ΔδD, difference between the bulk δD value of the oil and the average δD value of the *n*-alkanes (relative to VSMOW)

6.2.4 Compound-specific stable hydrogen isotopic analysis

The stable hydrogen isotopic compositions (δD) of individual *n*-alkanes (ca. *n*-C_{11} to *n*-C_{29}) and (in most oils) the regular isoprenoids pristane and phytane, were measured in the Perth Basin and Vulcan Sub-basin crude oils and condensates. Standard deviations for at least three replicate analyses are mostly within 5‰. In a minimal number of cases, standard deviations are as high as 12‰, but only for peaks of relatively low intensity or where minor co-elution was evident.

6.2.4.1 Perth Basin crude oils

The range of δD values of *n*-alkanes (ca. *n*-C_8 to *n*-C_{27}), and the δD values of pristane and phytane from the Perth Basin crude oils are summarised in Table 6.5. The δD values of the *n*-alkanes are plotted in Figure 6.7. The δD values of *n*-alkanes from the crude oils and condensates average between -125 and -89‰ (excluding Gage Roads-1, -198‰, attributed to a different source facies, see below), which are significantly more positive than that expected (~150‰) from marine-derived sedimentary organic matter (Smith and Epstein, 1970; Santos Neto and Hayes, 1999), indicating they were generated from mature source rocks.

Table 6.4 Bulk δD values and average *n*-alkane δD values of Vulcan Sub-basin crude oils and condensates determined by elemental analysis-isotope ratio mass spectrometry

Well name	Bulk δD_{oil} (‰)*	Average $\delta D_{n\text{-alkanes}}$ (‰)*	ΔδD (‰)
Birch-1	-127 (3)^5	-133 (3)^3	6
Tahbilk-1	-112 (3)^4	-110 (4)^3	-2
Cassini-1	-122 (2)^3	-125 (4)^3	3
Jabiru-2	-115 (2)^5	-120 (3)^3	5
Tenacious-1	-117 (1)^4	-113 (3)^3	-4
Challis-1	-125 (1)^5	-127 (3)^3	2
Oliver-1	-110 (2)^4	-108 (4)^3	-2
Montara-1	-103 (2)^5	-102 (4)^3	-1
Bilyara-1	-103 (2)^3	n.d.	n.d
Puffin-2	-118 (2)^3	-116 (5)^3	-2
Audacious-1	-110 (2)^4	-110 (4)^3	0

*Numbers in parentheses are standard deviations (average is shown for *n*-alkanes), superscript numbers are number of replicate analyses; ΔδD, difference between the bulk δD value of the oil and the average δD value of the *n*-alkanes (relative to VSMOW); n.d., not determined.

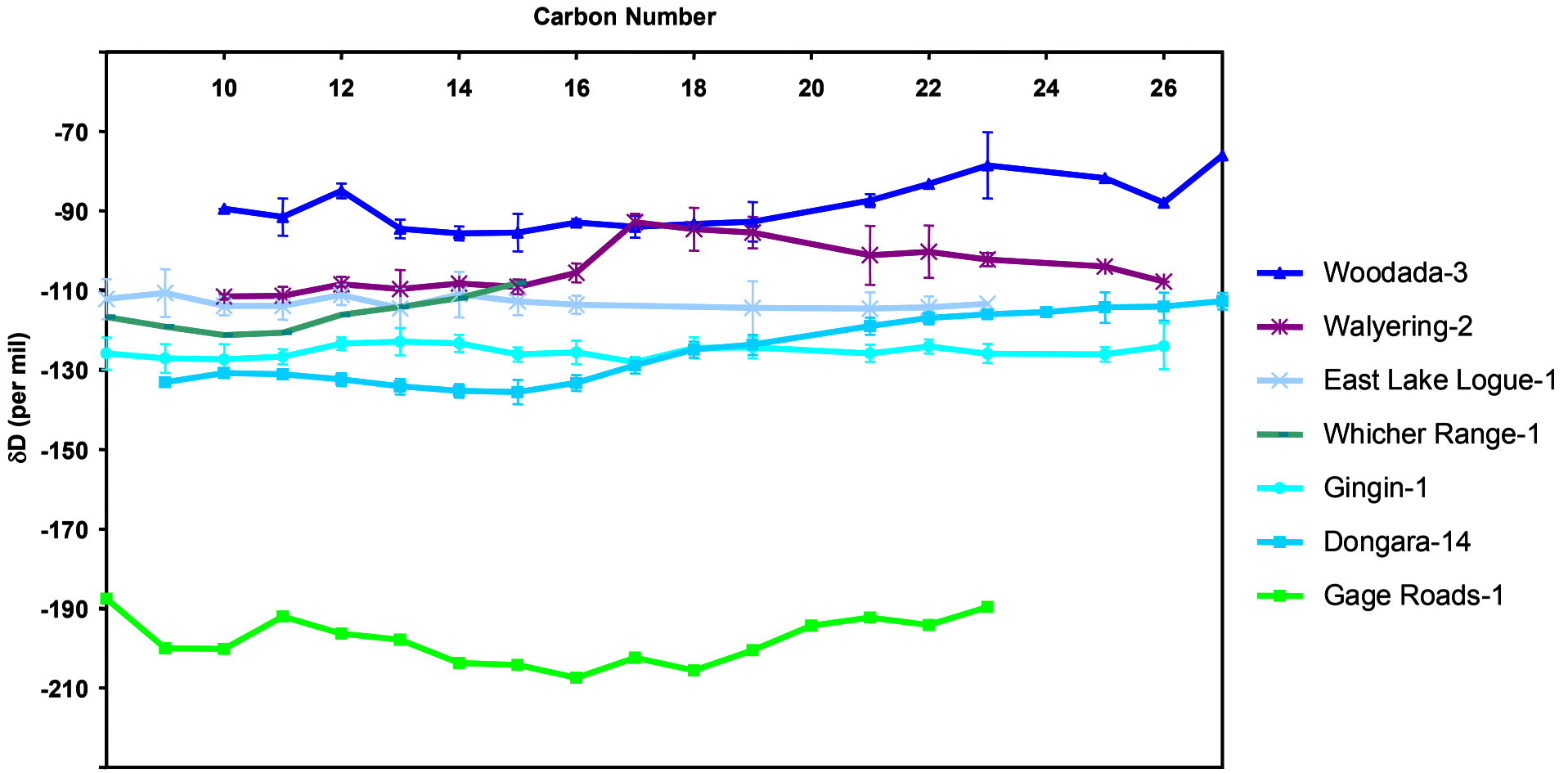

Figure 6.7 Plot of carbon number versus δD value for *n*-alkanes in Perth Basin crude oils and condensates

The *n*-alkanes and pristane from Gage Roads-1 (Jurassic) are significantly depleted in D (ca. 80‰) relative to the *n*-alkanes, pristane and phytane from the other crude oils analysed, including the two Jurassic-sourced condensates (Gingin-1, Walyering-2; Figure 6.7). This light isotopic signature is consistent with a source environment for Gage Roads-1 where meteoric waters were significantly depleted in D. Considering all crude oils and condensates analysed in this study are from the same geographical location, it is likely the D-depleted isotopic values are associated with the source rock for Gage Roads-1 having been deposited inland (i.e. lacustrine/ terrestrial source facies). In these regions, precipitation is typically depleted in D (due to the 'continentality' effect, see Chapter 4) relative to that nearer to the ocean, although this is highly variable. Indeed, such D-depleted *n*-alkanes have been reported for terrestrially-sourced crude oils from Australia (Schimmelmann *et al.*, 2004), and terrestrial source rocks from China (Xiong *et al.*, 2005). In addition, a flat $\delta^{13}C$ profile for the *n*-alkanes in Gage Roads-1 (Sec. 6.2.2.1) is also characteristic of a lacustrine source. Other evidence includes a high relative abundance of *n*-alkanes in the *n*-C_{23} to *n*-C_{29} carbon number range and a higher plant index of 0.67, both pointing to a significant terrestrial plant contribution to Gage Roads-1 (Eglinton and Hamilton, 1963; Boreham *et al.*, 2000).

The profile of δD values of *n*-alkanes from Dongara-14 (Early Triassic) displays a similar trend to that observed with their $\delta^{13}C$ values. The lower molecular weight *n*-alkanes (*n*-C_9 to *n*-C_{17}, Figure 6.8) are depleted in D relative to the higher molecular weight *n*-alkanes (*n*-C_{18} to *n*-C_{27}, Figure 6.8). Interestingly, the D-enrichment occurs earlier in the carbon number range with hydrogen compared to carbon. This profile of *n*-alkane δD values can also be explained in terms of a single mixed marine/terrestrial source rock for Dongara-14, with other possible reasons such as in-reservoir mixing of different oils or migration contamination being improbable based on the molecular analysis (Sec. 6.2.1.2). A comparison of the *n*-alkane δD profiles of two Early Triassic-sourced oils (Figure 6.8) suggests that the *n*-alkanes from East Lake Logue-1 have a predominant marine signature (i.e. relatively enriched in D), with the higher molecular weight *n*-alkanes (*n*-C_{21} to *n*-C_{27}) from Dongara-14 having a similar signature (Figure 6.8).

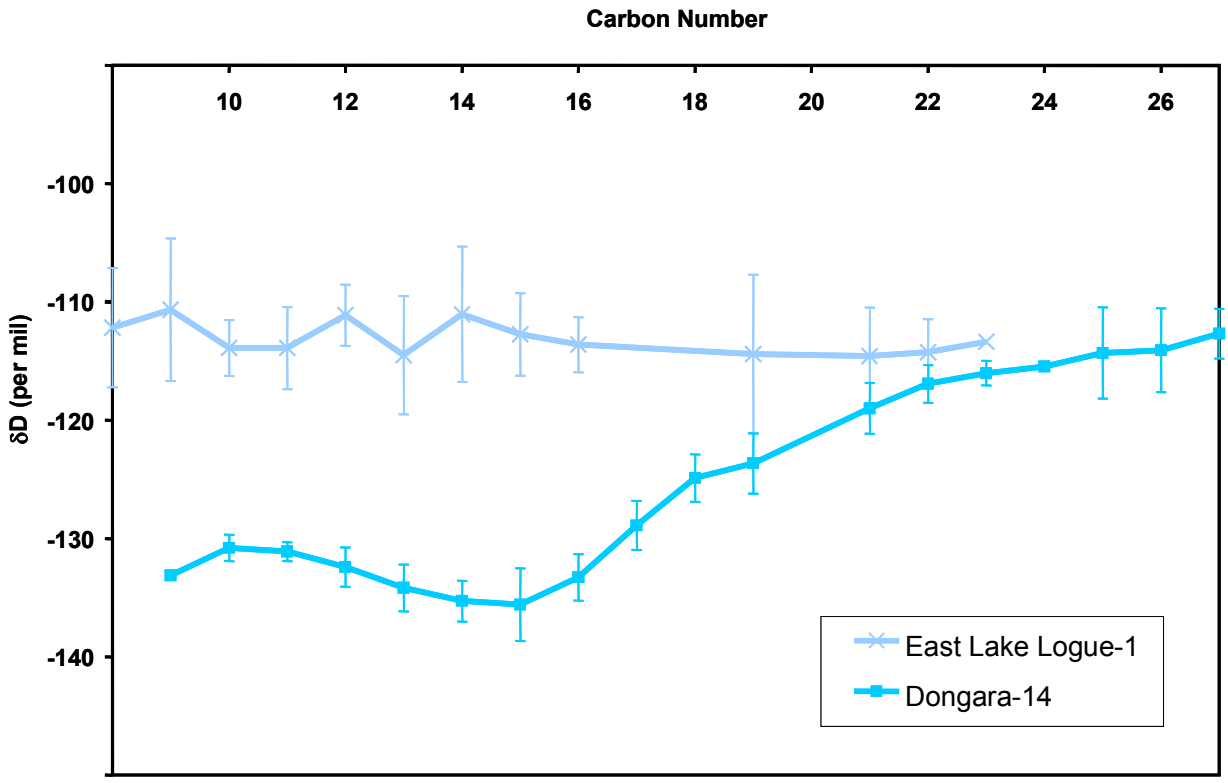

Figure 6.8 Plot of carbon number versus δD value for *n*-alkanes in Dongara-14 crude oil and East Lake Logue-1 condensate

The *n*-alkanes from the Woodada-3 crude oil are the most enriched in D (-95 to -75‰) in comparison to those from the other marine Perth Basin crude oils analysed (Figure 6.7). This is possibly due to the Woodada-3 oil having been affected by the high thermal maturity in the Woodada area (Thomas and Barber, 2004), supported to some extent by the $\delta^{13}C$ values of the *n*-alkanes (Sec. 6.2.2.1). Furthermore, Woodada-3 has been identified as a 'vagrant' in the northern Perth Basin, based on molecular and isotopic parameters (Boreham *et al.*, 2000).

The crude oils and condensates all contain pristane, and phytane where measured, with δD values that are similar (within ca. 14‰) to the δD values of their associated *n*-alkanes. For the Early Triassic crude oils and condensates, in particular, this is consistent with the results obtained from the supposed source rocks (Hovea Member, Kockatea Shale) for these Perth Basin oils (see Chapter 5), where the biological δD signature (i.e. the large δD offset between isoprenoids and *n*-alkanes, see Chapters 4 and 5) is lost at R_e values of 0.78–1.13% representing the peak oil-generative window. The δD value of pristane in Gage Roads-1 is significantly depleted in D (by 60 to 100‰) relative to pristane and phytane from the other Perth Basin oils,

consistent with what was observed with the *n*-alkanes and again attributed to a lacustrine/terrestrial depositional environment for the source rock. In Early Triassic-sourced crude oils and condensates (e.g. Dongara-14 and East Lake Logue-1), phytane is enriched in D relative to pristane by up to 17‰ which is consistent with the results obtained from their supposed Early Triassic source rocks (Chapter 5). The opposite is observed in Permian and Jurassic condensates (Whicher Range-1 and Gingin-1, respectively), where pristane is enriched in D relative to phytane.

Li *et al.* (2001) measured the δD values of individual *n*-alkanes and acyclic isoprenoids from a number of crude oils from the Western Canada Sedimentary Basin. The *n*-alkanes from a marginally mature crude oil ranged from -155 to -120‰ (averaging -134‰), while pristane and phytane had δD values of -188 and -168‰, respectively (average -178‰). The *n*-alkanes from a mature crude oil ranged from -131 to -97‰ (averaging -110‰), and pristane and phytane from these oils had δD values of -144 and -136‰, respectively (average -140‰). The *n*-alkanes, pristane and phytane were enriched in D in the more mature crude oil (generated from a more mature source rock) relative to respective δD values from the less mature crude oil. These data show trends consistent with the results obtained in this study.

Table 6.5 Range of δD values of *n*-alkanes, δD values of pristane (Pr) and phytane (Ph), and ΔδD values (see below for definition) for the Perth Basin crude oils and condensates

Well, Depth (m)	*n*-Alkanes δD Range (‰)	δD Pr (‰)	δD Ph (‰)	ΔδD (‰)
Whicher Range-1	-121 to -108 (3)[5]	-126 (2)[3]	-127 (0)[3]	-11
Woodada-3	-96 to -76 (3)[5]	n.d.	n.d.	n.d.
East Lake Logue-1	-114 to -111 (4)[4]	-112 (2)[3]	-95 (0)[3]	+13
Dongara-14	-136 to -113 (2)[3]	-119 (2)[3]	-104 (4)[3]	+14
Gingin-1	-128 to -123 (3)[4]	-111 (2)[3]	-132 (5)[3]	+3 (0)
Walyering-2	-112 to -93 (3)[4]	n.d.	n.d.	n.d.
Gage Roads-1	-207 to -188 (2)[4]	-191 (0)[3]	n.d.	+6

ΔδD, difference between the average δD value of Pr and Ph and the average δD value of the *n*-alkanes (relative to VSMOW); * Numbers in parentheses are standard deviations (average is shown for *n*-alkanes), superscript number are number of replicate analyses; n.d., not determined.

6.2.4.2 Vulcan Sub-basin crude oils

The range of δD values of *n*-alkanes (ca. *n*-C_{11} to *n*-C_{28}), and the δD values of pristane and phytane from the crude oils are summarised in Table 6.6. Figure 6.9 is a plot of δD versus number of carbons for the *n*-alkanes in the Vulcan Sub-basin crude oils. The δD values of *n*-alkanes average between -133 and -102‰, which are again significantly more positive than δD values that are expected (~ -150‰) for marine-derived *n*-alkanes (Smith and Epstein, 1970; Santos Neto and Hayes, 1999).

Edwards *et al.* (2004) divided a series of Vulcan Sub-basin crude oils (including those analysed in this study) into two broad groups (A and B) based on molecular and carbon isotope analysis (see Sections 6.2.1.2 and 6.2.2.2, respectively). With the Group A and Group B classifications being based on different relative inputs of marine versus terrigenous organic matter, the δD values of individual hydrocarbons in the crude oils appear to reflect this based on differences in the isotopic composition of marine and terrestrial source waters (see Chapter 4). The majority of Group A crude oils (excluding Tenacious-1, see below) plot in a similar region in Figure 6.9, with a typical marine signature, depleted in D in comparison to the Group B and mixed crude oils. Birch-1 (Group A oil) is the most negative end-member, with δD values of the *n*-alkanes ranging between -141 and -122‰; while Montara-1 (Group B oil) is the most positive end-member, with δD values of the *n*-alkanes ranging between -108 and -94‰. The oils thought to be of mixed origin plot in a region between the Group A oils and the Group B oil. Based on these results, the terrigenous input to Group B crude oils appears to cause the *n*-alkanes to become enriched in D. Typically, terrestrially-derived organic matter is depleted in D relative to marine-derived organic matter, because the δD values of meteoric source waters are almost always more negative than ocean water (Craig, 1961; Dansgaard, 1964). In some cases, significant D-enrichment of meteoric waters can take place in hot, arid environments so that the biosynthetic products of aquatic organisms (due to evaporation) and terrestrial plants (due to evapotranspiration) are significantly enriched in D. In general, terrestrially-derived organic matter has been shown to display a wide variation in δD values (e.g. Schimmelmann *et al.*, 2004; Xiong *et al.*, 2005). While temperature and latitude are the most important determining factors, the D/H composition of meteoric waters in the terrestrial hydrological cycle are additionally affected by altitude and continentality (see Chapter 4). These additional

effects are highly variable, leading to the large isotopic variations observed in terrigenous organic matter. For example, Schimmelmann *et al.* (2004) measured the D/H composition of the individual fractions of 75 terrestrially-derived crude oils and found that the bulk δD values of saturated fractions spanned a large range, from -245 to -62‰. Xiong *et al.* (2005) measured the δD values of individual *n*-alkanes in terrestrial source rocks from the Liaohe and Turpan Basins (China), which ranged from -250 to -140‰. Furthermore, the bulk δD values of saturated hydrocarbon fractions of representative marine-evaporitic, lacustrine and mixed oils reported by Santos Neto and Hayes (1999) showed that the lacustrine oils were enriched in D (by 10–26‰) relative to other oils in the basin.

As mentioned above, the δD values of the *n*-alkanes from Tenacious-1 crude oil (Group A) are more positive than those for other Group A oils (Figure 6.9). In fact, the *n*-alkane δD values for Tenacious-1 are similar to those of mixed oils (Table 6.6). The bulk δD value of Tenacious-1 is also similar to those other mixed oils, and is within 4‰ of the average δD value of the *n*-alkanes (Table 6.4). One possible explanation for this is that Tenacious-1 is more mature than other Group A oils, or has been mixed with more mature hydrocarbons. On a ternary plot of TMNr, TeMNr and PMNr (Figure 6.4), Tenacious-1 plots outside the 'maturity centre', towards the TMNr corner indicating mixing with more mature hydrocarbons (see Sec. 6.2.1.2). The majority of Group A oils (i.e. Birch-1, Cassini-1, Challis-1, Jabiru-2) are believed to have been generated from the Lower Vulcan formation in the Swan Graben and to have migrated over varying distances within the Vulcan Sub-basin (Chen *et al.*, 2002; Liu *et al.*, 2005). However, it is conceivable that the hydrocarbons in Tenacious-1 may have originated from the Paqualin Graben, which may also account for the differences observed in both the *n*-alkane $\delta^{13}C$ (Figure 6.6; Edwards *et al.*, 2004) and δD (Figure 6.9) isotopic profiles relative to those of other Group A oils.

The Group A crude oils and condensates have a 'bowl-shaped' profile of *n*-alkane δD values (Figure 6.9). Edwards *et al.* (2004) observed a 'lazy-S' shaped profile of *n*-alkane $\delta^{13}C$ values in the same samples, a common occurrence in many marine-sourced oils in the North West Shelf of Australia. This is thought to represent an addition of a more mature wet gas/condensate to the initial oil charge, resulting in an upward inflection of the $\delta^{13}C$ profile in the *n*-C_7 to *n*-C_{12} range (Edwards *et al.*,

2004). An upward inflection of the *n*-alkane δD profile occurs in the *n*-C_{11} to *n*-C_{15} range (Figure 6.9), and presumably this trend continues to lower-molecular-weights (< *n*-C_{11} were not measured due to their low abundance). This could also be attributed to contribution from a more mature wet gas/condensate, which would result in the addition of D-enriched lower molecular weight *n*-alkanes to the initial charge.

The Vulcan Sub-basin crude oils all contain pristane and phytane with δD values that are similar (within ca. 15‰) to the δD values of their associated *n*-alkanes (ΔδD values range from -15 to +13‰). This is consistent with the results obtained from the more mature Lower Vulcan formation sediments (see Chapter 5). It suggests that significant H/D exchange (D-enrichment) has occurred, implying that the crude oils and condensates were generated from mature source rocks. As indicated in Chapter 5, the Paqualin-1 sediments appear to be more mature than their R_o data suggest. Based on ΔδD values, the majority of the Vulcan Sub-basin crude oils have less mature isotopic signatures compared to most of the Paqualin-1 sediments, including those with R_o values representing the peak oil-generative window (i.e. ~ 0.7–1.1%). This is further evidence that the Paqualin-1 sediments are more mature than indicated by their R_o data if significant quantities of oil have been generated from the Paqualin-1 sequence. In the Vulcan Sub-basin crude oils and condensates, pristane is generally enriched in D relative to phytane by up to 25‰, consistent with the Vulcan Sub-basin sediments analysed in Chapter 5.

Table 6.6 Range of δD values of *n*-alkanes, δD values of pristane (Pr) and phytane (Ph), and ΔδD values (see below for definition) for the Vulcan Sub-basin crude oils and condensates

Well, Depth (m)	*n*-Alkanes δD Range (‰)*	δD Pr (‰)*	δD Ph (‰)*	ΔδD (‰)
Birch-1	-141 to -122 (3)[3]	-135 (4)[3]	-155 (7)[3]	-13
Tahbilk-1	-115 to -103 (4)[3]	-97 (0)[4]	-114 (2)[4]	+5
Cassini-1	-134 to -115 (4)[3]	-124 (1)[3]	-125 (7)[3]	0
Jabiru-2	-127 to -107 (3)[3]	-113 (0)[3]	-138 (5)[3]	-5
Tenacious-1	-118 to -107 (3)[3]	-101 (3)[3]	-100 (12)[3]	+13
Challis-1	-136 to -119 (3)[3]	-132 (2)[3]	-150 (9)[3]	-15
Oliver-1	-111 to -102 (4)[3]	n.d.	n.d.	n.d.
Montara-1	-108 to -94 (4)[3]	-84 (10)[3]	-112 (12)[3]	+8
Puffin-2	-118 to -112 (5)[3]	n.d.	n.d.	n.d.
Audacious-1	-116 to -99 (4)[3]	-94 (2)[3]	-108 (3)[3]	+9

ΔδD, difference between the average δD value of Pr and Ph and the average δD value of the *n*-alkanes (relative to VSMOW); * Numbers in parentheses are standard deviations (average is shown for *n*-alkanes), superscript number are number of replicate analyses; n.d., not determined.

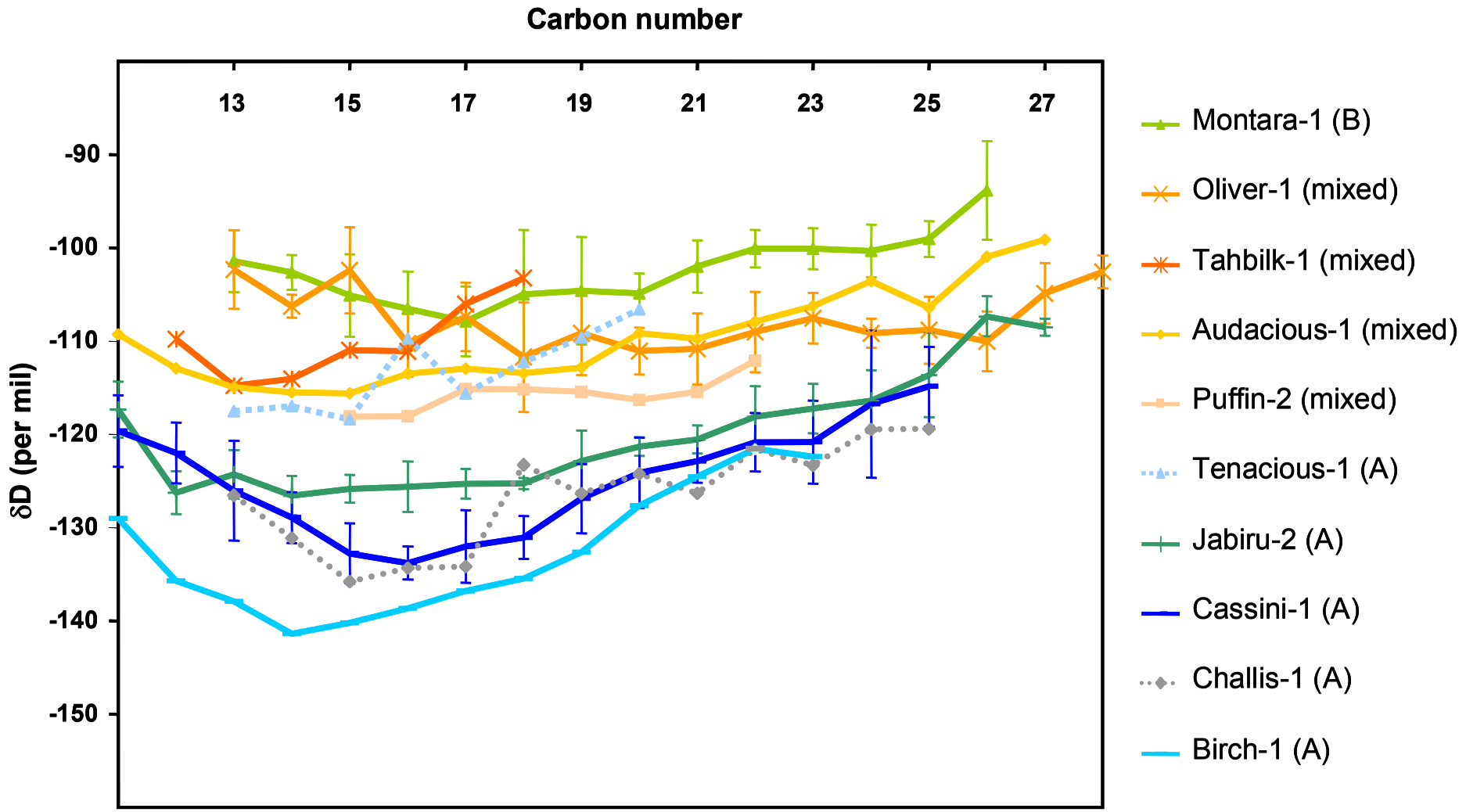

Figure 6.9 Plot of carbon number versus δD value for *n*-alkanes in Vulcan Sub-basin crude oils and condensates. The expressions in parentheses are source classifications based on work by Edwards *et al.* (2004), where A = marine influenced and B = terrestrial influenced.

6.3 SUMMARY AND CONCLUSIONS

1. The bulk δD values of the Perth Basin crude oils and condensates vary quite significantly from the average δD value of the *n*-alkanes determined by CSIA. However in the Vulcan Sub-basin, bulk δD values of crude oils and condensates are similar in most cases to the average δD value of the *n*-alkanes.

2. The δD values of *n*-alkanes in crude oils and condensates derived from a marine source are more positive than that expected for marine-derived organic matter, indicating they were generated from mature source rocks.

3. A Perth Basin crude oil (Gage Roads-1) derived from a lacustrine/terrestrial source contains *n*-alkanes and pristane which are significantly depleted in D relative to those from predominantly marine-derived crude oils. This is attributed to isotopic variability of marine versus terrestrial source waters.

4. The *n*-alkane δD profile for a marine-derived Perth Basin crude oil (Dongara-14) suggests that the oil is derived from a mixed marine/terrestrial source rock. The lower molecular weight *n*-alkanes are depleted in D relative to the higher molecular weight *n*-alkanes.

5. The *n*-alkanes from the Woodada-3 crude oil are the most enriched in D in comparison to those from the other marine Perth Basin crude oils, possibly due to the Woodada-3 oil having been affected by the high thermal maturity in the Woodada area. Furthermore, Woodada-3 has been identified as a 'vagrant' in the northern Perth Basin, based on molecular and isotopic parameters.

6. The relatively small differences between the δD values of *n*-alkanes and isoprenoids in the crude oils and condensates indicate they were generated from

mature source rocks. The biosynthetic δD differences between *n*-alkanes and isoprenoids would have probably been altered *via* hydrogen exchange reactions associated with thermal maturation.

7. The differences between the δD values of pristane and phytane in the crude oils and condensates are consistent with the differences seen in their supposed source rocks. Opposing trends between the Perth Basin and Vulcan Sub-basin are suggested to be due to quantitatively different algal inputs to the source organic matter for the crude oils and condensates in each basin.

8. In the Vulcan Sub-basin, the δD values of *n*-alkanes in the crude oils and condensates support their prior classification into two end-member groups based on molecular and stable carbon isotopic analyses: Group A, having a marine source affinity; and Group B, having a terrigenous source affinity. Some are suggested to be mixtures of sources A and B, or A and other as yet unknown sources. An exception was Tenacious-1 crude oil (Group A), which contained *n*-alkanes with more positive δD values compared to other Group A oils, and thus is suggested to have been mixed with another source of more mature hydrocarbons.

9. The Group A crude oils and condensates have a 'bowl shaped' profile of *n*-alkane δD values which is thought to represent an addition of a more mature wet gas/condensate to an initial oil charge, resulting in a upward inflection of the *n*-alkane δD profile in the *n*-C_{11} to *n*-C_{15} range.

10. Based on ΔδD values, the majority of the Vulcan Sub-basin crude oils have less mature isotopic signatures compared to most of the Paqualin-1 sediments. Thus it can be speculated that the Paqualin-1 sediments appear to be more mature than their R_o data suggest.

CHAPTER 7

7 CONCLUSIONS AND SUGGESTIONS FOR FUTURE WORK

7.1 CONCLUSIONS

This study aimed to establish the usefulness and reliability of stable hydrogen isotopic compositions of individual compounds for geochemical applications. The overall conclusions are summarised below.

7.1.1 Stable hydrogen isotopic compositions of petroleum hydrocarbons reflecting source and palaeoclimate

Based on the work presented in Chapter 4, the stable hydrogen isotopic compositions (δD) of individual saturated hydrocarbons extracted from thermally immature torbanites (bog-head coals) have been shown to reflect the main source of hydrogen (i.e. meteoric waters) in their depositional environments. A series of torbanites reflecting similar organic matter inputs, but deposited under different climate regimes, were chosen for this study. Previous biomarker studies on torbanites attest to the occurrence of well-preserved organic matter derived predominantly from *Botryococcus braunii* remains. Thus, the δD values of *n*-alkanes are representative of the different climate conditions under which the torbanites were deposited, varying from tropical (equatorial) to cool-temperate (mid-latitude) to glacial (high latitude). The reflection of climate is based primarily on the δD values of source meteoric waters produced from the global hydrological cycle, which vary significantly with latitude/temperature. The photosynthetic incorporation of the source water's D/H signature and subsequent biosynthesis leads to precursor lipids with δD values representative of the environmental waters.

The δD values of *n*-alkanes are also indicative of multiple source inputs. For example, the *n*-alkanes extracted from the Australian torbanites have been attributed to a dual-source system with predominant *Botryococcus braunii* input, and a terrestrial plant input favouring odd-carbon-numbered *n*-alkanes in the range *n*-C_{20} to

n-C_{29}. This interpretation is based on a saw-toothed profile of *n*-alkane δD values, with the odd-carbon-numbered *n*-alkanes being enriched in deuterium (D) relative to those with even-carbon-numbers attributed to the evapotranspiration effect in plants.

There is a significant disparity between the δD values of *n*-alkanes and acyclic isoprenoids (pristane and phytane) in two Permian torbanites from Australia. This offset is similar to that observed in extant organisms, suggesting that an apparent biological δD signal has been preserved for at least 260–280 million years. This preservation potential is appreciably greater than previously thought. There is no evidence that diagenetic and catagenetic processes have affected the δD values of the hydrocarbons to any significant extent.

In summary, it is apparent that important source and palaeoenvironmental information can be obtained from the δD values of individual hydrocarbons preserved in thermally immature sedimentary organic matter.

7.1.2 Alteration of stable hydrogen isotopic compositions of petroleum hydrocarbons in the subsurface

Based on the work presented in Chapters 4 and 5, the δD values of *n*-alkanes from immature sediments are representative of their source. In Chapter 5, it is shown that the δD values of *n*-alkanes and isoprenoids (pristane and phytane) extracted from immature-early mature Perth Basin sediments (marine shale/siltstone) and Vulcan Sub-basin sediments (marine mudstones) are consistent with that expected of marine-derived *n*-alkyl and isoprenoid lipids. With increasing thermal maturity, pristane and phytane are rapidly enriched in D, compared to slower D-enrichment of the *n*-alkanes. Over the studied range of maturity (%R_o= 0.53–1.6), the enrichment of D in isoprenoids is shown to correlate strongly with several traditional maturity parameters such as vitrinite reflectance (R_o) and the molecular parameters *Ts*/(*Ts*+*Tm*), MPI-1 and TNR-1 (see Appendix 1). Based on fundamental chemical principles, the more rapid enrichment of D in isoprenoids relative to *n*-alkanes suggests that H/D exchange occurs *via* a mechanism that proceeds faster with compounds containing tertiary carbon centres, i.e. one involving carbocation-like intermediates. Significant epimerisation of pristane and phytane coincides with their D-enrichment, suggesting that hydrogen exchange occurs at the tertiary carbons.

Pristane and phytane are significantly enriched in D (ca. 40‰) relative to the *n*-alkanes in the most mature Paqualin-1 sample (post-mature; $\%R_o$ = 1.6). This indicates that D-enrichment persists at very high maturity, and more so for regular isoprenoids than *n*-alkanes. This supports the notion that the observed shift in δD values is due to H/D exchange, and not free-radical hydrogen transfer which would more likely affect the *n*-alkanes to a larger extent than the regular isoprenoids. On the basis of this work, a mechanism is proposed which could occur on a reactive clay surface, involving the formation of an intermittent alkene structure *via* a tertiary carbocation-like species, which then promotes H/D exchange at the adjacent carbon. The resulting sp^2 hybridised tertiary carbocation then undergoes ^1H (or D) reattachment resulting in additional H/D exchange along with epimerisation of the chiral centre. This process would account for both H/D exchange, and the epimerisation of pristane and phytane in the sedimentary environment. However, the fact that pristane and phytane appear to retain the isotopic composition of their precursors in immature sediments indicates that the epimerisation mechanism does not alter their δD values to any significant extent during early maturation.

The enrichment of D in hydrocarbons from Paqualin-1 appears to occur at lower maturity (based on R_o) compared to Vulcan-1B and Perth Basin sediments. Notably, from the least mature sample at 3159 m to the one at 3354 m, there is a significant enrichment of D in pristane and phytane. Thus, it appears that the Paqualin-1 sediments may be more mature than suggested by their R_o values. Alternatively, the isoprenoids from the least mature Paqualin-1 sample could be derived from a different or additional D-depleted source.

In the Perth Basin, phytane is shown to be enriched in D relative to pristane, similar to that observed in the torbanites (Chapter 4), and thus is suggested to be a result of a dominant algal source contributing to the organic matter. In the Vulcan Sub-basin, however, pristane is enriched in D relative to phytane, and thus is suggested to have a lower relative input of algal organic matter. In both cases, the difference between the δD values of pristane and phytane is generally constant throughout the maturity range providing evidence that pristane and phytane exchange hydrogen at similar rates.

An understanding of the effect of sedimentary processes on δD values of individual petroleum hydrocarbons is implicit in their interpretation. This study

shows that the δD values of certain compound types is largely dependent on their reactivity towards hydrogen exchange, thus caution is required when interpreting δD values of hydrocarbons, particularly in sediments of high thermal maturity. It is suggested that samples retaining an offset between the δD values of *n*-alkanes and isoprenoids will have relatively well preserved D/H compositions. The results also suggest that δD values of individual hydrocarbons may be used to assess the thermal maturity of sedimentary organic matter, which will be particularly valuable for samples lacking vitrinite, or where traditional molecular maturity parameters are anomalous.

7.1.3 Stable hydrogen isotopic compositions of petroleum hydrocarbons for oil-source correlation

Based on the work presented in Chapter 6, it is shown that the δD values of individual hydrocarbons in crude oils and condensates can provide source and depositional information which is useful for oil-source correlation purposes. For example, it is shown in Chapter 5 that the δD values of *n*-alkanes in marine petroleum source rocks are indicative of marine-derived *n*-alkyl lipids. While this is somewhat true for marine-derived crude oils, the δD values of *n*-alkanes in crude oils and condensates are often more positive than their supposed source rock counterparts. The D-enriched *n*-alkanes are thought to be indicative of generation from mature source rocks. A mature source rock is supported by the relatively small difference between the δD values of *n*-alkanes and isoprenoids in the crude oils and condensates, which implies that significant H/D exchange has occurred.

A crude oil (Gage Roads-1, off-shore, southern Perth Basin), thought to be derived from a lacustrine/terrestrial source, contains hydrocarbons that are significantly depleted in D relative to those from marine-derived crude oils and condensates of the Perth Basin. This was attributed to terrestrial meteoric source waters being depleted in D relative to ocean water. Prior classification of Vulcan Sub-basin crude oils and condensates into separate marine-influenced (A) and terrestrially-influenced (B) groups is supported by the δD values of *n*-alkanes. One exception is Tenacious-1, previously classified as Group A, which contains *n*-alkanes that are more enriched in D relative to those from other Group A oils and

condensates. This discrepancy was attributed to mixing with another source containing relatively more mature hydrocarbons. Overall, the δD values of individual hydrocarbons are generally indicative of source rock depositional environments.

The profile of *n*-alkane δD values of crude oils have been shown to possibly relate to source and sedimentary processes. Dongara-14 crude oil (on-shore, northern Perth Basin) contains lower-molecular-weight *n*-alkanes that are depleted in D relative to higher-molecular-weight *n*-alkanes, which may be attributed to a mixed marine/terrestrial source rock for this oil. Group A crude oils and condensates from the Vulcan Sub-basin display a 'bowl-shaped' profile of *n*-alkane δD values, which is suggested to represent the addition of a more mature wet gas/condensate to a less mature initial oil charge. This would result in the addition of D-enriched lower-molecular-weight *n*-alkanes, thus causing the upward inflection observed in the *n*-alkane δD profile from *n*-C_{11} to *n*-C_{15}.

Woodada-3 crude oil (on-shore, northern Perth Basin), previously identified as a 'vagrant' in the northern Perth Basin, is also shown to contain *n*-alkanes which are the most enriched in D in comparison to those from the other northern Perth Basin crude oils. Thus, the vagrant nature of this oil is reflected in the δD values of its *n*-alkanes.

The above examples all demonstrate how the δD values of individual hydrocarbons in crude oils and condensates can assist in oil-source correlation studies.

7.2 SUGGESTIONS FOR FUTURE WORK

General suggestions for future development of compound-specific δD analysis of petroleum and other complex organic mixtures using gas chromatography-isotope ratio mass spectrometry (GC-irMS) follow. An improvement in the resolution of chromatographic separation of organic compounds would facilitate compound-specific δD analysis of a wider range of petroleum hydrocarbons (e.g. hopanes, steranes). Developments could include either the use of more advanced gas chromatographic (online separation) techniques such as GC-GC-irMS; or a more

comprehensive series of offline separation methods, e.g. advanced liquid chromatographic and molecular sieving techniques.

Suggestions for extension of the specific research areas (source, alteration and correlation) of this thesis are outlined below. Recent funding of an Australian Research Council Discovery grant (Grice and Greenwood, DP0662839) will allow an investigation of several of these.

7.2.1 Source

Although there has been some research into the biosynthetic fractionations of hydrogen isotopes in extant organisms (e.g. Estep and Hoering, 1980; 1981; Sessions *et al.*, 1999), there is a need for further work to better understand the complex fractionations that occur in specific biosynthetic pathways. This would allow for more comprehensive interpretation of the δD values of hydrocarbons derived from biological precursors *via* specific biosynthetic routes.

Future work could aim to achieve a more comprehensive understanding of source-derived δD values in a larger variety of depositional settings. For example, research into (hyper)saline depositional environments could give insights into the relationship of D/H with palaeosalinity. This research could involve the δD analysis of biomarkers derived from halophilic archaea, which include a series of extended acyclic isoprenoids (C_{21} to C_{25}). These compounds have been previously identified in sediments deposited in (hyper)saline environments (Grice *et al.*, 1998a; 1998c).

7.2.2 Alteration

It is clear that sedimentary processes such as thermal maturation alter the δD values of certain compound types to a greater extent than others; however the investigation of a wider range of compounds is necessary to confirm these findings. Although there is abundant evidence to suggest that hydrogen exchange is a fundamental process in altering the δD values of hydrocarbons during thermal maturation, δD analysis of a more diverse range of carbon-skeletons will serve to better understand the chemical mechanisms that lead to the alteration of δD values. Furthermore, additional field data showing evidence of more positive δD values of

isoprenoids than *n*-alkanes (as discussed in Chapter 5 of this thesis) would provide further evidence that the observed changes in δD values are due to H/D exchange, and not free-radical hydrogen transfer. δD analysis of model compounds before and after artificial maturation experiments could provide additional insight into the mechanisms altering δD values during maturation. In addition, the extent to which the δD values of hydrocarbons in hydrothermal systems are altered could provide another avenue to elucidate the incorporation of water-derived hydrogen into sedimentary hydrocarbons.

The potential of δD values of individual hydrocarbons to assess the thermal maturity of sedimentary organic matter also warrants further investigation. A maturity indicator based on compound-specific δD values may prove useful in cases where traditional biomarker maturity parameters are ineffective, for example at high maturity levels (i.e. $\%R_o > 1$) or where their associated reactants and products either equilibrate, or are thermally degraded. In addition, such a maturity measurement could be applicable to pre-Devonian sediments, where vitrinite reflectance measurements cannot be made because the higher-plant precursors of vitrinite had not yet evolved.

There has been little research into the effect that other alteration events such as in-reservoir biodegradation and water washing have on the δD values of individual petroleum hydrocarbons. Further work in this area would allow a more confident and comprehensive interpretation of the δD values of hydrocarbons present in samples exposed to these secondary processes.

7.2.3 Correlation

The δD values of individual hydrocarbons, in combination with other molecular and $\delta^{13}C$ parameters, have useful applications in oil-source correlation. However, further delineation of the factors determining *n*-alkane δD profiles is required. While the effects of in-reservoir biodegradation and water washing on the δD values of petroleum hydrocarbons are not well understood, there is some evidence that in-reservoir mixing of oils of different maturities affects *n*-alkane δD profiles. Presumably, migration contamination would have the same effect.

Further work could also focus on the δD analysis of a wider range of crude oils derived from source rocks deposited in various types of depositional environments, e.g. fluvio-deltaic, freshwater transitional, marine, lacustrine and (hyper)saline settings. An understanding of the effects of different depositional environments on the δD values of individual hydrocarbons, and particularly on *n*-alkane δD profiles, could prove to be useful when using these measurements for oil-source correlation.

REFERENCES

REFERENCES

AGSO and GEOMARK Research Inc., 2001. The oils of Eastern Australia. Petroleum Geochemistry and Correlation. Proprietary Report, Canberra and Houston, unpublished.

Alexander, R., Kagi, R.I., Larcher, A.V., 1982. Clay catalysis of aromatic hydrogen exchange reactions. Geochimica et Cosmochimica Acta 46, 219–222.

Alexander, R., Kagi, R.I., Larcher, A.V., 1984. Clay catalysis of alkyl hydrogen exchange reactions - reaction mechanisms. Organic Geochemistry 6, 755–760.

Alexander, R., Kagi, R.I., Larcher, A.V., Woodhouse, G.W., 1983. Aromatic hydrogen exchange in petroleum source rocks. In: M. Bjorøy (Ed.), Advances in Organic Geochemistry 1981. John Wiley & Sons Ltd., New York. pp. 69–71.

Alexander, R., Kagi, R.I., Rowland, S.J., Sheppard, P.N., Chirila, T.V., 1985. The effects of thermal maturity on distribution of dimethylnaphthalenes and trimethylnaphthalenes in some Ancient sediments and petroleums. Geochimica et Cosmochimica Acta 49, 385–395.

Andersen, N., Paul, H.A., Bernasconi, S.M., McKenzie, J.A., Behrens, A., Schaeffer, P., Albrecht, P., 2001. Large and rapid climate variability during the Messinian salinity crisis: Evidence from deuterium concentrations of individual biomarkers. Geology 29, 799–802.

Andrusevich, V.E., Engel, M.H., Zumberge, J.E., Brothers, L.A., 1998. Secular, episodic changes in stable carbon isotope composition of crude oils. Chemical Geology 152, 59–72.

Aquino Neto, F.R., Trendel, J.M., Restle, A., Connan, J., Albrecht, P.A., 1983. Occurrence and formation of tricyclic and tetracyclic terpanes in sediments and petroleums. In: M. Bjorøy (Ed.), Advances in Organic Geochemistry 1981. John Wiley & Sons Ltd., New York.

Audino, M., Grice, K., Alexander, R., Boreham, C.J., Kagi, R.I., 2001a. Unusual distribution of monomethylalkanes in *Botryococcus braunii*-rich samples: Origin and significance. Geochimica et Cosmochimica Acta 65, 1995–2006.

Audino, M., Grice, K., Alexander, R., Kagi, R.I., 2001b. Macrocyclic-alkanes: a new class of biomarker. Organic Geochemistry 32, 759–763.

Audino, M., Grice, K., Alexander, R., Kagi, R.I., 2002. Macrocyclic alkanes in crude oils from the algaenan of *Botryococcus braunii*. Organic Geochemistry 33, 979–984.

Barber, C.J., Grice, K., Bastow, T.P., Alexander, R., Kagi, R.I., 2001. The identification of crocetane in Australian crude oils. Organic Geochemistry 32, 943–947.

Bastow, T.P., Alexander, R., Fisher, S., Singh, R.K., van Aarssen, B.G.K., Kagi, R.I., 2000. Geosynthesis of organic compounds. Part V - methylation of alkylnaphthalenes. Organic Geochemistry 31, 523–534.

Bastow, T.P., van Aarssen, B.G.K., Lang, D., 2006. Rapid separation of saturate, aromatic and polar components in petroleum. Organic Geochemistry (in preparation).

Benton, M.J., 2003. When Life Nearly Died - the Greatest Mass Extinction of All Time. Thames & Hudson, London.

Berkaloff, C., Casadevall, E., Largeau, C., Metzger, P., Peracca, S., Virlet, J., 1983. The resistant polymer of the walls of the hydrocarbon-rich alga *Botryococcus braunii*. Phytochemistry 22, 389–397.

Berthéas, O., Delahais, V., Metzger, P., Largeau, C., 1997. Acetal-containing macromolecular lipids in *Botryococcus braunii* (B and L races). Chemical structure and relationship with algaenans. Abstracts of 18th International Meeting on Organic Geochemistry, Forschungszentrum Jülich GmbH, pp. 855–856.

Beveridge, R., Brown, S., Gallagher, J., Merritt, J.W., 1991. Economic geology. In: G.V. Craig (Ed.), Geology of Scotland, 3rd Edition. The Geological Society, London. pp. 545–595.

Bjorøy, M., Hall, K., Gillyon, P., Jumeau, J., 1991. Carbon isotope variations in *n*-alkanes and isoprenoids of whole oils. Chemical Geology 93, 13–20.

Boreham, C.J., Hope, J.M., Hartung-Kagi, B., 2001. Understanding source, distribution and preservation of Australian natural gas: A geochemical perspective. Australian Petroleum Production and Exploration Association Journal 41, 523–547.

Boreham, C.J., Hope, J.M., Hartung-Kagi, B., van Aarssen, B.G.K., 2000. More sources for gas and oil in the Perth Basin: Study highlights potential for multiple petroleum systems. In: AGSO Research Newsletter (December), pp. 5–9.

Boreham, C.J., Summons, R.E., Roksandic, Z., Dowling, L.M., Hutton, A.C., 1994. Chemical, molecular and isotopic differentiation of organic facies in the Tertiary lucastrine Duaringa oil shale deposit, Queensland, Australia. Organic Geochemistry 21, 685–712.

Brand, W.A., Tegtmeyer, A.R., Hilkert, A.W., 1994. Compound-specific isotope analysis: extending toward $^{15}N/^{14}N$ and $^{18}O/^{16}O$. Organic Geochemistry 21, 585–594.

Brooks, J.D., Gould, K., Smith, J., 1969. Isoprenoid hydrocarbons in coal and petroleum. Nature 222, 257–259.

Burgoyne, T.W., Hayes, J.M., 1998. Quantitative production of H_2 by pyrolysis of gas chromatographic effluents. Analytical Chemistry 70, 5136–5141.

Calvo, E., Pelejero, C., Logan, G.A., 2003. Pressurized liquid extraction of selected molecular biomarkers in deep sea sediments used as proxies in paleoceanography. Journal of Chromatography A 989, 197–205.

Caroll, P.G., Syme, A., 1994. Hydrocarbon habitat study of the Vulcan Graben (Browse and Bonaparte Basins) Permits: AC/P2 & AC/P4 and Licenses: AC/L1, 2, 3, 4. A study commissioned by the AC/P2 & AC/P4 Joint Ventures. BHP Petroelum Pty. Ltd. Report, unpublished.

Chen, G., Hill, K.C., Hoffman, N., 2002. 3D structural analysis of hydrocarbon migration in the Vulcan Sub-basin, Timor Sea. In: M. Keep, S.J. Moss (Eds), The Sedimentary Basins of Western Australia 3. Proceedings of the Petroleum Exploration Society of Australia Symposium. Perth, WA, 2002. pp. 377–388.

Chung, H.M., Rooney, M.A., Toon, M.B., Claypool, G.E., 1992. Carbon isotope composition of marine crude oils. American Association of Petroleum Geologists Bulletin 76, 1000–1007.

Clayton, C.J., 1991. Effect of maturity on carbon isotope ratios of oils and condensates. Organic Geochemistry 17, 887–899.

Clayton, C.J., Bjorøy, M., 1994. Effect of maturity on $^{13}C/^{12}C$ ratios of individual compounds in North-Sea oils. Organic Geochemistry 21, 737–750.

Coplen, T.B., 1988. Normalization of oxygen and hydrogen isotope data. Chemical Geology 72, 293–297.

Cox, R.E., Maxwell, J.R., Ackman, R.G., Hooper, S.N., 1974. Stereochemical studies of acyclic isoprenoid compounds IV. Microbial oxidation of 2,6,10,14-tetramethylpentadecane (pristane). Biochimica et Biophysica Acta 360, 166–173.

Craig, H., 1957. Isotopic standards for carbon and oxygen and correction factors for mass-spectrometric analysis of carbon dioxide. Geochimica et Cosmochimica Acta 12, 133–149.

Craig, H., 1961. Isotopic variations in meteoric waters. Science 133, 1702–1703.

Craig, H., Gordon, L.I., 1965. Deuterium and oxygen 18 variations in the ocean and the marine atmosphere. Symposium on Marine Geochemistry, Narraganset Marine Laboratory, University of Rhode Island Publication, Vol. 3, pp. 277–374.

Craig, H., Gordon, L.I., Horibe, Y., 1963. Isotopic exchange effects in the evaporation of water. 1. Low-temperature experimental results. Journal of Geophysical Research 68, 5079–5087.

Criss, R.E., 1999. Principles of Stable Isotope Distribution. Oxford University Press Inc., New York.

Dansgaard, W., 1964. Stable isotopes in precipitation. Tellus 16, 436–468.

Dawson, D., Grice, K., Alexander, R., 2005a. Effect of maturation on the indigenous δD signatures of individual hydrocarbons in sediments and crude oils from the Perth Basin (Western Australia). Organic Geochemistry 36, 95–104.

Dawson, D., Grice, K., Alexander, R., 2005b. Stable hydrogen isotope ratios of sedimentary hydrocarbons: A potential method for assessing thermal maturity? Australian Petroleum Production and Exploration Association Journal 45, 253–260.

Dawson, T.E., 1993. Water sources of plants as determined from xylem-water isotopic composition: perspectives on plant competition, distribution, and water relations. In: J.R. Ehleringer, A.E. Hall, G.D. Farquhar (Eds), Stable Isotopes and Plant Carbon-Water Relations. Academic Press Inc., San Diego. pp. 465–496.

Derenne, S., Largeau, C., Casadevall, E., Berkaloff, C., 1989. Occurence of a resistant biopolymer in the L race of *Botryococcus braunii*. Phytochemistry 28, 1137–1142.

Derenne, S., Largeau, C., Casadevall, E., Connan, J., 1988. Comparison of torbanites of various origins and evolutionary stages. Bacterial contribution to their formation. Cause of the lack of botryococcane in bitumens. Organic Geochemistry 12, 43–59.

Derenne, S., Largeau, C., Hatcher, P.G., 1992. Structure of *Chorella fusca* algaenan: relationships with ultralaminae in lacustrine kerogens; species and environment-dependant variations in the composition of fossil ultralaminae. Organic Geochemistry 19, 345–350.

Didyk, B.M., Simoneit, B.R.T., Brassell, S.C., Eglinton, G., 1978. Organic geochemical indicators of palaeoenvironmental conditions of sedimentation. Nature 272, 216–222.

Dongmann, G., Nurnber, H.W., Forstel, H., Wagner, K., 1974. The contribution of land photosynthesis to the stationary enrichment of ^{18}O in the atmosphere. Radiation and Environmental Biophysics 11, 41–52.

Edwards, D.S., Preston, J.C., Kennard, J.M., Boreham, C.J., van Aarssen, B.G.K., Summons, R.E., Zumberge, J.E., 2004. Geochemical characteristics of hydrocarbons from the Vulcan Sub-basin, western Bonaparte Basin, Australia. In: G.K. Ellis, P.W. Baillie, T.J. Munson (Eds), Timor Sea Petroleum Geoscience: Proceedings of the Timor Sea Symposium, Darwin, Northern Territory, 19-20 June 2003. Northern Territory Geological Survey, pp. 169–201.

Eglinton, G., Hamilton, R.J., 1963. The distribution of *n*-alkanes. In: T. Swain (Ed.), Chemical Plant Taxonomy. Academic Press, London. pp. 187–217.

Ehleringer, J.R., Hall, A.E., Farquhar, G.D., 1993. Stable Isotopes and Plant-Carbon Water Relations. Academic Press, San Diego.

Ensminger, A., Albrecht, P., Ourisson, G., Tissot, B., 1977. Evolution of polycyclic alkanes under the effect of burial. In: R. Campo, J. Goni (Eds), Advances in Organic Geochemistry 1975. ENADIMSA, Madrid. pp. 45–52.

Epstein, S., Yapp, C.J., Hall, J.H., 1976. The determination of the D/H ratio of non-exchangeable hydrogen in cellulose extracted from aquatic and land plants. Earth and Planetary Science Letters 30, 241–251.

Erwin, D., 1994. The Permo-Triassic extinction. Nature 367, 231–236.

Espitalié, J., Laporte, J.L., Madec, M., Marquis, F., Leplat, P., Paulet, J., Boutefeu, A., 1977. Méthode rapide de charactérisation des roches méres, de leur potential pétrolier et de leur degré d'évolution. Revue de l'Institut Français du Pétrole 32, 23–42.

Estep, M.F., Hoering, T.C., 1980. Biogeochemistry of the stable hydrogen isotopes. Geochimica et Cosmochimica Acta 44, 1197–1206.

Estep, M.F., Hoering, T.C., 1981. Stable hydrogen isotope fractionations during autotrophic and mixotrophic growth of microalgae. Plant Physiology 67, 474–477.

Evans, R.J., Felbeck, G.T., 1983. High temperature simulation of petroelum formation. I. The pyrolysis of Green River Shale. Organic Geochemistry 4, 135-144.

Farquhar, G.D., Gan, K.S., 2003. On the progressive enrichment of the oxygen isotopic composition of water along a leaf. Plant, Cell and Environment 26, 1579–1597.

Foster, C.B., Logan, G.A., Summons, R.E., Gorter, J.D., Edwards, D.S., 1997. Carbon isotopes, kerogen types and the Permian-Triassic boundary in Australia: Implications for Exploration. Australian Petroleum Production and Exploration Association Journal 37, 472–489.

Frakes, L.A., 1979. Climates Throughout Geologic Time. Elsevier Scientific, Amsterdam.

Freeman, K.H., Hayes, J.M., Trendel, J.M., Albrecht, P., 1990. Evidence from carbon isotope measurements for diverse origins of sedimentary hydrocarbons. Nature 343, 254–256.

Gan, K.S., Wong, S.C., Yong, J.W.H., Farquhar, G.D., 2003. Evaluation of models of leaf water ^{18}O enrichment using measurements of spatial patterns of vein xylem, leaf water and dry matter in maize leaves. Plant, Cell and Environment 26, 1479–1495.

Gatellier, J.-P.L.A., de Leeuw, J.W., Sinninghe Damsté, J.S., Derenne, S., Largeau, C., Metzger, P., 1993. A comparative study of macromolecular substances of a Coorongite and cell walls of the extant alga *Botryococcus braunii*. Geochimica et Cosmochimica Acta 57, 2053–2068.

Gelin, F., De Leeuw, J.W., Sinninghe Damsté, J.S., Derenne, S., Largeau, C., Metzger, P., 1994. The similarity of the chemical structures of the soluble aliphatic polyaldehyde and insoluble algaenan in the green microalga *Botryococcus braunii* race A as revealed by analytical pyrolysis. Organic Geochemistry 21, 423–435.

George, S.C., Boreham, C.J., Minifie, S.A., Teerman, S.C., 2002. The effect of minor to moderate biodegradation on C_5 to C_9 hydrocarbons in crude oils. Organic Geochemistry 33, 1293–1317.

Gilmour, I., Swart, P.K., Pillinger, C.T., 1984. The carbon isotopic composition of individual petroleum lipids. Organic Geochemistry 6, 665–670.

Goericke, R., Montoya, J.P., Fry, B., 1994. Physiology of isotope fractionation in algae and cyanobacteria. In: K. Lajtha, B. Michener (Eds), Stable Isotopes in Ecology and Environmental Science. Blackwell Scientific Publications, Oxford. pp. 187–221.

Goosens, H., de Leeuw, J.W., Schenck, P.A., Brassell, S.C., 1984. Tocopherols as likely precursors of pristane in sediments and crude oils. Nature 312, 440–442.

Greenwood, P.F., Summons, R.E., 2003. GC-MS detection and significance of crocetane and pentamethylicosane in sediments and crude oils. Organic Geochemistry 34, 1211–1222.

Grice, K., Audino, M., Boreham, C.J., Alexander, R., Kagi, R.I., 2001. Distributions and stable carbon isotopic compositions of biomarkers in torbanites from different palaeogeographical locations. Organic Geochemistry 32, 1195–1210.

Grice, K., Cao, C., Love, G.D., Böttcher, M.E., Twitchett, R.J., Grosjean, E., Summons, R.E., Turgeon, S.C., Dunning, W., Jin, Y., 2005a. Photic zone euxinia during the Permian-Triassic superanoxic event. Science 307, 706–709.

Grice, K., Schaeffer, P., Schwark, L., Maxwell, J.R., 1996. Molecular indicators of palaeoenvironmental conditions in an immature Permian shale (Kupferschiefer, Lower Rhine Basin, north-west Germany) from free and S-bound lipids. Organic Geochemistry 25, 131–147.

Grice, K., Schouten, S., Nissenbaum, A., Charrach, J., Sinninghe Damsté, J.S., 1998a. Isotopically heavy carbon in the C_{21} to C_{25} regular isoprenoids in halite-rich deposits from the Sdom Formation, Dead Sea Basin, Israel. Organic Geochemistry 28, 349–359.

Grice, K., Schouten, S., Nissenbaum, A., Charrach, J., Sinninghe Damsté, J.S., 1998b. A remarkable paradox: Sulfurised freshwater algal (*Botryococcus braunii*) lipids in an ancient hypersaline euxinic ecosystem. Organic Geochemistry 28, 195–216.

Grice, K., Schouten, S., Peters, K.E., Sinninghe Damsté, J.S., 1998c. Molecular isotopic characterization of hydrocarbon biomarkers in Palaeocene-Eocene evaporitic, lacustrine source rocks from the Jianghan Basin, China. Organic Geochemistry 29, 1745–1764.

Grice, K., Summons, R.E., Grosjean, E., Twitchett, R.J., Dunning, W., Wang, S.X., Böttcher, M.E., 2005b. Depositional conditions of the northern onshore Perth Basin (Basal Triassic). Australian Petroleum Production and Exploration Association Journal 45, 263–274.

Grice, K., Twitchett, R.J., Alexander, R., Foster, C.B., Looy, C., 2005c. A potential biomarker for the Permian-Triassic ecological crisis. Earth and Planetary Science Letters 236, 315–321.

Hansen, D., Bastow, T.P., van Aarssen, B.G.K., Alexander, R., Kagi, R.I., 2003. Maturation and biodegradation effects on the diastereomers of pristane and phytane. Book of Abstracts, Part II, 21st International Meeting on Organic Geochemistry, Kraków, pp. 355.

Hayes, J.M., 1993. Factors controlling the ^{13}C contents of sedimentary organic compounds: Principles and evidence. Marine Geology 113, 111–125.

Hayes, J.M., Freeman, K.H., Popp, B.N., Hoham, C.H., 1990. Compound-specific isotopic analyses: A novel tool for reconstruction of ancient biogeochemical processes. In: B. Durand, F. Behar (Eds), Advances in Organic Geochemistry 1989. Pergamon Press, Oxford. pp. 1115–1128.

Hilkert, A.W., Douthitt, C.B., Schlüter, H.J., Brand, W.A., 1999. Isotope ratio monitoring gas chromatography/mass spectrometry of D/H by high temperature conversion isotope ratio mass spectrometry. Rapid Communications in Mass Spectrometry 13, 1226–1230.

Hoefs, J., 1987. Stable Isotope Geochemistry. Springer-Verlag, Berlin.

Hoering, T.C., 1977. The stable isotopes of hydrogen in Precambrian organic-matter. In: C. Ponnamperuma (Ed.), Chemical Evolution of the Early Precambrian. Academic Press, New York. pp. 81–86.

Hoering, T.C., 1984. Thermal reactions of kerogen with added water, heavy water and pure organic substances. Organic Geochemistry 5, 267–278.

Huizinga, B.J., Tannenbaum, E., Kaplan, I.R., 1987. The role of minerals in the thermal alteration of organic matter. IV. Generation of *n*-alkanes, acyclic isoprenoids and alkenes in laboratory experiments. Geochimica et Cosmochimica Acta 51, 1083–1097.

Hunt, J.M., 1996. Petroleum Geochemistry and Geology, 2nd edition. W.H. Freeman and Co., San Fansisco.

Hutton, A.C., Kantsler, A.J., Cook, A.C., McKirdy, D.M., 1980. Organic-matter in oil shales. Australian Petroleum Exploration Association Journal 20, 44–65.

Jefferies, P.J., 1984. Petroleum geochemistry of the northern Perth Basin. Post-graduate Diploma dissertation, Western Australian Institute of Technology, Perth.

Kadouri, A., Derenne, S., Largeau, C., Casadevall, E., Berkaloff, C., 1988. Resistant biopolymer in the outer cell walls of *Botryococcus braunii,* B race. Phytochemistry 27, 551–557.

Kantsler, A.J., Cook, A.C., 1979. Maturation patterns in the Perth Basin. Australian Petroleum Exploration Association Journal 19, 94–107.

Kehew, A.E., 2001. Applied Chemical Hydrogeology. Prentice Hall, New Jersey.

Kennard, J.M., Deighton, I., Edwards, D.S., Colwell, J.B., O'Brien, G.W., Boreham, C.J., 1999. Thermal history modelling and transient heat pulses: New insights into hydrocarbon expulsion and 'hot flushes' in the Vulcan Sub-basin, Timor Sea. Australian Petroleum Production and Exploration Association Journal 39, 177–207.

Koepp, M., 1978. D/H isotope exchange reaction between petroleum and water: A contributory determinant for D/H-isotope ratios in crude oils? In: R.E. Zartman (Ed.), Short Papers of the Fourth International Conference, Geochronology, Cosmochronology, Isotope Geology. USGS Open-File Report 78-701. US Geological Survey, pp. 221–222.

Koopmans, M.P., Rijpstra, W.I.C., Klapwijk, M.M., De Leeuw, J.W., Lewan, M.D., Sinninghe Damsté, J.S., 1999. A thermal and chemical degradation approach to decipher pristane and phytane precursors in sedimentary organic matter. Organic Geochemistry 30, 1089–1104.

Krull, E.S., Retallack, G.J., Campbell, H.J., Lyon, G.L., 2000. $\delta^{13}C_{org}$ chemostratigraphy of the Permian-Triassic boundary in the Maitai Group, New Zealand: Evidence for high-latidudinal methane release. New Zealand Journal of Geology and Geophysics 43, 21–32.

Larcher, A.V., Alexander, R., Rowland, S.J., Kagi, R.I., 1986. Acid catalysis of alkyl hydrogen exchange and configurational isomerization reactions: acyclic isoprenoid acids. Organic Geochemistry 10, 1015–1021.

Largeau, C., Derenne, S., Casadevall, E., Kadouri, A., Menzger, P., 1984. Formation of *Botryococcus* derived kerogens. Comparative study of immature torbanites and of the extant alga *Botryococcus braunii*. Organic Geochemistry 6, 327–332.

Laws, E.A., Popp, B.N., Bidigare, R.R., Kennicutt, M.C., Macko, S.A., 1995. Dependence of phytoplankton isotopic composition on growth rate and $[CO_2]_{aq}$: Theoretical considerations and experimental results. Geochimica et Cosmochimica Acta 59, 1131–1138.

Leif, R.N., Simoneit, R.T., 2000. The role of alkenes produced during hydrous pyrolysis of a shale. Organic Geochemistry 31, 1189–1208.

Lewan, M.D., Winters, J.C., MacDonald, J.H., 1979. Generation of oil-like pyrolysates from organic-rich shales. Science 203, 897–899.

Li, M., Huang, Y., Obermajer, M., Jiang, C., Snowdon, L.R., Fowler, M.G., 2001. Hydrogen isotopic compositions of individual alkanes as a new approach to petroleum correlation: case studies from the Western Canada Sedimentary Basin. Organic Geochemistry 32, 1387–1399.

Lis, G., Schimmelmann, A., Mastalerz, M., Stankiewicz, B.A., 2005. D/H ratios and hydrogen exchangeability of type-II kerogens with increasing maturity. Organic Geochemistry 37, 342–353.

Liu, K., Fenton, S., Bastow, T.P., van Aarssen, B.G.K., Eadington, P., 2005. Geochemical evidence of multiple hydrocarbon charges and long distance oil migration in the Vulcan Sub-basin, Timor Sea. Australian Petroleum Production and Exploration Association Journal 45, 493–510.

Mackenzie, A.S., Brassell, S.C., Eglinton, G., Maxwell, J.R., 1982. Chemical fossils: the geological fate of steroids. Science 217, 491–504.

Mackenzie, A.S., Patience, R.L., Maxwell, J.R., 1980. Molecular parameters of maturation in the Toarcian shales, Paris Basin, France - I. Changes in the configurations of acyclic isoprenoid alkanes, steranes and triterpanes. Geochimica et Cosmochimica Acta 44, 1709–1721.

Matthews, D.E., Hayes, J.M., 1978. Isotope-ratio-monitoring gas chromatography-mass spectrometry. Analytical Chemistry 50, 1465–1473.

McIldowie, M., Alexander, R., 2005. Identification of a novel C_{33} *n*-alkylcyclohexane biomarker in Permian-Triassic sediments. Organic Geochemistry 36, 1454–1458.

Metzger, P., Templier, J., Largeau, C., Casadevall, E., 1986. A *n*-alkatriene and some *n*-alkadienes from the A race of the green alga *Botryococcus braunii.* Phytochemistry 25, 1869–1872.

Morante, R., Veevers, J.J., Andrew, A.S., Hamilton, P.J., 1994. Determination of the Permian-Triassic boundary in Australia from carbon isotope stratigraphy. Australian Petroleum Exploration Association Journal 34, 330–336.

Morrison, R.T., Boyd, R.N., 1992. Organic Chemistry, 6th Edition. Prentice Hall, New Jersey.

Murray, A.P., Summons, R.E., Boreham, C.J., Dowling, L.M., 1994. Biomarkers and *n*-alkane isotope profiles for Tertiary oils: relationship to source rock depositional setting. Organic Geochemistry 22, 521–542.

Pallasser, R.J., 2000. Recognising biodegradation in gas/oil accumulations through the $\delta^{13}C$ compositions of gas components. Organic Geochemistry 31, 1363–1373.

Patience, R.L., Rowland, S.J., Maxwell, J.R., 1978. The effect of maturation on the configuration of pristane in sediments and petroleum. Geochimica et Cosmochimica Acta 42, 1871–1875.

Patience, R.L., Yon, D.A., Ryback, G., Maxwell, J.R., 1980. Acyclic isoprenoid alkanes and geochemical maturation. In: A.G. Douglas, J.R. Maxwell (Eds), Advances in Organic Geochemistry 1979. Pergamon Press, Oxford. pp. 287–294.

Pedentchouk, N., Freeman, K.H., Harris, N.B., 2006. Different response of δD values of *n*-alkanes, isoprenoids, and kerogen during thermal maturation. Geochimica et Cosmochimica Acta 70, 2063–2072.

Peters, K.E., Moldowan, J.M., 1993. The Biomarker Guide. Interpreting Molecular Fossils in Petroleum and Ancient Sediments. Prentice Hall, New Jersey.

Peters, K.E., Walters, C.C., Moldowan, J.M., 2005. The Biomarker Guide, second edition. Volume 2. Biomarkers and Isotopes in Petroleum Exploration and Earth History. Cambridge University Press, Cambridge.

Pond, K.L., Huang, Y., Wang, Y., Kulpa, C.F., 2002. Hydrogen isotopic composition of individual *n*-alkanes as an intrinsic tracer for bioremediation and source identification of petroleum contamination. Environmental Science and Technology 36, 724–728.

Popp, B.N., Laws, E.A., Bidigare, R.R., Dore, J.E., Hanson, K.L., Wakeham, S.G., 1998. Effect of phytoplankton cell geometry on carbon isotopic fractionation. Geochimica et Cosmochimica Acta 62, 69–79.

Powell, T.G., McKirdy, D.M., 1973. Relationship between ratio of pristane to phytane, crude oil composition and geological environment in Australia. Nature 243, 37–39.

Radke, J., Bechtel, A., Gaupp, R., Püttmann, W., Schwark, L., Sachse, D., Gleixner, G., 2005. Correlation between hydrogen isotope ratios of lipid biomarkers and sediment maturity. Geochimica et Cosmochimica Acta 69, 5517–5530.

Radke, M., Welte, D.H., 1983. The methylphenanthrene index (MPI): A maturity parameter based on aromatic hydrocarbons. In: M. Bjorøy (Ed.), Advances in Organic Geochemistry 1981. John Wiley & Sons Ltd., New York. pp. 504–512.

Radke, M., Welte, D.H., Willsch, H., 1982. Geochemical study on a well in the Western Canada Basin: relation of the aromatic distribution pattern to maturity of organic matter. Geochimica et Cosmochimica Acta 46, 1–10.

Rieley, G., Collier, R.J., Jones, D.M., Eglinton, G., Eakin, P.A., Fallick, A.E., 1991. Sources of sedimentary lipids deduced from stable carbon isotope analyses of individual compounds. Nature 352, 425–427.

Rigby, D., Batts, B.D., Smith, J.W., 1981. The effect of maturation on the isotopic composition of fossil fuels. Organic Geochemistry 3, 29–36.

Rooney, M.A., Vuletich, A.K., Griffith, C.E., 1998. Compound-specific isotope analysis as a tool for characterizing mixed oils: An example from the west of Shetlands area. Organic Geochemistry 29, 241–254.

Ross, D., 1992. Comments on the source of petroleum hydrocarbons in hydrous pyrolysis. Organic Geochemistry 18, 79–81.

Rowland, S.J., 1990. Production of acyclic isoprenoid hydrocarbons by laboratory maturation of methanogenic bacteria. Organic Geochemistry 15, 9-16.

Santos Neto, E.V., Hayes, J.M., 1999. Use of hydrogen and carbon stable isotopes characterizing oils from the Potiguar Basin (onshore), Northeastern Brazil. American Association of Petroleum Geologists Bulletin 83, 496–518.

Sauer, P.E., Eglinton, T.I., Hayes, J.M., Schimmelmann, A., Sessions, A.L., 2001. Compound-specific D/H ratios of lipid biomarkers from sediments as a proxy for environmental and climatic conditions. Geochimica et Cosmochimica Acta 65, 213–222.

Schimmelmann, A., 1991. Determination of the concentration and stable isotopic composition of non-exchangeable hydrogen in organic matter. Analytical Chemistry 63, 2456–2459.

Schimmelmann, A., Boudou, J.-P., Lewan, M.D., Wintsch, R.P., 2001. Experimental controls on D/H and $^{13}C/^{12}C$ ratios of kerogen, bitumen and oil during hydrous pyrolysis. Organic Geochemistry 32, 1009–1018.

Schimmelmann, A., Lewan, M.D., Wintsch, R.P., 1999. D/H isotope ratios of kerogen, bitumen, oil, and water in hydrous pyrolysis of source rocks containing kerogen types I, II, IIS, and III. Geochimica et Cosmochimica Acta 63, 3751–3766.

Schimmelmann, A., Sessions, A.L., Boreham, C.J., Edwards, D.S., Logan, G.A., Summons, R.E., 2004. D/H ratios in terrestrially sourced petroleum systems. Organic Geochemistry 35, 1169–1195.

Schimmelmann, A., Sessions, A.L., Mastalerz, M., 2006. Hydrogen isotopic (D/H) composition of organic matter during diagenesis and thermal maturation. Annual Review of Earth and Planetary Science 34, 501–533.

Schouten, S., Klein Breteler, W.C.M., Blokker, P., Schogt, N., Rijpstra, W.I.C., Grice, K., Baas, M., Sinninghe Damsté, J.S., 1998. Biosynthetic effects on the stable carbon isotopic compositions of algal lipids: Implications for deciphering the carbon isotopic biomarker record. Geochimica et Cosmochimica Acta 62, 1397–1406.

Scotese, C.R., 1997. Paleogeographic Atlas. PALAEOMAP Progress Report 90-0497. Department of Geology, University of Texas, Arlington, Texas.

Seifert, W.K., Moldowan, J.M., 1978. Applications of steranes, terpanes and monoaromatics to the maturation, migration and source of crude oils. Geochimica et Cosmochimica Acta 42, 77–95.

Seifert, W.K., Moldowan, J.M., 1981. Paleoreconstruction by biological markers. Geochimica et Cosmochimica Acta 45, 783–794.

Sessions, A.L., 2001. Hydrogen Isotope Ratios of Individual Organic Compounds. PhD dissertation, Indiana University, Bloomington, Indiana, 149p.

Sessions, A.L., Burgoyne, T.W., Schimmelmann, A., Hayes, J.M., 1999. Fractionation of hydrogen isotopes in lipid biosynthesis. Organic Geochemistry 30, 1193–1200.

Sessions, A.L., Sylva, S.P., Summons, R.E., Hayes, J.M., 2004. Isotopic exchange of carbon-bound hydrogen over geologic timescales. Geochimica et Cosmochimica Acta 68, 1545–1559.

Sieskind, O., Joly, G., Albrecht, P., 1979. Simulation of the geochemical transformations of sterols: superacid effect of clay minerals. Geochimica et Cosmochimica Acta 43, 1675–1679.

Smith, B.N., Epstein, S., 1970. Biogeochemistry of the stable isotopes of hydrogen and carbon in salt marsh biota. Plant Physiology 46, 738–742.

Smith, J.W., Gould, K.W., Rigby, D., 1982. The stable isotope geochemistry of Australian coals. Organic Geochemistry 3, 111–131.

Smith, P.M., Sutherland, N.D., 1991. Discovery of salt in the Vulcan Graben: A geophysical and geological evaluation. Australian Petroleum Exploration Association Journal 31, 229–243.

Sofer, Z., 1984. Stable carbon isotope compositions of crude oils: Application to source depositional environments and petroleum alteration. American Association of Petroleum Geologists Bulletin 68, 31–49.

Sternberg, L., 1988. D/H ratios of environmental water recorded by D/H ratios of plant lipids. Nature 333, 59–61.

Summons, R.E., Boreham, C.J., Foster, C.B., Murray, A.P., Gorter, J.D., 1995. Chemostratigraphy and the composition of oils in the Perth Basin, Western Australia. Australian Petroleum Exploration Association Journal 35, 613–631.

Summons, R.E., Jahnke, L.L., Roksandic, Z., 1994. Carbon isotopic fractionation in lipids from methanotrophic bacteria: Relevance for interpretation of the geochemical record of biomarkers. Geochimica et Cosmochimica Acta 13, 2853–2863.

Sun, Y., Chen, Z., Xu, S., Cai, P., 2005. Stable carbon and hydrogen isotopic fractionation of individual *n*-alkanes accompanying biodegradation: evidence from a group of progressively biodegraded oils. Organic Geochemistry 36, 225–238.

Tang, Y., Huang, Y., Ellis, G.S., Wang, Y., Kralert, P.G., Gillaizeau, B., Ma, Q., Hwang, R., 2005. A kinetic model for thermally induced hydrogen and carbon isotope fractionation of individual *n*-alkanes in crude oil. Geochimica et Cosmochimica Acta 69, 4505–4520.

Thomas, B.M., Barber, C.J., 2004. A re-evaluation of the hydrocarbon habitat of the northern Perth Basin. Australian Petroleum Production and Exploration Association Journal 44, 59–92.

Thomas, B.M., Willink, R.J., Grice, K., Twitchett, R.J., Purcell, R.R., Archbold, N.W., George, A.D., Tye, S., Alexander, R., Foster, C.B., Barber, C.J., 2004. Unique marine Permian-Triassic boundary section from Western Australia. Australian Journal of Earth Sciences 51, 423–430.

Tyson, R.V., 1995. Sedimentary Organic Matter. Organic Facies and Palynofacies. Chapman and Hall, New York.

Urey, H.C., Lowenstam, H.A., Epstein, S., McKinney, C.R., 1951. Measurement of palaeotemperatures and temperatures of the upper Cretaceous of England, Denmark, and Southeastern United States. American Association of Petroleum Geologists Bulletin 62, 399–416.

van Aarssen, B.G.K., Alexander, R., Kagi, R.I., 1996. The origin of Barrow Sub-basin crude oils: A geochemical correlation using land-plant biomarkers. Australian Petroleum Exploration Association Journal 36, 465–476.

van Aarssen, B.G.K., Alexander, R., Kagi, R.I., 1998a. Higher plant biomarkers on the North West Shelf: Application in stratigraphic correlation and palaeoclimate reconstruction. In: P.G. Purcell, R.R. Purcell (Eds), The Sedimentary Basins of Western Australia 2: Proceedings of the Petroleum Exploration Society of Australia Symposium. Perth. pp. 123–128.

van Aarssen, B.G.K., Alexander, R., Kagi, R.I., 1998b. Molecular indicators for palaeoenvironmental changes. Petroleum Exploration Society of Australia Journal 26, 98–105.

van Aarssen, B.G.K., Bastow, T.P., Alexander, R., Kagi, R.I., 1999. Distributions of methylated naphthalenes in crude oils: indicators of maturity, biodegradation and mixing. Organic Geochemistry 30, 1213–1227.

van Aarssen, B.G.K., Bastow, T.P., Alexander, R., Kagi, R.I., 2004. Trend reversal in depth profiles of molecular maturity parameters. In: C. McIntyre (Ed.), Conference Program and Abstracts, Combined National Conference of the Australian Organic Geochemists and the International Humic Substances Society, Blue Mountains NSW, Australia. pp. 22–23.

van Kaam-Peters, H.M.E., Köster, J., van der Gaast, S.J., Dekker, M., De Leeuw, J.W., Sinninghe Damsté, J.S., 1998. The effect of clay minerals on diasterane/sterane ratios. Geochimica et Cosmochimica Acta 62, 2923–2929.

Volk, H., George, S.C., Boreham, C.J., Kempton, R.H., 2004. Geochemical and compound specific carbon isotopic characterisation of fluid inclusion oils from the offshore Perth Basin, Western Australia: implications for recognising effective oil source rocks. Australian Petroleum Exploration Association Journal 44, 223–239.

Volkman, J.K., 1986. A review of sterol markers for marine and terrigenous organic matter. Organic Geochemistry 9, 83–99.

Werner, R.A., Brand, W.A., 2001. Referencing strategies and techniques in stable isotope ratio analysis. Rapid Communications in Mass Spectrometry 15, 501–519.

White, M.E., 1993. The Greening of Gondwana. The 400 Million Year Story of Australias Plants. Reed, Australia.

Wignall, P.B., Twitchett, R.J., 1996. Late Permian extinctions. Response. Science 272, 1155–1158.

Wilkins, R.W.T., Wilmshurst, J.R., Russel, N.J., Hladky, G., Ellacott, M.V., Buckingham, C., 1992. Fluorescence alteration and the supression of vitrinite reflectance. Organic Geochemistry 18, 629–640.

Xie, S., Nott, C.J., Avsejs, L.A., Volders, F., Maddy, D., Chambers, F.M., Gledhill, A., Carter, J.F., Evershed, R.P., 2000. Palaeoclimate records in compound-specific δD values of a lipid biomarker in ombrotrophic peat. Organic Geochemistry 31, 1053–1057.

Xiong, Y., Geng, A., Pan, C., Liu, D., Peng, P., 2005. Characterization of the hydrogen isotopic composition of individual *n*-alkanes in terrestrial source rocks. Applied Geochemistry 20, 455–464.

Yang, H., Huang, Y., 2003. Preservation of lipid hydrogen isotope ratios in Miocene lacustrine sediments and plant fossils at Clarkia, northern Idaho, USA. Organic Geochemistry 34, 413–423.

Yeh, H-W., Epstein, S., 1981. Hydrogen and carbon isotopes of petroleum and related organic matter. Geochimica et Cosmochimica Acta 45, 753–762.

APPENDICES

APPENDIX 1

Glossary of geochemical parameters used in this study

BULK PARAMETERS

Vitrinite Reflectance

A maturity parameter for sedimentary organic matter. Vitrinite is a group of macerals derived from land plant tissues. Vitrinite particles are used for vitrinite reflectance (R_o) determinations of thermal maturity. The reflectance of vitrinite depends on its chemical composition. Irreversible chemical changes in vitrinite (e.g. increase in aromaticity) occur with ongoing maturaton, resulting in increased reflectance. R_o values are determined from the average reflectance of a specific number of vitrinite particles (typically 50–100; Peters and Moldowan, 1993) in a polished slide of kerogen. The term $\%R_o$ refers to the percentage of incident light (546 nm) reflected from the particles back through a microscope using an oil-immersion objective.

T_{max}, hydrogen index and oxygen index from Rock-Eval pyrolysis

Rock-Eval pyrolysis (Espitalié *et al.*, 1977) is a programmed temperature pyrolysis technique used for source rock assessment. The crushed sediment is heated in an inert atmosphere over a programmed temperature range from 300 to 550ºC. Free or adsorbed hydrocarbons (S_1) are thermally distilled at 300ºC and measured with a flame ionisation detector (FID). Hydrocarbons bound within the kerogen (S_2) are then thermally cracked during the temperature increase from 300 to 550ºC and also measured with the FID. CO_2 released during the cracking process (S_3) is trapped and subsequently measured by a thermal conductivity detector. Figure A.1a shows a typical Rock-Eval pyrolysis pyrogram and the related parameters. T_{max} is the temperature which corresponds to the maximum hydrocarbon generation during pyrolysis (S_2; see Figure A.1a), and is a maturity indicator, e.g. T_{max} values below ~ 430ºC are characteristic of immature samples, while values in excess of 460ºC are typical of overmature samples. T_{max} also varies with the type of organic matter, e.g.

in oil-prone Type I kerogen the generation of hydrocarbons will commence later, i.e. at higher temperatures, than in Type III kerogen. Hydrogen index (HI) and oxygen index (OI) are used as measures of source rock quality. HI ((S_2/TOC)x100), expressed as mg hydrocarbons/g total organic carbon (mg HC/g TOC); and OI ((S_3/TOC)x100), expressed as mg CO_2/g TOC, are used in combination to determine the type of organic matter present in a source rock. For example, high HI and low OI is indicative of oil-prone Type I kerogen, while low HI and high OI is characteristic of gas-prone Type III kerogen. HI and OI are often plotted together in van Krevelen diagrams (e.g. Figure A.1b).

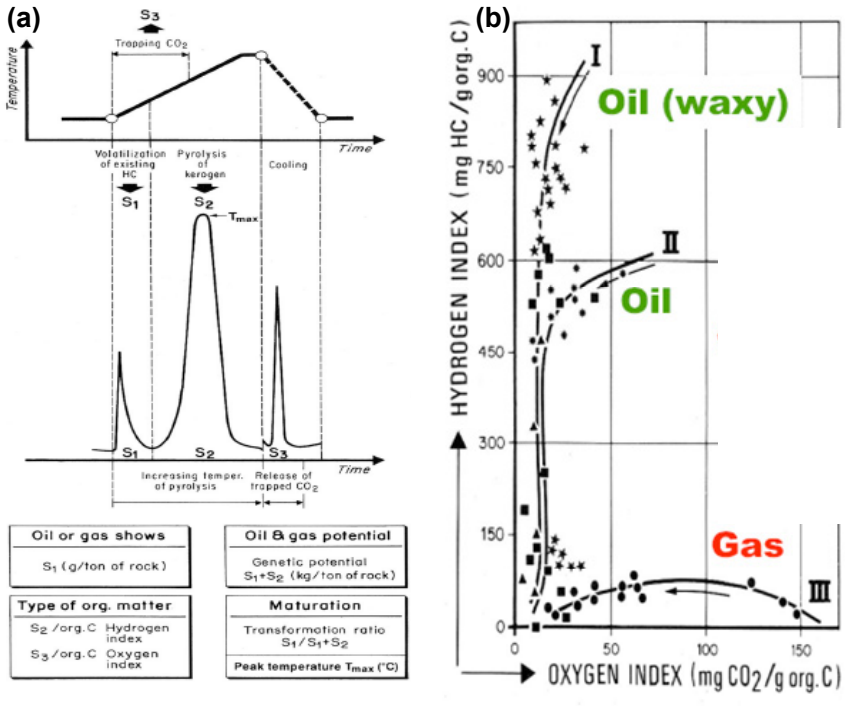

Figure A.1. (a) Cycle of analysis and example of record obtained by Rock-Eval pyrolysis (Espitalié *et al.*, 1977); and (b) a typical van Krevelen diagram.

MOLECULAR SOURCE AND DEPOSITIONAL PARAMETERS

n-Alkane profile

The distribution patterns of *n*-alkanes can be indicative of their origin. For example, a predominance of *n*-alkanes in the C_{23} to C_{30} range with an odd-over-even carbon number preference is associated with a terrestrial higher plant source (e.g. see

Chapter 3), while an even-over-odd carbon number preference can be associated with carbonate-evaporite source rocks (Peters and Moldowan, 1993). These interpretations can be complicated by the fact that secondary processes such as maturation, biodegradation, in-reservoir mixing of different oils and migration contamination can alter *n*-alkane distributions.

Pristane/Phytane ratio

The ratio of pristane (Appendix 2, **VI**) to phytane (**III**) (Pr/Ph) has been used as an indicator of the oxicity of depositional environments (e.g. Brooks *et al.*, 1969; Powell and McKirdy, 1973; Didyk *et al.*, 1978). This is based on the assumption that both pristane and phytane originate from the phytol side chain of chlorophyll *a* (**IV**). Early work suggested that low Pr/Ph (i.e. less than 1) were indicative of anoxic depositional environments while higher Pr/Ph (greater than 1) were ascribed to oxic depositional environments (Didyk *et al.*, 1978). However two main problems with this interpretation are, (i) there are other sources of pristane and phytane which include archaebacterial lipids (Rowland, 1990), while pristane is also derived from tocopherol (**XVI**) of higher plants (Goosens *et al.*, 1984); (ii) crocetane (**XVII**) co-elutes with phytane under typical GC conditions (Barber *et al.*, 2001; Greenwood and Summons, 2003), thus its presence can ambiguously alter Pr/Ph; (iii) thermal stress has been shown to alter Pr/Ph during both artificial and natural maturation (e.g. Brooks *et al.*, 1969; Lewan *et al.*, 1979; Evans and Felbeck, 1983; Huizinga *et al.*, 1987); and (iv) sulfur-bound Ph is abundant in NSO, asphaltene and kerogen fractions of immature sediments, which may be released upon breakage of relatively weak carbon-sulfur bonds during thermal maturation, and thus alter Pr/Ph (Koopmans *et al.*, 1999 and references therein). Peters and Moldowan (1993) summarised that Pr/Ph greater than 3.0 indicate terrestrial organic matter input under oxic conditions, and Pr/Ph less than 0.6 indicate anoxic, often hypersaline environments. They suggested that Pr/Ph in the range 0.8 to 2.5 should not be interpreted in terms of depositional conditions, and that Pr/Ph should not be used to describe the depositional environment of samples of low thermal maturity.

$C_{29}/(C_{29}+C_{27})$ sterane ratio

Steranes (e.g. cholestane, **XIX**) in petroleum are derived from sterols (e.g. cholesterol, **XX**) in eukaryotic organisms (Mackenzie *et al.*, 1982). The steranes commonly utilised in petroleum geochemical studies are the C_{27} to C_{30} homologues. There are three structural types of steranes, which include regular steranes, diasteranes (rearranged steranes, see below) and methyl steranes. One parameter is based on the abundance of the algal-derived C_{27} steranes with respect to C_{29} steranes derived from terrestrial higher plants (but see Volkman, 1986), i.e. $C_{29}/(C_{29}+C_{27})$. For example a dominance of C_{27} steranes with respect to C_{29} steranes, i.e. a low $C_{29}/(C_{29}+C_{27})$ sterane ratio, is characteristic of a predominant marine source.

$C_{19}/(C_{19}+C_{23})$ tricyclic terpane ratio

Tricyclic terpanes (e.g. **XXI**) ranging from C_{19} to C_{30} are common in petroleum, with the C_{23} homologue typically being the most prominent (Aquino Neto *et al.*, 1983). A parameter based on the distribution of tricyclic terpanes is the $C_{19}/(C_{19}+C_{23})$ tricyclic terpane ratio, which can be used to differentiate between marine and terrestrial source inputs. For example, a high abundance of the C_{23} tricyclic terpane relative to the terrestrial higher plant-derived (Peters *et al.*, 2005) C_{19} homologue, i.e. a low $C_{19}/(C_{19}+C_{23})$ tricyclic terpane ratio, is indicative of a predominant marine input.

Higher Plant Index

Higher plant index (HPI) is a parameter based on the distributions of various aromatic hydrocarbons. The higher plant input is represented by the abundance of the higher plant markers cadalene (**XXII**), retene (**XXIII**) and 6-isopropyl-1-isohexyl-2-methylnaphthalene (iP-iHMN; **XXIV**), relative to the bacterially-derived 1,3,6,7-tetramethylnaphthalene (1,3,6,7-TeMN; e.g. **XIV**). HPI is calculated using the equation (retene + cadalene + iP-iHMN)/1,3,6,7-TeMN (van Aarssen *et al.*, 1996), and increases with increasing higher plant input to sediments.

MOLECULAR MATURITY PARAMETERS

22*S*/(22*S*+22*R*) 17α(H),21β(H)-hopanes

Hopanes are pentacyclic triterpanes derived from a range of sources including bacteria, blue-green algae (cyanobacteria) and terrestrial higher plants. Hopanes are commonly present in petroleum as a homologous series ranging from C_{29} to C_{35}. The C_{31} to C_{35} homologues, often referred to as extended hopanes, contain an asymmetric centre at the C-22 position giving rise to two diastereomers: 22*R* and 22*S* (e.g. Appendix 2, **XXV**). In the sedimentary environment, hopanes initially retain the 22*R* configuration of the biologically-produced hopanoid precursor. With ongoing maturation, the relative abundance of the 22*S* hopane increases relative to the 22*R* hopane, resulting in an increase in the ratio of 22*S*/(22*S*+22*R*). Thus, the ratio of 22*S*/(22*S*+22*R*) 17α(H) 21β(H)-hopanes (Ensminger *et al.*, 1977) is often used to assess the thermal maturity of sedimentary organic matter.

Ts/(*Ts*+*Tm*), diahopanes/regular hopanes and diasteranes/regular steranes

Some hopane maturity parameters include those based on the rearrangement of hopane structures. These include the parameter based on the 18α(H)/17α(H)-trisnorhopane (**XXVI**) ratio, or *Ts*/*Tm*, calculated as *Ts*/(*Ts*+*Tm*), and that based on the ratio of diahopanes to regular hopanes. During catagenesis, *Ts* is more resistant to degradation than *Tm* (Seifert and Moldowan, 1978), thus *Ts*/(*Ts*+*Tm*) generally increases with ongoing maturation. Diahopanes are formed in clay-rich source rocks *via* carbocation-rearrangement of regular hopanes, where the methyl group attached to C-14 is 'rearranged' to C-15. The rearrangement of regular steranes to diasteranes also occurs in clay-rich source rocks (e.g. Sieskind *et al.*, 1979; van Kaam-Peters *et al.*, 1998). Diahopanes and diasteranes are considered to be more stable than their regular counterparts, therefore diahopane/hopane (e.g. C_{30}-diahopane/$C_{30}\alpha\beta$-hopane) and diasterane/sterane (e.g. $C_{27}\beta\alpha$-diasterane (20*S*)/$C_{27}\alpha\alpha\alpha$-sterane (20*R*)) ratios generally increase with increasing maturity.

Methylphenanthrene index

The methylphenanthrene index (e.g. MPI-1; Radke and Welte, 1983) is a maturity parameter based on the distributions of methylphenanthrene (MP) isomers, relative to the presumed parent compound phenanthrene (P, **XXVII**). MPI-1 is based on the presumption that the MP isomers with methyl groups in the α-position of the phenanthrene structure (e.g. 1-MP, 9-MP) are less stable than those with methyl groups in the β-position (e.g. 2-MP, 3-MP), and thus are more susceptible to change with increasing thermal maturity. The parameter MPI-1 is calculated using the equation (1.5 x (2MP + 3MP))/(P + 9MP + 1MP), and increases with increasing thermal maturity.

Trimethylnaphthalene ratio

The trimethylnaphthalene ratio (e.g. TNR-1; Alexander *et al.*, 1985) is a maturity parameter based on the distribution of methylated naphthalenes. TNR-1, like MPI-1, relies on a shift with maturity in the trimethylnaphthalene (TMN) distributions towards predominance of the more stable β-substituted (**XIV**) isomers (Alexander *et al.*, 1985). The more stable β,β,β-substituted TMN isomer (2,3,6-TMN) increases in abundance relative to the α,α,β-substituted TMN isomers (1,4,6- and 1,3,5-TMN) with increasing thermal maturity. Thus, TNR-1 is calculated using the formula 2,3,6-TMN/(1,4,6-TMN + 1,3,5-TMN) (Alexander *et al.*, 1985).

Trimethylnaphthalene ratio, tetramethylnaphthalene ratio and pentamethylnaphthalene ratio in a ternary diagram

The three parameters TMNr (trimethylnaphthalene ratio), TeMNr (tetramethylnaphthalene ratio) and PMNr (pentamethylnaphthalene ratio), when plotted in a ternary diagram (van Aarssen *et al.*, 1999), can be used as an indicator for secondary alteration. Maturation leads to an increase in the abundance of the more stable methylnaphthalene isomers (e.g. 1, 3, 7-trimethylnaphthalene; 1, 3, 6, 7-tetramethylnaphthalene; 1, 2, 4, 6, 7-pentamethylnaphthalene) relative to the less stable isomers (e.g. 1, 2, 5-trimethylnaphthalene; 1, 2, 5, 6-tetramethylnaphthalene; 1, 2, 3, 5, 6-pentamethylnaphthalene), and the three parameters appear to be linearly

related when determined by thermal stress alone (van Aarssen *et al.*, 1999). Therefore, when plotted on a ternary diagram, crude oils with parameters that are determined only by thermal stress locate inside the 'maturity centre' (Figure A.2). The maturity centre (e.g. see Chapter 6) is defined as the area within a 10% margin around a mathematically-determined centre which, in theory, is a single point on the diagram representing a case where TMNr, TeMNr and PMNr are perfectly linearly related (van Aarssen *et al.*, 1999). Samples that deviate from the maturity centre are affected by additional secondary processes, such as in-reservoir mixing of oils of different maturities, by biodegradation, or by migration contamination (van Aarssen *et al.*, 1999).

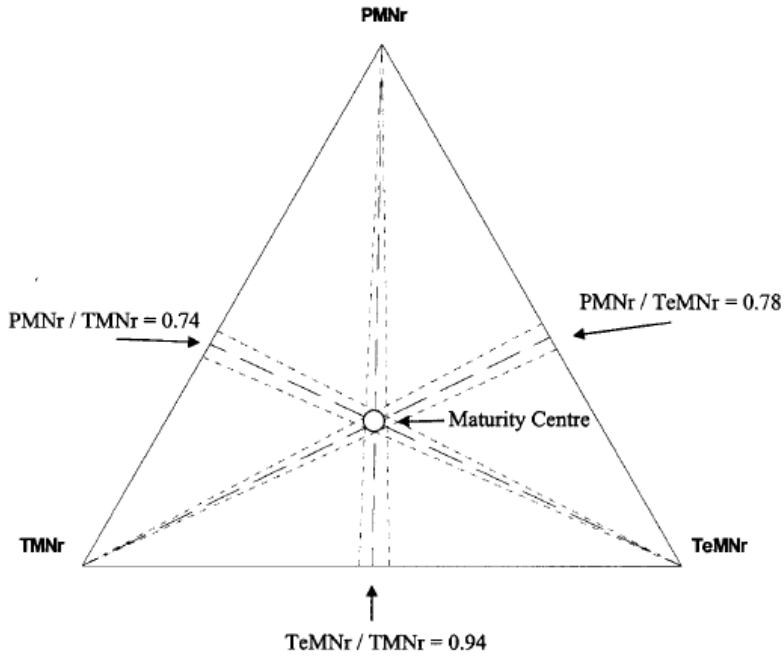

Figure A.2. A ternary plot displaying the linear relationships between TMNr, TeMNr and PMNr as dashed lines. The crosspoint of these lines is where samples that fit all three equations plot (van Aarssen *et al.*, 1999).

APPENDIX 2

Structures referred to in text

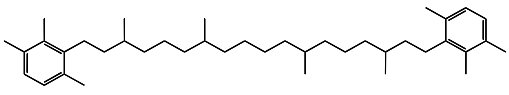

I

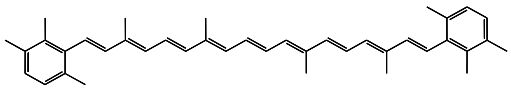

II

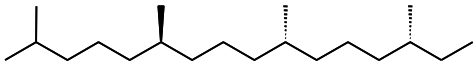

6(*R*), 10(*R*), 14(*R*)-Phytane

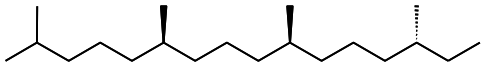

6(*R*), 10(*S*), 14(*R*)-Phytane

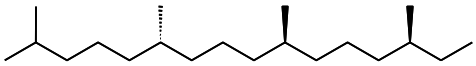

6(*S*), 10(*S*), 14(*S*)-Phytane

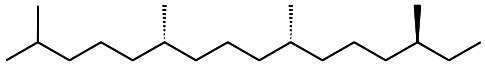

6(*S*), 10(*R*), 14(*S*)-Phytane

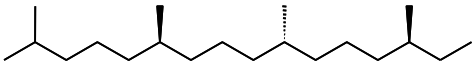

6(*R*), 10(*R*), 14(*S*)-Phytane

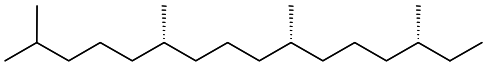

6(*S*), 10(*R*), 14(*R*)-Phytane

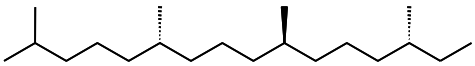

6(*S*), 10(*S*), 14(*R*)-Phytane

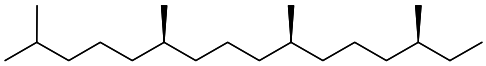

6(*R*), 10(*S*), 14(*S*)-Phytane

III

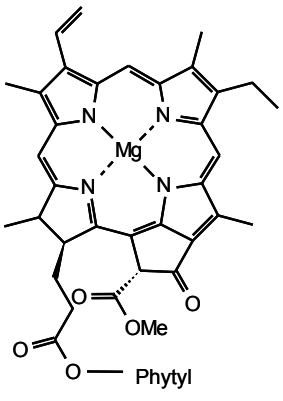

IV

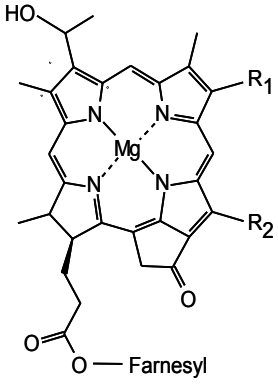

V

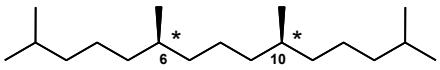

6(*R*), 10(*S*)-Pristane (*meso*-Pristane)

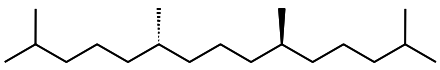

6(*S*), 10(*S*)-Pristane

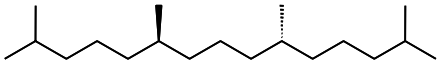

6(*R*), 10(*R*)-Pristane

VI

C_{30} Hopanes

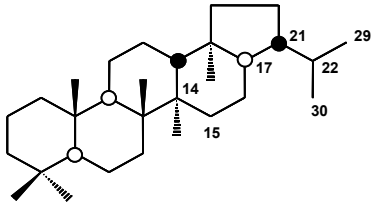

17α(H)21β(H)-Hopane

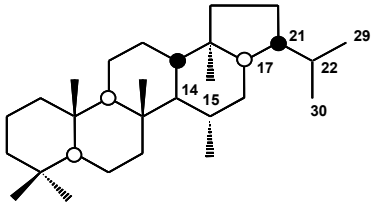

17α(H)21β(H)-Diahopane

VII

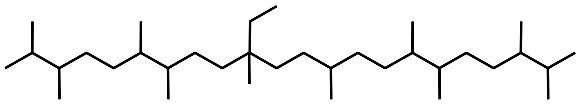

VIII

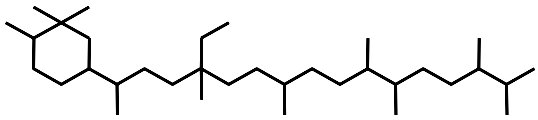

X

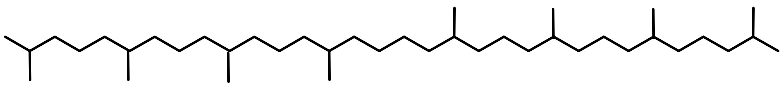

IX

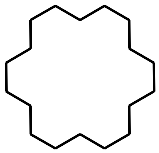

XI

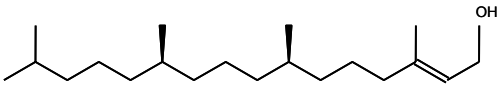

XII

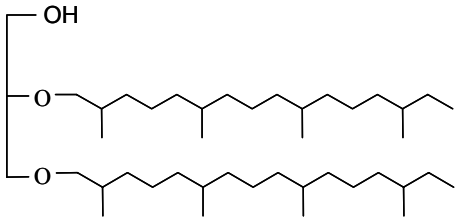

XIII

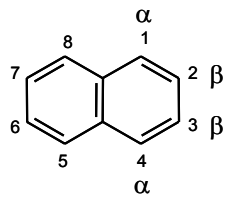

XIV

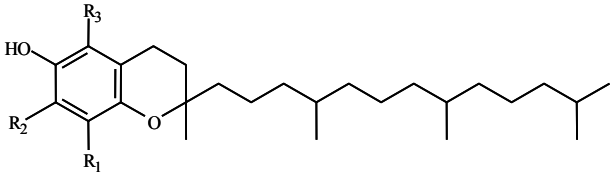

XVI

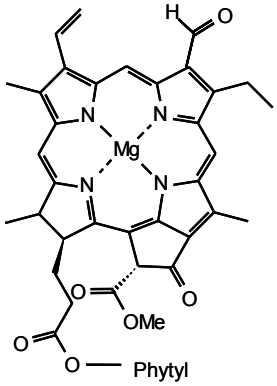

XV

α-Tocopherol $R_1 = CH_3$ $R_2 = CH_3$ $R_3 = CH_3$
β-Tocopherol $R_1 = CH_3$ $R_2 = H$ $R_3 = CH_3$
γ-Tocopherol $R_1 = CH_3$ $R_2 = CH_3$ $R_3 = H$
δ-Tocopherol $R_1 = CH_3$ $R_2 = H$ $R_3 = H$

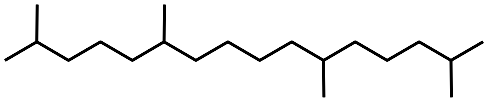

XVII

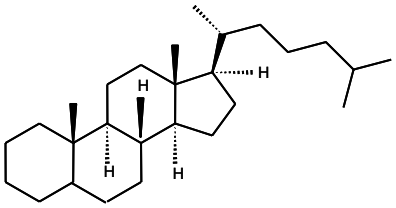

XIX

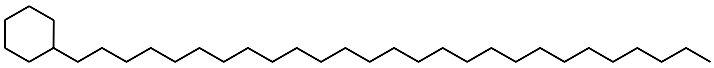

XVIII

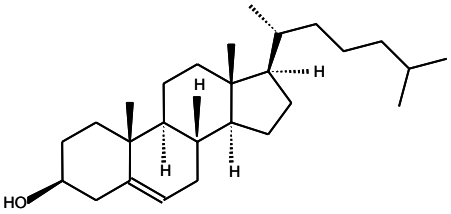

XX

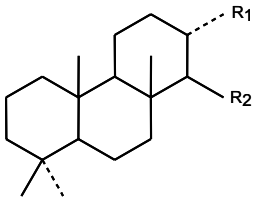

XXI

e.g. C_{19}: R_1=H; R_2=CH_3

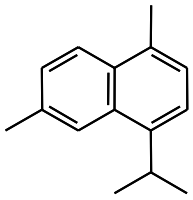

XXII

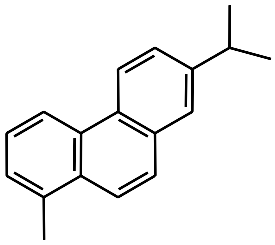

XXIII

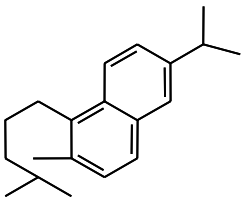

XXIV

C_{31} Extended Hopanes

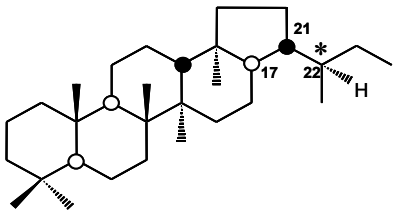

17α(H)21β(H)-Hopane (22*R*)

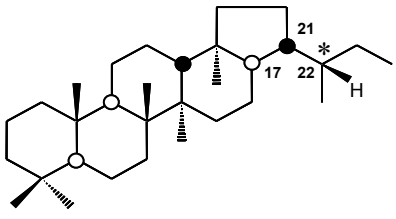

17α(H)21β(H)-Hopane (22*S*)

XXV

22,29,30-Trisnorhopanes (C_{27})

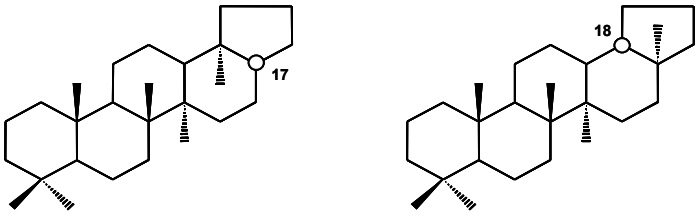

Tm ***Ts***

XXVI

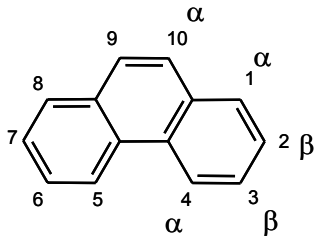

XXVII